Université de Montréal

# Photochemical Synthesis of Macrocyclic Disulfides in Continuous Flow and Photocatalytic Thiol-Yne Reactions of Alkynyl Sulfides

*Par*

Olivier Bleton

Département de Chimie, Faculté des Arts et des Sciences

Mémoire présenté en vue de l'obtention du grade de Maitrise

en Chimie

Août, 2023

Université de Montréal

Unité académique: Département de Chimie/ Faculté des Arts et Sciences

---

*Ce mémoire intitulé*

**Photochemical Synthesis of Macrocyclic Disulfides in Continuous Flow and Photocatalytic Thiol-Yne Reactions of Alkynyl Sulfides**

*Présenté par*

**Olivier Bleton**

*A été évalué par un jury composé des personnes suivantes*

**William Lubell**
Président-rapporteur

**Shawn Collins**
Directeur de recherche

**Stephen Hanessian**
Membre du jury

# Résumé

Le grand thème unifiant le présent travail est celui de la chimie du souffre. La première partie de ce travail traite de la macrocyclisation photochimique. Les macrocycles nécessitent de conditions de dilution élevées, avec de grandes quantités de solvant, généralement incompatibles avec les conditions photocatalytiques en raison de l'absorption de la lumière par le solvant. Pour remédier à ce problème, notre groupe a développé un réacteur hybride pour l'oxydation aérobique photocatalytique des thiols en disulfures dans des conditions de flux continu. Auparavant, des réactions ont été examinées en utilisant de l'octanediol, du PEG et des liants aromatiques pour préparer des macrocycles contenant des peptides allant jusqu'à quatre acides aminés. Le champ d'application a été élargi pour inclure des linkers, tels que le BINOL qui peut former des atropisomères, ainsi que des peptides composés de séquences plus longues d'acides aminés. Le chapitre 1 présentera les concepts de macrocycles et de photochimie, le chapitre 2 décrira la chimie de flux et les recherches du Dr Émilie Morin sur la macrocyclisation à l'aide du réacteur hybride. Le chapitre 3 présente les efforts déployés pour élargir la gamme des macrocycles pouvant être préparés à l'aide du réacteur hybride.

La deuxième partie de ce travail traite des réactions thiol-yne des sulfures d'alcynyle. Les réactions thiol-yne ont de nombreuses applications, notamment dans la chimie des polymères et la macrocyclisation. Les réactions thiol-yne peuvent se dérouler par des voies radicalaires rendues possibles par la photocatalyse à la lumière visible. Cependant, les réactions thiol-yne sont généralement réalisées avec des thiols et des alcynes terminaux. Les alcynes internes représentent un plus grand défi en raison de l'absence de régiocontrôle, mais les sulfures d'alcynyle constituent une solution viable au problème en polarisant la triple liaison de l'alcyne et en offrant une réactivité et une régiosélectivité améliorées par rapport à leurs homologues "tout carbone". Le chapitre 4 présentera les réactions thiol-yne et les différents mécanismes qui y sont associés, ainsi que les sulfures d'alkyles et les méthodes de leur synthèse. Le chapitre 5 présentera les recherches effectuées sur les réactions thiol-yne photocatalytiques des sulfures d'alcynyle.

**Mots-clés**: macrocycle, photocatalyse, peptide, flux continu, thiol-yne, sulfure d'alcynyle

# Abstract

The unifying theme of the present work is sulfur chemistry. The first section of the work deals with photochemical macrocyclization. Macrocyclic peptides are important molecules in the pharmaceutical domain for numerous reasons. Macrocyclizations require high dilution conditions, i.e., large amounts of solvent, typically incompatible with photocatalytic conditions due to the absorption of light by the solvent. To remedy the problem, our group developed a hybrid reactor for the photocatalytic aerobic oxidation of thiols into disulfides in flow conditions. Prior work included several examples using octanediol, PEG, and haloaromatic linker molecules, and of macrocyclic peptides containing up to four amino acids The scope, however, did not include linkers such as BINOL which can exhibit atropisomers as well as peptide macrocycles composed of longer sequences of amino acids. Chapter 1 will introduce the concepts of macrocycles and photochemistry, while Chapter 2 will describe flow chemistry and the research of Dr. Émilie Morin on macrocyclization using the novel reactor. Chapter 3 will discuss the attempted, and ultimately successful, synthesis of a macrocycle intended to further the scope of macrocycles that can be prepared using the hybrid reactor.

The second section of the present work deals with thiol-yne reactions of alkynyl sulfides. Thiol-yne reactions have many applications including uses polymer and macrocyclization chemistry. Thiol-yne reactions can proceed via radical-mediated pathways made possible with visible light photocatalysis. However, thiol-yne reactions are typically accomplished with thiols and terminal alkynes. Internal alkyne functionalization is challenging due to the need of regiocontrol, but alkynyl sulfides present a viable solution to the problem by polarizing the triple bond of the alkyne and offering improved reactivity and regioselectivity over “all-carbon” counterparts. Thiol-yne reactions and different mechanisms associated with them are featured in Chapter 4, as well as alkynyl sulfides and methods for their synthesis. Work done on photocatalytic thiol-yne reactions of alkynyl sulfides will be presented in Chapter 5.

**Key words**: macrocycle, photocatalysis, peptide, continuous flow, thiol-yne, alkynyl sulfide

# Table of content

Résumé ..... 3

Abstract ..... 4

Table of content ..... 5

List of tables ..... 8

List of figures ..... 9

List of schemes ..... 11

List of abbreviations and acronyms ..... 14

Acknowledgements ..... 20

Chapter 1 – Introduction to Macrocyclization and Photochemistry ..... 21

1.1 Macrocycles ..... 21

1.1.1 Definition and Utility ..... 21

1.1.2 Challenges in Macrocycle Synthesis ..... 22

1.1.3 Macrocyclic Peptides ..... 23

1.1.4 “Linker” Molecules and Amino Acids as Building Blocks for Macrocycles ..... 24

1.2 Photochemistry ..... 27

1.2.1 Basics of Photochemistry ..... 27

1.2.2 Photocatalysts ..... 29

1.2.2.1 Eosin Y ..... 31

1.2.3 PCET and Photochemical Oxidation of Thiols into Disulfides ..... 32

1.2.4 Photochemical Macrocyclizations ..... 34

1.3 References ..... 36

Chapter 2 – Flow Chemistry and the Hybrid Reactor ..... 40

2.1 Flow Chemistry ..... 40
2.1.1 Basics of Flow Chemistry ..... 40
2.1.2 Macrocyclization in Flow Chemistry ..... 41
2.1.3 Continuously Stirred Tank Reactor (CSTR) Setups ..... 44
2.2 The Hybrid Reactor ..... 45
2.2.1 Design of the Reactor ..... 45
2.2.2 Model Reaction, Comparison and Scale-Up ..... 49
2.2.3 Scope of the Reaction ..... 52
2.3 References ..... 55
Chapter 3 – Photocatalytic Synthesis of a Macrocyclic Polypeptide ..... 57
3.1 Project Goals ..... 57
3.2 Attempted Synthesis of a Tetrapeptide-Containing Macrocycle Incorporating a BINOL Motif. ..... 57
3.3 Attempted Synthesis of a Hexapeptide-Containing Macrocycle Incorporating an Octanediol Motif ..... 62
3.4 Synthesis of a Hexapeptide-Containing Macrocycle Incorporating a Haloaromatic Motif. 67
3.5 References ..... 72
Chapter 4 – Thiol-Yne Reactions and Alkynyl Sulfides ..... 73
4.1 Thiol-Yne Reactions ..... 73
4.1.1 Generalities and Utility ..... 73
4.1.2 Mechanisms ..... 75
4.1.3 Use of Visible Light for Thiol-Yne Reactions ..... 77
4.2 Alkynyl Sulfides ..... 79
4.2.1 Synthesis of Alkynyl Sulfides ..... 79

4.2.1 Previous Work from the Collins Group ..... 80
4.3 References ..... 83
Chapter 5 – Photocatalytic Thiol-Yne Reactions of Alkynyl Sulfides ..... 86
5.1 Abstract ..... 86
5.2 Introduction ..... 87
5.3 Results ..... 89
5.4 Conclusion ..... 92
5.5 References ..... 94
Chapter 6 – Conclusions and Perspectives ..... 99
6.1 Conclusions ..... 99
6.2 Perspectives ..... 99
Appendix 1: Experimental Procedures and Spectral Data for Chapter 3 ..... 101
Appendix 2: Experimental Procedures and Spectral Data for Chapter 5 ..... 118

# List of tables

Table **2.1** – Comparison of the efficiency of different reaction setups for the model reaction ... 51

Table **2.2** – Scale-up of the model reaction. ..... 52

# List of figures

Figure **1.1** – Examples of macrocycles ..... 21
Figure **1.2** – The intramolecular and intermolecular pathways possible for a linear precursor and their associated rate equations. ..... 22
Figure **1.3** – Examples of FDA approved drugs containing macrocyclic peptides. ..... 24
Figure **1.4** – Use of a linker molecule in A) an EGFR Tyrosine Kinase Inhibitor and B) a JAK2 macrocyclic inhibitor to increase biological activity. ..... 25
Figure **1.5** – Examples of aromatic linkers found in natural products. ..... 26
Figure **1.7** – Interaction of light with molecule *A* to promote it to its excited state $A^*$. ..... 28
Figure **1.8** – Jablonski diagram. ..... 29
Figure **1.9** – General mechanisms for a) triplet-triplet energy transfer (TTET) and b) single electron transfer (SET) in photocatalysis. ..... 30
Figure **1.10** – General mechanisms for a) reductive and b) oxidative PCETs. ..... 33
Figure **2.1** – Example of a continuous flow setup designed by the Jamison group for the synthesis of Ibuprofen. ..... 40
Figure **2.2** – Example of a PFR with a coiled tubing structure (top) and of a PFR used for photochemical reactions developed by the Collins group (bottom).[11] The LED tower goes inside the coiled-tubing structure to irradiate the entire length of the tubing evenly. ..... 42
Figure **2.3** – Difference between a) a slow addition setup and b) a CSTR setup. ..... 44
Figure **2.4** – The Collins group hybrid reactor for photochemical macrocyclizations. ..... 46
Figure **2.5** – The Teflon insert serving as the centre of the reactor. ..... 46
Figure **2.6** – The metal frames of the reactor. ..... 47
Figure **2.7** – The LED plates that cover the reactor. ..... 47
Figure **2.8** – Mixing of Eosin Y without (top) and with (bottom) bubbling of oxygen. ..... 48
Figure **2.9** – The reaction setup including (from left to right) the syringe pump, an injection loop, the hybrid reactor, a LED plate, a collection vessel, the gas source, and a *Syrris* pump. ..... 49
Figure **2.10** – Different setups for model macrocyclization reaction comparisons. From left to right: Traditional batch, CSTR, and PFR ..... 50

Figure **2.11** – Three reactors place in series with two Syrris pumps ..... 52
Figure **2.12** – Scope of the reaction achieved by Dr. Émilie Morin, William Neiderer, Corentin Cruché and Charlotte Cave. ..... 53
Figure **3.1** – Envisioned tetrapeptide atropisomeric macrocyclic precursor and resulting macrocycle. ..... 58
Figure **4.1** – General a) thiol-ene reaction and b) thiol-yne reaction. ..... 73
Figure **4.2** – Reaction of 4-pentyn-1-thiol with various β-substituted propiolates ..... 74
Figure **5.1** – Thiol-yne reactions ..... 87
Figure **5.2** – Developing a photocatalytic thiol-yne reaction of alkynyl sulfides. ..... 89
Figure **5.3** – *Top:* Substrate scope [a] Major *cis*-product shown. Minor product is *trans*-isomer. Isolated yields. *Bottom:* Plausible mechanism and catalytic cycle. ..... 91
Figure **6.1** – Examples of reactions to try in the hybrid reactor. Thiol-ene (top) and thiol-yne (bottom). ..... 100
Figure **6.2** – Examples of thiol-yne reactions with different heteroatoms. ..... 100
Figure **S1** – Homemade photoreactor used for the photochemical thiol-yne reaction. ..... 121

# List of schemes

Scheme **1.1** – Olefin metathesis leading to a cyclic peptide. ..... 27

Scheme **1.2** – Use of $Ru(bpy)_3Cl_2$ photocatalyst by a) Yoon, b) MacMillan and c) Stephenson. .. 31

Scheme **1.3** – Use of Eosin Y photocatalyst by a) Yadava, b) Wang and c) Zeitler. ..... 32

Scheme **1.4** – Aerobic oxidation of thiols to disulfides developed by the Noël group with proposed mechanism. ..... 33

Scheme **1.5** – Photocatalyzed macrocyclization by dimerization of alkynes developed by the Collins group. ..... 34

Scheme **2.1** – Synthesis of poly(3-hexylthiophene) using a droplet flow setup. ..... 41

Scheme **2.2** – Synthesis of an alkynyl sulfide macrocycle using continuous flow and photochemical conditions. ..... 43

Scheme **2.3** – Gram scale photochemical Diels Alder macrocyclization. ..... 43

Scheme **2.4** –Macrocyclization via olefin metathesis using a CSTR setup. ..... 45

Scheme **2.5** – Synthesis of the model substrate used for macrocyclization. ..... 50

Scheme **2.6** – Macrocyclization to form the disulfide **2.19** via photocatalysis. ..... 50

Scheme **3.1** - Linear retrosynthesis of a tetrapeptide macrocycle containing two cysteines and a BINOL linker molecule ..... 59

Scheme **3.2** – Coupling of Alanine **3.2** to BINOL **3.1** through an esterification reaction. ..... 59

Scheme **3.3** – Attempted Fmoc deprotection of dipeptide **3.3** ..... 60

Scheme **3.4** – Alternate retrosynthesis of a tetrapeptide macrocycle containing two cysteines and a BINOL linker molecule. ..... 61

Scheme **3.5** – Attempted synthesis of a tetrapeptide macrocyclic precursor ..... 62

Scheme **3.6** – Linear retrosynthesis of a hexapeptide octanediol-based macrocyclic precursor. 63

Scheme **3.7** – Attempted synthesis of a hexapeptide macrocyclic precursor through an esterification of two tripeptides and an octanediol. ..... 64

Scheme **3.8**– Alternate retrosynthesis of a hexapeptide octanediol-based macrocyclic precursor. ..... 65

Scheme **3.9** – Attempted synthesis of a diamine dipeptide through a double esterification to an octanediol followed by Boc-deprotection. ..... 66

Scheme **3.10** – Attempted synthesis of a diamine dipeptide through a double esterification to an octanediol followed by Fmoc-deprotection. ..... 67

Scheme **3.11** – Retrosynthesis of a hexapeptide macrocycle containing a haloaromatic motif. . 68

Scheme **3.12** – Synthesis of the haloaromatic core-containing dipeptide substrate. ..... 69

Scheme **3.13** – Synthesis of a hexapeptide haloaromatic macrocyclic precursor. ..... 70

Scheme **3.14** – Synthesis of a hexapeptide haloaromatic macrocycle in flow using the hybrid reactor. ..... 71

Scheme **4.1** – Photocatalyzed radical addition of octanethiol to phenylacetylene leading to an α-substituted sulfoxide. ..... 74

Scheme **4.2** –Hydrothiolation of alkyne initiated by cesium carbonate base. ..... 75

Scheme **4.3** – Palladium-catalyzed hydrothiolation of 1-alkynylphosphines. ..... 76

Scheme **4.4** – Radical-mediated thiol-yne chain reaction mechanism. 1) Addition to a terminal alkyne. 2) Subsequent addition to the vinyl sulfide. ..... 77

Scheme **4.5** – Thiol-yne dihydrothiolation macrocyclization reaction of dithiol precursors with acetylene using an iridium catalyst. ..... 78

Scheme **4.6** – Metal-free thiol-yne reaction using visible light catalyzed by Eosin Y. ..... 79

Scheme **4.7** – Dehalogenation of a bromo-vinyl precursor to give an alkynyl sulfide..... 80

Scheme **4.8** – Thiolation reaction using a sulfur umpolung strategy. ..... 80

Scheme **4.9** – Thiol alkynylation reaction with alkyne umpolung using EBX reagent. ..... 80

Scheme **4.10** – Synthesis of an alkynyl sulfide using continuous flow and photochemical conditions. ..... 81

Scheme **4.11** – Cu-catalyzed $C_{sp}$–S coupling for alkynyl sulfide synthesis. ..... 81

Scheme **4.12** – General Cu-catalyzed $C_{sp}$–S coupling for alkynyl sulfide macrocyclization. ..... 82

# List of abbreviations and acronyms

| | |
|---|---|
| 4CzIPN | 2,4,5,6-Tetra(9*H*-carbazol-9-yl)isophthalonitrile |
| ΔG | Gibbs Free Energy |
| ΔH | Enthalpy change |
| ΔS | Change in Entropy |
| ε | Molar absorption coefficient |
| λmax | Maximum absorption wavelength |
| µg | Microgram |
| µL | Microliter |
| ν | Frequency |
| π | Pi |
| ω | Omega |
| Å | Angström |
| A | Absorption/Absorbance |
| Ac | Acetyl |
| Aq | Aqueous |
| atm | Atmosphere (pressure) |
| BINOL | 1,1'-Bi-2-naphthol |
| BPR | Back pressure regulator |
| Bpy | 2,2'-Bipyridine |
| Boc | tert-Butoxycarbonyl |
| br | Broad |
| Bu | Butyle |
| c | Concentration |
| °C | Celsius degree |
| cat. | Catalytic amount |
| cm | Centimetre |

| | |
|---|---|
| CSTR | Continuous stirred tank reactor |
| Cz | Carbazole |
| d | Days |
| d | Doublet |
| dr | Diastereomeric ration |
| dba | Dibenzylideneacetone |
| DCC | *N,N'*-Dicyclohexylcarbodiimide |
| DCM | Dichloromethane |
| DIPEA | *N,N*-Diisopropylethylamine |
| DMAP | 4-Dimethylaminopyridine |
| DPAP | 2,2-dimethoxy-2-phenylacetophenone |
| dppp | 1,3-Bis(diphenylphosphino)propane |
| DMF | *N,N*-Dimethylformamide |
| DMS | Dimethylsulfate |
| DMSO | Dimethylsulfoxide |
| dtbbpy | 4,4'-di-*tert*-butyl-2,2'-dipyridyl |
| EBX | Ethynyl benziodoxolone |
| ee | Enantiomeric excess |
| EDC | 1-Ethyl-3-(3-dimethylaminopropyl)carbodiimide |
| EFGR | Epidermal growth factor receptor |
| ET | Electron transfer |
| Et | Ethyl |
| Eq. | Equivaents |
| F | Fluorescence |
| FDA | Food Drug Administration |
| Fmoc | Fluorenylmethoxycarbonyl |
| g | Gram |
| GC-MS | Gas chromatography-mass spectrometry |
| h | Hour |

| | |
|---|---|
| h | Planck's constant |
| HATU | 1-[Bis(dimethylamino)methylene]-1*H*-1,2,3-triazolo[4,5-*b*]pyridinium 3-oxid hexafluorophosphate |
| HBTU | *N,N,N',N'*-Tetramethyl-*O*-(1*H*-benzotriazol-1-yl)uronium hexafluorophosphate |
| HCTU | O-(1H-6-Chlorobenzotriazole-1-yl)-1,1,3,3-tetramethyluronium hexafluorophosphate |
| HOBt | Hydroxybenzotriazole |
| HOMO | Highest occupied molecular orbital |
| HOSu | *N*-Hydroxysuccinimide |
| HPLC | High pressure liquid chromatography |
| HRMS | High resolution mass spectrometry |
| Hz | Hertz |
| IC | Internal conversion |
| ISC | Intersystem crossing |
| Inter | Intermolecular |
| Intra | Intramolecular |
| IR | Infra-red |
| *i*-Pr | Isopropyl |
| IUPAC | International Union of Pure and Applied Chemistry |
| J | Coupling constant |
| JAK2 | Janus Kinase 2 |
| k | Reaction rate constant |
| $K_d$ | dissociation constant |
| kg | Kilogram |
| L | Litre |
| $\ell$ | Optical pathlength |
| LED | Light emitting diode |
| LUMO | Lowest unoccupied molecular orbitals |
| m/z | Mass to charge |

| | |
|---|---|
| m | meta |
| m | Multiplet |
| M | Molar |
| Me | Methyl |
| mg | Milligram |
| MHz | Megahertz |
| min | Minute |
| mL | Millilitre |
| mm | Milimetre |
| mM | Millimolar |
| mmol | Millimole |
| mol | Mole |
| MS | Mass spectometry |
| MS | Molecular sieves |
| ng | Nanogram |
| $NEt_3$ | Triehtylamine |
| nm | Nanometre |
| nM | Nanomolar |
| NMR | Nuclear magnetic resonance |
| o | Ortho |
| OAc | Acetate |
| p | para |
| P | Phosphorescence |
| PCC | Pyridinium chlorochromate |
| PCat | Photocatalyst |
| PCET | Proton coupled electron transfer |
| PEG | Poly(ethylene) glycol |
| PFA | Polyfluoroalkoxy alkane |
| PFR | Plug-flow reactor |

| | |
|---|---|
| Ph | Phenyl |
| pKa | Acid dissociation constant |
| ppm | Parts per million |
| psi | Pound per square inch |
| PT | Proton transfer |
| q | Quartet |
| ref. | Reference |
| r. t. | Room temperature |
| s | second |
| s | singlet |
| $S_0$ | Singlet ground state |
| SET | Single electron transfer |
| $SN_2$ | Bimolecular nucleophilic substitution |
| t | tert |
| t | Triplet |
| T | Transmittance |
| $T_n$ | Triplet state |
| TBD | 1,5,7-triazabicyclo[4.4.0]dec-5-ene |
| t-Bu | Tert-butyl |
| TBTU | 2-(1H-Benzotriazole-1-yl)-1,1,3,3-tetramethylaminium tetrafluoroborate |
| temp | Temperature |
| TES-H | Triethylsilyl |
| Teflon | Tetrafluoroethylene |
| TFA | Trifluroacetic acid |
| THF | Tetrahydrofurane |
| TKI | Tyrosine Kinase Inhibitors |
| TLC | Thin-Layered Chromatography |
| TMEDA | *N,N,N',N'*-Tetramethylethylenediamine |
| TMS | Trimethylsilyl |

| | |
|---|---|
| $t_{res}$ | Residence time |
| Trt | Triphenylmethyl |
| TTET | Triplet-triplet energy transfer |
| UV | Ultraviolet |
| v | speed |
| Vis | Visible |
| W | Watt |
| Y | Yield |

# Acknowledgements

I want to express my sincere gratitude to the people who have played vital roles in helping me complete this Chemistry master's thesis. First and foremost is Professor Shawn Collins who gave me a chance to work in his lab even though I was completely inexperienced. I learned quite a bit and Prof. Collins was a major factor, guiding me through all the highs and lows and instilling in me a very persistent work ethic. It wasn't always easy, but it was nonetheless a privilege to be able to work in the Collins lab, so thank you again Prof. Collins. I want to thank my parents, Paul and Irène, for their incredible support throughout the years, and though my father was given very challenging news at the beginning of my master's program, he is still with us at the time of this writing, and his strength has been a true inspiration. I can't thank the love of my life, Lorissa, enough. She has been an incredible partner and support throughout the years of hard work we've gone through together. She is always there for me (and usually cooks delicious dinners… usually…I love you!). I'd like to thank my brother Jérôme and his soon-to-be wife Téo for their support, their good humor and all their advice. Finally, I want to thank my amazing lab colleagues, without whom this journey would have been much more demanding. I have made friendships I will keep for a lifetime in that lab. But for the love of God, please choose somewhere other than McCarold's for celebrations!

# Chapter 1 – Introduction to Macrocyclization and Photochemistry

## 1.1 Macrocycles

### 1.1.1 Definition and Utility

Macrocycles are molecules that contain at least one large ring composed of 12 or more atoms.[1] Examples include crown ethers, calixarenes, porphyrins, and cyclodextrins, among others.[2] Macrocyclic structures have been used as chemosensors for small metal ions,[3] to construct supramolecular structures,[4] and to form pi-conjugated nanostructures,[5] but perhaps most importantly they form a variety of bioactive compounds that are prevalent in the realm of pharmaceuticals.

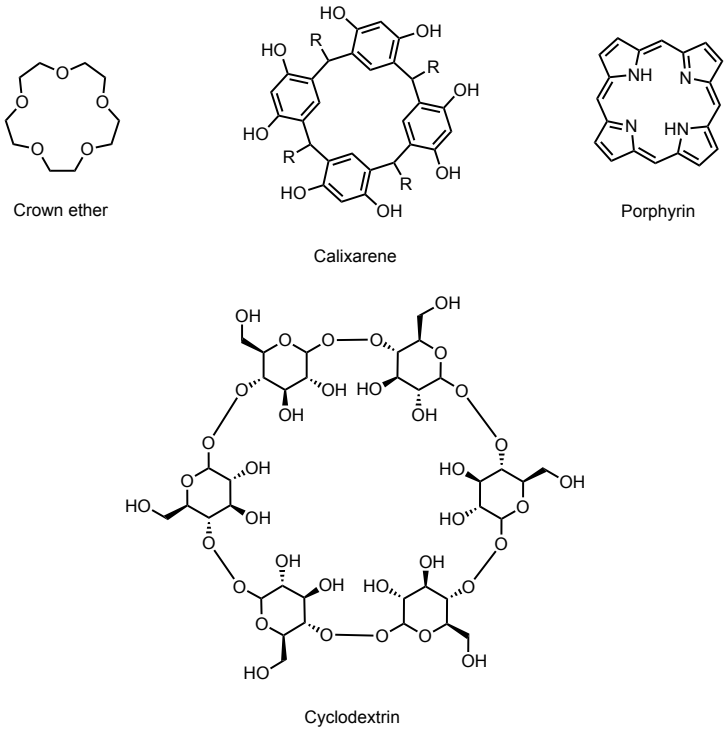


Figure **1.1** – Examples of macrocycles

### 1.1.2 Challenges in Macrocycle Synthesis

A linear precursor containing functional groups at each end can undergo a desired intramolecular, "head-to-tail" reaction leading to the formation of a macrocyclic product (Figure **1.2**). To cyclize, the precursor must overcome the loss of entropy due to bond angle deformations (Baeyer strain), forced adoption of eclipsed conformations (Pitzer strain), and transannular interactions.[6] A competing pathway involves the precursor molecule reacting intermolecularly with another equivalent of itself to form dimers. Subsequent reactions could potentially form polymers or even larger rings.

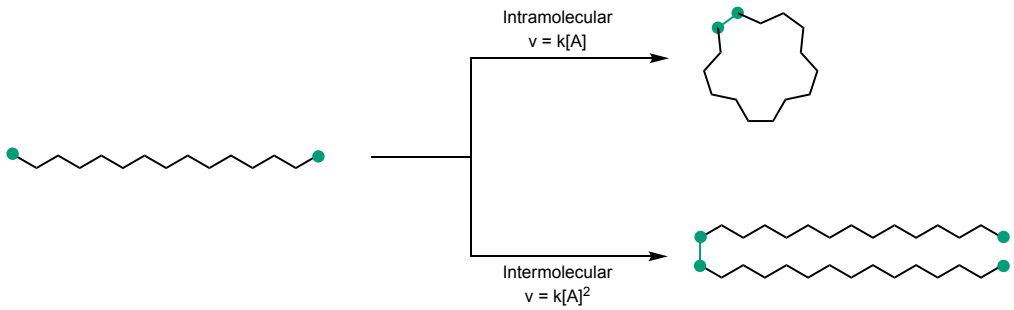


Figure **1.2** – The intramolecular and intermolecular pathways possible for a linear precursor and their associated rate equations.

Kinetics play a critical role in determining which pathway is followed. Because a dimerization/polymerization reaction is bimolecular, and the intramolecular macrocyclization is unimolecular, changes in concentration affect the kinetics of the bimolecular reaction to a greater degree since an increase in the rate of the reaction is proportional to the square of an increase in substrate concentration (Figure **1.2**). To favor the intramolecular pathway, the reaction should be performed at low concentrations.[7] Typically, macrocyclization reactions are carried out in the millimolar (mM) range. Such constraints can pose problems when scaling up macrocyclization processes to gram scales due to the amount of solvent necessary to achieve such concentrations. One method to overcoming the problem is to use slow addition strategies,[8] in which a concentrated solution of substrate is slowly added to another flask containing a greater amount of solvent and reagents, to mimic high dilution conditions and disfavor intermolecular reaction.

### 1.1.3 Macrocyclic Peptides

Peptides play a crucial role in various biological functions. However, the pharmacological application of linear peptides is limited due to their vulnerability to degradation by proteases and peptidases.[9] Moreover, their conformational flexibility can negatively impact their biological activity, as they need to adopt the correct conformation to bind effectively to their target proteins. When a polypeptide exhibits high flexibility, it can exist in different conformations, many of which could be biologically inactive. Consequently, the binding affinity is considerably diminished, primarily due to the influence of entropy on the free Gibbs free energy (ΔG) of binding and, consequently, the molecule's dissociation constant ($K_d$). In contrast, cyclic peptides offer distinct advantages by pre-organizing amino acid side-chains, leading to a decrease in polar surface area and promoting the formation of intramolecular hydrogen bond networks, restricting the number of possible conformations, and increasing membrane permeability and cytoplasmic delivery of the molecule.[10] Examples of the Food Drug Administration (FDA) approved macrocyclic peptide drugs include Lupkynis (**1.1**), an immunosuppressant, Signifor (**1.2**), for treatment of Cushing's disease, and Somatuline (**1.3**), used to treat acromegaly.[11]

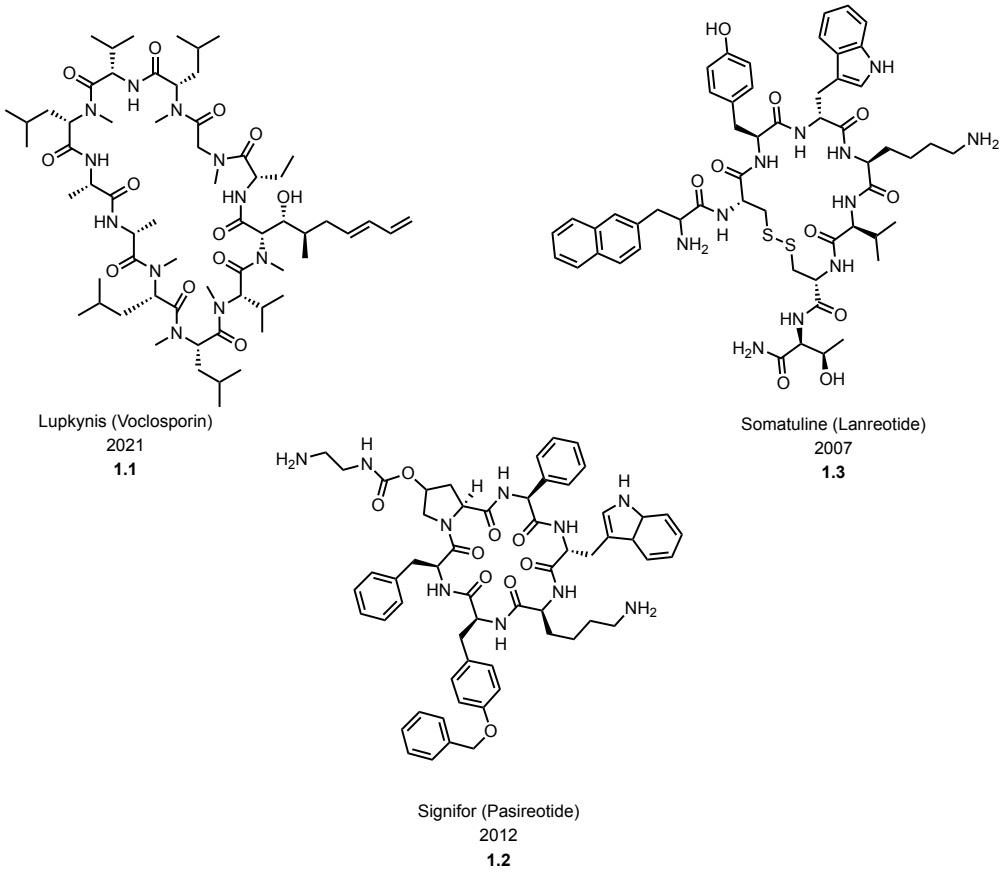


Figure **1.3** – Examples of FDA approved drugs containing macrocyclic peptides.

### 1.1.4 "Linker" Molecules and Amino Acids as Building Blocks for Macrocycles

Some macrocycles include "linkers" or certain scaffolding motifs that link together a pharmacophore forming a macrocycle and in turn improving biological activity. An example is found with epidermal growth factor receptor (EFGR) Tyrosine Kinase Inhibitors (TKIs) used for their anti-tumor activity. Though TKIs can shrink tumors significantly, the response from the tumors is not usually durable. To improve the activity of TKI **1.4**, which can exist in both its active (**1.4a**) and inactive (**1.4b**) conformations, a linker was added to synthesize macrocycle **1.5**, confining the inhibitor to the active binding conformation (Figure **1.3**). Improvement of the potency of the TKI was solely due to the conformational restrictions, as an X-ray structure of compound **1.5** complexed with EGFR showed no newly formed interactions with active site

residues.[12] The linker can also be chosen to introduce certain properties to the macrocycle. Pacritinib (**1.7**), a Janus Kinase 2 (JAK2) macrocyclic inhibitor used to treat myelofibrosis and lymphoma, incorporated a hydrophilic, oxygen-containing linking chain to help ensure better solubility and metabolic stability.[13]

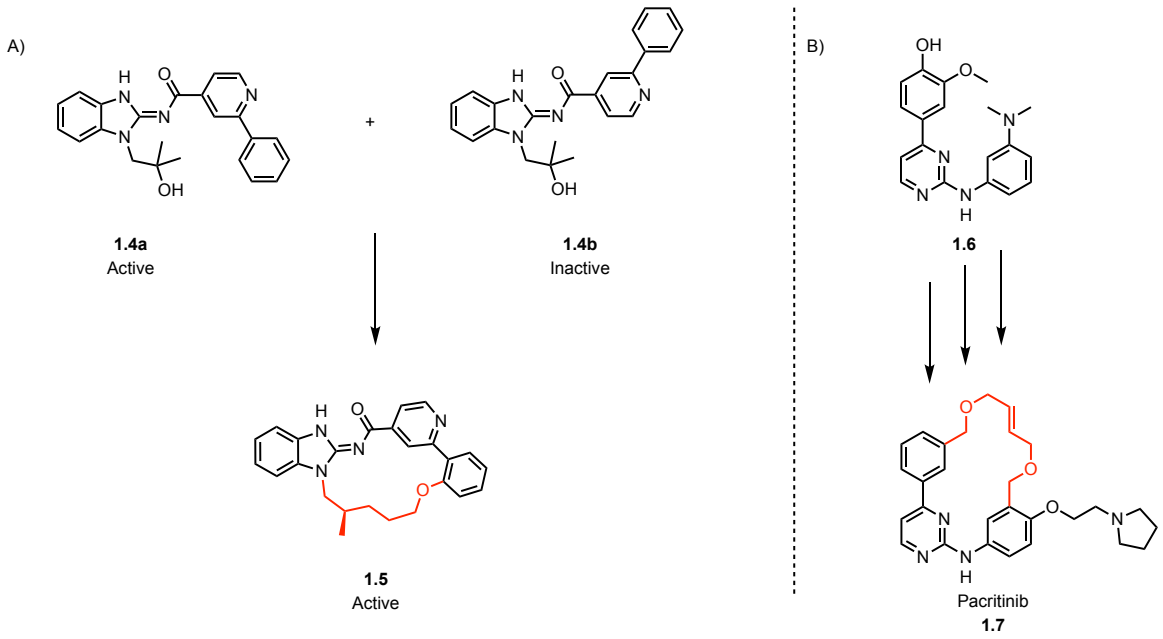


Figure **1.4** – Use of a linker molecule in A) an EGFR Tyrosine Kinase Inhibitor and B) a JAK2 macrocyclic inhibitor to increase biological activity.

In cyclic peptides, the addition of flat, aromatic motifs often results in the stabilization of their secondary structures by conserving intramolecular networks of hydrogen bonds.[14] Outside of ester, amide, and disulfide groups, Nature also uses cyclophane-type linkers to cyclize polypeptide natural products. Examples include the antipyretic hibispeptin A (**1.8**) or the antimitotic celogentin C (**1.9**) (Figure **1.5**). As opposed to flexible linkers such as disulfides, the rigid, planar, and hydrophobic cyclophane linkers can be fully integrated into the main skeletons of peptide macrocycles and form unique structures with unusual arrangements of side chains and peptide backbones.[15]

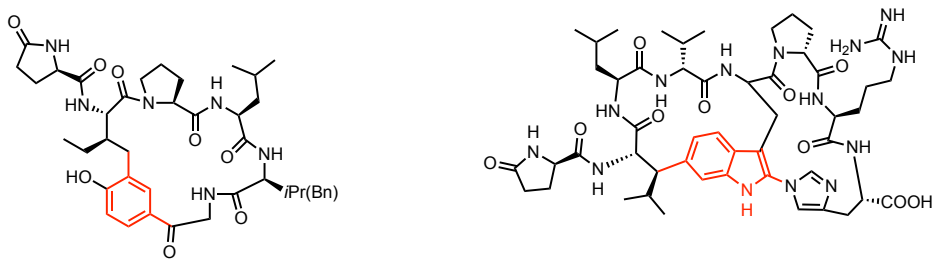

hibispeptin A
**1.8**

celogentin C
**1.9**

Figure **1.5** – Examples of aromatic linkers found in natural products.

Macrocycles are important molecules that occupy the region of chemical space between small molecules and proteins, exploiting the specificity of biological drugs and the accessibility of small molecule drugs.[16] Amino acids are ideal building blocks to synthesize macrocycles. Their *N*-terminals and C-terminals can be reacted to form amide bonds. Esterification reactions between amino acids and linkers or other structural elements can be carried out with the aid of coupling agents such as 1-ethyl-3-(3-dimethylaminopropyl) carbodiimide (EDC) and hydroxybenzotriazole (HOBt). Cysteine residues can be exploited to form disulfide bridges. Furthermore, amino acids are widely available and inexpensive. Various side chains can be used to add further functionalization to a macrocyclic molecule, and, outside of the 20 natural amino acids, unnatural amino acids can also be synthesized and incorporated. For example, the White group used a synthetic amino acid containing an allyl side chain used to carry out a catalytic olefin metathesis macrocyclization (Scheme **1.1**).[17]

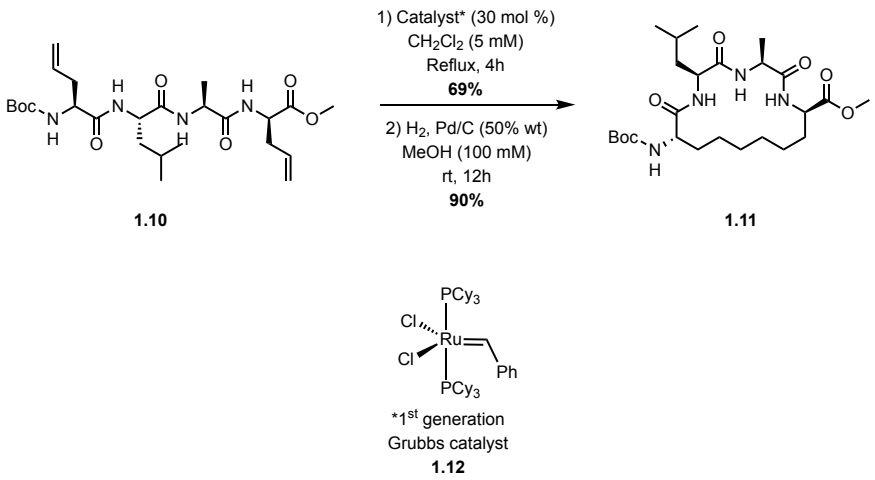


Scheme **1.1** – Olefin metathesis leading to a cyclic peptide.

Though peptide coupling is a trusted method for forming macrocyclic peptides, it requires stoichiometric amounts of reagents and generates a lot of waste. A greener option would be to use catalysis. Photocatalysis is cutting-edge, alternative technology. It has various advantages, including functioning at normal temperatures and atmospheric pressure, reduced waste, and being readily available and easily accessible. There is a growing interest in applying the technology; for example, as a technique for water treatment and decontamination.[18]

## 1.2 Photochemistry

### 1.2.1 Basics of Photochemistry

Photochemistry is the branch of chemistry concerned with the chemical effects of light; chemical reactions caused by the absorption of ultraviolet (UV), visible, or infrared (IR) radiation.[19] Photochemical reactions play a vital role in Nature by driving biological processes like photosynthesis in plants and synthesis of vitamin D in humans.[20] According to the Grotthuss-Draper law, light must first be absorbed by a chemical substance for a photochemical process to take place, and furthermore, the Stark-Einstein law states that for each photon absorbed, only one molecule or atom can be activated for a photochemical reaction.[21]

In the wave model, a photon of light is characterized by its wavelength l and frequency n, travelling at the speed of light c according to the relationship ln=c. A photon of light can transfer

enough energy *E* to an atom or molecule *A* to take it from its ground state to an electronic state of higher energy, the excited state, a new chemical species *A** with its own chemical and physical properties (Figure **1.7**). *E* is related to $\nu$ through the formula $E=h\nu$, where *h* is Planck's constant ($6.63 \times 10^{-34}$ J s). [22]

$$A + h\nu \rightarrow A^*$$

Figure **1.7** – Interaction of light with molecule *A* to promote it to its excited state $A^*$.

Molecules in their excited states reach higher energy levels than they otherwise could in a thermal process, allowing them to overcome activation energy barriers they could not while in the ground state. The ground state is responsible for the absorption spectrum, that is, for the color. The excited states are responsible for deactivation processes that can be chemical in nature (photochemical reactions) or involve energy loss processes, either radiative or nonradiative.[21]

The electronic transitions in the photochemical process can be represented in a Jablonski energy diagram (Figure **1.8**). Radiative transitions represent energy gain or loss in the form of electromagnetic radiation. Nonradiative transitions represent energy gain or loss in the form of thermal vibrational agitation. Absorption (A) describes a radiative transition where the molecule absorbs radiation. The molecule finds itself in an excited state at a higher energy level, while the excited electron retains its spin. The new electronic state is called the singlet state ($S_n$). Subsequently, the molecule relaxes to the lower-energy excited level $S_1$ through a nonradiative transition called internal conversion (IC). From the $S_1$ level, the excited substrate can relax radiatively back to the ground state ($S_0$), through the process of fluorescence (F). Under the right conditions however, the excited molecule in the $S_1$ state can relax through intersystem conversion (ISC). The transition is nonradiative and occurs by reversing the spin of the excited electron to form a state known as a triplet state ($T_n$). The molecule can relax to the more stable and lower energy level $T_1$ through internal conversion. To relax back to its ground state, the system must invert its spin to respect electronic symmetry. The relaxation is known as phosphorescence (P). Since it takes a certain amount of time to invert the spin, phosphorescence is a slower process than fluorescence. $S_0 \rightarrow T_n$ absorptions cannot take place because of the spin selection rule, which states that transitions can only be made between states of same spin multiplicity.[21]

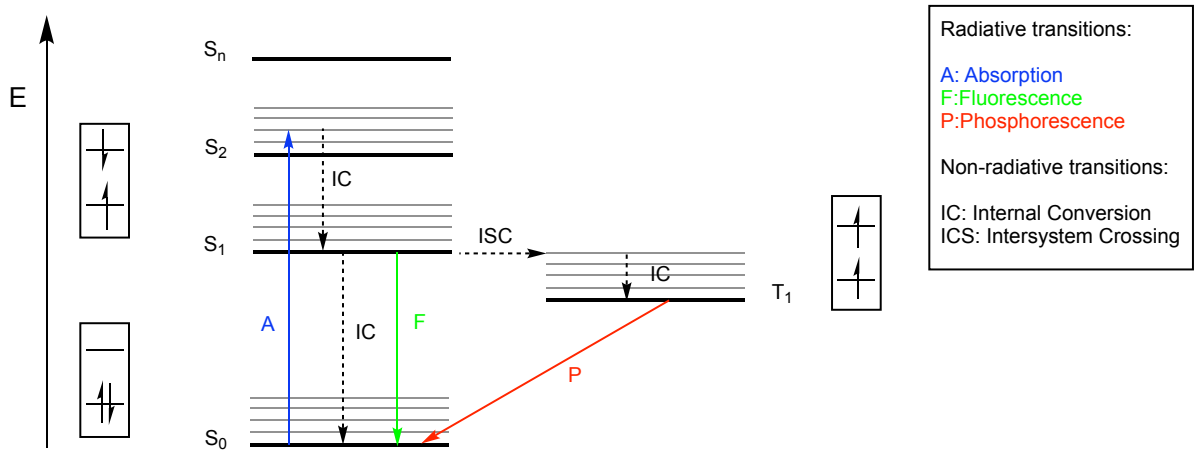


Figure **1.8** – Jablonski diagram.

### 1.2.2 Photocatalysts

Photocatalysis is the acceleration of a photochemical reaction through the aid of a photocatalyst, which can produce, upon absorption of light, chemical transformations of the reaction partners. The excited state of the photocatalyst interacts with the reaction partners forming reaction intermediates and must regenerate itself after each cycle.[18] There are three types of photocatalysts: heterogeneous, where the catalyst is in a different phase from the reactants, homogeneous, where the catalyst and reactants are in the same phase, and plasmonic, where plasmons are used to increase the rate of reaction.[21]

Once a photocatalyst is in its excited state, it can react with a molecule through a triplet-triplet energy transfer (TTET) or through a single electron transfer (SET) (Figure **1.9**). In the case of TTET, the photocatalyst (Pcat*) is excited to its triplet energy level and then transfers its energy to molecule A, returning to its ground state, while promoting an electron in molecule A to a lower triplet energy state $T_1$. The now-excited A* can participate in a chemical reaction. In the case of SET, when the photocatalyst is in its excited state, it simultaneously becomes a better oxidant and a better reductant. Excitation of an electron results in an electron/hole pair separation. After excitation, an electron found in the highest occupied molecular orbital (HOMO) can jump to a

higher energy level to the lowest unoccupied molecular orbital (LUMO), leaving behind a "hole" where the electron used to be. Because the electron is at a higher energy level than it used to be, donation to an acceptor is more favourable than it was before, making the compound a more effective reducing agent through photoexcitation. Also, since the hole is lower in energy than the LUMO of the ground state, it will more easily accept an electron from a donor.[21] The resulting mechanism depends on the preferred redox potential of the species involved in the reaction. The photocatalyst can either give or abstract an electron from the quencher (Q) before either reducing an electron acceptor (A) or by oxidating an electron donor (D). Ideally, there is no need for a sacrificial electron donor or acceptor and the two-electron transfer is connected by intermediates in the reaction.[23]

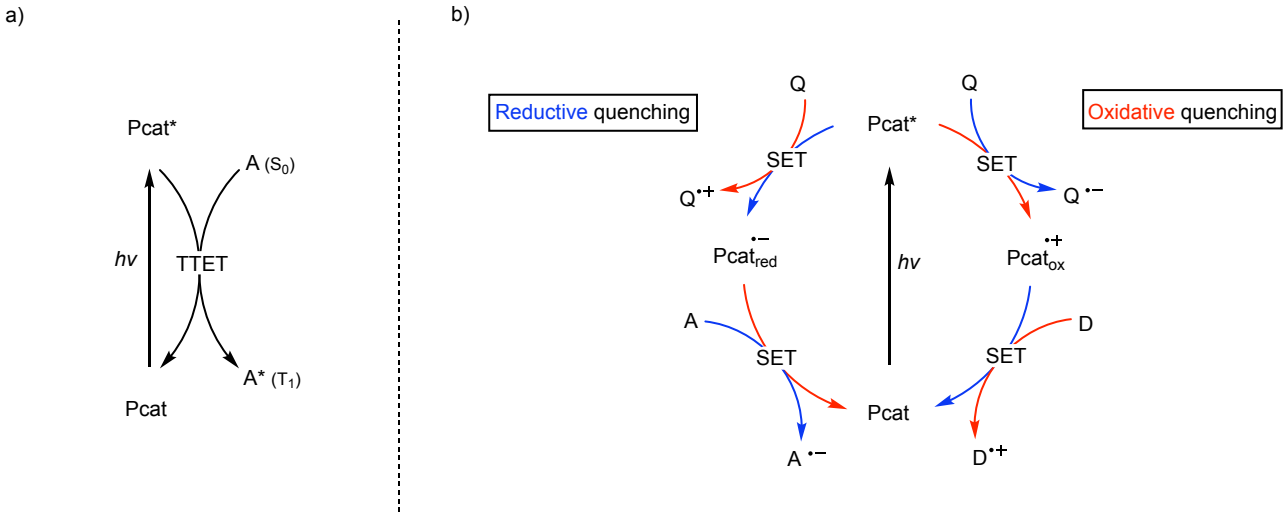


Figure **1.9** – General mechanisms for a) triplet-triplet energy transfer (TTET) and b) single electron transfer (SET) in photocatalysis.

Among the most extensively studied photocatalysts are the organometallic ruthenium (II) polypyridine complexes (e.g., $Ru(bpy)_3^{2+}$), in part due to their ability to absorb light in the visible range.[22] Several examples, namely from Yoon,[24] MacMillan,[25] and Stephenson[26] show the powerful efficiency of the catalysts (Scheme **1.2**). Other sought-after catalysts are also iridium-based, but ruthenium and iridium are rare, expensive metals, and are associated with certain levels of toxicity in pharmaceutical products if not properly eliminated.

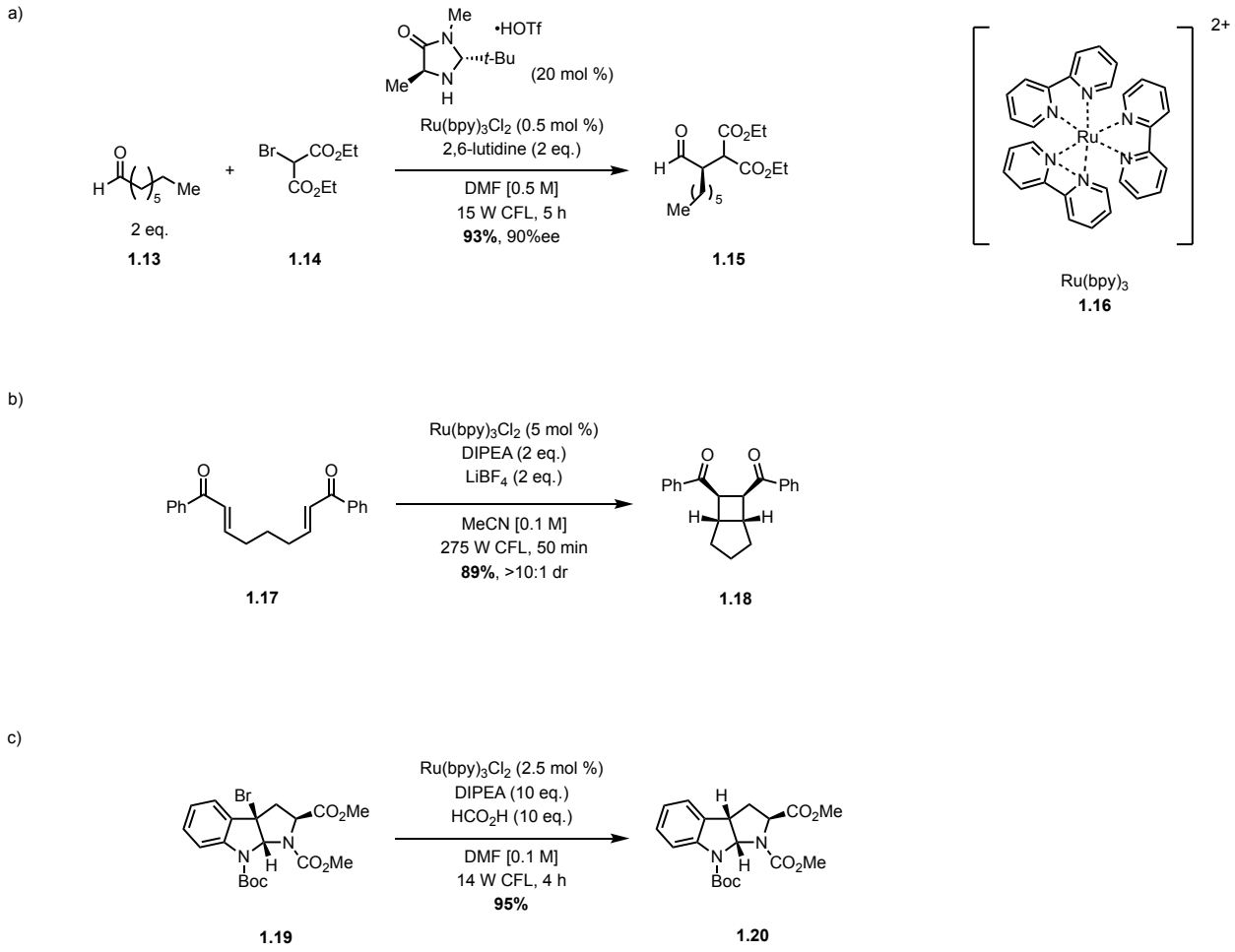


Scheme **1.2** – Use of $Ru(bpy)_3Cl_2$ photocatalyst by a) MacMillan, b) Yoon and c) Stephenson.

### 1.2.2.1 Eosin Y

Eosin Y, a tetrabromo derivative of fluorescein, is an organic dye often used as a histologic stain.[27] In organic chemistry, it is used as a greener, less toxic, and much less expensive photocatalyst alternative to the ruthenium and iridium-based ones. It absorbs green light and upon excitation, it undergoes rapid intersystem crossing to the lowest energy triplet state.[28] Examples such as those from Yadav,[29] Wang,[30] and Zeitler[31] demonstrate the capabilities of Eosin Y as an effective photocatalyst (Scheme **1.3**).

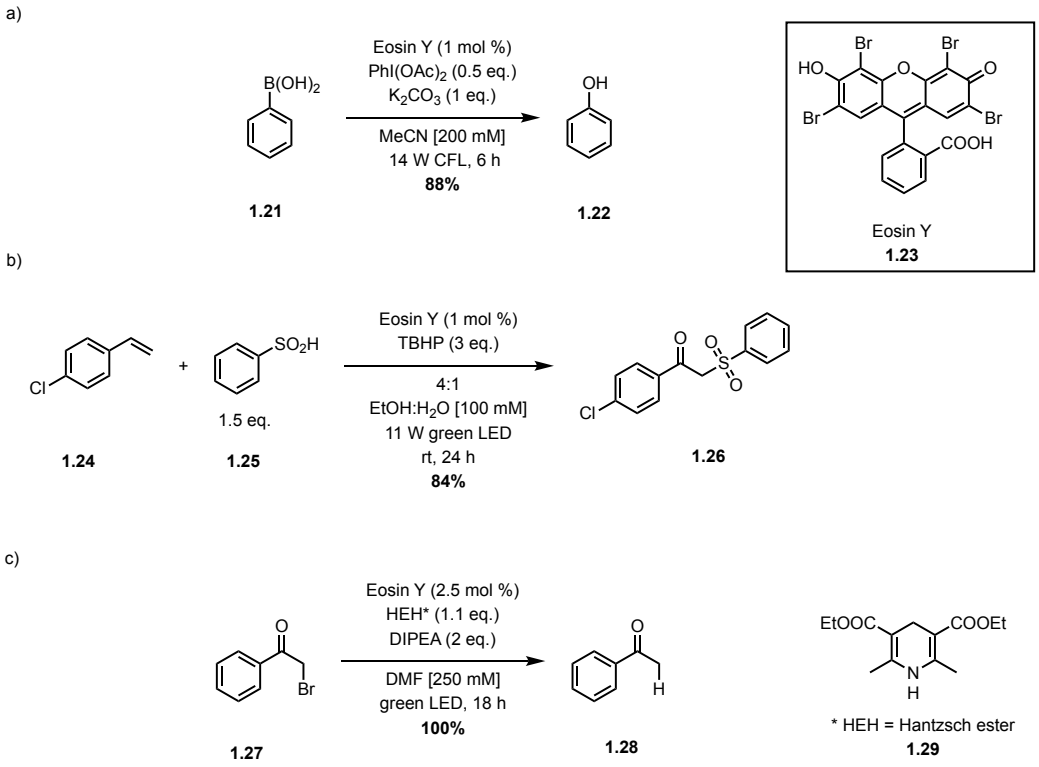


Scheme **1.3** – Use of Eosin Y photocatalyst by a) Yadava, b) Wang and c) Zeitler.

### 1.2.3 PCET and Photochemical Oxidation of Thiols into Disulfides

Other photoredox mechanisms also exist, such as proton-coupled electron transfers (PCETs) in which both an electron and proton are exchanged, often in a concerted elementary step. Since PCETs transfer an electron and proton together, they can function as a non-traditional mechanism for homolytic bond cleavage.[32] Sequential electron transfer (ET) and proton transfer (PT) steps each generate high energy intermediates. The concerted step in a PCET allows to bypass the high energy intermediates to obtain the product of lowest energy directly.[33] PCETs can be reductive or oxidative in nature. In the first case (Figure **1.11a**), the substrate accepts an electron from the photocatalyst and a proton from an acid. In the opposite case (Figure **1.11b**), a base takes a proton from the substrate as the photocatalyst takes an electron from the substrate.[31]

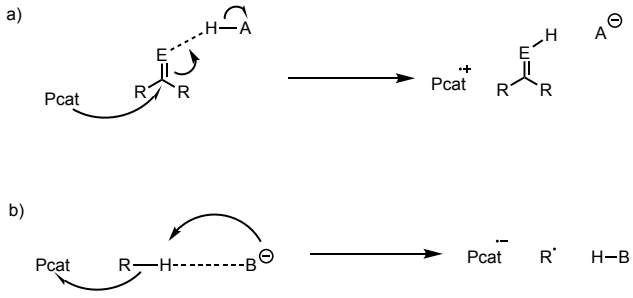


Figure **1.10** – General mechanisms for a) reductive and b) oxidative PCETs.

Researchers have been able to exploit the PCET mechanism for various types of reactions, including work from the Noël group with the aerobic oxidation of thiols into disulfides catalyzed by Eosin Y. The mechanism (Scheme **1.4**) proposes that Eosin Y is promoted to its excited state, and then takes an electron from the thiol substrate as it gives a proton to the TMEDA base in a PCET mechanism. The thiol radical reacts with another thiol radical to form the disulfide, while oxygen acts as the sacrificial electron acceptor to help complete the catalytic cycle.[34]

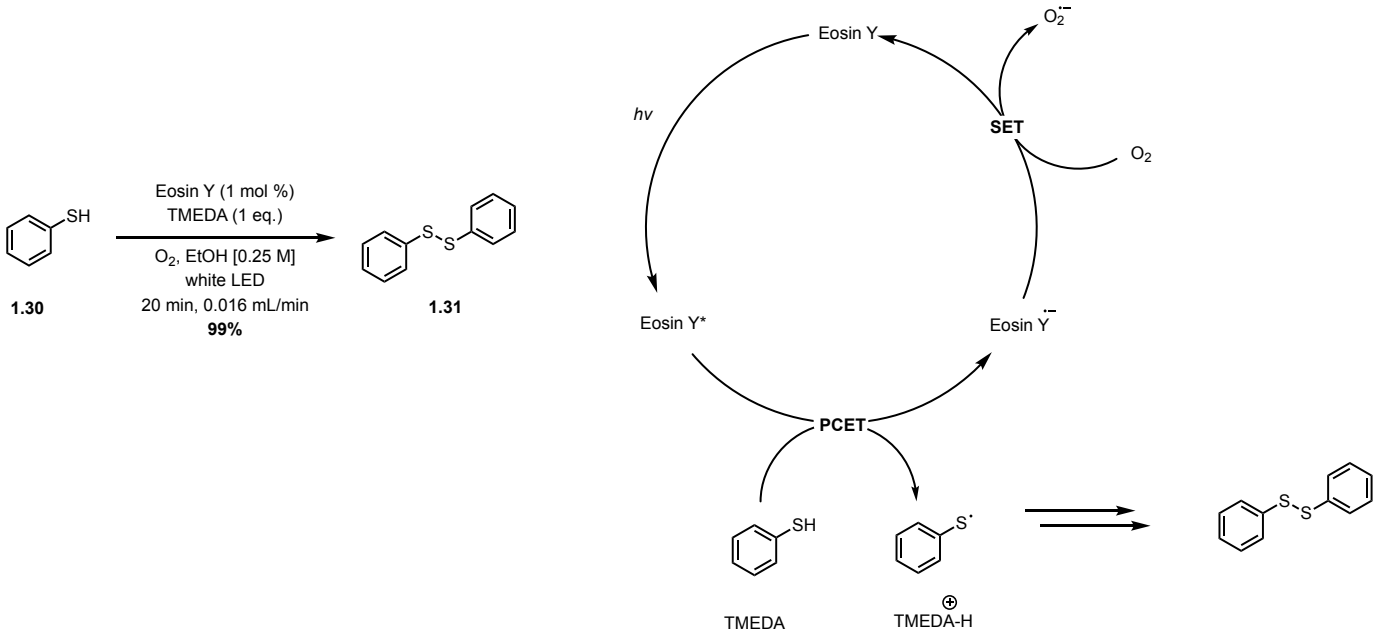


Scheme **1.4** – Aerobic oxidation of thiols to disulfides developed by the Noël group with proposed mechanism.

### 1.2.4 Photochemical Macrocyclizations

There are very few examples of photochemical macrocyclizations done in batch because photochemistry and macrocyclizations have conflicting reaction parameters. As has been discussed earlier, macrocyclizations typically require very low concentrations, or in other words, a large amount of solvent. However, the absorbance *A* of light by the solution respects the Beer-Lambert law $A = -\log T = \varepsilon \ell c$, where $\varepsilon$ is the absorptivity of the attenuating species, $\ell$ is the optical pathlength, and c is the concentration of the solution.[35] The formula implies in part that the longer the pathlength light needs to travel through the solvent, the more it will get absorbed. Light tends to mostly get absorbed in the first millimeter of solution,[36] so attempting to carry out macrocyclization reactions photochemically in large reaction vessels with a large volume of solvent will not be very efficient, since the molecules in the middle of the vessel will not get excited.

The Collins group has developed a successful photochemical macrocyclization reaction in batch through the dimerization of alkynes, aided by a cobalt complex and the organic photocatalyst 4CzIPN, which helps change the oxidation state of the metal throughout the mechanism. The reaction was carried out at a concentration of 10 mM, the solution being irradiated by blue LEDs for 18 hours. The macrocyclic product **1.33** isolated in 91% yield and an *E/Z* ratio of 17:1.[37]

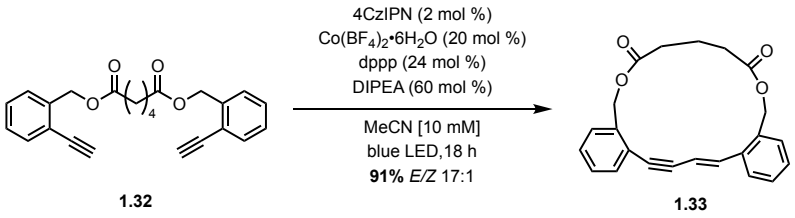


Scheme **1.5** – Photocatalyzed macrocyclization by dimerization of alkynes developed by the Collins group.

Considering examples such as the one seen above, to expand the use of photochemistry and photocatalysis for macrocyclization reactions, other solutions are required to overcome the limitation of carrying out reactions in typical glassware vessels like round-bottom flasks, which

cannot maximize the potential of photochemical setups. Continuous flow chemistry presents a promising avenue for enhancing the efficiency of photochemistry. The technology boasts numerous advantages that are conducive to a wide variety of reactions and conditions, which will be explored in the upcoming chapter.

## 1.3 References


(1) Marsault, E.; Peterson, M. L. Macrocycles Are Great Cycles: Applications, Opportunities, and Challenges of Synthetic Macrocycles in Drug Discovery. *J. Med. Chem.* **2011**, *54* (7), 1961-2004.

(2) Liu, Z.; Nalluri, S. K. M.; Stoddart, J. F. Surveying Macrocyclic Chemistry: From Flexible Crown Ethers to Rigid Cyclophanes. *Chem. Soc. Rev.* **2017**, *46* (9), 2459–2478.

(3) Marsella, M. J.; Swager, T. M. Designing Conducting Polymer-Based Sensors: Selective Ionochromic Response in Crown Ether-Containing Polythiophenes. *J. Am. Chem. Soc.* **1993**, *115* (25), 12214–12215.

(4) Zhao, D.; Moore, J. S. Shape-Persistent Arylene Ethynylene Macrocycles: Syntheses and Supramolecular Chemistry. *Chem. Commun. (Camb.)* **2003**, No. 7, 807–818.

(5) Iyoda, M.; Yamakawa, J.; Rahman, M. J. Conjugated Macrocycles: Concepts and Applications. *Angew. Chem. Int. Ed Engl.* **2011**, *50* (45), 10522–10553.

(6) Allinger, N. L.; Tribble, M. T.; Miller, M. A.; Wertz, D. H. Conformational Analysis. LXIX. Improved Force Field for the Calculation of the Structures and Energies of Hydrocarbons. *J. Am. Chem. Soc.* **1971**, *93* (7), 1637–1648

(7) Illuminati, G.; Mandolini, L. Ring Closure Reactions of Bifunctional Chain Molecules. *Acc. Chem. Res.* **1981**, *14* (4), 95–102.

(8) Osvath, P. A Simple and Inexpensive Device for Slow, Controlled Addition of a Solution to a Reaction Mixture. *J. Chem. Educ.* **1995**, *72* (7), 658.

(9) Haines, D. J.; Swan, C. H.; Green, J. R.; Woodley, J. F. Mucosal Peptide Hydrolase and Brush-Border Marker Enzyme Activities in Three Regions of the Small Intestine of Rats with Experimental Uraemia. *Clin. Sci. (Lond.)* **1990**, *79* (6), 663–668.

(10) Rezai, T.; Bock, J. E.; Zhou, M. V.; Kalyanaraman, C.; Lokey, R. S.; Jacobson, M. P. Conformational Flexibility, Internal Hydrogen Bonding, and Passive Membrane Permeability: Successful in Silico Prediction of the Relative Permeabilities of Cyclic Peptides. *J. Am. Chem. Soc.* **2006**, *128* (43), 14073–14080.

(11) Garcia Jimenez, D.; Poongavanam, V.; Kihlberg, J. Macrocycles in Drug Discovery–Learning from the Past for the Future. *J. Med. Chem.* **2023**, *66* (8), 5377–5396.

(12) Harald, E.; Dietrich, B.; Scharn, P.M.; Bader, D.; Baum, G.; Bergner, A.; Chong, A.; Doebel, E.; Egger, S.; Engelhardt, G.C.; et al. Start Selective and Rigidify: The Discovery Path toward a Next Generation of EGFR Tyrosine Kinase Inhibitors. *J. Med. Chem.* **2019**, *62*, 10272–10293.

(13) William, A. D.; Lee, A. C.-H.; Blanchard, S.; Poulsen, A.; Teo, E. L.; Nagaraj, H.; Tan, E.; Chen, D.; Williams, M.; Sun, E. T.; Goh, K. C.; Ong, W. C.; Goh, S. K.; Hart, S.; Jayaraman, R.; Pasha, M. K.; Ethirajulu, K.; Wood, J. M.; Dymock, B. W. Discovery of the Macrocycle 11-(2-Pyrrolidin-1-Yl-Ethoxy)-14,19-Dioxa-5,7,26-Triaza-Tetracyclo[19.3.1.1(2,6).1(8,12)]Heptacosa-1(25),2(26),3,5,8,10,12(27),16,21,23-Decaene (SB1518), a Potent Janus Kinase 2/Fms-like Tyrosine Kinase-3 (JAK2/FLT3) Inhibitor for the Treatment of Myelofibrosis and Lymphoma. *J. Med. Chem.* **2011**, *54* (13), 4638–4658.

(14) Zaretsky, S.; Yudin, A. K. Recent Advances in the Synthesis of Cyclic Pseudopeptides. *Drug Discov. Today Technol.* **2017**, *26*, 3–10

(15) Li, B.; Li, X.; Han, B.; Chen, Z.; Zhang, X.; He, G.; Chen, G. Construction of Natural-Product-like Cyclophane-Braced Peptide Macrocycles via $Sp^3$ C–H Arylation. *J. Am. Chem. Soc.* **2019**, *141* (23), 9401–9407.

(16) Smolyar, I. V.; Yudin, A. K.; Nenajdenko, V. G. Heteroaryl Rings in Peptide Macrocycles. *Chem. Rev.* **2019**, *119* (17), 10032–10240.

(17) Osberger, T. J.; Rogness, D. C.; Kohrt, J. T.; Stepan, A. F.; White, M. C. Oxidative Diversification of Amino Acids and Peptides by Small-Molecule Iron Catalysis. *Nature* **2016**, *537* (7619), 214–219.

(18) Al-Nuaim, M. A.; Alwasiti, A. A.; Shnain, Z. Y. The Photocatalytic Process in the Treatment of Polluted Water. *Chem. Pap.* **2023**, *77* (2), 677–701.

(19) *The IUPAC Compendium of Chemical Terminology: The Gold Book*; Gold, V., Ed.; International Union of Pure and Applied Chemistry (IUPAC): Research Triangle Park, NC, 2019; p 2259.

(20) Glusac, K. What has light ever done for chemistry?. *Nat. Chem.* **2016**, *8* (8): 734–735.

(21) *A Dictionary of Chemistry*, 6th ed.; Daintith, J., Ed.; Oxford University Press: London, England, 2008; p 108.

(22) Balzani, V.; Ceroni, P.; Juris, A. *Photochemistry and Photophysics: Concepts, Research, Applications*; Wiley-VCH Verlag: Weinheim, Germany, 2014; p 94-96.

(23) Zeitler, K. Photoredox Catalysis with Visible Light. *Angew. Chem. Int. Ed Engl.* **2009**, *48* (52), 9785–9789.

(24) Ischay, M. A.; Anzovino, M. E.; Du, J.; Yoon, T. P. Efficient Visible Light Photocatalysis of [2+2] Enone Cycloadditions. *J. Am. Chem. Soc.* **2008**, *130* (39), 12886–12887.

(25) Nicewicz, D. A.; MacMillan, D. W. C. Merging Photoredox Catalysis with Organocatalysis: The Direct Asymmetric Alkylation of Aldehydes. *Science* **2008**, *322* (5898), 77–80

(26) Narayanam, J. M. R.; Tucker, J. W.; Stephenson, C. R. J. Electron-Transfer Photoredox Catalysis: Development of a Tin-Free Reductive Dehalogenation Reaction. *J. Am. Chem. Soc.* **2009**, *131* (25), 8756–8757.

(27) *Theory and Practice of Histological Techniques*, 4th ed.; Bancroft, J. D., Stevens, A., Eds.; Churchill Livingstone: London, England, 1995; pp 173-186.

(28) Penzkofer, A.; Beidoun, A.; Daiber, M. Intersystem-Crossing and Excited-State Absorption in Eosin Y Solutions Determined by Picosecond Double Pulse Transient Absorption Measurements. *J. Lumin.* **1992**, *51* (6), 297–314.

(29) Paul, A.; Chatterjee, D.; Rajkamal; Halder, T.; Banerjee, S.; Yadav, S. Metal Free Visible Light Photoredox Activation of PhI(OAc)2 for the Conversion of Arylboronic Acids to Phenols. *Tetrahedron Lett.* **2015**, *56* (19), 2496–2499.

(30) Yang, D.; Huang, B.; Wei, W.; Li, J.; Lin, G.; Liu, Y.; Ding, J.; Sun, P.; Wang, H. Visible-Light Initiated Direct Oxysulfonylation of Alkenes with Sulfinic Acids Leading to β-Ketosulfones. *Green Chem.* **2016**, *18* (20), 5630–5634.

(31) Neumann, M.; Füldner, S.; König, B.; Zeitler, K. Metal-Free, Cooperative Asymmetric Organophotoredox Catalysis with Visible Light. *Angew. Chem. Int. Ed Engl.* **2011**, *50* (4), 951–954.

(32) Murray, P. R. D.; Cox, J. H.; Chiappini, N. D.; Roos, C. B.; McLoughlin, E. A.; Hejna, B. G.; Nguyen, S. T.; Ripberger, H. H.; Ganley, J. M.; Tsui, E.; Shin, N. Y.; Koronkiewicz, B.; Qiu, G.;

Knowles, R. R. Photochemical and Electrochemical Applications of Proton-Coupled Electron Transfer in Organic Synthesis. *Chem. Rev.* **2022**, *122* (2), 2017–2291.

(33) Qiu, G.; Knowles, R. R. Understanding Chemoselectivity in Proton-Coupled Electron Transfer: A Kinetic Study of Amide and Thiol Activation. *J. Am. Chem. Soc.* **2019**, *141* (42), 16574–16578.

(34) Talla, A.; Driessen, B.; Straathof, N. J. W.; Milroy, L.-G.; Brunsveld, L.; Hessel, V.; Noël, T. Metal-Free Photocatalytic Aerobic Oxidation of Thiols to Disulfides in Batch and Continuous-Flow. *Adv. Synth. Catal.* **2015**, *357* (10), 2180–2186.

(35) Swinehart, D. F. The Beer-Lambert Law. *J. Chem. Educ.* **1962**, *39* (7), 333.

(36) Su, Y.; Straathof, N. J. W.; Hessel, V.; Noël, T. Photochemical Transformations Accelerated in Continuous-Flow Reactors: Basic Concepts and Applications. *Chemistry* **2014**, *20* (34), 10562–10589

(37) Grenier-Petel, J.-C.; Collins, S. K. Photochemical Cobalt-Catalyzed Hydroalkynylation to Form 1,3-Enynes. *ACS Catal.* **2019**, *9* (4), 3213–3218.

# Chapter 2 – Flow Chemistry and the Hybrid Reactor

## 2.1 Flow Chemistry

### 2.1.1 Basics of Flow Chemistry

Continuous flow refers to chemical reactions pumped in a pipe or through reactors in a continuous manner, as exemplified by the setup by the Jamison group for the synthesis of Ibuprofin (Figure **2.1**),[1] rather than in a traditional batch stirred vessel. For lab-scale purposes, syringes, HPLC systems, or peristaltic pumps drive fluid through reactor coils or microfluidic chips, with the residence time ($t_R$) of the fluid dictated by the total flow rate and reactor volume.[2] Setups are modular and can be adapted for various types of reactions.[1]

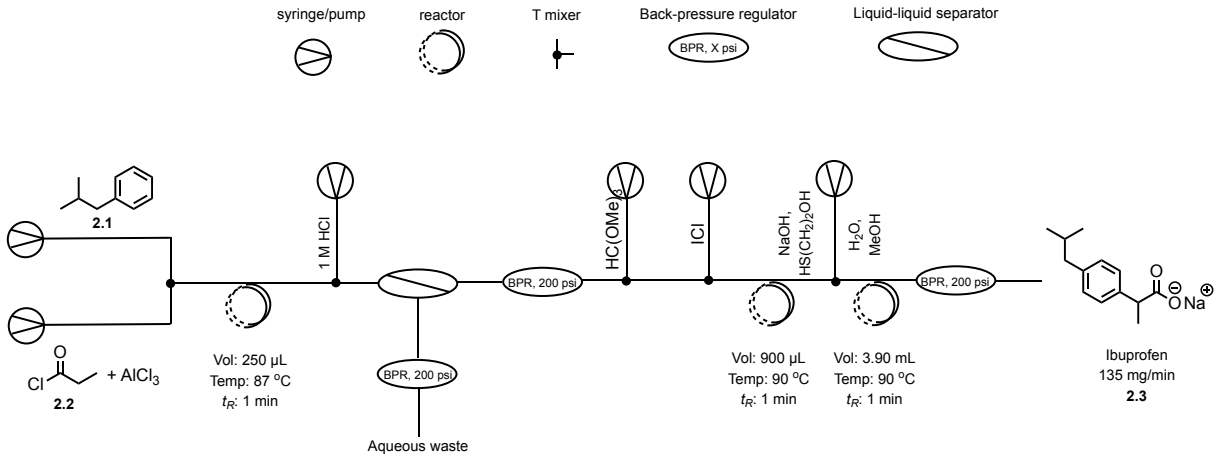


Figure **2.1** – Example of a continuous flow setup designed by the Jamison group for the synthesis of Ibuprofen.[1]

Moving to continuous flow for chemical reactions allows a much greater amount of control and automation that can't be achieved in batch conditions. Continuous flow improves the energy transfer by improving heat or radiation penetration,[3,4] while also improving mass transfer through increased micromixing that improves the homogeneity,[5,6,7] thus increasing the overall efficiency

of a reaction. Continuous flow also provides greater safety for the handling of hazardous species, as well as allowing for immediate consumption of toxic substances, generated *in situ*, thus avoiding any significant build-up of risk-prone compounds.[8] In general, continuous flow systems have enabled reactions for which processing conditions are difficult to control in batch reactors. Multistep continuous flow systems have provided rapid syntheses of active pharmaceutical ingredients (APIs), natural-product intermediates, and effective functional-group transformations.[9]

An example of a reaction taking advantage of the increased control of reaction conditions for better mass and energy transfer from continuous flow is the de Melo group's synthesis of poly(3-hexylthiophene) (**2.7**) by Grignard metathesis polymerization using droplet-based reactors (Scheme **2.1**).[10] A Ni(dppp)$Br_2$ catalyst was generated *in situ* under an argon atmosphere. The use of the droplet-based flow and of perfluorinated polyether as carrier fluid in polytetrafluoroethylene tubing eliminated fouling, a common problem observed in polymerization reactions. Furthermore, full conversion was achieved in less than 1 minute, at 65 $^{o}$C, and an average molecular weight of 44 kg/mol was obtained from the flow synthesis i.e., low molecular weight polymers compared to those attained from the batch synthesis. Batch conditions resulted in a yield of 85% at 75 $^{o}$C and an average molecular weight of 134 kg/mol.

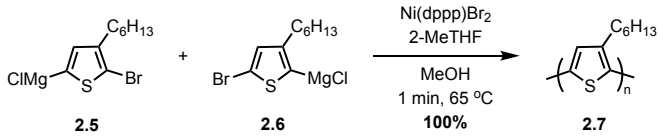


Scheme **2.1** – Synthesis of poly(3-hexylthiophene) using a droplet flow setup.

## 2.1.2 Macrocyclization in Flow Chemistry

A standard type of reactor used generally for flow reactions is the plug-flow reactor (PFR), consisting of thin, small diameter tubing of a defined length (Figure **2.2** top). In the case of photochemistry, transparent tubing can be irradiated much more efficiently than a reaction flask, PFR-based reactors can be effectively exploited in photochemical processes to improve efficiency.

For example, tubing can be coiled around a light source to allow for constant and even irradiation throughout the entire length of the tubing (Figure **2.2** bottom).

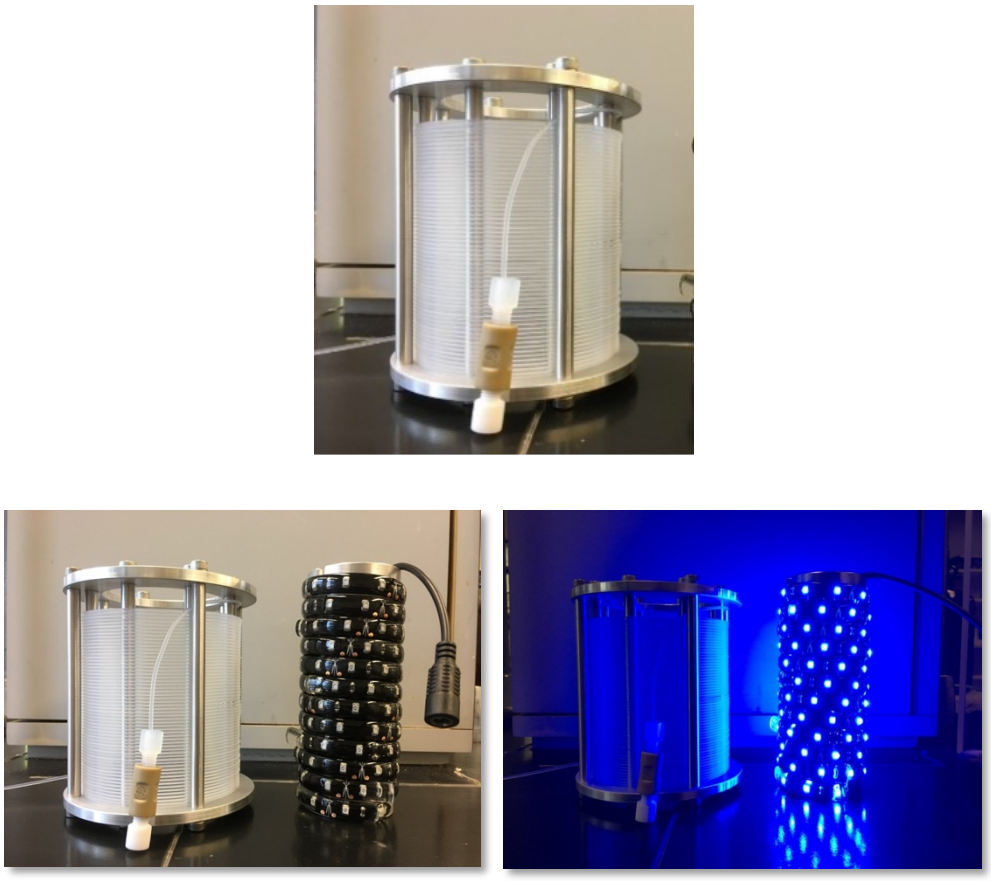

Figure **2.2** – Example of a PFR with a coiled tubing structure (top) and of a PFR used for photochemical reactions developed by the Collins group (bottom).[11] The LED tower goes inside the coiled-tubing structure to irradiate the entire length of the tubing evenly.

Images source: Ph.D thesis by Dr.Émilie Morin[11]

An interest of the Collins group is to combine the advantages provided by photochemistry and flow chemistry and apply them to macrocyclization. The group showed the effectiveness of doing so with the synthesis of a macrocyclic alkynyl sulfide, catalyzed by 4CzIPN and a nickel complex, using blue light emitting diodes (LEDs) (Scheme **2.2**).[12] The original batch conditions of the reaction led to the formation of the desired product **2.11** in a 17% yield after 20 hours of irradiation. On the other hand, when using the PFR reactor, pictured and described above (Figure

**2.2**), a noticeable improvement of the reaction with a yield of 28% after only 2 hours of irradiation was observed.

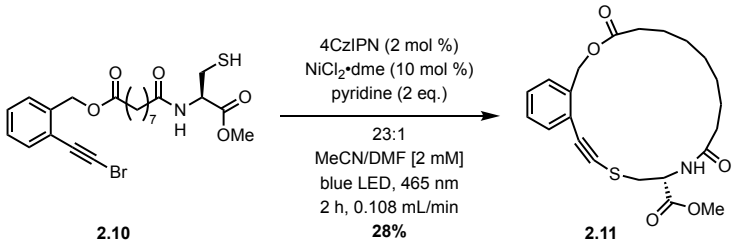


Scheme **2.2** – Synthesis of an alkynyl sulfide macrocycle using continuous flow and photochemical conditions.

Another example of the effectiveness of combining flow chemistry with photochemistry for macrocyclization is in a rare instance of gram-scale macrocyclization, in which the Zhang group used a 200 mL PFR to cyclize one gram of linear polymer **2.11** in a 90% yield and 2 minutes resident time of the reaction mixture using UV light (Scheme **2.3**). The group was able to pump 17.3 L through the reactor in 3 hours thanks to the volume of the reactor and the very high flow rate (100 mL/min).[13]

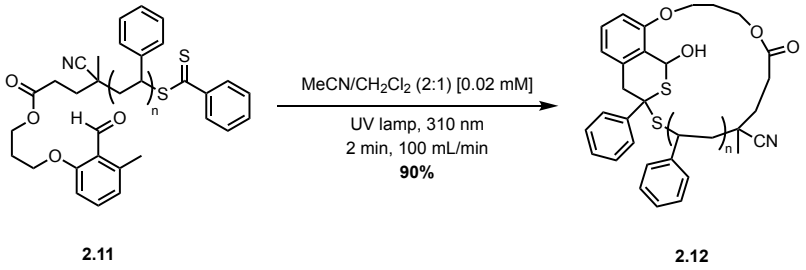


Scheme **2.3** – Gram scale photochemical Diels Alder macrocyclization.

The PFR-based reactor setups may improve the irradiation process, but the need for large quantities of solvent necessary for the high dilution conditions required for macrocyclization remains. Reconciling continuous flow processes and high dilution conditions to make them more efficient for macrocyclization while adhering to green chemistry principles is challenging.

### 2.1.3 Continuously Stirred Tank Reactor (CSTR) Setups

The process of slow addition, where a concentrated solution of substrate is slowly added to another flask containing more solvent and the other reagents, mimicking high dilution conditions, has been discussed earlier. To render the process continuous, a second pump needs to be added to remove solvent from the flask. The exit tube of the second pump can be placed at the meniscus of the solution in the flask (Figure **2.3**). As such, for every drop added, one drop can be pumped out to a receiving flask, maintaining a constant volume in the reaction flask. The process would allow for much less solvent to be used and permit a more efficient scale-up.

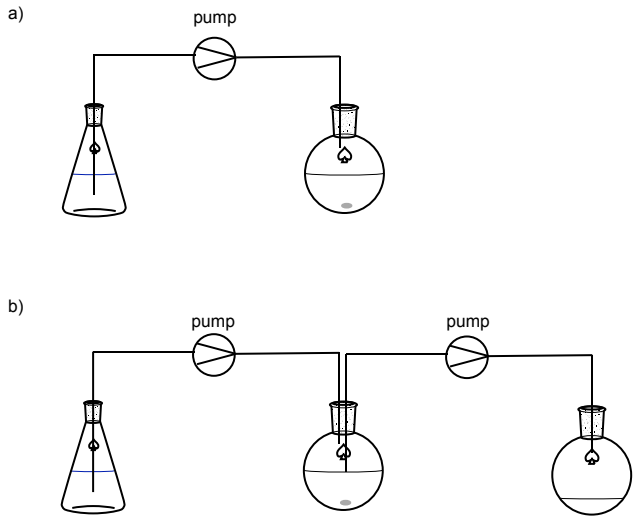


Figure **2.3** – Difference between a) a slow addition setup and b) a CSTR setup.

An example of the utility of CSTRs for thermally promoted macrocyclizations can be found with the Fogg group's successful macrocyclization reaction via olefin metathesis (Scheme **2.4**).[14] They were able to isolate macrocyclic product **2.15** in quantitative yield within 20 minutes. The round bottom flask was heated during the process. The conditions would be less than efficient for use in photocatalysis since it would be problematic to irradiate the round bottom flask effectively. If it were possible to reduce the thickness of the flask to make it as flat (two-dimensional) as possible to mimic small diameter tubing, then light penetration would improve. It would then be possible to combine the advantages of slow addition, continuous flow and photocatalysis all at once in an attempt at improving macrocyclization conditions for a variety of reactions.

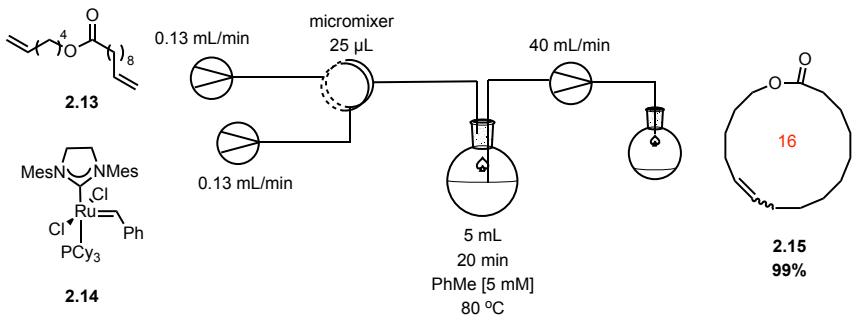


Scheme **2.4** –Macrocyclization via olefin metathesis using a CSTR setup.

## 2.2 The Hybrid Reactor

### 2.2.1 Design of the Reactor

The hybrid reactor designed by the Collins group, most notably by Dr. Émilie Morin, is a solution to the reaction vessel problem discussed earlier. The reactor has 10 cm x 5 cm x 0.8 cm dimensions, for a total volume of 40 mL (Figure **2.4**). A Teflon insert is sandwiched between two glass plates, each 3 mm thick, that make up the two faces of the reactor. The glass and Teflon insert are held together by two metal frames tightly screwed together. The Teflon insert is perforated at different points along its lateral faces: one hole on the top left for the input of the reaction mixture, one on the top right to evacuate excess gas, one at the top of the right side as the output where the solution is pumped out, and 5 on the bottom to bubble gas into the reactor (Figure **2.5**). There is a wall carved in the Teflon insert, which is there to increase the residence time of the substrate, forcing the molecules to travel under the wall before being pump out at the exit, giving them more time to mix efficiently. The Teflon insert, including the wall, is lined with silicon joints to ensure proper sealing. The metal frames are drilled and threaded, and like the Teflon insert, have carved grooves lined with silicon joints to ensure proper sealing as well (Figure **2.6**). Once assembled, the unit is covered by two plates covered in LED stripes purchased from *Creatives Lighting Solution* (Figure **2.7**) which allows for even irradiation throughout the entire reaction mixture volume.

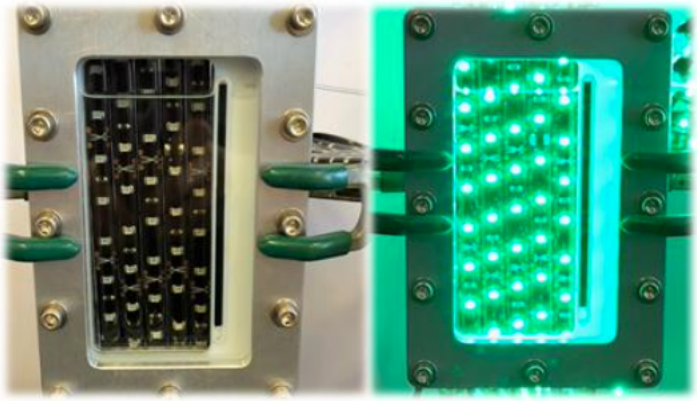

Figure **2.4** – The Collins group hybrid reactor for photochemical macrocyclizations.

Image source: Ph.D thesis by Dr.Émilie Morin[11]

Figure **2.5** – The Teflon insert serving as the centre of the reactor.

Images source: Ph.D thesis by Dr.Émilie Morin[11]

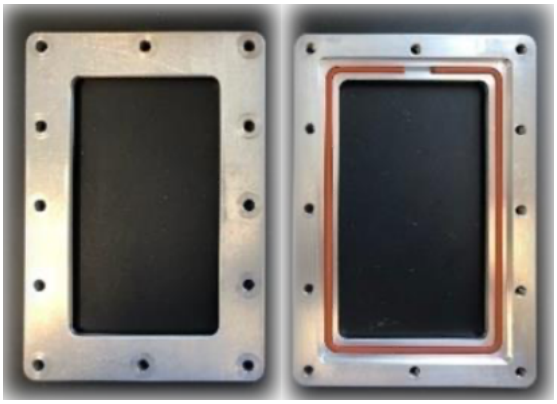

Figure **2.6** – The metal frames of the reactor.

Image source: Ph.D thesis by Dr.Émilie Morin[11]

Figure **2.7** – The LED plates that cover the reactor.

Image source: Ph.D thesis by Dr.Émilie Morin[11]

Initially, the Teflon insert did not have the 5 bottom holes. Tests with Eosin Y showed poor mixing leading to a heterogenous solution (Figure **2.8**). The holes were added so that gas, inert or otherwise, could be bubbled in and act as a mechanical mixer, and/or as a reagent if necessary. The gas bubbling strategy proved to be successful for mixing and further tests with the dye showed proper mixing and a homogeneous solution.

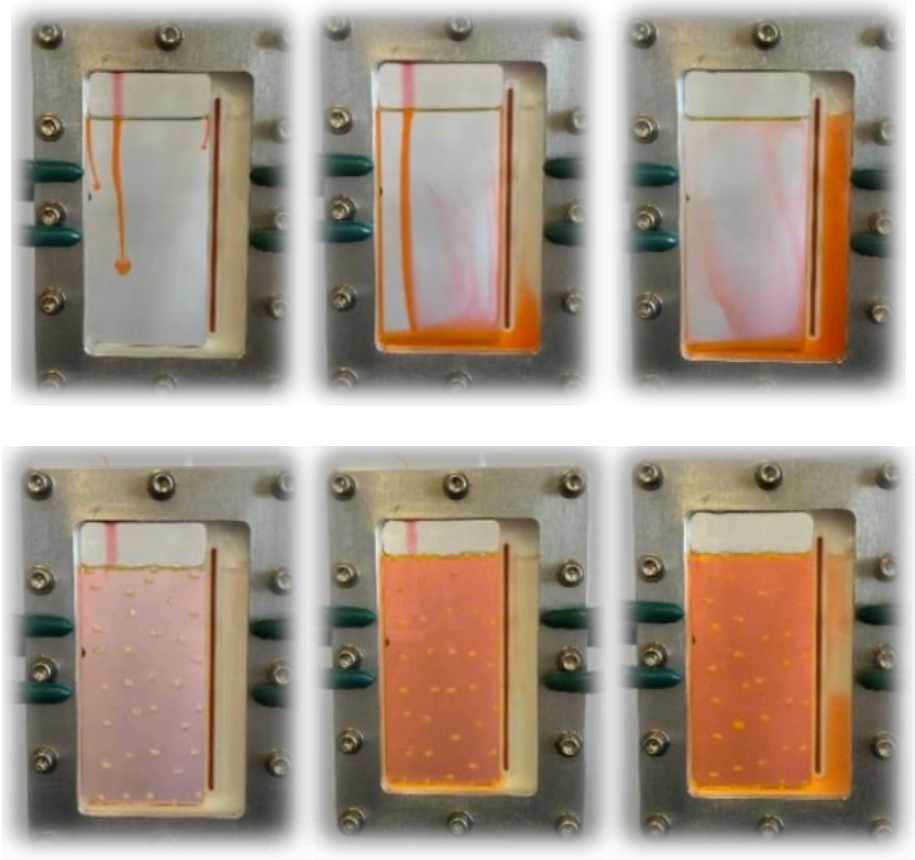

Figure **2.8** – Mixing of Eosin Y without (top) and with (bottom) bubbling of oxygen.

Images source: Ph.D thesis by Dr.Émilie Morin[11]

The reactor is the centerpiece of a modular setup for photochemical macrocyclization (Figure **2.9**). Moving from left to right in the figure, a *KD Scientific* syringe pump is observed delivering the reaction mixture (an injection loop can also be used depending on scale) through the top of the reactor, which is held vertically in place using clamps and bars. The gas enters from the bottom of the reactor and exits from the top right outlet. The reaction mixture exits the reactor through the lateral outlet located on the upper right side, behind the Teflon wall. An LED panel is positioned behind the reactor, and one in front is lifted in the image to view the reactor's content. An *Asia Syrris* pump enables the evacuation of the reactor into a round-bottom collection flask. The collection rate is maintained at 1.25 mL/min, higher than the inlet rate, to prevent any possibility of reactor overflow. Since the reactor volume is maintained throughout the reaction, the set-up can be described as a pseudo CSTR. Through controlled addition the setup mimics

highly diluted conditions, all while allowing efficient irradiation of the solution. The residence time distribution of the hybrid reactor does not resemble those typically observed for CSTR or PFR setups, therefore we refer to the design as a "hybrid" reactor.

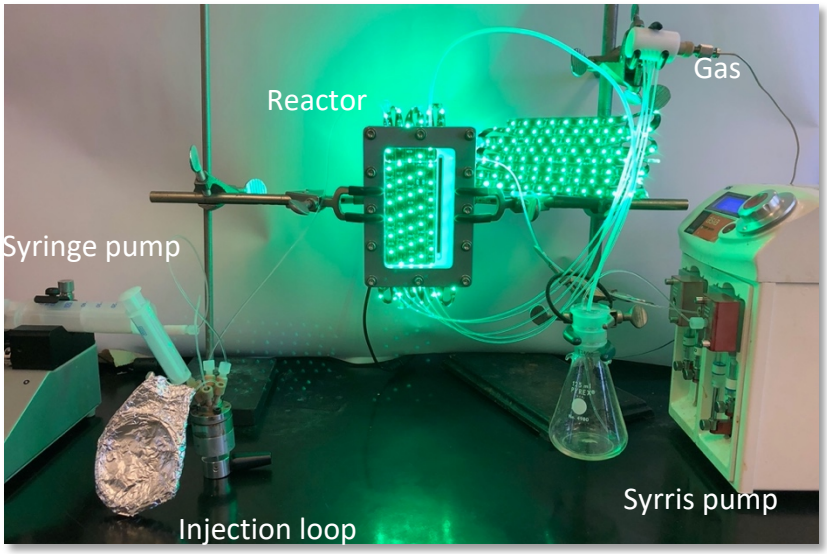


Figure **2.9** – The reaction setup including (from left to right) the syringe pump, an injection loop, the hybrid reactor, a LED plate, a collection vessel, the gas source, and a *Syrris* pump.

Image source: Ph.D thesis by Dr.Émilie Morin[11]

### 2.2.2 Model Reaction, Comparison and Scale-Up

To demonstrate the efficiency of the reactor, a model reaction was chosen, inspired by the work of Noël referenced earlier (Scheme **1.4)** (section 1.2.3).[34, 35] It was chosen for several practical reasons. First, the synthesis of substrates is potentially simplified since the chemical reaction involves thiol dimerization and compounds can be prepared by branching off a central motif. Another motivating factor for choosing the model reaction was the inclusion of disulfide bridges in the final macrocycle, which are a common motif in peptides and proteins and helps contribute to their tertiary structure. The model substrate (**2.18**) used to compare and optimize the reaction conditions was synthesized through a double Fisher esterification of octanediol (**2.16**) with 3-mercaptopropionic acid (**2.17**), catalyzed by *p*-toluenesulfonic acid (Scheme **2.5**).

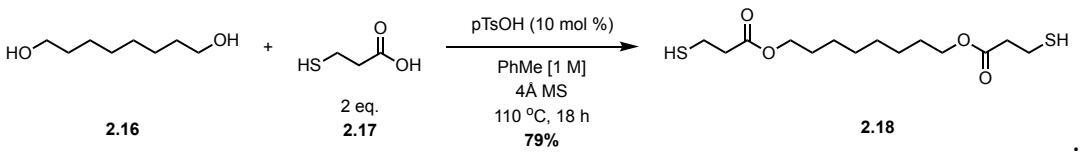


Scheme **2.5** – Synthesis of the model substrate used for macrocyclization.

The model reaction (Scheme **2.6**), the aerobic oxidation of a dithiol into a disulfide catalyzed by Eosin Y, was carried out in a traditional round bottom flask setup, in a PFR, and in a CSTR (Figure **2.10**) to compare the efficiency of each method with that of the hybrid reactor.

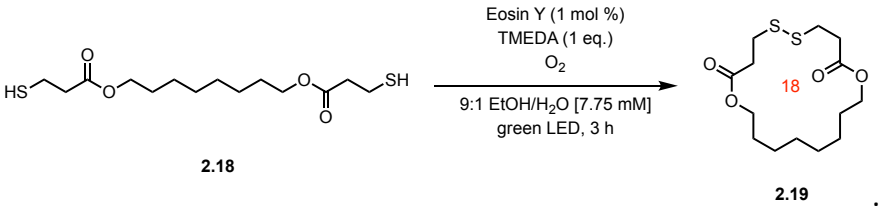


Scheme **2.6** – Macrocyclization to form the disulfide **2.19** via photocatalysis.

The batch setup afforded an 11% yield of **2.19**. The CSTR setup did poorly and gave less than 5% of the desired macrocycle. An improvement was observed with the PFR, but only yielded 17% of 2.19. The 47% yield of the desired macrocycle obtained with the hybrid reactor clearly demonstrated its superior efficiency for the reaction (Table **2.1**).

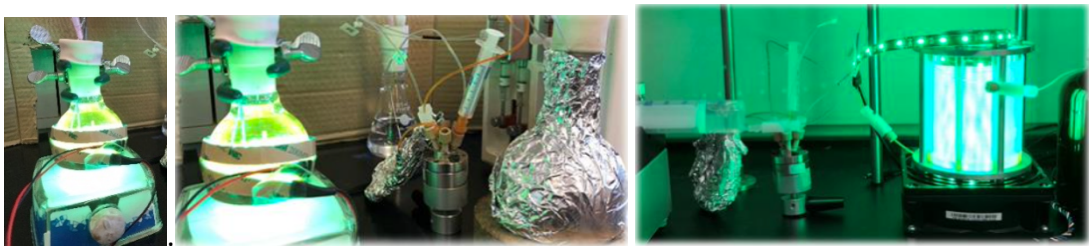

Figure **2.10** – Different setups for model macrocyclization reaction comparisons. From left to right: Traditional batch, CSTR, and PFR

Table **2.1** – Comparison of the efficiency of different reaction setups for the model reaction

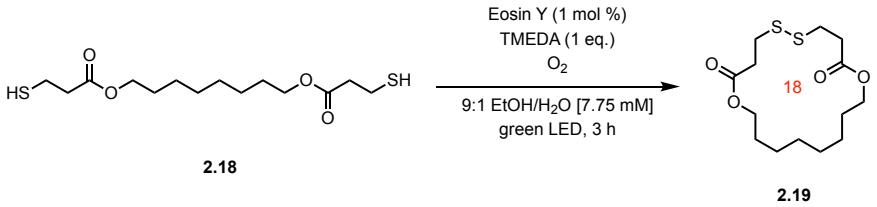


**2.18** **2.19**

All results taken from by Dr.Émilie Morin's Ph.D thesis[11]

| **Setup** | **Yield (%)*** | **RSM (%)*** |
|---|---|---|
| *Hybrid Reactor* | *47* | *0* |
| Batch | 11 | >5 |
| PFR | 17 | 6 |
| CSTR | >5 | 10 |

*$^1$H NMR yield, determined with internal standard 1,4-dimethoxybenzene

Scale up of the model macrocyclization was also investigated with a single reactor (Table **2.2**). Increasing the amount of starting material from 100 mg to 250 mg affected the yield negatively and increasing further to 1 g gave only traces of the product. To remedy the issue, three hybrid reactors were placed in series, increasing the total volume capacity (Figure **2.9**). By using such a strategy, it was possible to conduct a gram scale macrocyclization to afford macrocycle **2.19** with a 48% yield.

Table **2.2** – Scale-up of the model reaction.

All results taken from by Dr.Émilie Morin's Ph.D thesis[11]

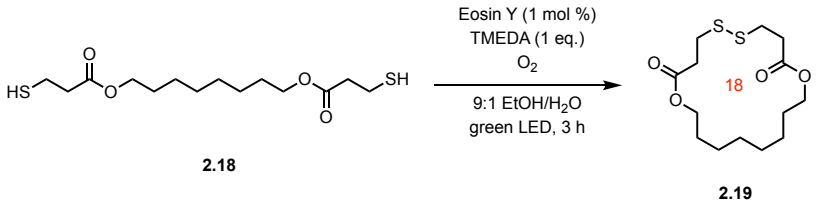


**2.18** **2.19**

| # reactors | Scale (mg) | Yield (%)* |
|---|---|---|
| *1* | *100* | *47* |
| 1 | 250 | 5 |
| 1 | 1000 | traces |
| *3* | *1000* | *48* |

*$^1$H NMR yield, determined with internal standard 1,4-dimethoxybenzene

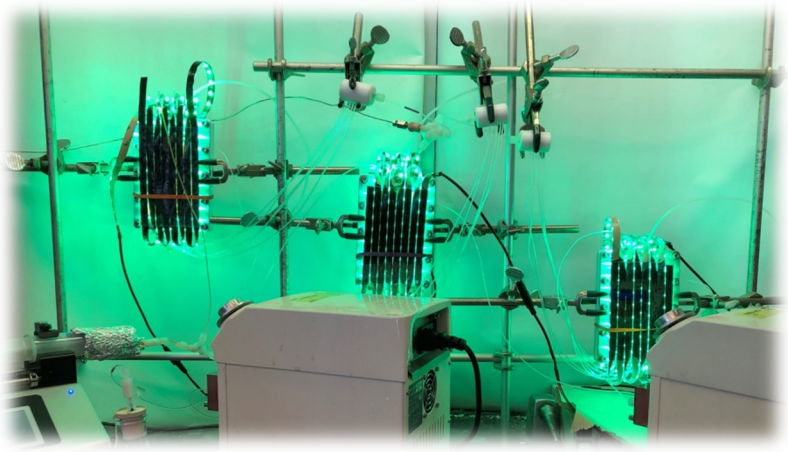

Figure **2.11** – Three reactors place in series with two Syrris pumps

Image source: Ph.D thesis by Dr.Émilie Morin[11]

### 2.2.3 Scope of the Reaction

After demonstrating the power of the reactor, a reaction scope was explored by Dr. Morin, William Neiderer, Corentin Cruché, and Charlotte Cave (Figure **2.12**). Other than the model

macrocycle, the group was able to isolate different macrocycles from various precursors. In general, macrocycles containing aliphatic or polyethylene glycol (PEG) linkers had lower yields (25%-44%) than the more rigid cyclophanes (46%-54%). The exception was **2.23**, with a yield of 52%, which also happened to be the only example used to make a dual macrocycle (**2.24**) through a Glaser-Hay reaction, coupling two alkynyl side chains to complete the second ring.

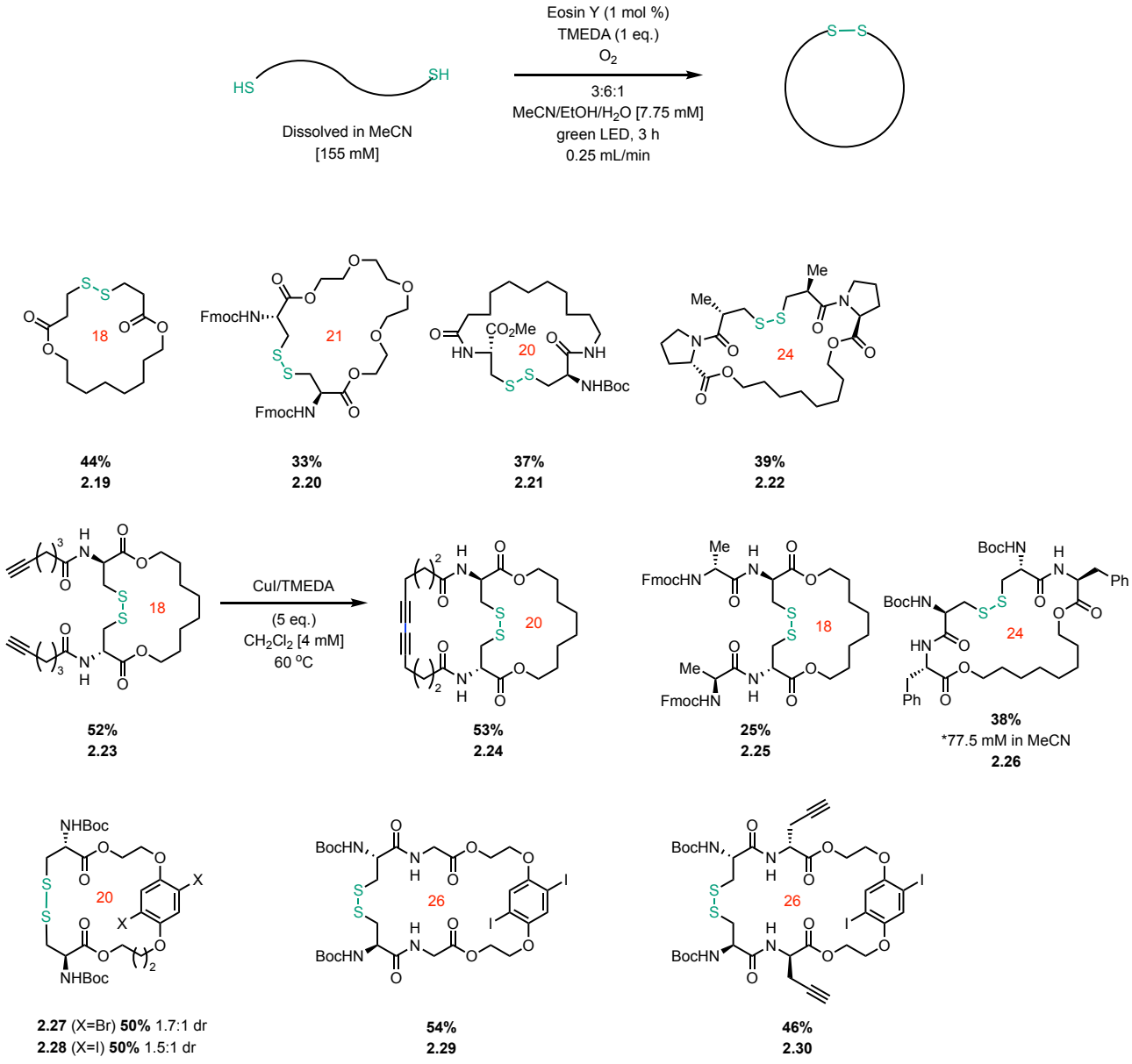


Figure **2.12** – Scope of the reaction achieved by Dr. Émilie Morin, William Neiderer, Corentin Cruché and Charlotte Cave.

The next chapter will be a description and discussion of the attempted synthesis of a new macrocycle to help further the scope that has been achieved by the group so far. Some missing elements of scope will be addressed such as new linker molecules, as well as exploring the cyclization of larger peptides from PEG and haloaromatic linkers.

## 2.3 References


(1) Snead, D. R.; Jamison, T. F. A Three-Minute Synthesis and Purification of Ibuprofen: Pushing the Limits of Continuous-Flow Processing. *Angew. Chem. Int. Ed Engl.* **2015**, *54* (3), 983–987.

(2) Britton, J.; Jamison, T. F. The Assembly and Use of Continuous Flow Systems for Chemical Synthesis. *Nat. Protoc.* **2017**, *12* (11), 2423–2446.

(3) Jähnisch, K.; Hessel, V.; Löwe, H.; Baerns, M. Chemistry in Microstructured Reactors. *Angew. Chem. Int. Ed Engl.* **2004**, *43* (4), 406–446.

(4) Su, Y.; Straathof, N. J. W.; Hessel, V.; Noël, T. Photochemical Transformations Accelerated in Continuous-Flow Reactors: Basic Concepts and Applications. *Chemistry* **2014**, *20* (34), 10562–10589

(5) Sahoo, H. R.; Kralj, J. G.; Jensen, K. F. Multistep continuous-flow microchemical synthesis involving multiple reactions and separations. *Angew. Chem. Weinheim Bergstr. Ger.* **2007**, *119* (30), 5806–5810.

(6) Wörz, O.; Jäckel, K.-P.; Richter, T.; Wolf, A. Microreactors – A New Efficient Tool for Reactor Development. *Chem. Eng. Technol.* **2001**, *24* (2), 138.

(7) Ley, S. V.; Fitzpatrick, D. E.; Ingham, R. J.; Myers, R. M. Organic Synthesis: March of the Machines. *Angew. Chem. Int. Ed Engl.* **2015**, *54* (11), 3449–3464.

(8) Wiles, C.; Watts, P. Continuous Flow Reactors: A Perspective. *Green Chem.* **2012**, *14* (1), 38–54.

(9) Britton, J.; Raston, C. L. Multi-Step Continuous-Flow Synthesis. *Chem. Soc. Rev.* **2017**, *46* (5), 1250–1271.

(10) Bannock, J. H.; Xu, W.; Baïssas, T.; Heeney, M.; de Mello, J. C. Rapid Flow-Based Synthesis of Poly(3-Hexylthiophene) Using 2-Methyltetrahydrofuran as a Bio-Derived Reaction Solvent. *Eur. Polym. J.* **2016**, *80*, 240–246.

(11) Morin, É. Applications de la macrocyclisation par métathèse d'alcènes en flux continu et développement d'un réacteur facilitant la macrocyclisation photochimique. Ph. D. Thesis, University of Montreal, Montreal, CA, 2022; pp 171-206. https://papyrus.bib.umontreal.ca/xmlui/handle/1866/26806?show=full

(12) Santandrea, J.; Minozzi, C.; Cruché, C.; Collins, S. K. Photochemical Dual-Catalytic Synthesis of Alkynyl Sulfides. *Angew. Chem. Int. Ed Engl.* **2017**, *56* (40), 12255–12259.

(13) Sun, P.; Liu, J.; Zhang, Z.; Zhang, K. Scalable Preparation of Cyclic Polymers by the Ring-Closure Method Assisted by the Continuous-Flow Technique. *Polym. Chem.* **2016**, *7* (12), 2239–2244.

(14) Monfette, S.; Eyholzer, M.; Roberge, D. M.; Fogg, D. E. Getting Ring-Closing Metathesis off the Bench: Reaction-Reactor Matching Transforms Metathesis Efficiency in the Assembly of Large Rings. *Chemistry* **2010**, *16* (38), 11720–11725.

# Chapter 3 – Photocatalytic Synthesis of a Macrocyclic Polypeptide

## 3.1 Project Goals

Given the success of the hybrid reactor to form macrocyclic disulfides in the metal-free catalyzed oxidation of thiols, the goal of the project was to expand the scope of the reaction through the synthesis of peptide macrocycles, either by introducing a new linker molecule, to assess the feasibility and potential for improvement of macrocyclic yields, or by preparing more complex peptides, increasing the size of macrocycles already found in the scope, in order to create a greater amount of amino acid residues that mimic biologically active cyclic peptides and pharmaceuticals. The insertion of disulfide bonds into macrocyclic peptides using N-protected cysteines allows for post-cyclization functionalization of cysteine N-terminals, opening more potential avenues for biological activity mimicry. The following chapter will describe two attempted failed syntheses, and one successful synthesis of complex peptide-based macrocycles.

## 3.2 Attempted Synthesis of a Tetrapeptide-Containing Macrocycle Incorporating a BINOL Motif.

Given the interest in atropisomerism in modern drug discovery ,[1] a macrocycle containing an axially chiral element was envisioned. Atropisomerism is a type of stereoisomerism that arises due to hindered rotation around a single bond in a molecule. It occurs when 2 stereoisomers of a compound are conformationally stable because rotation around a single bond is hindered by a bulky group creating a high barrier to rotation. As a result, the 2 stereoisomers, known as atropisomers, can exist as separate entities with different physical and chemical properties.[2]

1,1’-Bi-2-naphthol (BINOL) was picked as the linker molecule (Section 1.1.4) for a tetrapeptide macrocycle to be added to the scope of the aerobic photocatalytic oxidation of thiols into disulfides using the Collins group hybrid reactor (Section 2.2). It was picked because it is an

axially chiral molecule with a high configurational stability and is commercially available as both (*R*)- and (*S*)-BINOL in enantiomerically pure forms. Substituted BINOL derivatives have well-established synthetic chemistry serving as chiral supports for many stereoselective applications, such as metal- and organocatalysis and stereoselective chemosensing.[3,4,5] The BINOL linker, thus, would make a good addition to the variety already used in the scope since it would be the first one used to include, or impose, a certain chirality.

A precursor built around a BINOL coupled to two symmetrical dipeptide arms was envisioned (Figure **3.1**). A first amino acid (red), either alanine or glycine, would connect to both sides of the linker (black), creating a diester. Two *N*-protected cysteines (green) would constitute the ends of the arms, connected through peptide bonds to the first amino acid, and supply the thiol groups to be oxidized in the macrocyclization using the reaction conditions outlined in Chapter 2 (Section 2.2). Alanine or glycine are envisioned as a building block to be used as part of the dipeptide arms to limit the bulkiness of the side-chain group, while also giving the flexibility of either having additional stereocenters or not. Glycine doesn't add a stereocenter to the equation, while alanine is the smallest side-chain group.

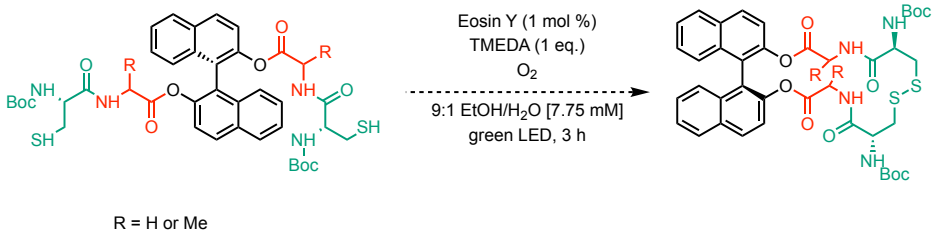


Figure **3.1** – Envisioned tetrapeptide atropisomeric macrocyclic precursor and resulting macrocycle.

Two potential retrosynthetic pathways were considered for exploring the synthesis of the macrocyclic precursor. The first approach involved sequentially and symmetrically adding amino acids to the BINOL linker, constructing the macrocyclic precursor from the BINOL outward (Scheme **3.1**). Macrocyclization would be achieved through the oxidation of thiols, forming a disulfide bond after the removal of the trityl protection group from cysteine. Prior to the deprotection step, the protected cysteine would be coupled to the substrate via peptide coupling

with alanine, which would undergo Fmoc group deprotection after being previously linked to the BINOL linker through an esterification reaction.

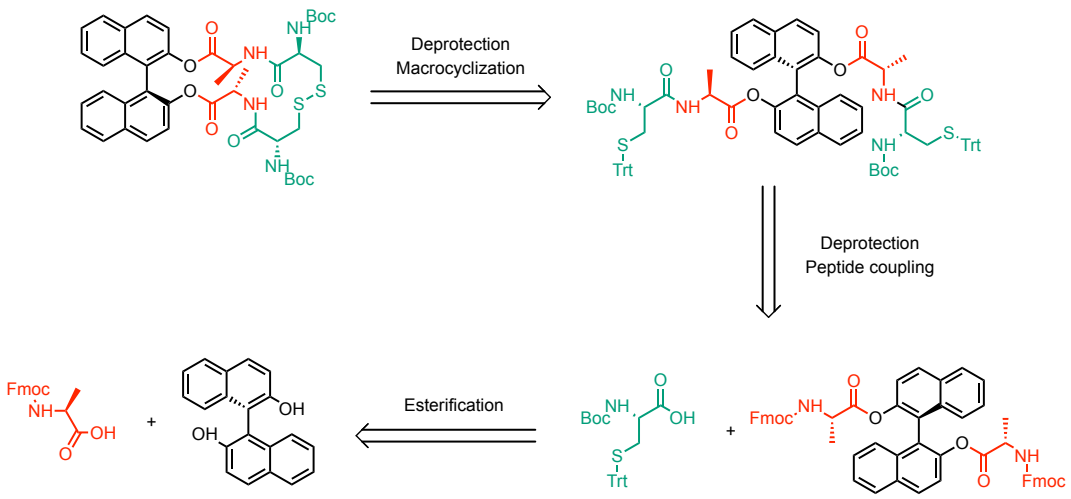


Scheme **3.1** - Linear retrosynthesis of a tetrapeptide macrocycle containing two cysteines and a BINOL linker molecule.

Two equivalents of commercially available Fmoc L-alanine (**3.2**) were coupled to commercially available (*R*)-(+)-BINOL (**3.1**) through a double esterification, using 3 equivalents of DCC and 20 mol % of DMAP, to yield 70% of the desired diester product **3.3** (Scheme **3.2**).

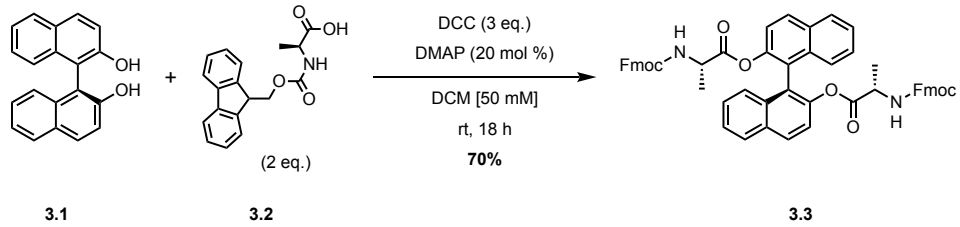


Scheme **3.2** – Coupling of Alanine **3.2** to BINOL **3.1** through an esterification reaction.

Problems occurred during the following Fmoc deprotection step (Scheme **3.3**). TLC analysis of the reaction revealed the presence of the BINOL starting material, suggesting that the reaction conditions may have been sufficiently basic to cause hydrolysis of the ester bonds

between the amino acids and the phenols of the BINOL linker. It is likely that free amines, liberated by the deprotection conditions, were reacting with the ester bonds as well. In either case, the resulting phenolate anions represent good leavings groups for hydrolysis. Formation of the deprotected alanine amide was not observed but could have occurred. Non-peptidic sulfide linkers were not considered since the goal of the project was to build peptide macrocycles and to use cysteines as to have the possibility for future post-functionalization of the macrocycle.

Consequently, efforts were redirected towards the second potential synthesis pathway, which involved the synthesis of a dipeptide that would subsequently be coupled to the BINOL linker.

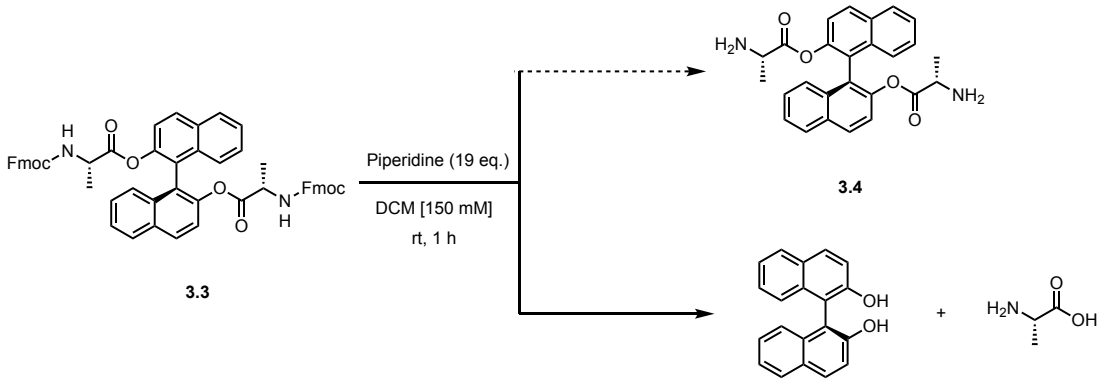


Scheme **3.3** – Attempted Fmoc deprotection of dipeptide **3.3**

The second prospective retrosynthetic pathway (Scheme **3.4**) explores the synthesis of a dipeptide before its coupling with the BINOL linker. A cysteine, protected by N-Boc and S-trityl groups, and alanine are coupled via an amidation reaction. The coupling leaves the carboxyl group of the alanine available for a double-esterification reaction with the BINOL linker. Subsequently, the trityl group is removed from the thiol, paving the way for the completion of the macrocycle through the formation of a disulfide bond.

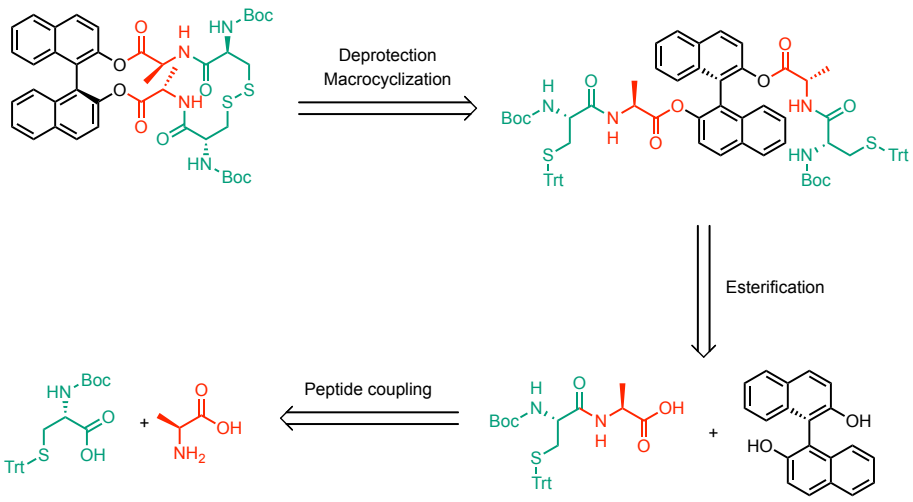


Scheme **3.4** – Alternate retrosynthesis of a tetrapeptide macrocycle containing two cysteines and a BINOL linker molecule.

Peptide coupling between commercially available cysteine **3.5** and glycine was carried out in 2 steps (Scheme **3.5**). The first step involved the activation of the cysteine's carboxyl group using 1.1 equivalent of hydroxysuccinimide (HOSu) and EDC in DMF. After 24 h, 1.2 equivalent of glycine and DIPEA each was added to the reaction mixture and allowed to react for 6 h. Dipeptide **3.6**, as reported in the literature,[6] was obtained with 50% yield over 2 steps. Glycine was used in place of alanine to try and eliminate issues of epimerization and formation of diastereomers in the target precursor. Due to known epimerization issues dealing with cysteine residues,[7] HOBt was used as a coupling reagent in conjunction with EDC during the esterification of the dipeptides to the BINOL linker, because HOBt suppresses the risk of racemization.[8] The approach proved however to be ineffective, and no product was observed. Three equivalents each of DCC and DMAP were then used, and although the mass of the desired product could be observed using mass spectroscopy, 1H NMR analysis revealed epimerization of the cysteine residue. In addition, the desired product could not be isolated from its diastereomer, hindering the synthesis and characterization. It was then decided that the BINOL-based tetrapeptide macrocyclic precursor would be abandoned in favor of a hexapeptide octanediol-based macrocyclic precursor.

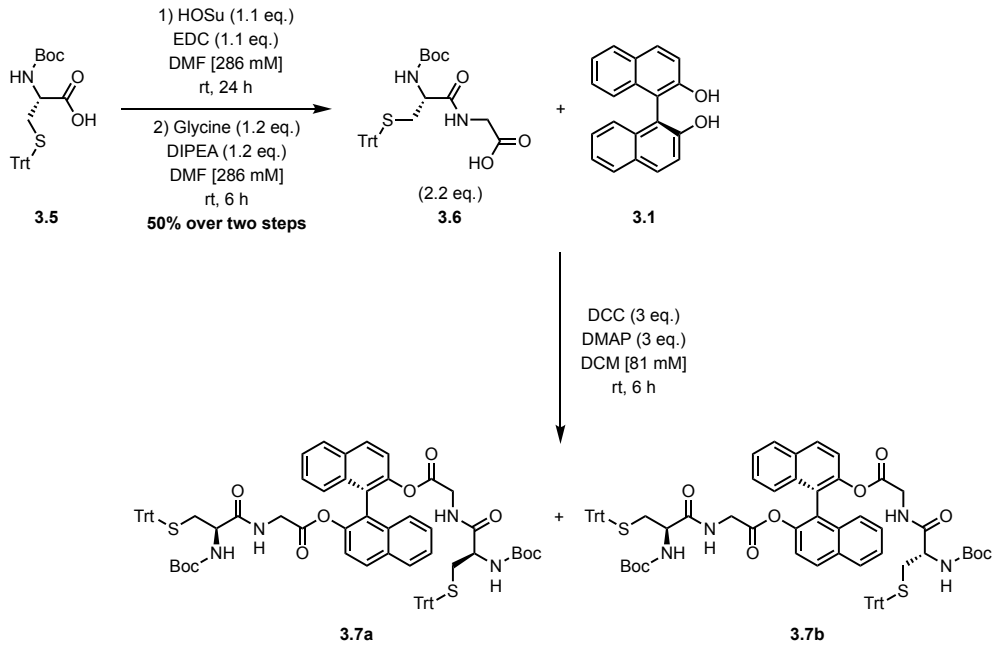


Scheme **3.5** – Attempted synthesis of a tetrapeptide macrocyclic precursor

## 3.3 Attempted Synthesis of a Hexapeptide-Containing Macrocycle Incorporating an Octanediol Motif

Given that our group had already synthesized several tetrapeptide macrocycle examples using the oxidative coupling of thiols in the hybrid reactor, a bigger hexapeptide macrocycle was envisioned as the next challenge. It was decided that the 1,8-octanediol linker molecule, which had been successfully used in the scope to make several tetrapeptide macrocycles, was chosen as the linker for a hexapeptide macrocycle. Using an octanediol linker would give the macrocycle flexibility and an extremely non-polar moiety, though no modeling was attempted to determine the possible conformations of such macrocycles. The first retrosynthetic pathway to be explored (Scheme **3.6**) involved a tripeptide composed of a cysteine residue protected by N-Boc and S-trityl groups, a glycine residue, and an alanine residue, synthesized through two sequential peptide coupling reactions. Two equivalents of the tripeptide would then be coupled to the 1,8-octanediol linker through a double esterification, before the resulting precursor would undergo trityl deprotection and finally macrocyclization.

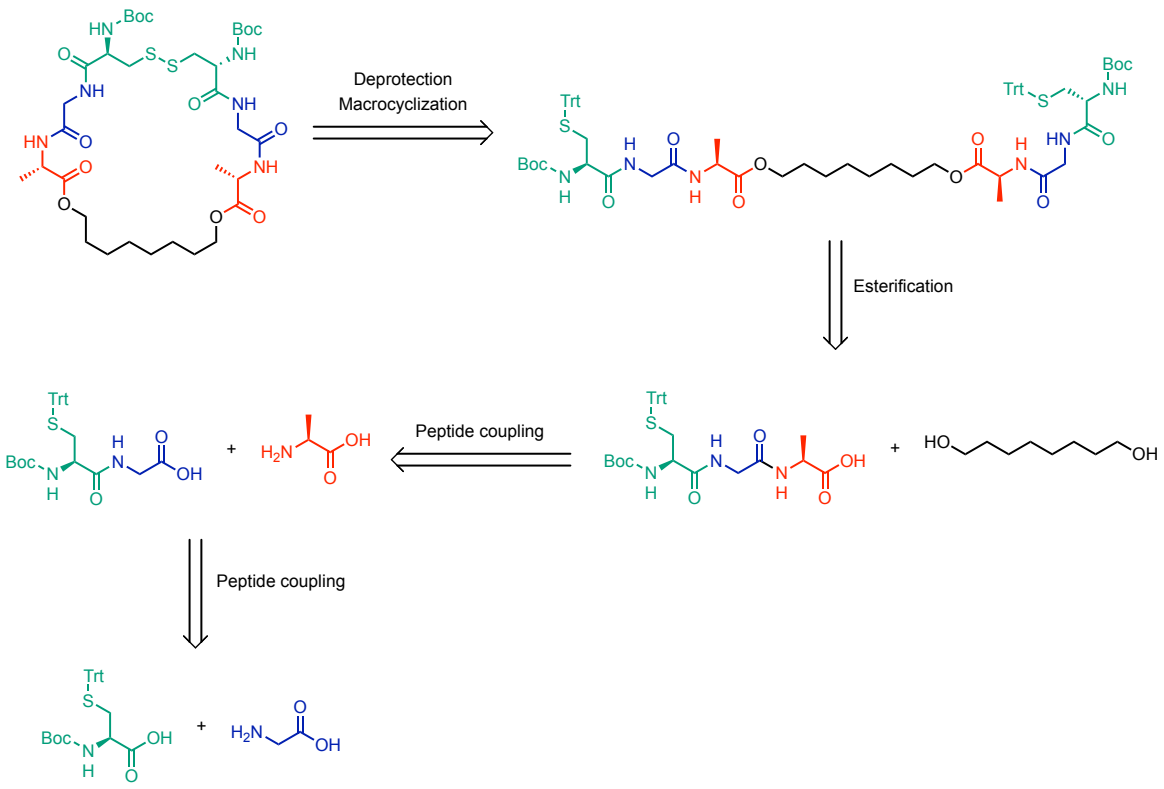


Scheme **3.6** – Linear retrosynthesis of a hexapeptide octanediol-based macrocyclic precursor.

Dipeptide **3.6** was synthesized in the same fashion as earlier, using 1.1 equivalent of hydroxysuccinimide (HOSu) and EDC in DMF. After 24 h, 1.2 equivalent of glycine and DIPEA each was added to the reaction mixture and allowed to react for 6 h. The same procedure was repeated for the addition of commercially available L-alanine to the peptide chain after activation of the carboxylic acid of dipeptide **3.6**, as reported in the literature,[6] using 1.1 equivalent each of HOSu and EDC in DMF. After 24 hours of stirring, 1.2 equivalent each of L-alanine and DIPEA were added to the reaction mixture and left to mix for 6 h. The resulting tripeptide **3.8** (spectral data in Annex 1) was obtained in 25% yield over the two steps (Scheme **3.7**). Further evaluation of the synthetic route suggested that the yields were too low to afford enough material. In addition, the synthesis demanded an excessive quantity of starting materials due to the need for at least two equivalents of the tripeptide for each reaction with one hydroxyl group of the octanediol.

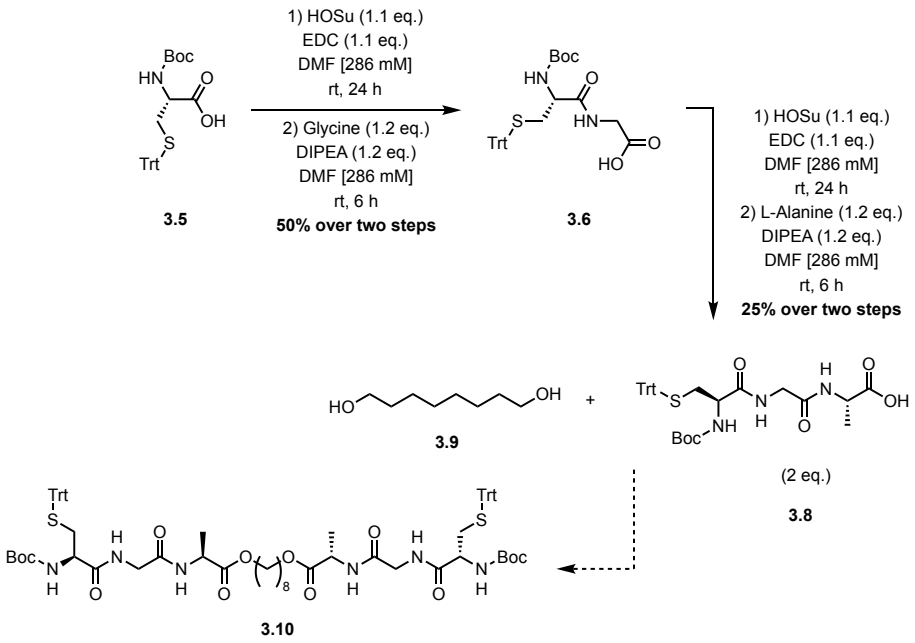


Scheme **3.7** – Attempted synthesis of a hexapeptide macrocyclic precursor through an esterification of two tripeptides and an octanediol.

An alternative retrosynthetic pathway was therefore investigated, aiming to construct the macrocyclic precursor through the peptide coupling of 2 smaller dipeptides. The dipeptides would contain a cysteine residue and be coupled to a previously deprotected alanine residue, which itself would be coupled to the octanediol linker. Following the second peptide coupling, the precursor would undergo trityl deprotection, and the two thiols would be oxidized into a disulfide, resulting in the formation of the desired macrocycle (Scheme **3.8**).

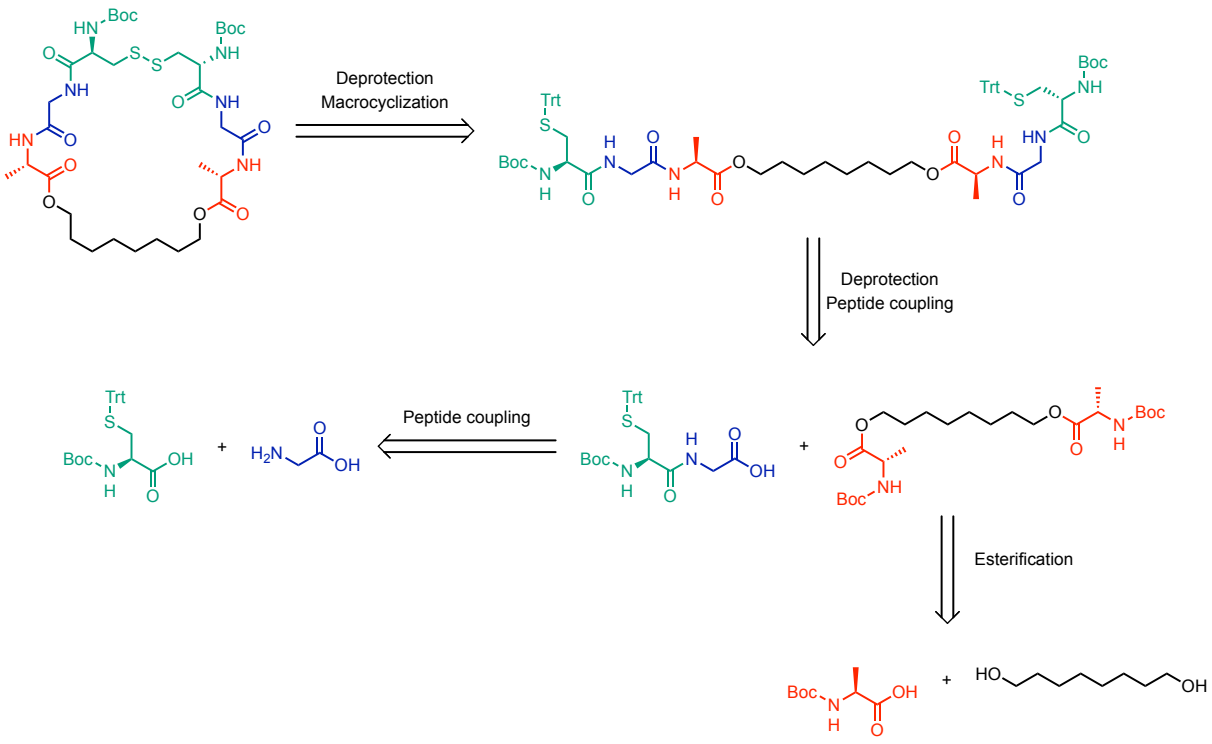


Scheme **3.8**– Alternate retrosynthesis of a hexapeptide octanediol-based macrocyclic precursor.

Alanine **3.11** was coupled to 1,8-octanediol in a double-esterification reaction, after activation of the carboxylic acid by 2.2 equivalents of TBTU and 4 equivalents of DIPEA in DMF, yielding 81% of the desired dipeptide **3.12** (Scheme **3.9**). Purification of the following Boc-deprotection step to obtain the diamine substrate using 4M HCl in dioxane was problematic, as complete deprotection of the product was never observed and the present single-deprotected side-product **3.13** could not be separated from the desired product **3.14a**.

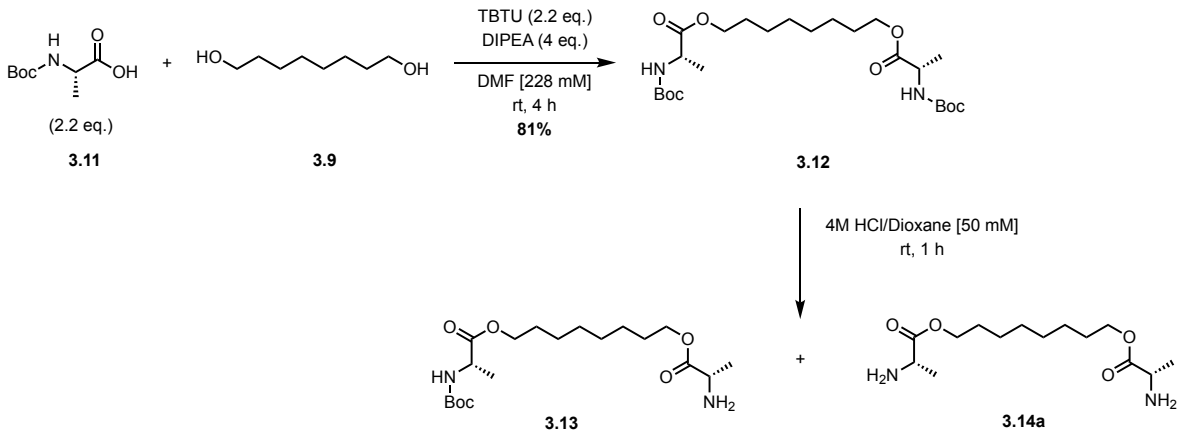


Scheme **3.9** – Attempted synthesis of a diamine dipeptide through a double esterification to an octanediol followed by Boc-deprotection.

A second attempt was made to synthesize the target substrate, utilizing Fmoc-protected alanine **3.15** (Scheme **3.10**). By employing 4 equivalents each of TBTU and DIPEA to activate the carboxyl group of alanine, the desired protected diester product was successfully obtained with a yield of 67%. However, like the previous attempt, isolating the desired deprotected diester proved challenging. This may have been due to acyl migration of alanine during the deprotection, leading to the formation of dipeptide octanol **3.25**, which has the same mass as the desired double-deprotected product, and which could potentially co-elute with the desired product. Since the part of the goal of the project was to simply use a linker molecule already found in the scope, to build larger peptide macrocycles, the 1,8-octanediol linker was abandoned in favor of a more rigid haloaromatic linker molecule, which had been successfully used in the synthesis of a tetrapeptide macrocycle and afforded some of the best yields, in the goal of building a bigger hexapeptide macrocycle.

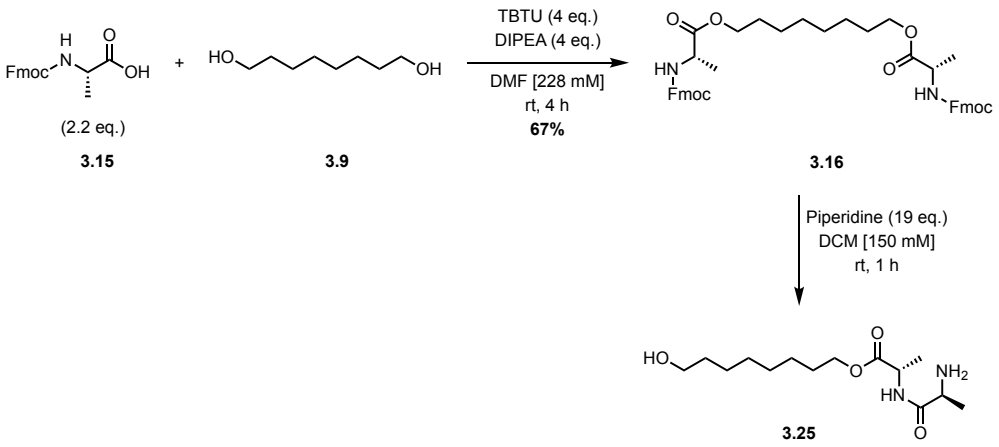


Scheme **3.10** – Attempted synthesis of a diamine dipeptide through a double esterification to an octanediol followed by Fmoc-deprotection.

## 3.4 Synthesis of a Hexapeptide-Containing Macrocycle Incorporating a Haloaromatic Motif

Dr. Émilie Morin, Charlotte Cave, and William Neiderer from our group had reported successful synthesis of peptides when employing a dihalogenated phenyl ring linker, so the previous objective of synthesizing a hexapeptide macrocycle was altered slightly to contain a haloaromatic core rather than an octanediol one. Since the flexibility of the octanediol linker seemed to hinder the synthesis of the hexapeptide macrocycle, the haloaromatic linker was chosen in part for its rigidity. The bromo and iodo haloaromatic linkers used in the scope gave some of the best yields, so the hopes were that similar or better results would ensue with an increased number of peptides, due to increased intramolecular hydrogen bonding. A similar retrosynthetic strategy as for the previously attempted precursor was adopted, in which Boc-alanine would be coupled to the linker and deprotected, after which the resulting substrate would be coupled to a cysteine-glycine dipeptide (Scheme **3.11**).

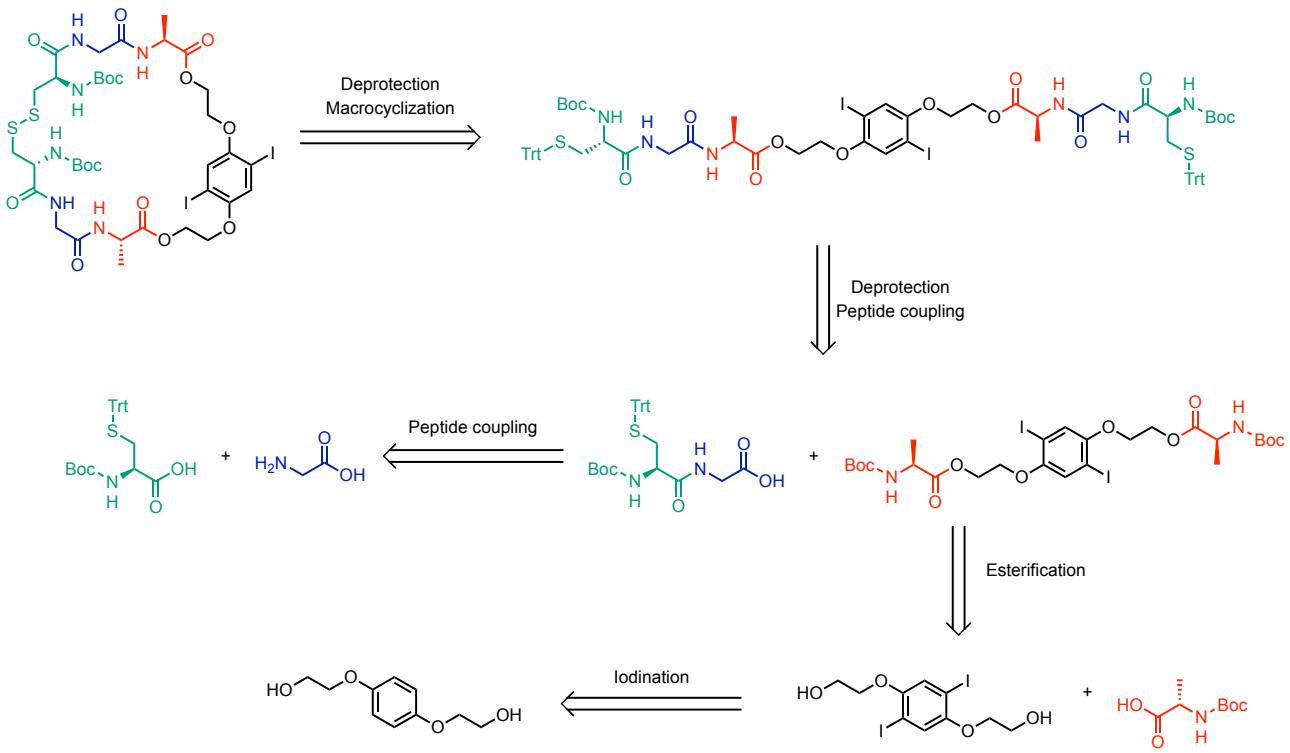


Scheme **3.11** – Retrosynthesis of a hexapeptide macrocycle containing a haloaromatic motif.

Hydroquinone bis(2-hydroxyethyl) ether was doubly iodinated, with the halogens in para positions from each other, using iodine monochloride in methanol under reflux conditions at 85 °C for 5 hours to afford a 66% yield of product **3.18** (Scheme **3.12**), as reported in the literature.[10] Next, 2.5 equivalents of N-Boc L-alanine were then reacted with the diiodobenzene diol in a double esterification reaction with 3 equivalents each of HOBt and EDC as coupling agents, and 3 equivalents of DIPEA as a base, in DMF, to afford a 58% yield of protected peptide **3.19**. Deprotection was carried out in 4M HCl/dioxane conditions to afford the deprotected dipeptide **3.20** in 83% yield. No epimerization was observed, nor did any singly deprotected side product complicate purification.

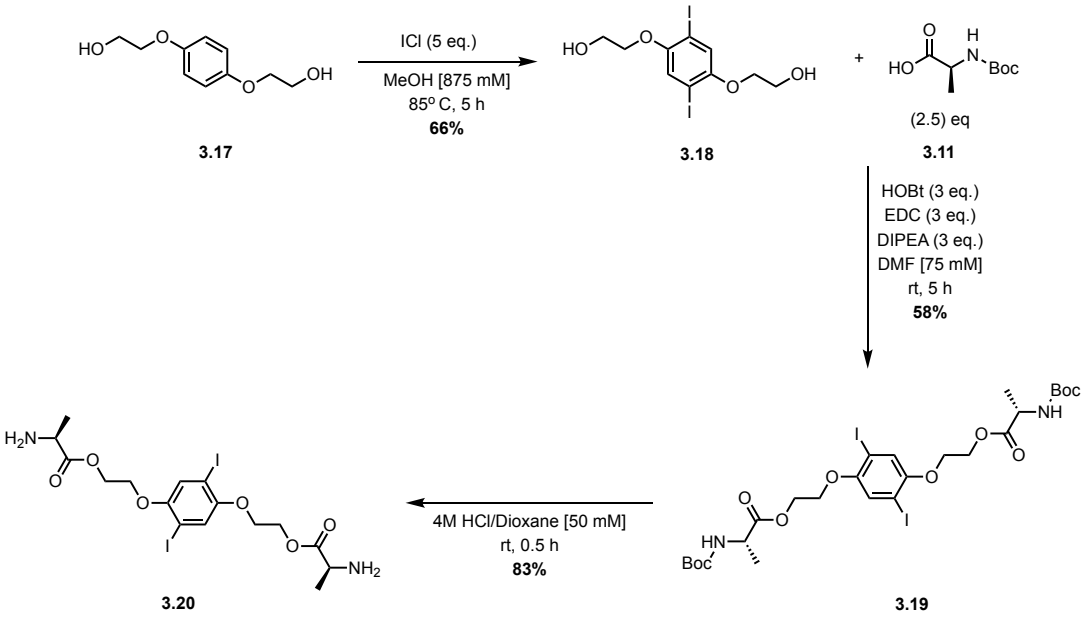


Scheme **3.12** – Synthesis of the haloaromatic core-containing dipeptide substrate.

The cysteine dipeptide **3.6** was activated using 1.1 equivalents each of HOSu and EDC in DMF for 24 hours. Then, 0.42 equivalents of deprotected dipeptide **3.20** were added to the mixture for a double peptide bond coupling to afford the protected hexapeptide precursor **3.22** in 40% yield over two steps. Trityl deprotection was carried out using 9 equivalents of triethyl silane and trifluoroacetic acid (TFA) for one hour in DCM, before quenching the reaction with 19 equivalents of triethylamine ($NEt_3$), affording the deprotected hexapeptide precursor **3.23** in 86% yield.

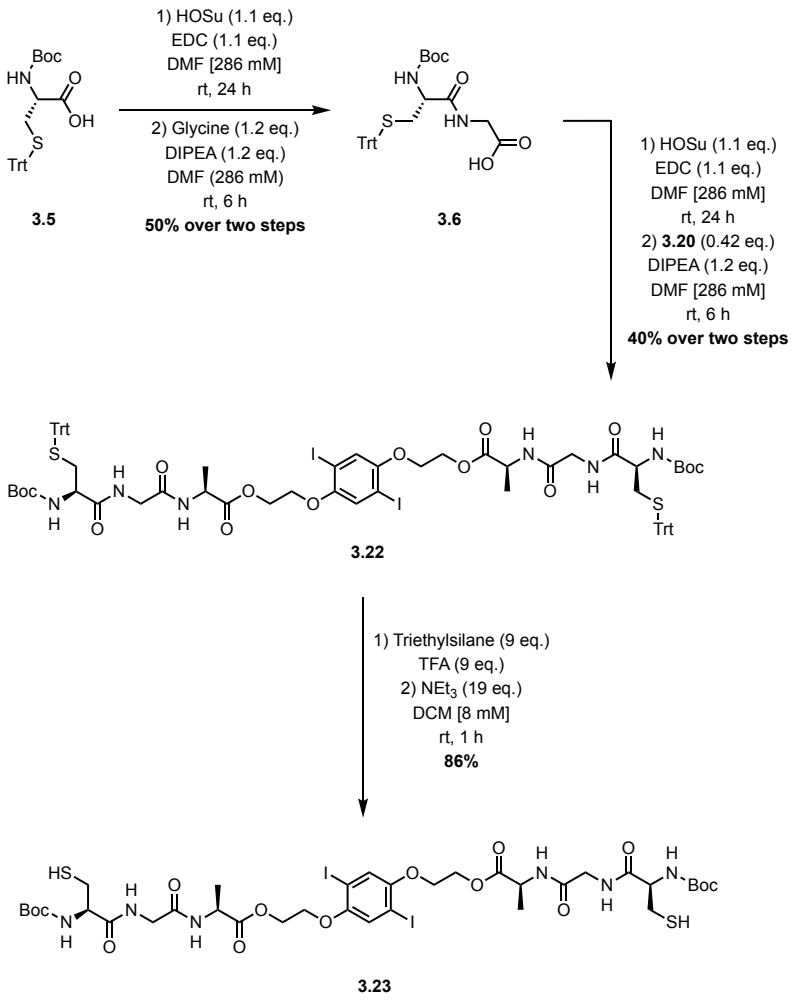


Scheme **3.13** – Synthesis of a hexapeptide haloaromatic macrocyclic precursor.

Finally, the precursor underwent macrocyclization in flow using the hybrid reactor. The macrocycle **3.24** was isolated in 71% (Scheme **3.14**). The cyclization was the highest yielding out of all the molecules investigated in the scope. A comparison can be made with the cyclophane tetrapeptide haloaromatic macrocycles in the scope, which tended to have better yields than the aliphatic or PEG linker macrocycles. The highest yield observed from the tetrapeptide cyclophane macrocycles was 54%. The rigid linker molecule seems to help the precursor assume a conformation suitable for macrocyclization. It is plausible that when adding more amino acids to the precursor, as in the case of the hexapeptide precursor, the number of potential intramolecular hydrogen bonds increases, which in turn increases the precursor's likeliness to favor the cyclization pathway, which could be an explanation for the observed large increase in

yield. It only remains an assumption however, since neither X-ray crystal structure analysis nor detailed conformational analysis by $^{1}H$ NMR were undertaken.

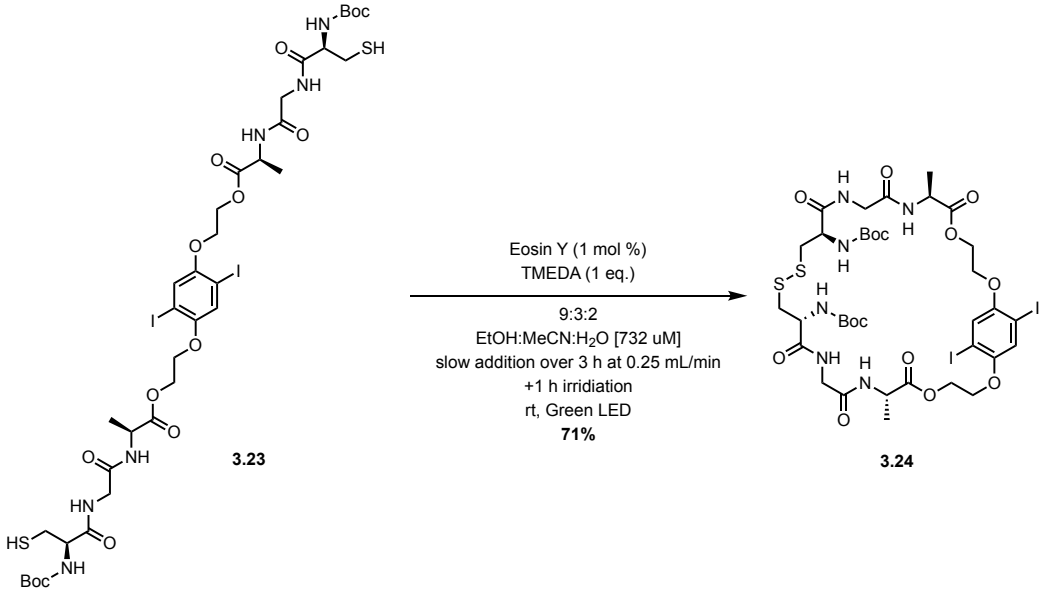


Scheme **3.14** – Synthesis of a hexapeptide haloaromatic macrocycle in flow using the hybrid reactor.

## 3.5 References


(1) Perreault, S.; Chandrasekhar, J.; Patel, L. Atropisomerism in Drug Discovery: A Medicinal Chemistry Perspective Inspired by Atropisomeric Class I PI3K Inhibitors. *Acc. Chem. Res.* **2022**, *55* (18), 2581–2593

(2) Toenjes, S. T.; Gustafson, J. L. Atropisomerism in Medicinal Chemistry: Challenges and Opportunities. *Future Med. Chem.* **2018**, *10* (4), 409–422.

(3) Brunel J M. *Chem. Rev.* **2005** *105* (3), 857-898

(4) Parmar D, Sugiono E, Raja S, Rueping M. *Chem Rev*. **2014**;114:9047–9153

(5) Pu, L. Enantioselective Fluorescent Sensors: A Tale of BINOL. *Acc. Chem. Res.* **2012**, *45* (2), 150–163

(6) Lu, X.; Olsen, S. K.; Capili, A. D.; Cisar, J. S.; Lima, C. D.; Tan, D. S. Designed Semisynthetic Protein Inhibitors of Ub/Ubl E1 Activating Enzymes. *J. Am. Chem. Soc.* **2010**, *132* (6), 1748–1749.

(7) Arbour, C. A.; Kondasinghe, T. D.; Saraha, H. Y.; Vorlicek, T. L.; Stockdill, J. L. Epimerization-Free Access to C-Terminal Cysteine Peptide Acids, Carboxamides, Secondary Amides, and Esters via Complimentary Strategies. *Chem. Sci.* **2018**, *9* (2), 350–355.

(8) Windridge, G. C.; Jorgensen, E. C. 1-Hydroxybenzotriazole as a Racemization-Suppressing Reagent for the Incorporation of Im-Benzyl-L-Histidine into Peptides. *J. Am. Chem. Soc.* **1971**, *93* (23), 6318–6319.

(9) Smith, G. G.; Williams, K. M.; Wonnacott, D. M. *J. Org. Chem.* **1978**, 43, 1-5.

(10) Wariishi, K.; Morishima, S.-I.; Inagaki, Y. A Facile Synthesis of 1,4-Dialkoxy-2,5-Diiodobenzenes: Reaction of Dialkoxybenzenes with Iodine Monochloride in Alcoholic Solvents. *Org. Process Res*. Dev. **2003**, 7 (1), 98–100.

(11) Still, W. C.; Kahn, M.; Mitra, A. Rapid Chromatographic Technique for Preparative Separations with Moderate Resolution. *J. Org. Chem.* **1978**, *43* (14), 2923–2925.

# Chapter 4 – Thiol-Yne Reactions and Alkynyl Sulfides

## 4.1 Thiol-Yne Reactions

### 4.1.1 Generalities and Utility

Thiol-ene and thiol-yne reactions have been known since the turn of the 20th century.[1,2] They involve the reaction between a thiol and an alkene, in the case of thiol-ene reaction, or an alkyne, in the case of thiol-yne reaction, resulting in a thioether or an alkenyl sulfide product respectively (Figure **4.1**). They are considered "click" reactions, defined as "a reaction that must be modular, wide in scope, give very high yields, generate only inoffensive byproducts that can be removed by nonchromatographic methods, and be stereospecific (but not necessarily enantioselective), due to their often-high yields, chemoselectivity, high rates, and thermodynamic driving forces".[3,4] The two reactions are very similar, but the focus of the present work will mainly be on thiol-yne reactions. Similarities of thiol-ene and thiol-yne are: 1) alkene or alkyne reactivity under radical-mediated conditions varies depending on the electronic nature of the unsaturation, 2) side reactions can happen with unsaturations that are electron deficient, 3) terminal alkenes or alkynes are much more reactive than internal ones, with anti-Markovnikov products favored, and 4) thiol-ene or thiol-yne reactions with electron-deficient bonds are best performed using catalyzed Michael-addition conditions.[5] Thiol-ynes reactions can proceed through radical addition or catalyzed Michael addition pathways.[4]

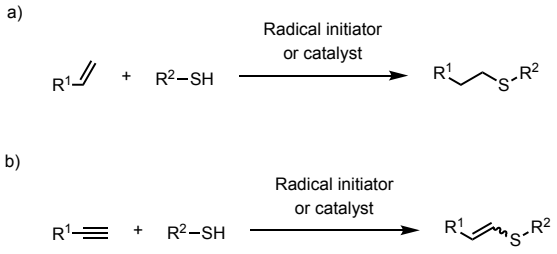


Figure **4.1** – General a) thiol-ene reaction and b) thiol-yne reaction.

An example of a thiol-yne reaction involving a free radical addition is the photocatalytic visible-light-initiated hydrothiolation of alkenes and alkynes in a green solvent by the Li group (Scheme **4.1**).[6] They used $ZnIn_2S_4$ catalyst and methanol as the solvent to couple phenylacetylene and benzyl mercaptan with 94% yield over 15 h. In the absence of either light or $ZnIn_2S_4$, no product was observed, indicating the hydrothiolation was induced by irradiated $ZnIn_2S_4$.

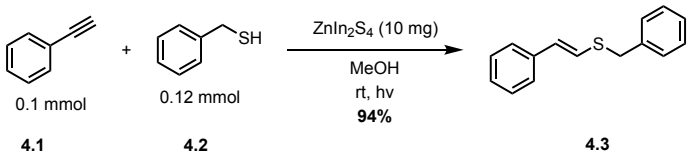


Scheme **4.1** – Photocatalyzed radical addition of octanethiol to phenylacetylene leading to an α-substituted sulfoxide.

An example of a catalyzed Michael addition for thiol-yne reactions is the synthesis of β-substituted propiolates by the Larsen group (Figure **4.2**).[7] The mercaptans are added onto an activated triple bond using *N*-methylmorpholine as the base in dichloromethane in good yields as a mixture of separable *E*-and *Z*-isomers.

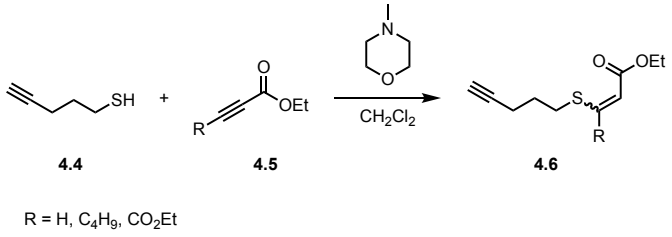


Figure **4.2** – Reaction of 4-pentyn-1-thiol with various β-substituted propiolates

Thiol-yne reactions have been used for the synthesis and modification of macromolecules and polymers.[8] They have provided novel hydrogels and hyperbranched polymers with low dispersity.[9,10] They have been used as biomaterials for synthetic extracellular materials.[11] Polymerization and functionalization using thiol-yne reactions have given high porosity microspheres,[12] access to modified quantum dots,[13] and ways to decorate the surface of carbon rich nanoparticles.[14] The thiol-yne reaction can be used as a "click" strategy for bioconjugation,[15] or to prepare linkages in macrocyclic peptides.[16]

### 4.1.2 Mechanisms

Alkyne hydrothiolation is one of the most atom-economical approaches to produce alkenyl sulfides from thiols and alkynes. Thiol-yne reactions can proceed through different mechanistic pathways, including in the presence of bases, transition metals, or free radicals, and favor an anti-Markovnikov addition.[17] Alkyne and thiol groups are both nucleophilic, so a method must be used to activate either one or both groups for the construction of the vinyl sulfide.

As an example of a base activated thiol-yne reaction, the Oshima group used cesium carbonate in catalytic amounts to synthesize 1-alkenylsulfides (Scheme **4.2**).[18] They were able to isolate vinyl sulfide **4.9** in 87% yield and 10:90 *E/Z* selectivity. The mechanism is proposed to start with deprotonation of the thiol by the carbonate base. Nucleophilic addition of a thiolate anion to an alkyne in an *anti* fashion then yields an alkenyl anion. Subsequently, hydrogen abstraction from a thiol produces the product while regenerating the thiolate anion, propagating the cycle.

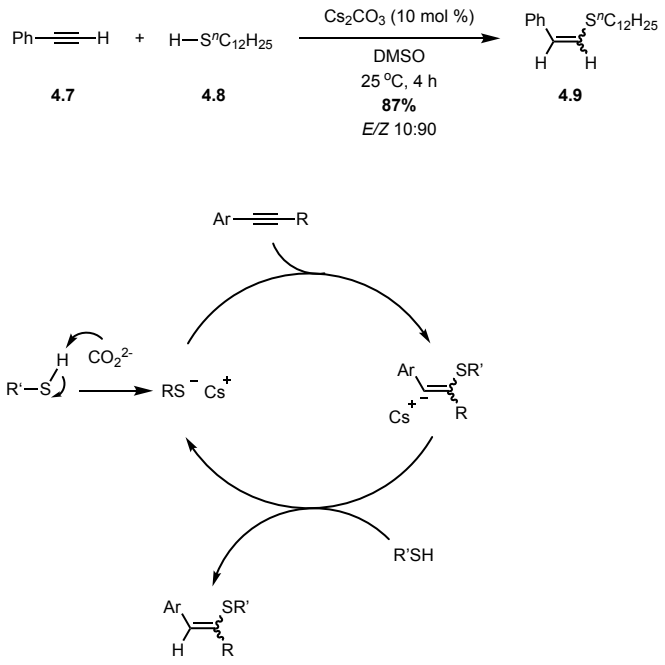


Scheme **4.2** –Hydrothiolation of alkyne initiated by cesium carbonate base.

As an example of a thiol-yne reaction activated by a transition-metal catalyst, the Oshima group demonstrated the palladium-catalyzed *anti*-hydrothiolation of 1-alkynylphosphines (Scheme **4.3**).[19] The reaction was carried out with $Pd(OAc)_2$ catalyst and afforded product **4.12** in 90% yield after one hour. The group suggested a plausible mechanism for the catalytic cycle. A palladium salt first reacts with the 1-alkynylphosphine to generate a palladium(1-alkynylphosphine) complex. A thiol then attacks the triple bond which has become activated by the coordination to form an intermediate which undergoes protonolysis to generate the (*Z*)-isomer product while regenerating the initial palladium species. The stereochemistry of the product suggests that the reaction proceeds via coordination-assisted activation of the triple bond and not oxidative addition of the thiol to a palladium complex followed by thiopalladation or hydropalladation.

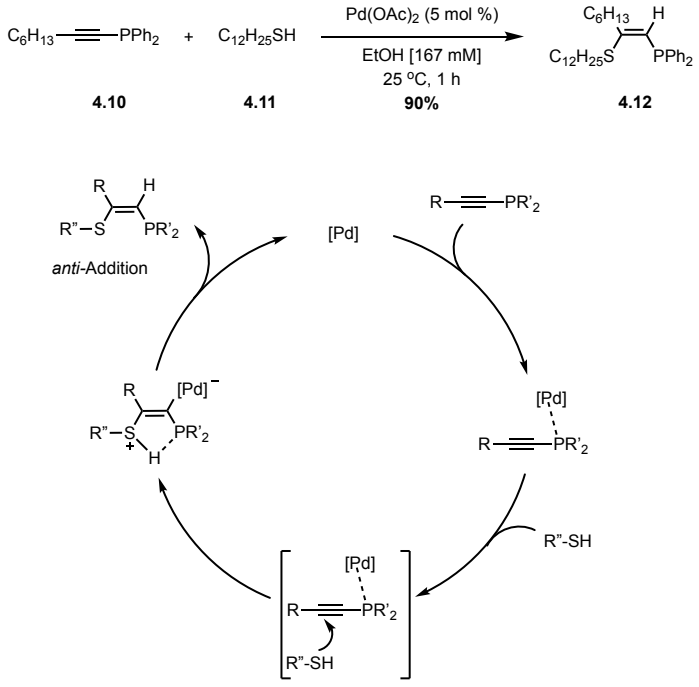


Scheme **4.3** – Palladium-catalyzed hydrothiolation of 1-alkynylphosphines.

As an example of a thiol-yne reaction activated by radical initiation, the Dondoni group demonstrated the photoinduced addition of glycosyl thiols to alkynyl peptides (Scheme **4.4**).[20] They performed propargylation on cysteine **4.13** followed by coupling with glycosyl thiols in a one-pot glycosylation using UV light (365 nm) and 2,2-dimethoxy-2-phenylacetophenone (DPAP)

as a sensitizer to obtain glycosylated product **4.15** in a 53% yield. Radically mediated thiol-yne reactions begin by the radical activation of the thiol using an initiator. The addition of the thiyl radical to an alkyne follows, in a similar fashion to the thiol-ene reaction. The resulting radical then abstracts a hydrogen from another thiol, generating a vinyl sulfide, and propagating another thiyl radical. Unlike the thiol-ene reaction, which results in a thioether, the vinyl sulfide can go through a second thyil radical addition. After the second addition, each alkyne functional group has combined with two thiols generating a dithioether.

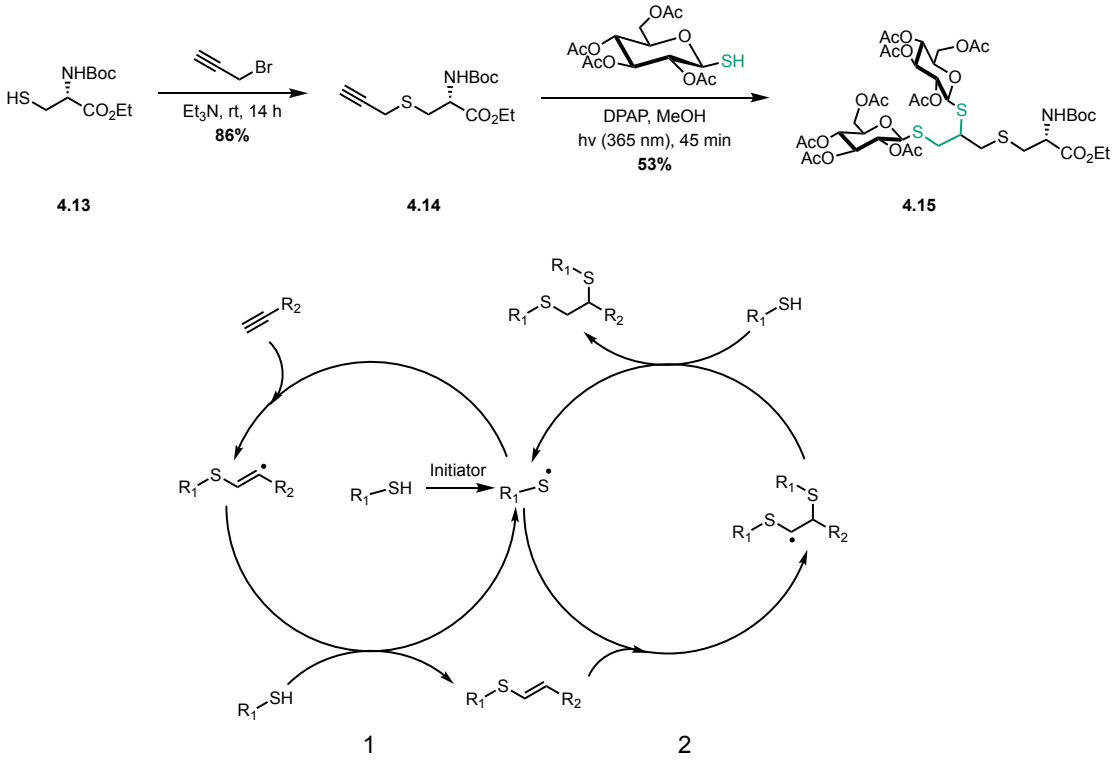


Scheme **4.4** – Radical-mediated thiol-yne chain reaction mechanism. 1) Addition to a terminal alkyne. 2) Subsequent addition to the vinyl sulfide.

### 4.1.3 Use of Visible Light for Thiol-Yne Reactions

Many thiol-yne reactions proceed via a radical pathway.[21] To obtain the anti-Markovnikov products that are generally initiated by thermal or UV-light activation, stoichiometric radical initiators are necessary.[22,23] The disadvantage of such procedures is that they often require either

stoichiometric reagents and/or a specialized UV photochemistry apparatus. The stoichiometric reagents produce stoichiometric waste that can complicate purification of the products.[21] The focus has therefore turned to developing milder and greener methodologies to achieve the "click" reaction. Due to its potential for sustainability, visible-light photoredox catalysis has become an attractive strategy for thiol-yne processes.[21]

As an example of visible light-mediated thiol-yne reaction, the Zhu group demonstrated visible light-mediated thiol-acetylene click macrocyclization (Scheme **4.5**).[5] The group was able to synthesize a large library of macrocycles (up to 35-membered rings) in a dihydrothiolation process, using iridium catalyst **4.16** and blue LEDs in the presence of DIPEA as a base, with yields ranging from 8 to 42%.

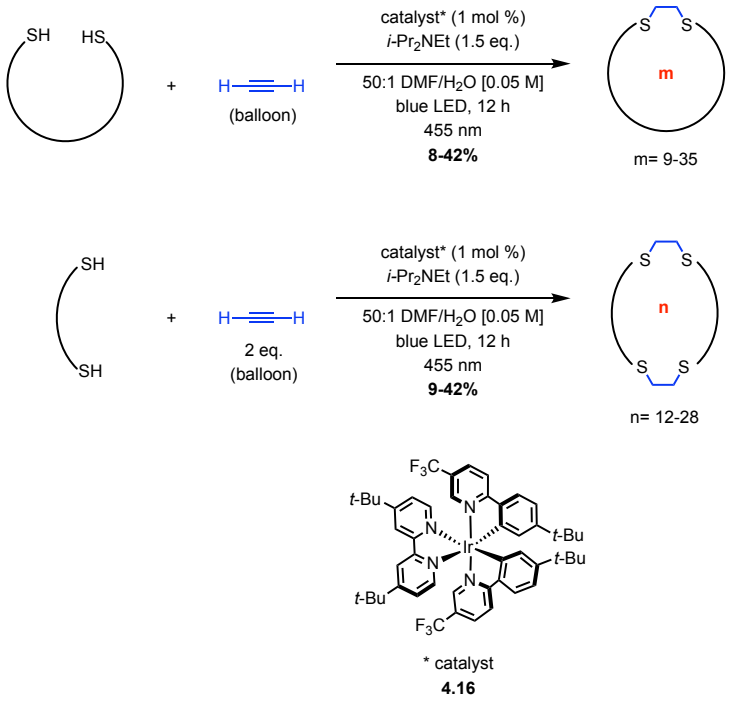


Scheme **4.5** – Thiol-yne dihydrothiolation macrocyclization reaction of dithiol precursors with acetylene using an iridium catalyst.

An example of a thiol-yne reaction using visible light and metal-free photocatalysis is that reported by the Ananikov group (Scheme **4.6**).[24] The group used Eosin Y as a catalyst with

irradiation by green LEDs, and the reaction afforded a variety of vinyl sulfides with yields ranging from 55-91%, with regioselectivity favoring the (*E*)-isomer (25-60:1 *E*/*Z* ratio).

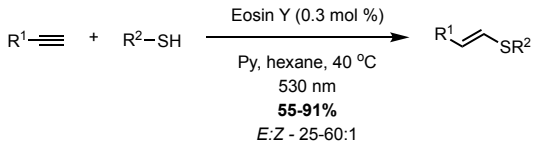


Scheme **4.6** – Metal-free thiol-yne reaction using visible light catalyzed by Eosin Y.

Though the examples above yielded interesting results, both the reactions used terminal alkynes. For the intermolecular process described by Ananikov, the products were isolated with high levels of selectivity.[24] Thiol-yne reactions using internal alkynes would be more challenging, since, in theory, four different vinyl sulfides could be formed, namely the *cis*- and *trans*- isomers of the products resulting of thiyl addition to either carbon. To help control selectivity, one strategy would be to have a substituent of the di-substituted alkyne capable to stabilize reaction intermediates, favoring addition at one carbon of the internal alkyne.

## 4.2 Alkynyl Sulfides

### 4.2.1 Synthesis of Alkynyl Sulfides

Alkynyl sulfides, or thioalkynes, are bench stable compounds containing a polarized triple bond due to conjugation of the heteroatom lone pair into the pi-orbitals of the alkyne. The prominence of sulfur in biomolecules and materials makes alkynyl sulfides attractive as sulfur-containing building blocks.[25] Different strategies can be employed to synthesize thioalkynes. The earliest attempts carried out by Arens consisted of using dehydrohalogenation conditions (Scheme **4.7**).[26] The bromo-vinyl precursor **4.17** was heated with potassium hydroxide in the absence of solvent, generating alkynyl sulfide **4.18** in 57% yield. The reaction was done with KOH and no solvent to prevent unwanted nucleophilic addition to the alkyne.

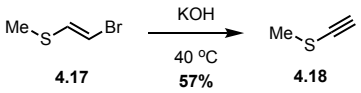


**4.17** **4.18**

Scheme **4.7** – Dehalogenation of a bromo-vinyl precursor to give an alkynyl sulfide.

Later, umpolung strategies were exploited to generate alkynyl sulfides. An example of a sulfur umpolung was reported by the Menezes group in their synthesis of alkynyl sulfide **4.21** (Scheme **4.8**).[27] They used a copper catalyst, CuI, to make a copper acetylide with alkyne **4.19**, to act as a nucleophile and react with disulfide **4.20**, acting as the electrophile. The result was alkynyl sulfide **4.21** isolated in 90% yield**.**

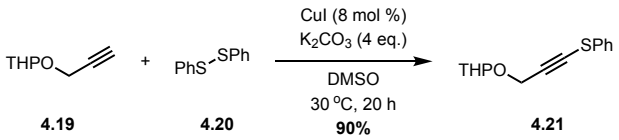


Scheme **4.8** – Thiolation reaction using a sulfur umpolung strategy.

An example of umpolung strategy of alkynes for a thiol-yne reaction can be seen from the Waser group, who efficiently synthesized alkynyl sulfides using ethynyl benziodoxolone (EBX) reagents (Scheme **4.9**).[28] Using 1,5,7-triazabicyclo[4.4.0]dec-5-ene (TBD) as a base allowed for the use of different EBX reagents, bearing aliphatic- and mesityl-substituted alkynes, with a broad scope of thiols as demonstrated by the chemoselective reaction of thiol **4.22** with EBX reagent **4.23** giving alkynyl sulfide **4.24**, isolated in 95% yield.

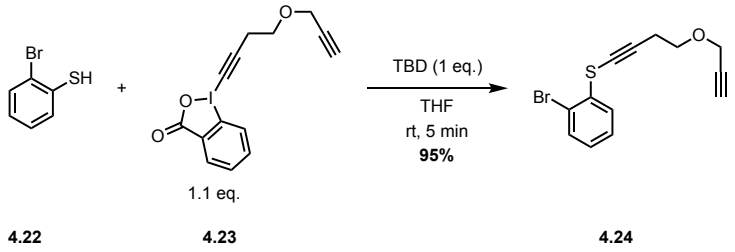


Scheme **4.9** – Thiol alkynylation reaction with alkyne umpolung using EBX reagent.

## 4.2.1 Previous Work from the Collins Group

As has already been discussed in Chapter 2, the Collins group developed a catalytic metallaphotoredox approach to preparing alkynyl sulfides (Scheme **2.2**, Section 2.1.2).[29] The

group used 4CzIPN, a nickel catalyst, and irradiation with blue LEDs in a dual-catalytic thiolation using continuous flow techniques with short reaction times (30 min) (Scheme **4.10**). Alkynyl sulfide products were obtained in 50-96% yields. Though highly efficient for the preparation of aromatic alkynyl sulfides, it failed with aliphatic alkyne coupling partners.[29]

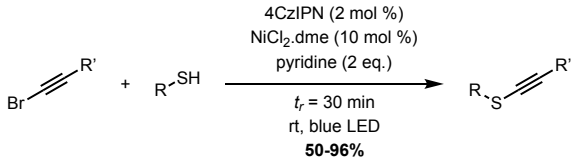


Scheme **4.10** – Synthesis of an alkynyl sulfide using continuous flow and photochemical conditions.

The Collins group then developed a more "universal" catalytic protocol for the synthesis of alkynyl sulfides from bromoalkynes. They developed a Cu-catalyzed cross-coupling of bromoalkynes with thiols to make a large library of alkynyl sulfides (Scheme **4.11**).[30] The catalytic system employed $Cu(MeCN)_4PF_6$, 4,4'-di-*tert*-butyl-2,2'-dipyridyl (dtbbpy) ligand, and 2,6-lutidine, affording yields ranging from 50-99%. The substrate scope included the functionalization of cysteine in dipeptides as well the synthesis of rare bis-heteroatom-substituted alkynes.

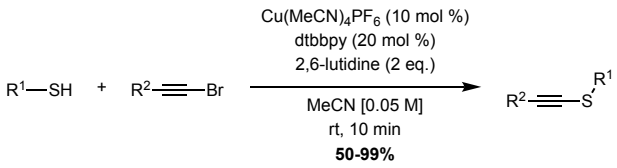


Scheme **4.11** – Cu-catalyzed $C_{sp}$–S coupling for alkynyl sulfide synthesis.

The method was effective at forming rare macrocyclic alkynyl sulfides (Scheme **4.12**).[31] The group was able to create a library of cysteine-derived macrocycles, along with dipeptide and tripeptide macrocycles, at ambient temperature, in yields ranging from 23-73%. The reaction conditions were also chemoselective with regards to terminal alkynes versus bromoalkynes.

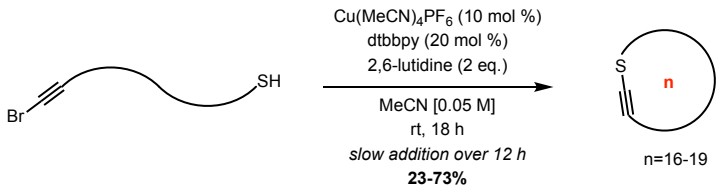


Scheme **4.12** – General Cu-catalyzed $C_{sp}$–S coupling for alkynyl sulfide macrocyclization.

Alkynyl sulfides are interesting candidates for thiol-yne reactions since they are heteroatom-substituted internal alkynes. The sulfur atom on the di-substituted alkyne polarizes the carbon-carbon triple bond, which may favor certain regio- and chemoselective pathways. It would seem like a strategy to gain greater control over reactions with internal alkynes. Initiation of the reaction could be achieved through photocatalytic conditions using visible light, promoting a green process. The next chapter will be the research performed on the metal-free photocatalytic thiol-yne reaction of alkynyl sulfides using visible light.

## 4.3 References


(1) Posner, T. Beiträge Zur Kenntniss Der Ungesättigten Verbindungen. II. Ueber Die Addition von Mercaptanen an Ungesättigte Kohlenwasserstoffe. *Ber. Dtsch. Chem. Ges.* **1905**, *38* (1), 646–657.

(2) Ruhemann, S.; Stapleton, H. E. CIX.—Condensation of Phenols with Esters of the Acetylene Series. Part III. Synthesis of Benzo-γ-Pyrone. *J. Chem. Soc.* **1900**, *77* (0), 1179–1185.

(3) Lowe, A. B. Thiol-Ene "Click" Reactions and Recent Applications in Polymer and Materials Synthesis. *Polym. Chem.* **2010**, *1* (1), 17–36.

(4) Lowe, A. B. Thiol-Yne 'Click'/Coupling Chemistry and Recent Applications in Polymer and Materials Synthesis and Modification. *Polymer* **2014**, *55* (22), 5517–5549.

(5) Lü, S.; Wang, Z.; Zhu, S. Thiol-Yne Click Chemistry of Acetylene-Enabled Macrocyclization. *Nat. Commun.* **2022**, *13* (1), 1–11.

(6) Li, Y.; Cai, J.; Hao, M.; Li, Z. Visible Light Initiated Hydrothiolation of Alkenes and Alkynes over $ZnIn_2S_4$. *Green Chem.* **2019**, *21* (9), 2345–2351.

(7) [1] Journet, M.; Rouillard, A.; Cai, D.; Larsen, R. D. Double Radical Cyclization/β-Fragmentation of Acyclic ω-Yne Vinyl Sulfides. Synthesis of 3-Vinyldihydrothiophene and Dihydrothiopyran Derivatives. A New Example of a 5-*Endo*-*Trig* Radical Cyclization. *J. Org. Chem.* **1997**, *62* (25), 8630–8631.

(8) Lowe, A. B. Thiol-Yne 'Click'/Coupling Chemistry and Recent Applications in Polymer and Materials Synthesis and Modification. *Polymer* **2014**, *55* (22), 5517–5549.

(9) Macdougall, L. J.; Truong, V. X.; Dove, A. P. Efficient in Situ Nucleophilic Thiol-Yne Click Chemistry for the Synthesis of Strong Hydrogel Materials with Tunable Properties. *ACS Macro Lett.* **2017**, *6* (2), 93–97.

(10) Cook, A. B.; Barbey, R.; Burns, J. A.; Perrier, S. Hyperbranched Polymers with High Degrees of Branching and Low Dispersity Values: Pushing the Limits of Thiol-Yne Chemistry. *Macromolecules* **2016**, *49*, 1296-1304.

(11) MacDougall, L. J.; Wiley, K. L.; Kloxin, A. M.; Dove, A. P. Design of synthetic extracellular matrices for probing breast cancer cell growth using robust cyctocompatible nucleophilic thiol-yne addition chemistry. *Biomaterials* **2018**, *178*, 435-447.

(12) Cai, S.; Weng, Z.; Zheng, Y.; Zhao, B.; Gao, Z.; Gao, C. High porosity microspheres with functional groups synthesized by thiol-yne click suspension polymerization. *Polym. Chem*. **2016**, *7*, 7400-7407.

(13) Stewart, M. H.; Susumu, K.; Oh, E.; Brown, C. G.; McClain, C. C.; Gorzkowski, E. P.; Boyd, D. A. Fabrication of Photoluminescent Quantum Dot Thiol-yne Nanocomposites via Thermal Curing or Photopolymerization. *ACS Omega* **2018**, *3*, 3314-3320.

(14) Picard-Lafond, A.; Morin, J.-F. Low-Temperature Synthesis of Carbon-Rich Nanoparticles with a Clickable Surface for Functionalization. *Langmuir* **2017**, *33*, 5385-5392.

(15) Zhang, C.; Dai, P.; Vinogradov, A. A.; Gates, Z. P.; Pentelute, B. L. Site-Selective Cysteine-Cyclooctyne Conjugation. *Angew. Chem., Int*. *Ed*. **2018**, *57*, 6459-6463.

(16) Wang, Y.; Bruno, B. J.; Cornillie, S.; Nogieira, J. M.; Chen, D.; Cheatham, T. E. III; Lim, C. S.; Chou, D. H.-C. Application of Thiol-yne/Thiol-ene Reactions for Peptide and Protein MacrocyclizationsApplication of Thiol-yne/Thiol-ene Reactions for Peptide and Protein Macrocyclizations. *Chem. Eur. J*. **2017**, *23*, 7087-7092.

(17) Nador, F.; Mancebo-Aracil, J.; Zanotto, D.; Ruiz-Molina, D.; Radivoy, G. Thiol-Yne Click Reaction: An Interesting Way to Derive Thiol-Provided Catechols. *RSC Adv.* **2021**, *11* (4), 2074–2082.

(18) Kondoh, A.; Takami, K.; Yorimitsu, H.; Oshima, K. Stereoselective Hydrothiolation of Alkynes Catalyzed by Cesium Base: Facile Access to (*Z*)-1-Alkenyl Sulfides. *J. Org. Chem.* **2005**, *70* (16), 6468–6473.

(19) Kondoh, A.; Yorimitsu, H.; Oshima, K. Palladium-Catalyzed *Anti*-Hydrothiolation of 1-Alkynylphosphines. *Org. Lett.* **2007**, *9* (7), 1383–1385.

(20) Lo Conte, M.; Pacifico, S.; Chambery, A.; Marra, A.; Dondoni, A. Photoinduced Addition of Glycosyl Thiols to Alkynyl Peptides: Use of Free-Radical Thiol−Yne Coupling for Post-Translational Double-Glycosylation of Peptides. *J. Org. Chem.* **2010**, *75* (13), 4644–4647.

(21) Xiao, Q.; Tong, Q.-X.; Zhong, J.-J. Recent Advances in Visible-Light Photoredox Catalysis for the Thiol-Ene/Yne Reactions. *Molecules* **2022**, *27* (3), 619.

(22) Kumar, R.; Saima; Shard, A.; Andhare, N. H.; Richa; Sinha, A. K. Thiol-Ene “Click” Reaction Triggered by Neutral Ionic Liquid: The “Ambiphilic” Character of [Hmim]Br in the

Regioselective Nucleophilic Hydrothiolation. *Angew. Chem. Int. Ed Engl.* **2015**, *54* (3), 828–832.

(23) Vanslambrouck, S.; Riva, R.; Ucakar, B.; Préat, V.; Gagliardi, M.; Molin, D. G. M.; Lecomte, P.; Jérôme, C. Thiol-Ene Reaction: An Efficient Tool to Design Lipophilic Polyphosphoesters for Drug Delivery Systems. *Molecules* **2021**, *26* (6), 1750.

(24) Zalesskiy, S. S.; Shlapakov, N. S.; Ananikov, V. P. Visible Light Mediated Metal-Free Thiol–Yne Click Reaction. *Chem. Sci.* **2016**, *7* (11), 6740–6745.

(25) Santandrea, J.; Godin, E.; Collins, S. K. A Synthetic Guide to Alkynyl Sulfides. *Org. Biomol. Chem.* **2020**, *18* (26), 4885–4893.

(26) Arens, J. F.; Doornbos, T. The Chemistry of Acetylenic Ethers XVI. Acetylenic Thioethers. *Recl. Trav. Chim. Pays Bas* **1956**, *75* (4), 481–486.

(27) Bieber, L. W.; da Silva, M. F.; Menezes, P. H. Short and Efficient Preparation of Alkynyl Selenides, Sulfides and Tellurides from Terminal Alkynes. *Tetrahedron Lett.* **2004**, *45* (13), 2735–2737.

(28) Frei, R.; Waser, J. A Highly Chemoselective and Practical Alkynylation of Thiols. *J. Am. Chem. Soc.* **2013**, *135* (26), 9620–9623.

(29) Santandrea, J.; Minozzi, C.; Cruché, C.; Collins, S. K. Photochemical Dual-Catalytic Synthesis of Alkynyl Sulfides. *Angew. Chem. Int. Ed Engl.* **2017**, *56* (40), 12255–12259.

(30) Godin, É.; Santandrea, J.; Caron, A.; Collins, S. K. General Cu-Catalyzed $C_{sp}$–S Coupling. *Org. Lett.* **2020**, *22* (15), 5905–5909.

(31) Godin, É.; Nguyen Thanh, S.; Guerrero-Morales, J.; Santandrea, J.; Caron, A.; Minozzi, C.; Beaucage, N.; Rey, B.; Morency, M.; Abel-Snape, X.; Collins, S. K. Synthesis and Diversification of Macrocyclic Alkynediyl Sulfide Peptides. *Chemistry* **2020**, *26* (64), 14575–14579.

# Chapter 5 – Photocatalytic Thiol-Yne Reactions of Alkynyl Sulfides

Oliver Bleton and Shawn K. Collins*

Département de Chimie, Centre for Green Chemistry and Catalysis, Université de Montréal, Complexe des Sciences, 1375 Avenue Thérèse-Lavoie-Roux, Montréal, Québec H2V 0B3 CANADA

Submitted to Organic Letters

Contributions :

- Olivier Bleton carried out all reactions and purifications; as well as participating in the writing of the article and the experimental section.
- Shawn K. Collins helped set up the experiments and write the manuscript.

## 5.1 Abstract

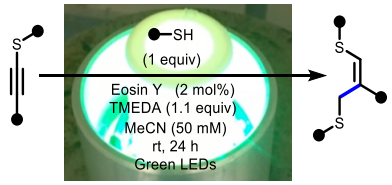


Thiol-yne reactions typically employ thiols and terminal alkynes as reaction partners. Thiol-yne reaction of alkynyl sulfides and thiols is possible when employing a non-metal photocatalyst Eosin Y, green LED irradiation, under an air atmosphere. Alkynyl sulfides were transformed in good overall yields (58-90% total yields, 10 examples) favoring the *cis*-isomer. No addition to the α-position of the alkynyl sulfide is observed, and regioselectivity is believed to be controlled through stabilization of radical intermediates by the adjacent sulfur atom. Furthermore, control experiments with "all-carbon" internal alkynes demonstrate that alkynyl sulfides possess improved reactivity and regioselectivity profiles during thiol-yne processes.

## 5.2 Introduction

The thiol-yne reaction has emerged as a powerful strategy for carbon-sulfur (C-S) bond formation.[1] The simplicity of the starting materials, free thiols and terminal alkynes, both versatile building blocks,[2] renders the process synthetically attractive. The formal hydrothiolation of the alkyne results in the formation of a thioalkene with high atom economy (Figure 1 **a**). Traditionally, such additions to inactivated alkynes occur with the aid of transition metal catalysis[3] and in a rare example, have occured without catalysis via the aid of weak S-H...π interactions using specific substituents.[4] The ease of C-S bond formation opens opportunities for applications in numerous fields. The thiol-yne process has proven utility in the synthesis and modification of macromolecules, polymers,[5] hydrogels,[6] hyperbranched polymers with low dispersity,[7] and biomaterials.[8]

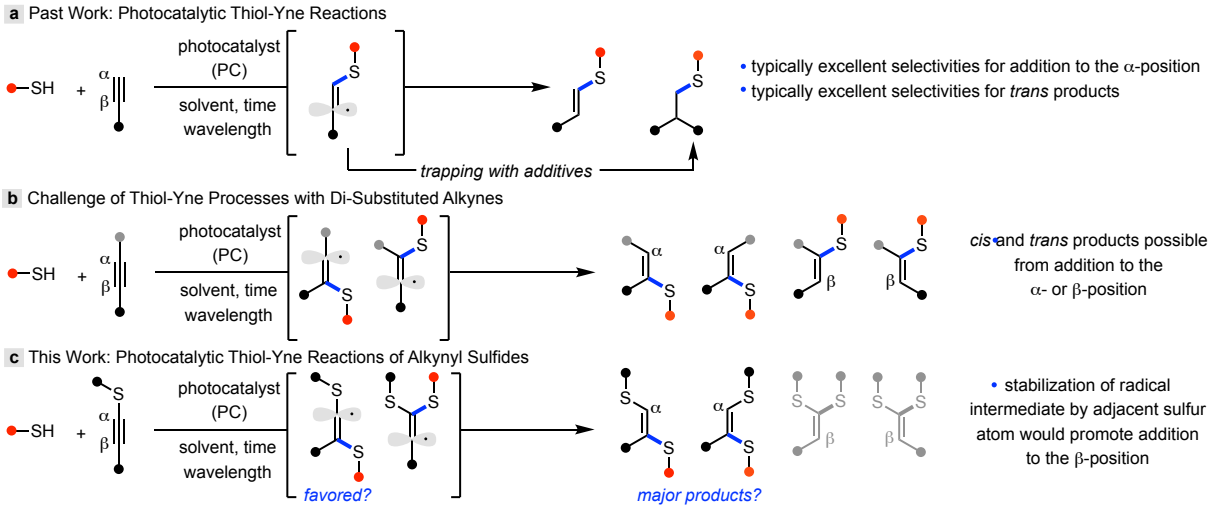


Figure **5.1** – Thiol-yne reactions

Polymerization and functionalization using thiol-yne reactions has afforded high porosity microspheres,[9] modified quantum dots,[10] and surface decorated carbon rich nanoparticles.[11] In chemical biology, the thiol-yne reaction has been used in a "click" strategy for bioconjugation,[12] as well as to prepare linkages in macrocyclic peptides.[13]

Recently, photocatalysis has materialized as an alternative means for achieveing thiol-yne reactions. Photocatalysis employing visible light is now considered a green and sustainable route for molecular synthesis. Li and co-workers reported heterogeneous photocatalysis could be

employed for hydrothiolation of alkynes. Visible light irradiation over $ZnIn_2S_4$ afforded good yields for both thiol-yne and thiol-ene reactions.[14] In 2016, Ananikov and co-workers reported a thiol-yne process between thiols and terminal alkynes using homogeneous catalysis.[15] Eosin Y combined with irradiation using green LEDs (530 nm) afforded good yields of hydrothiolated product. In 2019, Wang and co-workers also reported a method using acridinium salts as non-metal photocatalysts, to promote thiol-yne reactions.[16] Sterically unencumbered thiols reacted however in double additions of thiol to provide dithiolated product.[16] Zhu and co-workers exploited that reactivity pattern to design macrocyclization processes that involved dithiols and acetylene gas as starting materials.[17] Using Ir-based photocatalysts and blue LEDs, a broad substrate scope of structurally varied macrocycles were obtained. [17] Thiol-yne reactions have also attracted attention due to the potential to trap or intercept radical intermediates in cascade sequences that rapidly increase molecular complexity (Figure 1 **a**). For example, Volla et. al. intercepted the alkenyl radical formed from thiol-yne reaction with an intramolecular Michael acceptor, to afford polycyclic products.[18] Ananikov employed a similar strategy, however in an intermolecular sense to develop thiol-yne-ene couplings.[19] Such "modified" photocatalytic thiol-yne processes have resulted in new syntheses of indoles,[20] α,α-aminothioketones,[21] hydroxydithioacetals,[22] sulfoxides,[23] and vinyl sulfones.[24] The aforementioned syntheses all exploit terminal alkynes as reaction partners, which is not surprising given the high levels of selectivity observed. Thiol-yne processes using di-substituted alkynes would be considered challenging, because in theory four different alkene *cis*- and *trans*-isomers could be formed from addition to the alkyne carbons. (Figure 1 **b**). One strategy to control selectivity in additions to di-substituted alkynes would be judicious choice of one substituent, particularly one that could stabilize reaction intermediates. In that context, alkynyl sulfides are promising acceptors in thiol-yne reactions.[25] As heteroatom-substituted alkynes, the sulfur atom polarizes the carbon-carbon triple bond, and the predictive reactivity has allowed alkynyl sulfides to act as versatile synthons in a variety of transformations.[26] Addition of a thiol to an alkynyl sulfide at the β-position may allow for favorable stabilization of the resulting radical (Figure 1 **c**). Herein, we report on the development of a thiol-yne process employing a disubstituted alkynes, specifically alkynyl

sulfides. The process employs non-metal photocatalysts and affords useful selectivity for the *cis*-products resulting from addition to the β-carbon of the alkyne.

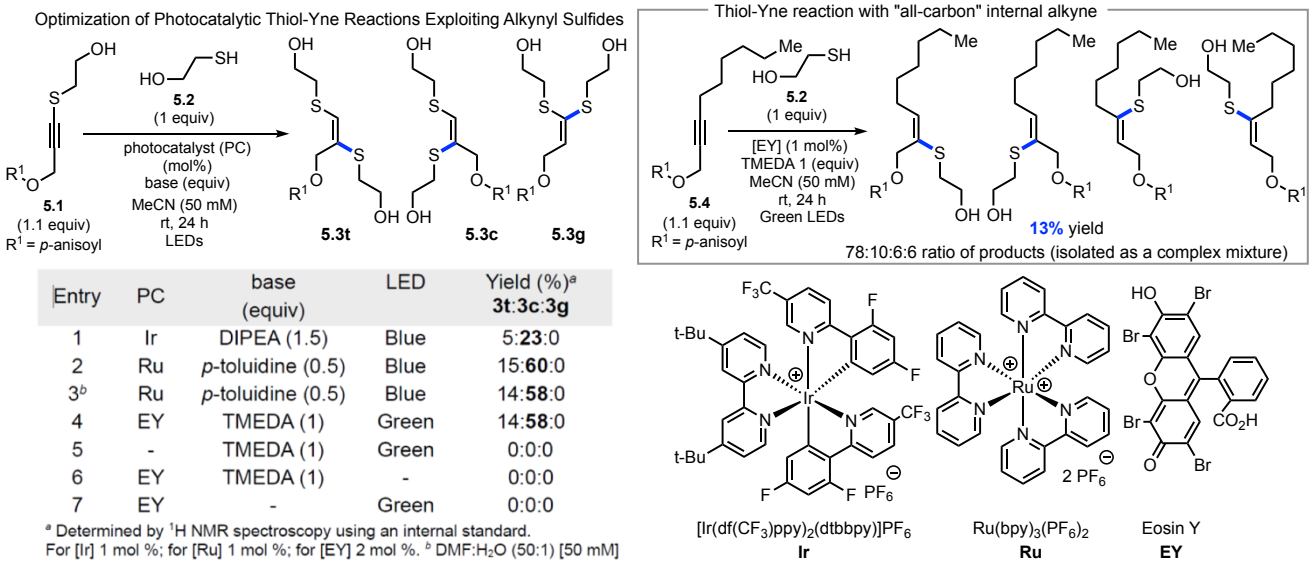


| Entry | PC | base (equiv) | LED | Yield (%)[a] 3t:3c:3g |
|---|---|---|---|---|
| 1 | Ir | DIPEA (1.5) | Blue | 5:**23**:0 |
| 2 | Ru | *p*-toluidine (0.5) | Blue | 15:**60**:0 |
| 3[b] | Ru | *p*-toluidine (0.5) | Blue | 14:**58**:0 |
| 4 | EY | TMEDA (1) | Green | 14:**58**:0 |
| 5 | - | TMEDA (1) | Green | 0:0:0 |
| 6 | EY | TMEDA (1) | - | 0:0:0 |
| 7 | EY | - | Green | 0:0:0 |

[a] Determined by $^1$H NMR spectroscopy using an internal standard. For [Ir] 1 mol %; for [Ru] 1 mol %; for [EY] 2 mol %. [b] DMF:$H_2O$ (50:1) [50 mM]



$[Ir(df(CF_3)ppy)_2(dtbbpy)]PF_6$ **Ir** $Ru(bpy)_3(PF_6)_2$ **Ru** Eosin Y **EY**

Figure **5.2** – Developing a photocatalytic thiol-yne reaction of alkynyl sulfides.

## 5.3 Results

Initial investigations into a thiol-yne reaction onto di-substituted alkynes began with alkynyl sulfide **5.1**, which was prepared via Cu-catalyzed $C_{sp}$-S coupling[27] (Figure 2). Mercaptoethanol was selected as the thiol coupling partner to simplify analysis of the reaction mixture (the product resulting from attack at the α-position does not afford *cis*- nor *trans* isomers). Treating alkynyl sulfide **5.1** with mercaptoethanol in MeCN with an iridium-based photocatalyst **Ir** and DIPEA under blue LED irradiation afforded 23% of the *cis*-product **5.3c** and 5% of the *trans*-product **5.3t**. The product resulting from attack at the α-position (**5.3g**) was not observed. NOESY experiments confirmed the stereochemistry of **5.3c**, through observation of interactions between the singlet of the vinylic proton and the singlet of the allylic protons of the *cis*-isomer. When a Ru-based photocatalyst with p-toluidine, conditions established by Yoon for thiol-ene reactions,[28] were explored, a significant increase in the yield of the *cis*-product **5.3c** was observed (60%) and the ratio between *cis*- and *trans*-products was 4:1 (total yield of 75%). Thiol-yne reaction with Eosin Y/TMEDA as the catalyst system under green LED irradiation afforded similar yields and selectivities as the Ru-based catalyst. Conditions employing Eosin Y were

selected based on the the appeal of a non-metal process. Further control reactions demonstrated the need for Eosin Y, TMEDA and light to promote the thiol-yne reaction. Using the optimized conditions, an "all-carbon" analogue **5.4** of alkynyl sulfide **5.1** was prepared and subjected to the thiol-yne reaction. A 13% yield of co-eluting thiol-yne products could be recovered via flash chromatography. Analysis of the mixture ($^1$H NMR) showed four different alkene products, suggesting a mixture of products resulting from reaction at both the α- and β-positions of the alkyne. The contrast in reactivity profile of alkyne **5.4** (13 % total yield) compared to alkynyl sulfide **5.1** (72 % total yield) demonstrates that the sulfur substituent is helping to augment reactivity and control regioselectivity during the thiol-yne reaction.

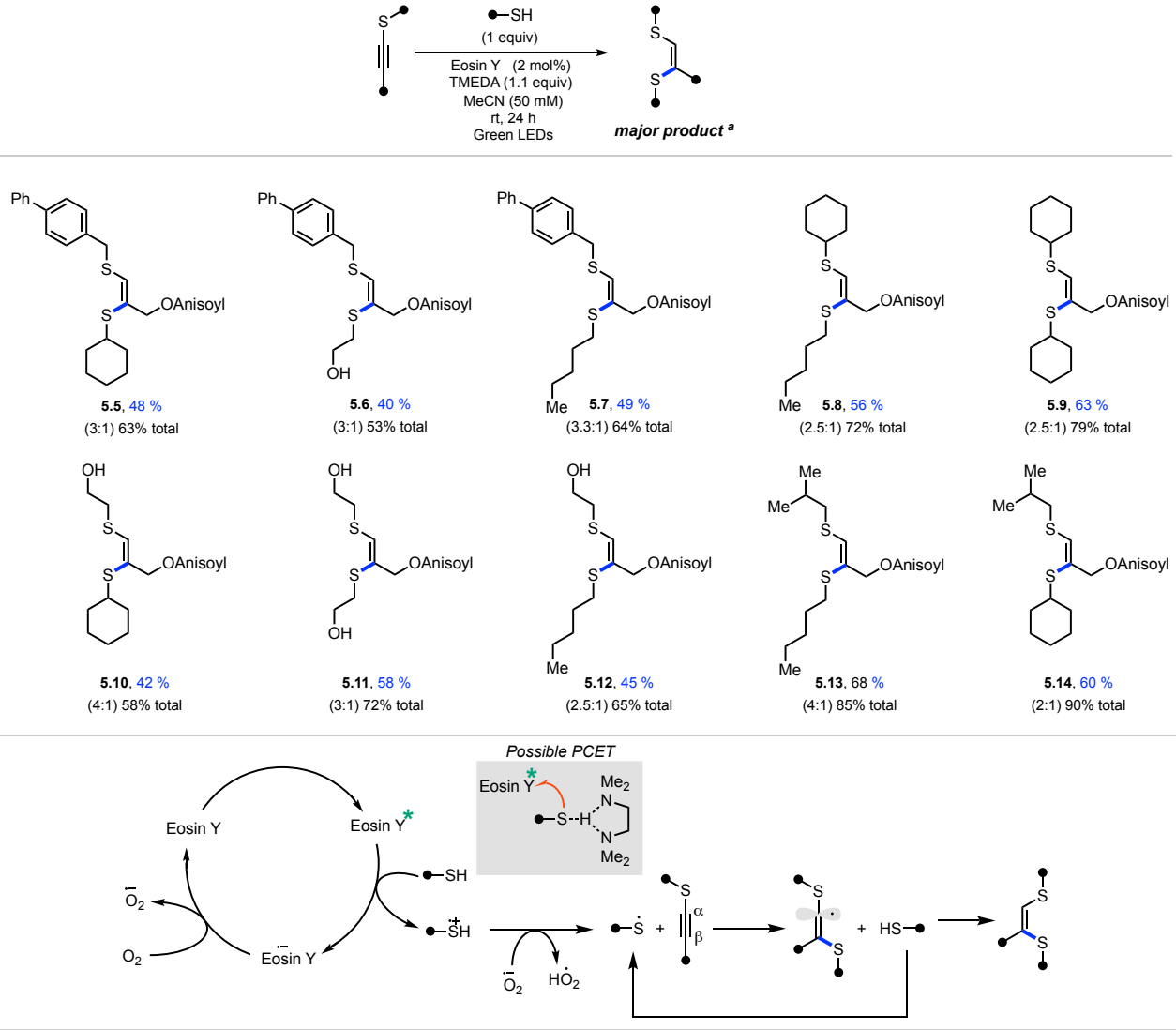

Figure **5.3** – *Top:* Substrate scope [a] Major *cis*-product shown. Minor product is *trans*-isomer. Isolated yields. *Bottom:* Plausible mechanism and catalytic cycle.

Using the optimized conditions, thiol-yne reaction with different alkynyl sulfides and thiols was investigated (Figure 3 *top*). First an alkynyl sulfide bearing a 4-(phenyl)benzylthio- group was reacted with three different thiols: cyclohexylthiol, mercatoethanol and *n*-pentylthiol. All three experiments afforded the *cis*-isomer as the major product (3-4:1 ratio *cis*: *trans*). The average yield of the *cis*-products (**5.5**→**5.7**) was approximately 50%, with slightly higher total yields of the *cis*- *trans* mixture (58-62%). Thiol-yne reaction with an alkynyl sulfide bearing a ($C_6H_{11}S$)-substituent afforded slightly higher yields when reacted with *n*-pentylthiol and cyclohexylthiol (56-63% total yields), but selectivities were slightly lower for the *cis*-isomer. Similar trends were again observed for thiol-yne processes with two other alkynyl sulfides bearing -$SCH_2CH_2OH$ or -$SCH_2CH(CH_3)_2$ groups. In all cases all three thiol reaction partners reacted efficiently and provided the *cis*-isomer as the major product. $^1$H NMR signals for the vinylic proton typically ranged roughly from 7 ppm to 6.5 ppm, *cis*-isomers generally having a displacement more downfield than their *trans*- counterparts. The thiol-yne process was efficient with overall yields reaching 90 %.

A plausible mechanism for the thiol-yne process would first involve promotion of Eosin Y to its excited state (Figure 3 *bottom*). The excited state of Eosin Y could abstract an electron from the thiol to create the corresponding radical cation. It has been proposed by others[29] that the subsequent transformation to the thiyl radical is aided by the radical anion of molecular oxygen (itself formed when the ground state radical anion of Eosin Y donates an electron to $O_2$ to close its catalytic cycle). Such a catalytic cycle is plausible, and the thiol-yne reactions are performed under an air atmosphere. Control reaction had shown TMEDA to be essential to the formation of the desired products. Consequently, it is possible that the thiyl radical is generated via a proton-coupled electron transfer (PCET) process aided by TMEDA acting as a base.[30] TMEDA may also be acting as a redox mediator similar to p-toluidine in photocatalytic thiol-ene processes.[26] Upon formation of a thiyl radical, addition to the β-position of the alkynyl sulfide generates an alkenyl radical form which possible stabilization exists with the adjacent sulfur atom. Hydrogen atom transfer could occur from another thiol, which would regenerate the thiyl radical as a chain process.[31]

## 5.4 Conclusion

Thiol-yne processes have found applications in materials science, chemical biology and complex molecule synthesis, but have found limited use in reaction with terminal alkyne partners. The thiol-yne reaction of alkynyl sulfides and thiols presented herein is operationally simple, employing a non-metal photocatalyst Eosin Y, green LED irradiation, under an air atmosphere. Alkynyl sulfides were reacted in good overall yields (40-90% total yields) favoring the *cis*-isomer. No addition to the α-position of the alkynyl sulfide was observed, and regioselectivity is believed to be controlled through stabilization of radical intermediates by the adjacent sulfur atom. Control experiments with "all-carbon" internal alkynes demonstrate that alkynyl sulfides possess improved reactivity and regioselectivity profiles during thiol-yne processes. The thiol-yne reactions described herein suggest that other heteroatom-substituted alkynes such as alkynyl ethers, alkynyl phosphonates or the popular ynamides could act as selective di-substituted alkynes in thiol-yne processes as well. As a number of "cascade" reactions employing terminal alkynes exist, it is plausible that new reaction processes that increase molecular complexity from simple building blocks could be achieved by exploiting alkynyl sulfide reaction partners.

**Supporting Information**

The Supporting Information is available free of charge on the ACS Publications website.

Experimental procedure, compound characterization data and $^{1}H$ and $^{13}C$ NMR spectra (PDF).

**Corresponding Author**

Shawn Collins − *Département de Chimie, Centre for Green Chemistry and Catalysis, Université de Montréal, 1375 Avenue Thérèse-Lavoie-Roux, Montréal, QC CANADA H2V 0B3; orcid.org/0000-0001-9206-5538; Email: shawn.collins@umontreal.ca*

**Acknowledgements**

The authors acknowledge the Natural Sciences and Engineering Research Council of Canada (NSERC, Discovery 1043344 and RGPIN-2020-05006) and the Fonds de recherche Nature et technologie via the Centre in Green Chemistry and Catalysis (FRQNT-2020-RS4-265155-CCVC) for generous funding.

## 5.5 References


(1) (a) Hoogenboom, R. Thiol–Yne Chemistry: A Powerful Tool for Creating Highly Functional Materials. *Angew. Chem., Int. Ed*. **2010**, *49*, 3415-3417. (b) Ogawa, A.; Ikeda, T.; Kimura, K.; Hirao, T. Highly Regio- and Stereocontrolled Synthesis of Vinyl Sulfides via Transition-Metal-Catalyzed Hydrothiolation of Alkynes with Thiols. *J. Am. Chem. Soc*. **1999**, *121*, 5108-5114. (c) Beletskaya, I. P.; Ananikov, V. P. Transition-Metal-Catalyzed C−S, C−Se, and C−Te Bond Formation via Cross-Coupling and Atom-Economic Addition Reactions. *Chem. Rev*. **2011**, *111*, 1596-1636. (d) Ogawa, A. Transition-Metal-Catalyzed S–H and Se–H Bonds Addition to Unsaturated Molecules. *Top. Organomet. Chem*. **2011**, *43*, 325-360.

(2) Trost, B. M.; Li, C.-J. Modern Alkyne Chemistry: Catalytic and Atom-Economic Transformations. Wiley-VCH , Weinheim, 2015.

(3) (a) Castarlenas, R.; Giuseppe, A. D.; Pérez-Torrente, J. J.; Oro, L. A. The emergence of transition-metal-mediated hydrothiolation of unsaturated carbon-carbon bonds: a mechanistic outlook. *Angew. Chem,. Int. Ed*. **2013**, *52*, 211-222. (b) L. Benati, L. Capella, P. C. Montevecchi and P. Spagnolo, J. Org. Chem., 1995, 60, 7941; (b) Griesbaum, K. Problems and Possibilities of the Free-Radical Addition of Thiols to Unsaturated Compounds. *Angew. Chem., Int. Ed*. **1970**, *9*, 273-287. (c) Kuniyasu, H.; Ogawa, A; Sato, K.; Ryu, I.; Kambe, N.; Sonoda, N. The first example of transition-metal-catalyzed addition of aromatic thiols to acetylenes. *J. Am. Chem. Soc*. **1992**, *114*, 5902-5903; (d) Ananikov, V. P.; Orlov, N. V.; Zalesskiy, S. S.; Beletskaya, I. P.; Khrustalev, V. N.; Morokuma, K.; Musaev, D. G. Catalytic adaptive recognition of thiol (SH) and selenol (SeH) groups toward synthesis of functionalized vinyl monomers. *J. Am. Chem. Soc*. **2012**, *134*, 6637-6649. (e) Weiss, C. J.; Marks, T. J. Organozirconium Complexes as Catalysts for Markovnikov-Selective Intermolecular Hydrothiolation of Terminal Alkynes: Scope and Mechanism. *J. Am. Chem. Soc*. **2010**, *132*, 10533-10546; (f) Weiss, C. J.;Wobser, S. D.; Marks, T. J. Organoactinide-Mediated Hydrothiolation of Terminal Alkynes with Aliphatic, Aromatic, and Benzylic Thiols*. J. Am. Chem. Soc*. **2009**, *131*, 2062-2063.

(4) Choudhuri, K.; Pramanik, M.; Mandal, A.; Mal, P. S-H···π Driven Anti-Markovnikov Thiol-Yne Click Reaction. *Asian J. Org. Chem*. **2018**, *7*, 1849-1855.

(5) (a) Lowe, A. B. Thiol-yne 'click'/coupling chemistry and recent applications in polymer and materials synthesis and modification. *Polymer* **2014**, *55*, 5517-5549. (b) Daglar, O.; Luleburgaz, S.; Baysak, E.; Gunay, U. S.; Hizal, G.; Tunca, U.; Durmaz, H. Nucleophilic Thiol-yne reaction in Macromolecular Engineering: From synthesis to applications. *Eur. Polym. J.* **2020**, *137*, 109926.

(6) (a) MacDougall, L. J.; Truong, V. X.; Dove, A. P. Efficient In Situ Nucleophilic Thiol-yne Click Chemistry for the Synthesis of Strong Hydrogel Materials with Tunable Properties. *ACS Macro Lett*. **2017**, *6*, 93-97. (b) Hu, X.; Tan, H.; Wang, X.; Chen, P. Surface functionalization of hydrogel by thiol-yne click chemistry for drug delivery. *Colloids and Surfaces, A: Physicochemical and Engineering Aspects* **2016**, *489*, 297-304.

(7) Cook, A. B.; Barbey, R.; Burns, J. A.; Perrier, S. Hyperbranched Polymers with High Degrees of Branching and Low Dispersity Values: Pushing the Limits of Thiol-Yne Chemistry. *Macromolecules* **2016**, *49*, 1296-1304.

(8) MacDougall, L. J.; Wiley, K. L.; Kloxin, A. M.; Dove, A. P. Design of synthetic extracellular matrices for probing breast cancer cell growth using robust cyctocompatible nucleophilic thiol-yne addition chemistry. *Biomaterials* **2018**, *178*, 435-447.

(9) Cai, S.; Weng, Z.; Zheng, Y.; Zhao, B.; Gao, Z.; Gao, C. High porosity microspheres with functional groups synthesized by thiol-yne click suspension polymerization. *Polym. Chem*. **2016**, *7*, 7400-7407.

(10) Stewart, M. H.; Susumu, K.; Oh, E.; Brown, C. G.; McClain, C. C.; Gorzkowski, E. P.; Boyd, D. A. Fabrication of Photoluminescent Quantum Dot Thiol-yne Nanocomposites via Thermal Curing or Photopolymerization. *ACS Omega* **2018**, *3*, 3314-3320.

(11) Picard-Lafond, A.; Morin, J.-F. Low-Temperature Synthesis of Carbon-Rich Nanoparticles with a Clickable Surface for Functionalization. *Langmuir* **2017**, *33*, 5385-5392.

(12) a) Zhang, C.; Dai, P.; Vinogradov, A. A.; Gates, Z. P.; Pentelute, B. L. Site-Selective Cysteine-Cyclooctyne Conjugation. *Angew. Chem., Int*. *Ed*. **2018**, *57*, 6459-6463. (b) Griebenow, N.; Dilmac, A. M.; Greven, S.; Braese, S. Site-Specific Conjugation of Peptides and Proteins via Rebridging of Disulfide Bonds Using the Thiol-Yne Coupling Reaction. *Bioconjugate Chem*. **2016**, *27*, 911-917.

(13) Wang, Y.; Bruno, B. J.; Cornillie, S.; Nogieira, J. M.; Chen, D.; Cheatham, T. E. III; Lim, C. S.; Chou, D. H.-C. Application of Thiol-yne/Thiol-ene Reactions for Peptide and Protein Macrocyclizations Application of Thiol-yne/Thiol-ene Reactions for Peptide and Protein Macrocyclizations. *Chem. Eur. J*. **2017**, *23*, 7087-7092.

(14) Li, Y.; Cai, J.; Hao, M.; Li, Z. Visible light initiated hydrothiolation of alkenes and alkynes over ZnIn2S4. *Green Chem*. **2019**, *21*, 2345-2351.

(15) Zalesskiy, S. S.; Shlapakov, N. S.; Ananikov, V. P. Visible Light Mediated Metal-Free Thiol-Yne Click Reaction. *Chem. Sci*. **2016**, *7*, 6740−6745

(16) Kaur, S.; Zhao, G.; Busch, E.; Wang, T. Metal-Free Photocatalytic Thiol-Ene/Thiol-Yne Reactions. *Org. Biomol. Chem*. **2019**, *17*, 1955−1961.

(17) Lü, S.; Wang, Z.; Zhu, S. Thiol-Yne click chemistry of acetylene-enabled macrocyclization. *Nature Commun*. **2022**, *13*, 5001-5012.

(18) Nair, A. M.; Kumar, S.; Volla, C. M. R. Visible Light Mediated Sulfenylation-Annulation Cascade of Alkyne Tethered Cyclohexadienones. *Adv. Synth. Catal*. **2019**, *361*, 4983−4988.

(19) Burykina, J. V.; Kobelev, A. D.; Shlapakov, N. S.; Kostyukovich, A. Y.; Fakhrutdinov, A. N.; König, B.; Ananikov, V. P. Intermolecular Photocatalytic Chemo-, Stereo- and Regioselective Thiol–Yne–Ene Coupling Reaction. *Angew. Chem*., *Int. Ed.* **2022**, *61*, e202116888.

(20) Tambe, S. D.; Rohokale, R. S.; Kshirsagar, U. A. Visible-Light Mediated Eosin Y Photoredox-Catalyzed Vicinal Thioamination of Alkynes: Radical Cascade Annulation Strategy for 2-Substituted-3- Sulfenylindoles. *Eur. J. Org. Chem*. **2018**, 2117−2121.

(21) Chalotra, N.; Rizvi, M. A.; Shah, B. A. Photoredox-Mediated Generation of Gem -Difunctionalized Ketones: Synthesis of α,α-Aminothioketones. *Org. Lett*. **2019**, *21*, 4793–4797.

(22) Manzer Manhas, F.; Kumar, J.; Raheem, S.; Thakur, P.; Rizvi, M. A.; Shah, B. A. Photoredox-Mediated Synthesis of β-Hydroxydithioacetals from Terminal Alkynes. *ChemPhotoChem* **2021**, *5*, 235–239.

(23) Kumar, J.; Ahmad, A.; Rizvi, M. A.; Ganie, M. A.; Khajuria, C.; Shah, B. A. Photoredox-Mediated Synthesis of Functionalized Sulfoxides from Terminal Alkynes. *Org. Lett*. **2020**, *22*, 5661–5665.

(24) Wang, H.; Lu, Q.; Chiang, C.-W.; Luo, Y.; Zhou, J.; Wang, G.; Lei, A. Markovnikov-Selective Radical Addition of S-Nucleophiles to Terminal Alkynes through a Photoredox Process. *Angew. Chem. Int. Ed*. **2017**, *56*, 595–599.

(25) Santandrea, J.; Godin, É.; Collins, S. K. A synthetic guide to alkynyl sulfides. *Org. Biomol. Chem*. **2020**, *18*, 4885-4893.

(26) (a) [3+2] Cycloaddition: Destito, P.; Couceiro, J. R.; Faustino, H.; López, F.; Mascareñas, J. L. Ruthenium-Catalyzed Azide-Thioalkyne Cycloadditions in Aqueous Media: A Mild, Orthogonal, and Biocompatible Chemical Ligation. *Angew. Chem. Int. Ed*. **2017**, *56*, 10766-10770; (b) [2+2+2] Cycloaddition: Xie, L. G.; Niyomchon, S.; Mota, A. J.; González, L.; Maulide, N. Metal-Free Intermolecular Formal Cycloadditions Enable an Orthogonal Access to Nitrogen Heterocycles. *Nat. Commun*. **2016**, *7*, 10914-10923; (c) Annulation: Zhang, Y.-Q.; Zhu, X.-Q.; Chen, Y.-B.; Tan, T.-D.; Yang, M.-Y.; Ye, L.-W. Synthesis of Isothiochroman-3-ones via Metal-Free Oxidative Cyclization of Alkynyl Thioethers. *Org. Lett*. **2018**, *20*, 7721-7725; (d) Annulation: Reddy, R. J.; Ball-Jones, M. P.; Davies, P. W. Alkynyl Thioethers in Gold-Catalyzed Annulations To Form Oxazoles. *Angew. Chem. Int. Ed*. **2017**, *56*, 13310-13313; (e) Hydrosilylation: Ding, S.; Song, L. J.; Wang, Y.; Zhang, X.; Chung, L. W.; Wu, Y. D.; Sun, J. Highly Regio- and Stereoselective Hydrosilylation of Internal Thioalkynes under Mild Conditions. *Angew. Chem. Int. Ed*. **2015**, *54*, 5632-5635; (f) 1,4-Chirality Transfer: Kaldre, D., Maryasin, B.; Kaiser, D.; Gajsek, O.; González, L.; Maulide, N. An Asymmetric Redox Arylation: Chirality Transfer from Sulfur to Carbon through a Sulfonium [3,3]-Sigmatropic Rearrangement. *Angew. Chem. Int. Ed*. **2017**, *56*, 2212-2215; (g) Hydrofluoration: Bello, D.; O'Hagan, D. Lewis Acid-Promoted Hydrofluorination of Alkynyl Sulfides to Generate α-Fluorovinyl Thioethers. *Beilstein J. Org. Chem*. **2015**, *11*, 1902-1909; (h) Hydroallylation: Kong, W.; Che, C.; Kong, L.; Zhu, G. Copper-Catalyzed Regio- and Stereoselective Hydroallylation of Thioalkynes with Allylboronates: A Facile and Convenient Synthesis of 1,4-Dienes. *Tetrahedron Lett*. **2015**, *56*, 2780-2782. (i)

Pommainville, A.; Campeau, D.; Gagosz, F. The Synthetic Potential of Thiophenium Ylide Cycloadducts. *Angew. Chem., Int. Ed*. **2022**, *61*, e202205963

(27) Godin, É.; Santandrea, J.; Caron, A.; Collins, S. K. General Cu-Catalyzed $C_{sp}$–S Coupling. *Org. Lett.* **2020**, *22*, 5905–5909.

(28) Tyson, E. L.; Niemeyer, Z. L. Yoon, T. P. Redox Mediators in Visible Light Photocatalysis: Photocatalytic Radical Thiol–Ene Additions. *J. Org. Chem*. **2014**, *79*, 1427–1436.

(29) Chand, S.; Pandey, A. K.; Singh, R.; Kumar, S.; Singh, K. N. Eosin-Y-Catalyzed Photoredox CS Bond Formation: Easy Access to Thioethers. *Chem. Asian J*. **2019**, 24, 4712-4716.

(30) Murray, P. R. D.; Cox, J. H.; Chiappini, N. D.; Roos, C. B.; McLoughlin, E. A.; Hejna, B. G.; Nguyen, S. T.; Ripberger, H. H.; Ganley, J. M.; Tsui, E. Photochemical and Electrochemical Applications of Proton-Coupled Electron Transfer in Organic Synthesis *Chem. Rev*. **2022**, *122*, 2017-2291.

(31) Cismesia, M. A.; Yoon, T. P Characterizing chain processes in visible light photoredox catalysis. *Chem*. *Sci*. **2015**, *6*, 5426-5434.

# Chapter 6 – Conclusions and Perspectives

## 6.1 Conclusions

The first research section of the synthesis concerned expanding the scope of peptidic macrocycles synthesized using a hybrid reactor designed in the Collins group. A hexapeptide macrocycle was successfully synthesized with a yield of 71% using a haloaromatic linker molecule. Despite the hexapepetide being the largest macrocycle to date prepared using the hybrid reactor, we obtained the best yield out of all the macrocycles found in the scope of the reaction. While it is difficult to discern the exact reason for the high yield, our group has found that the rigidity and polarity of the linker molecule has improved many macrocyclizations for peptides.

In the second research section of the thesis, thiol-yne reactions with alkynyl sulfides were investigated. It was found that having a sulfur atom polarizing the triple bond of an internal alkyne prevents the addition of the thiol to the α position, and the thiol-yne reactions favored the formation of a *cis* vinyl sulfide product. A control reaction demonstrated that alkynyl sulfides have greater reactivity than their "all-carbon" counterparts.

## 6.2 Perspectives

Future perspectives for the macrocyclization using the hybrid reactor could include testing different types of reactions outside of oxidation of thiols into disulfides. Considering the experience of our group in the photochemical generation of thiyl radicals, macrocyclic thiol-ene/thiol-yne reactions could be attempted (Figure **6.1**). If the macrocyclic precursors were constructed using terminal alkynes and alkenes, excellent regioselectivity should be observed in the products. Macrocyclic thiol-yne processes could be problematic in that mixtures of *E* and *Z*-isomers could be formed.

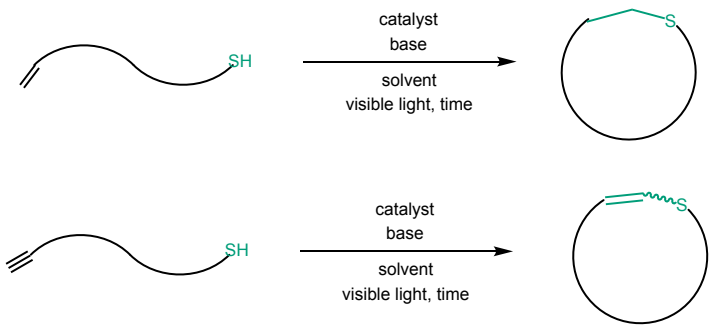


Figure **6.1** – Examples of photochemical thiol-ene (top) and thiol-yne (bottom) reactions that could be applied to macrocyclization using the hybrid reactor

Future perspectives for the thiol-yne reaction with alkynyl sulfides could include trying the thiol-yne reaction with different heteroatoms at the α position of the internal alkyne, such as oxygen or nitrogen (Figure **6.2**). The corresponding alkynyl ethers and ynamides are much more reactive than alakynyl sulfides, which may provide increased regiocontrol. However, the reactivity also means that there would be loss in terms of ease-of-handling of the compounds.

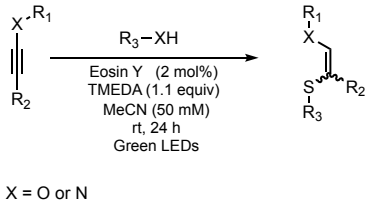


Figure **6.2** – Examples of thiol-yne reactions with different heteroatom-substituted alkynes.

# Appendix 1: Experimental Procedures and Spectral Data for Chapter 3

## Supplemental Information

General:

All reactions that were carried out under anhydrous conditions were performed under an inert argon or nitrogen atmosphere in glassware that had previously been dried overnight at 120 $^{o}$C or had been flame dried and cooled under a stream of argon or nitrogen. All chemical products were obtained from Sigma-Aldrich Chemical Company or Alfa Aesar and were reagent quality. Technical solvents were obtained from VWR International Co. Anhydrous solvents ($CH_2Cl_2$, $Et_2O$, THF, DMF, toluene, and *n*-hexane) were dried and deoxygenated using a GlassContour system (Irvine, CA). Methyl *S*-trityl-L-cysteinate, 2,2'-((2,5-dibromo-1,4-phenylene)bis(oxy)) bis(ethan-1-ol)[2] and 2,2'-((2,5-diiodo-1,4-phenylene)bis(oxy))bis(ethan-1-ol) were prepared according to their respective literature procedures. Isolated yields reflect the mass obtained following flash column silica gel chromatography. Organic compounds were purified using the method reported by W. C. Still[11] and using silica gel obtained from Silicycle Chemical division (40-63 nm; 230-240 mesh). Analytical thin-layer chromatography (TLC) was performed on glass-backed silica gel 60 coated with a fluorescence indicator (Silicycle Chemical division, 0.25 mm, $F_{254}$.). Visualization of TLC plate was performed by UV (254 nm), $KMnO_4$ or *p*-anisaldehyde stains. All mixed solvent eluents are reported as v/v solutions. Concentration refers to removal of volatiles at low pressure on a rotary evaporator. All reported compounds were homogeneous by thin layer chromatography (TLC) and by $^{1}$H NMR. NMR spectra were taken in deuterated $CDCl_3$ using Bruker AV-300 and AV- 400 instruments unless otherwise noted. Signals due to the solvent served as the internal standard ($CHCl_3$: δ 7.27 for $^{1}$H, δ 77.0 for $^{13}$C). The acquisition parameters are shown on all spectra. The $^{1}$H NMR chemical shifts and coupling constants were determined assuming first-order behavior. Multiplicity is indicated by one or more of the following: s (singlet), d (doublet), t (triplet), q (quartet), m (multiplet), br (broad); the list of couplings constants (*J*) corresponds to the order of the multiplicity assignment. High resolution mass spectrometry (HRMS) was done by the Centre régional de spectrométrie de masse at the Département de Chimie, Université de Montréal from an Agilent LC-MSD TOF system using ESI mode of ionization unless otherwise noted.

## Synthesis of macrocyclic peptide and precursor

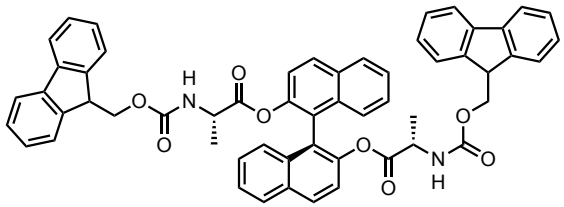

**(*S*)-[1,1'-Binaphthalene]-2,2'-diyl(2*S*,2'*S*)-bis(2-((((9*H*-fluoren-9-yl)methoxy)carbonyl)amino)propanoate) (3.3):** To a 15 mL round bottom flask equipped with a stir bar, the binol (100 mg, 0.349 mmol, 1 equiv.), Fmoc-L-alanine (269 mg, 0.864 mmol, 2.5 equiv.), EDC (8.5 mg, 0.069 mmol, 0.2 equiv.) and DIPEA (0.238 mL, 1.37 mmol, 4 equiv.) were added followed by $CH_2Cl_2$ (50 mM). The reaction mixture was stirred at room temperature overnight. The base was neutralized using 1M HCl and the solution was added to a separatory funnel containing water. The solution was extracted with $CH_2Cl_2$. The organic layer was washed with brine, dried using $MgSO_4$, filtered, and concentrated *in vacuo.* Following purification by column chromatography (3% diethyl ether in $CH_2Cl_2$), the desired product was obtained as a white solid (168 mg, 67%). $^1$H NMR (400 MHz, Methanol-*d*) δ 8.08 (d, *J* = 8.9 Hz, 2H), 8.01 (d, *J* = 8.2 Hz, 2H), 7.79 (d, *J* = 7.5 Hz, 4H), 7.64-7.14 (m, 20H), 4.31-4.04 (m, 8H), 0.60 (d, *J* = 7.2 Hz, 6H). $^{13}$C NMR (101 MHz, $CDCl_3$) δ 171.3, 155.4, 146.2, 143.9, 143.7, 141.3, 133.1, 131.8, 130.0, 128.1, 127.7, 127.1, 126.0, 125.1, 123.3, 121.6, 120.0, 67.0, 49.4, 47.1, 17.2; HRMS (ESI) m/z calculated for $C_{56}H_{44}N_2O_8$ $[M+Na]^+$ 895.2990; found 895.2987.

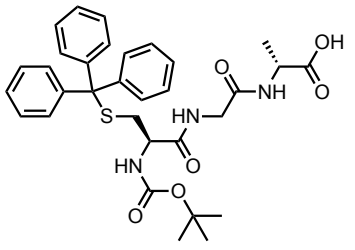

***N*-(*tert*-Butoxycarbonyl)-*S*-trityl-*L*-cysteinylglycyl-*D*-alanine (3.8):** To a 50 mL round bottom flask equipped with a stir bar was added dipeptide **3.6** activated by hydroxysuccinimide (1.19 g, 1.92

mmol, 1 equiv.), L-alanine (205 mg, 2.30 mmol, 1.2 equiv.), and DIPEA (0.401 mL, 2.30 mmol, 1.2 equiv.). DMF (6.71 mL) was added to the flask, and the reaction mixture was stirred at room temperature for 6h. The base was neutralized using 1M HCl and the solution was added to a separatory funnel containing water. The solution was extracted with EtOAc. The organic layer was washed with saturated LiCl solution and brine, dried using $MgSO_4$ and concentrated *in vacuo.* Following purification by column chromatography (40-70% EtOAc in Hexanes), the desired product was obtained as a white solid (476 mg, 42%). $^1$H NMR (400 MHz, Acetone-*d6*) δ 7.54 (br s, 1H), 7.44-7.25 (m, 16H), 6.24-6.17 (dd, *J* = 6 Hz, 1H), 4.43 (t, *J* = 5.6 Hz, 1H), 4.02-3.79 (m, 3H), 2.70-2.63 (m, 2H), 1.43 (s, 9H), 1.35 (d, *J* = 6 Hz, 4H). $^{13}$C NMR (101 MHz, $(CD_3)_2CO$) δ 173.1, 170.5, 168.4, 155.4, 144.8, 129.5, 128.0, 127.5, 126.8, 79.0, 78.3, 66.5, 54.01, 47.7, 42.4, 33.8, 27.7, 17.0; HRMS (ESI) m/z calculated for $C_{32}H_{37}N_3O_6S$ $[M+Na]^+$ 614.2295; found 614.2285.

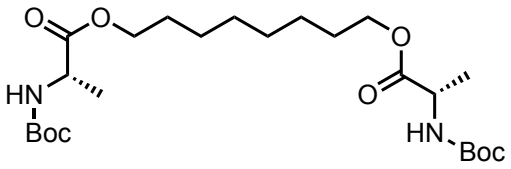


**Octane-1,8-diyl (2*S*,2'*S*)-bis(2-((*tert*-butoxycarbonyl)amino)propanoate) (3.12)**: To a 15 mL round bottom flask equipped with a stir bar was added diol **3.9** (100 mg, 0.684 mmol, 1 equiv.), *N*-Boc-L-alanine (285 mg, 1.50 mmol, 2.2 equiv.), TBTU (483 mg, 1.50 mmol, 2.2 equiv.) and DIPEA (0.476 mL, 2.74 mmol, 4 equiv.). DMF (228 mM) was added to the flask, and the reaction mixture was stirred at room temperature for 6h. The base was neutralized using 1M HCl and the solution was added to a separatory funnel containing water. The solution was extracted with EtOAc. The organic layer was washed with saturated LiCl solution and brine, dried using $MgSO_4$ and concentrated *in vacuo.* Following purification by column chromatography (30% EtOAc in Hexanes), the desired product was obtained as an oil (209 mg, 63%). $^1$H NMR (500 MHz, Chloroform-*d*) δ 5.09 (s, 2H), 4.31 (t, *J* = 6.9 Hz, 2H), 4.19-4.10 (m, 4H), 1.66-1.63 (m, 4H), 1.46 (s, 18H), 1.40 (d, *J* = 7.2 Hz, 6H), 1.34 (s, 8H). $^{13}$C NMR (101 MHz, $CDCl_3$) δ 173.5, 155.1, 79.8, 65.4, 49.3, 29.0, 28.3, 25.7, 18.8; HRMS (ESI) m/z calculated for $C_{24}H_{44}N_2O_8$ $[M+Na]^+$ 511.2990; found 511.2999.

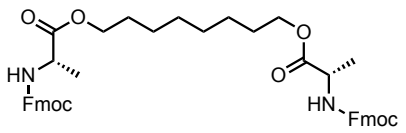


**Octane-1,8-diyl (2*S*,2'*S*)-bis(2-((((9*H*-fluoren-9-yl)methoxy)carbonyl)amino)propanoate) (3.16)**: To a 25 mL round bottom flask equipped with a stir bar was added the diol (50 mg, 0.342 mmol, 1 equiv.), Fmoc-L-alanine (234 mg, 0.752 mmol, 2.2 equiv.), TBTU (439 mg, 1.37 mmol, 4 equiv.) and DIPEA (0.238 mL, 1.37 mmol, 4 equiv.). DMF (228 mM) was added to the flask, and the reaction mixture was stirred at room temperature for 4h. The base was neutralized using 1M HCl and the solution was added to a separatory funnel containing water. The solution was extracted with EtOAc. The organic layer was washed with saturated LiCl solution and brine, dried using $MgSO_4$ and concentrated *in vacuo.* Following purification by column chromatography (30% EtOAc in Hexanes), the desired product was obtained as a white solid (168 mg, 67%). $^1$H NMR (400 MHz, Chloroform-*d*) δ 7.80-7.32 (m, 16H), 5.41 (br s, 2H), 4.45-4.15 (m, 11H), 1.66-1.33 (m, 18H). $^{13}$C NMR (101 MHz, $CDCl_3$) δ 173.2, 155.6, 143.9, 143.8, 141.3, 127.7, 127.1, 125.1, 120.0, 67.0, 65.6, 49.7, 47.2, 29.0, 28.5, 25.7, 18.8; HRMS (ESI) m/z calculated for $C_{44}H_{48}N_2O_8$ $[M+H]^+$ 733.3483; found 733.3517.

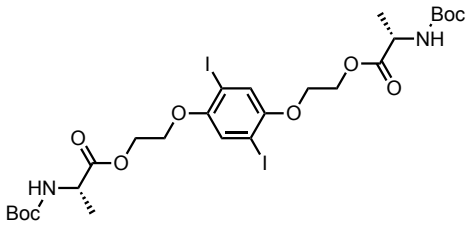


**((2,5-Diiodo-1,4-phenylene)bis(oxy))bis(ethane-2,1-diyl)(2*S*,2'*S*)-bis(2-((*tert*-butoxycarbonyl)amino)propanoate) (3.19):** To a solution of 2,2'-(2,5-diiodo-1,4-phenylene)bis(ethan-1-ol) (500 mg, 1.11 mmol, 1 eq.) in dry DMF (278 mM) was added (*tert*-butoxycarbonyl)-*L*-alanine (526mg, 2.78 mmol, 2.5 eq.), 1-Hydroxybenzotriazol hydrate (450 mg, 3.33 mmol, 3 eq.), 1-(3-dimethylaminopropyl)-3-ethylcarbodiimide HCl (639 mg, 3.33 mmol, 3 eq.) and DIPEA (718 mg, 5.56 mmol, 5 eq.). The solution was stirred at room temperature for 5h.

The base was neutralized using 1M HCl and the solution was added to a separatory funnel containing water. The solution was extracted with EtOAc. The organic layer was washed with brine, dried using $MgSO_4$ and concentrated *in vacuo.* Following purification by column chromatography (35% EtOAc in Hexanes), the desired product was obtained as a white solid (512 mg, 58%). $^1$H NMR (400 MHz, $CDCl_3$) δ 7.23(s, 2H), 5.10 (d, *J* = 5.3 Hz, 2H), 4.59-4.46 (m, 4H), 4.41(t, *J* = 6.8 Hz, 2H), 4.20-4.18 (m, 4H), 1.46 (s, 24H); $^{13}$C NMR (101 MHz, $CDCl_3$) δ 173.2, 155.1, 152.9, 123.6, 86.5, 79.9, 68.2, 63.2, 49.3, 28.3, 18.8; HRMS (ESI) m/z calculated for $C_{26}H_{38}I_2N_2O_{10}$ $[M+H]^+$ 793.0681; found 793.0689.

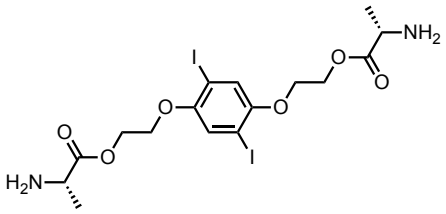


**((2,5-Diiodo-1,4-phenylene)bis(oxy))bis(ethane-2,1-diyl) (2S,2'S)-bis(2-aminopropanoate) (3.20):** ((2,5-Diiodo-1,4-phenylene)bis(oxy))bis(ethane-2,1-diyl) (2S,2'S)-bis(2-((tert-butoxycarbonyl)amino)propanoate) (511 mg, 645 mmol, 1 eq.) was added to 4M HCl in dioxane (72 mM). The solution was stirred at room temperature for 30 minutes. The solution was concentrated *in vacuo*, and the resulting solid was filtered and washed with $Et_2O$. The desired product was obtained as a white solid (316 mg, 83%).$^1$H NMR (400 MHz, $CD_3OD$) δ 7.41 (s, 2H), 4.70-4.56 (m, 4H), 4.28 (t, *J* = 4.5 Hz, 4H), 4.20 (q, *J* = 7.2 Hz, 2H), 1.63 (d, *J* = 7.2 Hz, 6H); $^{13}$C NMR (101 MHz, $CD_3OD$) δ 169.6, 153.0, 123.3, 85.8, 67.8, 64.3, 48.5, 15.0; HRMS (ESI) m/z calculated for $C_{16}H_{22}I_2N_2O_6$ $[M+H]^+$ 592.9642; found 592.9640.

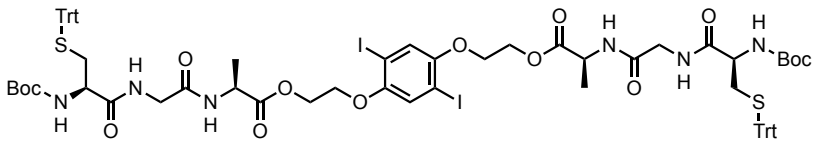

**((2,5-Diiodo-1,4-phenylene)bis(oxy))bis(ethane-2,1-diyl) (6R,6'R,12S,12'S)-bis(2,2,12-trimethyl-4,7,10-trioxo-6-((tritylthio)methyl)-3-oxa-5,8,11-triazatridecan-13-oate) (3.22):** To a solution of 2,5-dioxopyrrolidin-1-yl *N*-(*tert*-butoxycarbonyl)-*S*-trityl-*L*-cysteinylglycinate (365 mg, 701 umol, 1 eq.) in dry DMF (243 mM), was added diamine **3.20** (173 mg, 292 umol, 0.4 eq.) and DIPEA (91 mg, 701 umol, 1 eq.). The solution was stirred at room temperature 6h. The base was neutralized using 1M HCl and the solution was added to a separatory funnel containing water. The solution was extracted with EtOAc. The organic layer was washed with brine, dried using $MgSO_4$ and concentrated *in vacuo.* Following purification by column chromatography (25% Hexanes in EtOAc), the desired product was obtained as a white solid (189 mg, 40%). $^1$H NMR (400 MHz, $CDCl_3$) δ 7.46-7.21 (m, 32H), 6.90 (br s, 2H), 6.62 (d, *J* = 6 Hz, 2H), (dd, *J* = 6.2 Hz, 6 Hz, 2H), 4.61-4.44 (m, 5H), 4.16 (d, *J* = 4 Hz, 4H), 3.97-3.76 (m, 5H), 3.00-2.59 (m, 4H), 1.44 (s, 24 H); $^{13}$C NMR (101 MHz, $CDCl_3$) δ 172.3, 170.8, 155.9, 144.3, 129.5, 128.2, 127.0, 123.5, 86.5, 80.8, 68.1, 67.4, 63.3, 60.4, 54.0, 48.2, 43.1, 33.6, 29.7, 28.3, 21.1, 17.9, 17.6, 14.2; HRMS (ESI) m/z calculated for $C_{74}H_{82}I_2N_6O_{14}S_2$ $[M+H]^+$ 1597.3494; found 1597.3493.

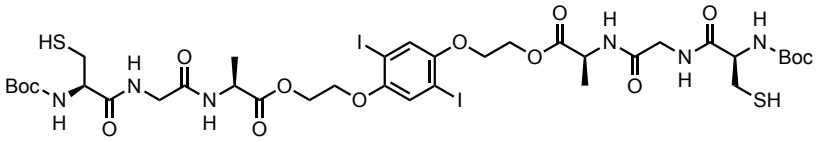

**((2,5-Diiodo-1,4-phenylene)bis(oxy))bis(ethane-2,1-diyl)(6R,6'R,12S,12'S)-bis(6-(mercaptomethyl)-2,2,12-trimethyl-4,7,10-trioxo-3-oxa-5,8,11-triazatridecan-13-oate) (3.23):** A solution of trityl-protected dithiol **3.22** (97 mg, 0.061 mmol, 1 eq.) in dry $CH_2Cl_2$ (7.7 mL, 7.9 mM) was bubbled with nitrogen. Triethylsilane (0.087 mL, 0.547 mmol, 9 eq.), then trifluoroacetic acid (0.047 mL, 0.607 mmol, 10 eq.) were added under nitrogen. The reaction was stirred at room temperature for 2h. Triethylamine (0.161 mL, 1.15 mmol, 19 eq.) was slowly added to quench the reaction and the reaction mixture was concentrated *in vacuo*. Following purification by

column chromatography (100% EtOAc), the desired product was obtained as a white solid (112 mg, 86%). $^{1}$H NMR (400 MHz, $CD_3OD$) δ 7.38 (s, 2H), 4.54-4.42(m, 6H), 4.23-4.18 (m, 6H), 3.94 (s, 4H), 3.06-2.84 (m, 4H), 1.48 (s, 24H); $^{13}$C NMR (101 MHz, $CD_3OD$) δ 172.4, 172.2, 172.1, 169.8, 153.0, 123.4, 85.9, 79.7, 68.1, 63.3, 57.2, 57.1, 42.0, 27.3, 25.7, 16.4 HRMS (ESI) m/z calculated for $C_{36}H_{54}I_2N_6O_{14}S_2$ $[M+H]^+$ 1113.1305; found 1113.1302.

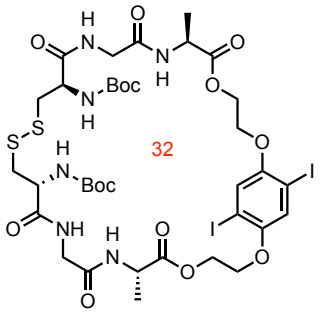


**Di-*tert*-butyl((7*S*,13*R*,18*R*,24*S*)-1$^2$,1$^5$-diiodo-7,24-dimethyl-6,9,12,19,22,25-hexaoxo-2,5,26,29-tetraoxa-15,16-dithia-8,11,20,23-tetraaza-1(1,4)-benzenacyclononacosaphane-13,18-diyl)dicarbamate (3.24):** In a pear-shaped flask, dithiol (1.0 equiv.) and eosin Y (1 mol%) were dissolved in EtOH/MeCN/$H_2O$ (9:3:1) [732 uM] before TMEDA (1 equiv.) was added. A syringe containing 45 mL of the solvent mixture and the reaction was placed in a KD Scientific syringe pump and pushed the reaction mixture at a rate of 0.250 mL/min into the photochemical reactor. The reactor was filled with 40 mL of the solvent mix and oxygen (5 psi) was bubbled through the five gas inputs. Two plates of green LEDs sandwiched the whole reactor. An Asia syringe pump by Syrris connected to the reactor by a PFA-tubing was set at a flow rate of 1.250 mL/min to remove any volume of solution in excess. After all the solvent was injected, for a total time of three hours, the lights were turned off. The reaction mixture from the reaction and the wash processes was collected in a round bottom flask covered with aluminum foil. Following concentration *in vacuo* and purification by column chromatography (0-2% MeOH in EtOAc), the desired product was obtained as a white powder (32 mg, 71 %). $^{1}$H NMR (400 MHz, $CD_3OD$) δ 7.40 (s, 2H), 4.50-4.31 (m, 8H), 4.26-4.24 (m, 4H), 3.91 (s, 4H), 3.27-2.87 (m, 4H), 1.47 (s, 24H); $^{13}$C NMR (101 MHz, DMSO) δ 172.2, 170.8, 170.6, 168.4, 155.4, 152.5, 123.4, 87.2, 79.2, 78.4,

68.1, 63.0, 47.6, 41.9, 28.2, 17.1 HRMS (ESI) m/z calculated for $C_{36}H_{52}I_2N_6O_{14}S_2$ $[M+H]^+$ 1111.1144; found 1111.1145

## Spectral data:

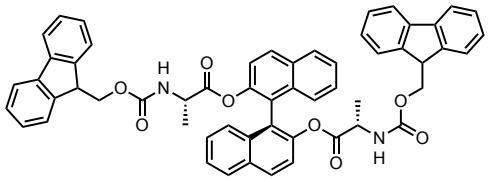

**3.3**

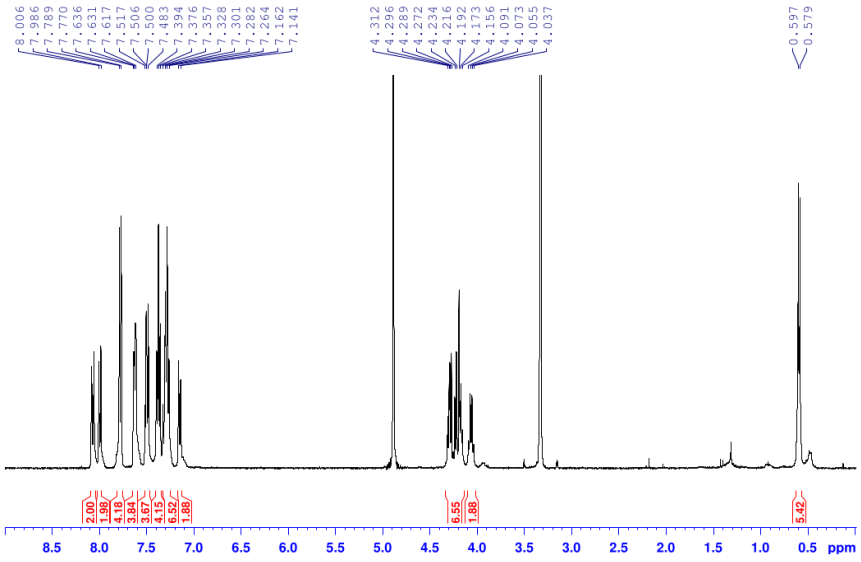


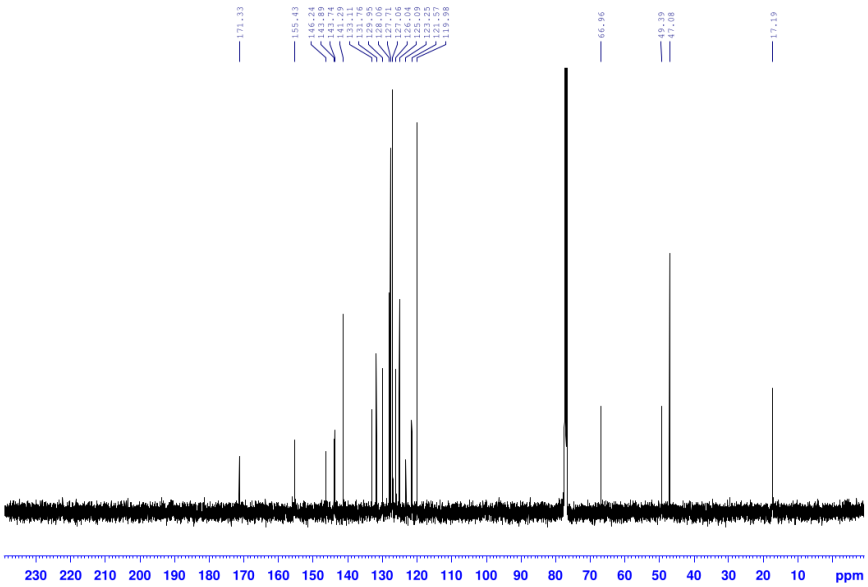

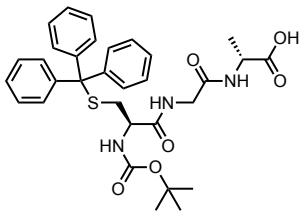
OH
O
NH
O
HN
S
HN
O
HN
O
O
O

**3.8**

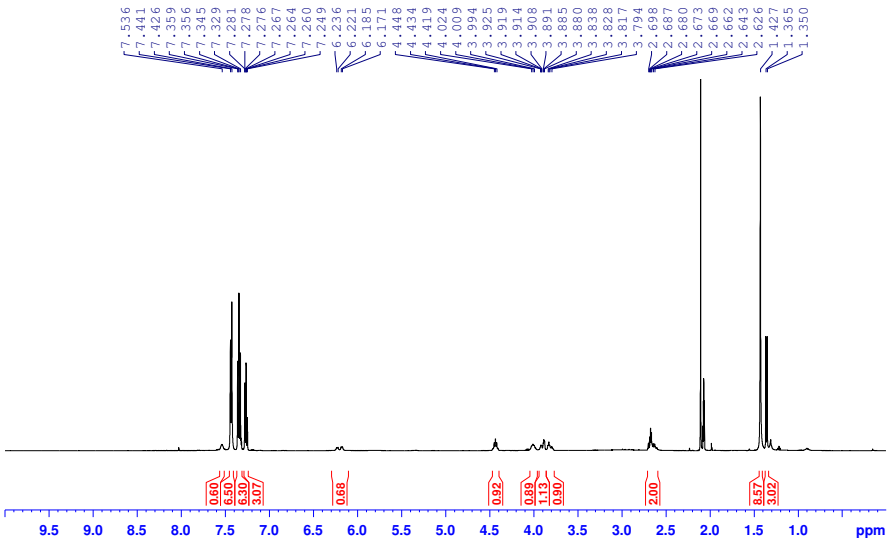
7.536
7.441
7.426
7.359
7.356
7.345
7.329
7.281
7.278
7.276
7.267
7.264
7.260
7.249
6.236
6.221
6.185
6.171
4.448
4.434
4.419
4.024
4.009
3.994
3.925
3.919
3.914
3.908
3.891
3.885
3.880
3.838
3.828
3.817
3.794
2.698
2.687
2.680
2.673
2.669
2.662
2.643
2.626
1.427
1.365
1.350
0.60
6.50
6.30
3.07
0.68
0.92
0.89
1.13
0.90
2.00
8.57
3.02
9.5
9.0
8.5
8.0
7.5
7.0
6.5
6.0
5.5
5.0
4.5
4.0
3.5
3.0
2.5
2.0
1.5
1.0
ppm

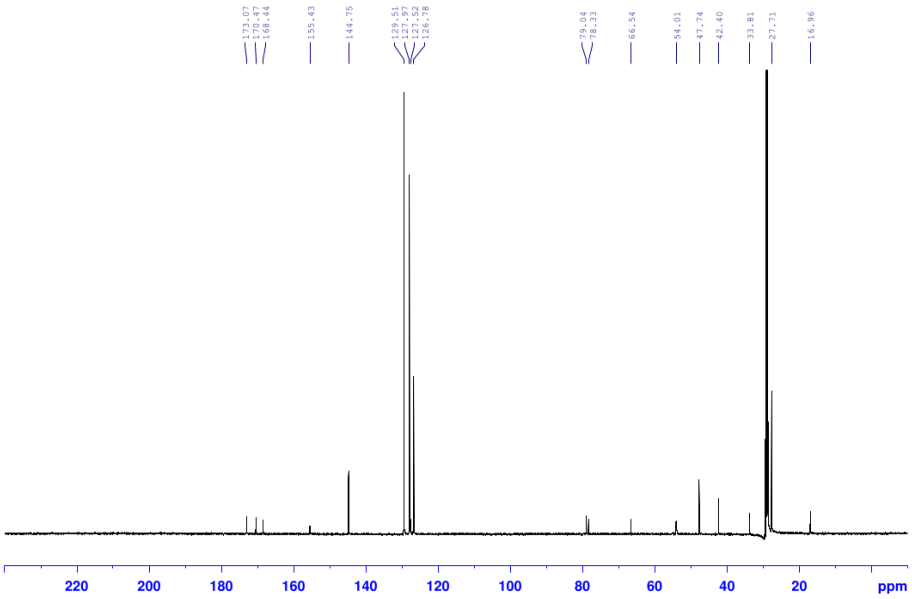
173.07
170.47
168.44
155.43
144.75
129.51
127.97
127.52
126.78
79.04
78.33
66.54
54.01
47.74
42.40
33.81
27.71
16.96
220
200
180
160
140
120
100
80
60
40
20
ppm

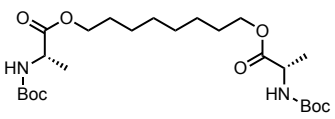
O
O
O
O
HN
Boc
HN
Boc

**3.12**

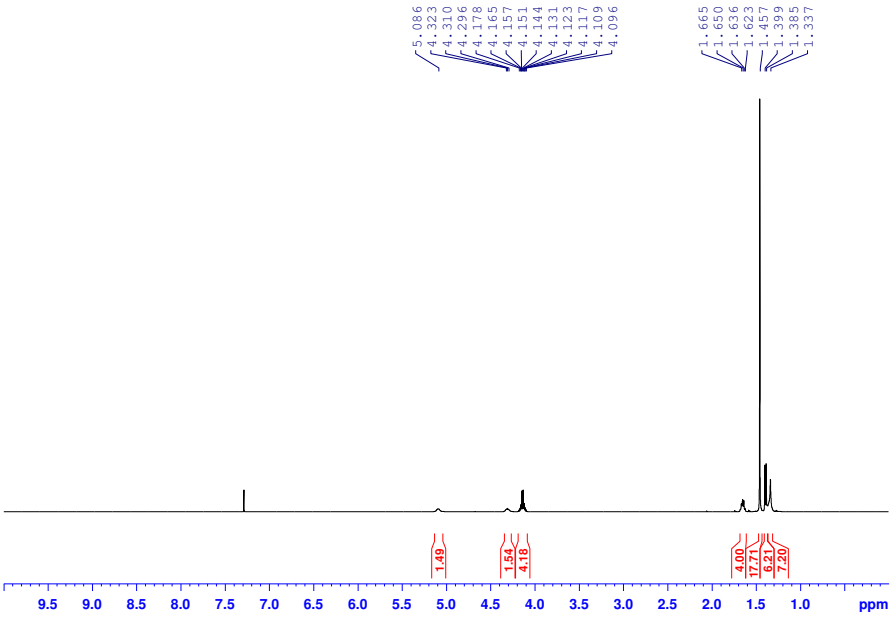
5.086
4.323
4.310
4.296
4.178
4.165
4.157
4.151
4.144
4.131
4.123
4.117
4.109
4.096
1.665
1.650
1.636
1.623
1.457
1.399
1.385
1.337
1.49
1.54
4.18
4.00
17.71
6.21
7.20
9.5
9.0
8.5
8.0
7.5
7.0
6.5
6.0
5.5
5.0
4.5
4.0
3.5
3.0
2.5
2.0
1.5
1.0
ppm

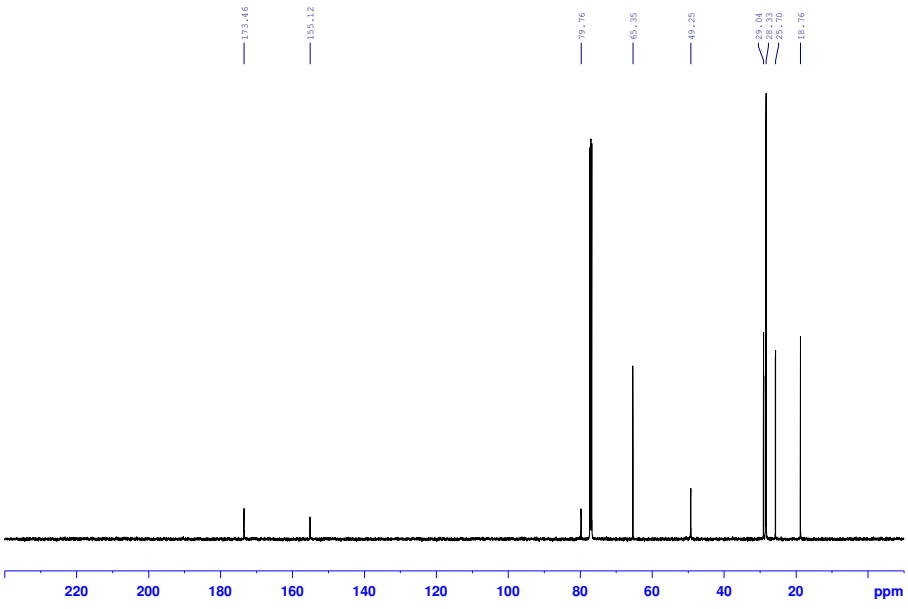
173.46
155.12
79.76
65.35
49.25
29.04
28.33
25.70
18.76
220
200
180
160
140
120
100
80
60
40
20
ppm

**3.16**

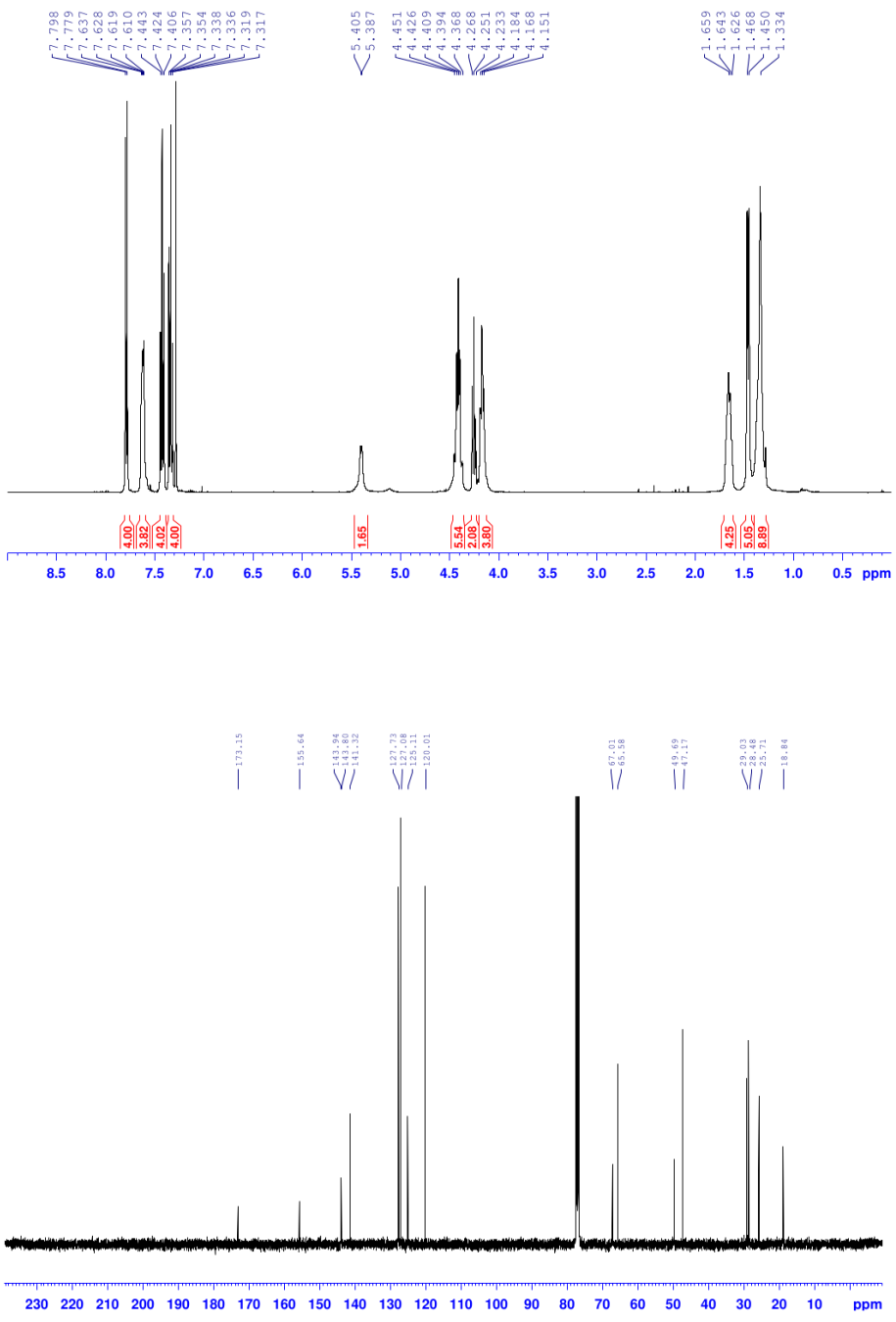
7.798
7.779
7.637
7.628
7.619
7.610
7.443
7.424
7.406
7.357
7.354
7.338
7.336
7.319
7.317
5.405
5.397
4.451
4.426
4.409
4.394
4.368
4.268
4.251
4.233
4.184
4.168
4.151
1.659
1.643
1.626
1.468
1.450
1.334
4.00
3.82
4.02
4.00
1.65
5.54
2.06
3.80
4.25
5.05
8.89
8.5 8.0 7.5 7.0 6.5 6.0 5.5 5.0 4.5 4.0 3.5 3.0 2.5 2.0 1.5 1.0 0.5 ppm
173.15
155.64
143.94
143.80
141.32
127.73
127.08
125.11
120.01
67.01
65.58
49.69
47.17
29.03
28.48
25.71
18.84
230 220 210 200 190 180 170 160 150 140 130 120 110 100 90 80 70 60 50 40 30 20 10 ppm

**3.19**

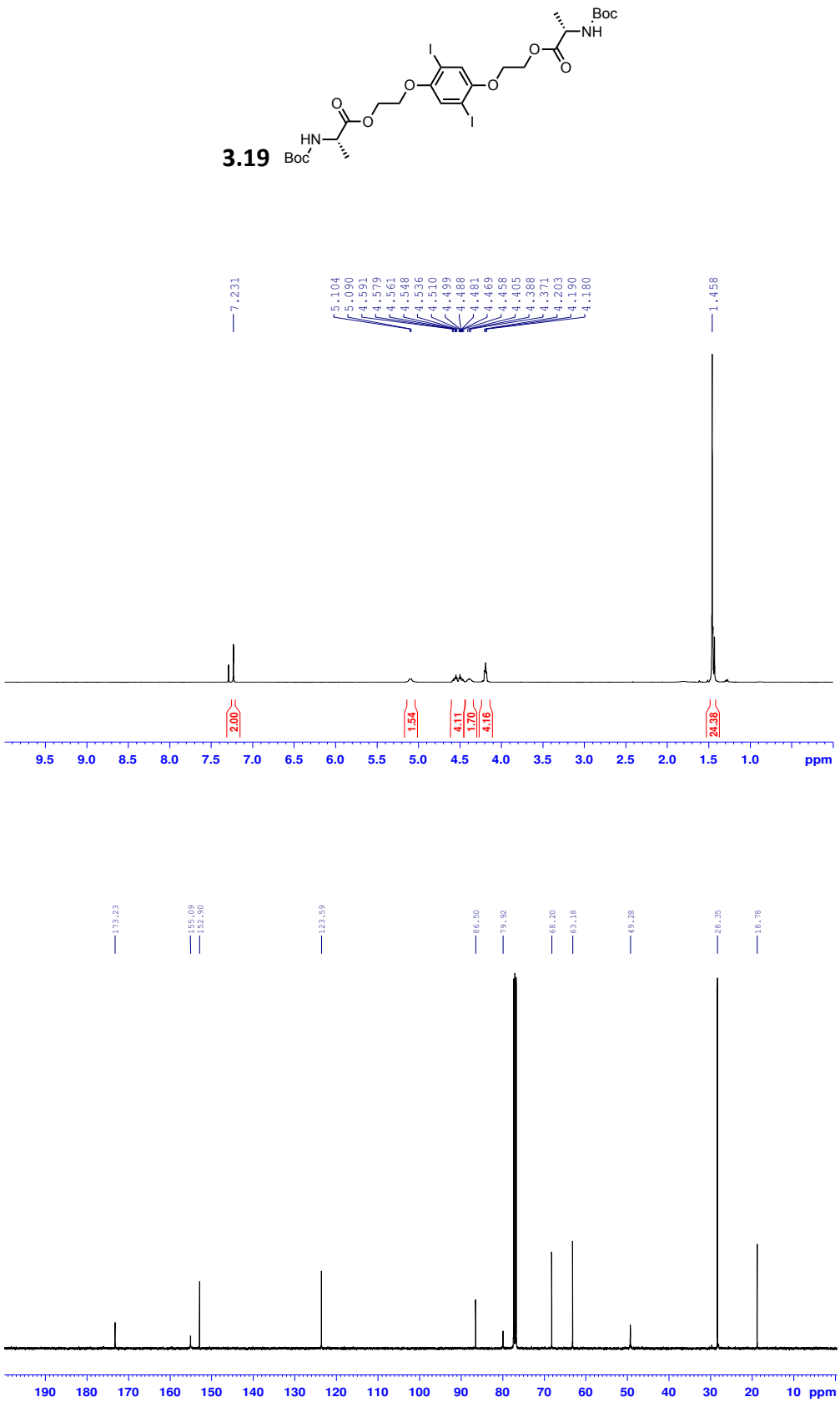
7.231
5.104
5.090
4.591
4.579
4.561
4.548
4.536
4.510
4.499
4.488
4.481
4.469
4.458
4.405
4.388
4.371
4.203
4.190
4.180
1.458
2.00
1.54
4.11
1.70
4.16
24.38
9.5 9.0 8.5 8.0 7.5 7.0 6.5 6.0 5.5 5.0 4.5 4.0 3.5 3.0 2.5 2.0 1.5 1.0 ppm
173.23
155.09
152.90
123.59
86.50
79.92
68.20
63.18
49.28
28.35
18.78
190 180 170 160 150 140 130 120 110 100 90 80 70 60 50 40 30 20 10 ppm

**3.20**

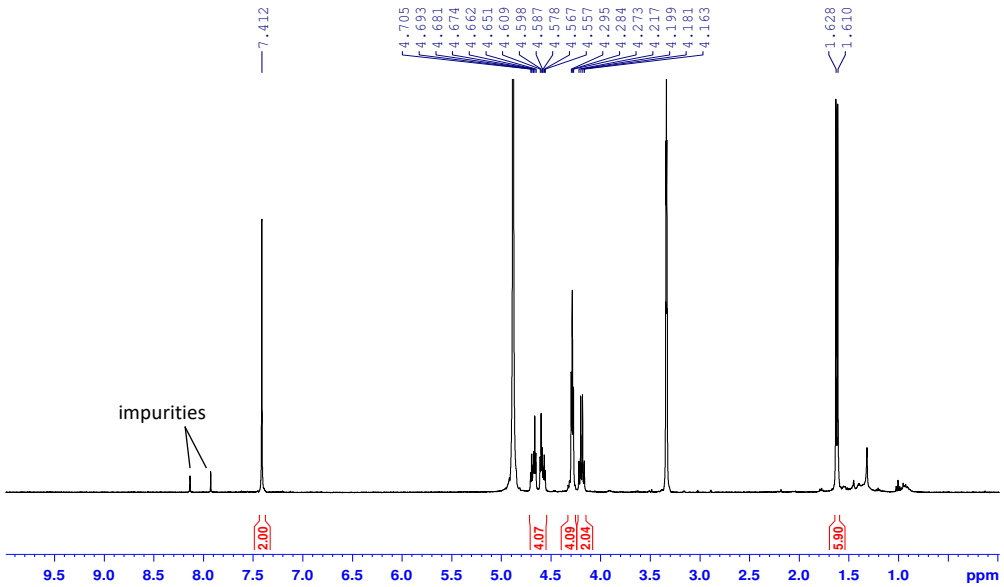
7.412
4.705
4.693
4.681
4.674
4.662
4.651
4.609
4.598
4.587
4.578
4.567
4.557
4.295
4.284
4.273
4.217
4.199
4.181
4.163
1.628
1.610
impurities
2.00
4.07
4.09
2.04
5.90
9.5 9.0 8.5 8.0 7.5 7.0 6.5 6.0 5.5 5.0 4.5 4.0 3.5 3.0 2.5 2.0 1.5 1.0 ppm

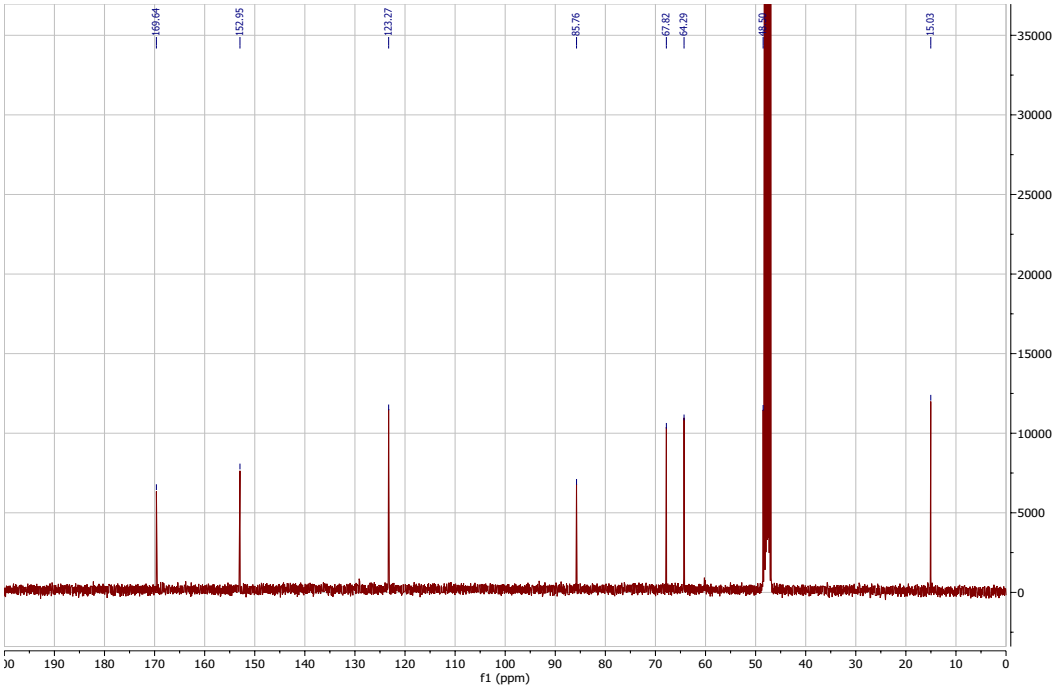
169.64
152.95
123.27
85.76
67.82
64.29
48.50
15.03
35000
30000
25000
20000
15000
10000
5000
0
190 180 170 160 150 140 130 120 110 100 90 80 70 60 50 40 30 20 10 0
f1 (ppm)

**3.22**

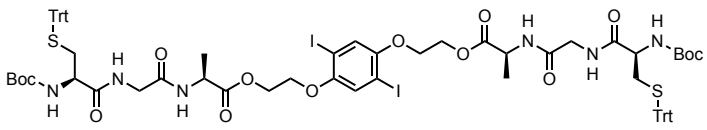
Trt
S
Boc
N
H
O
H
N
O
N
H
O
O
O
I
O
O
O
I
O
H
N
O
N
H
O
H
N
Boc
S
Trt

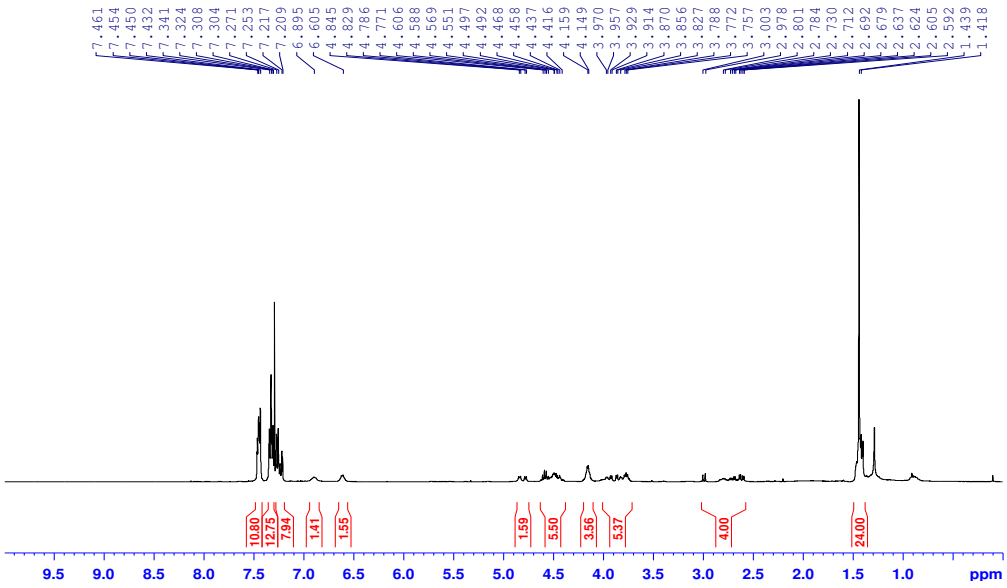
7.461
7.454
7.450
7.432
7.341
7.324
7.308
7.304
7.271
7.253
7.217
7.209
6.895
6.605
4.845
4.829
4.786
4.771
4.606
4.588
4.569
4.551
4.497
4.492
4.468
4.458
4.437
4.416
4.159
4.149
3.970
3.957
3.929
3.914
3.870
3.856
3.827
3.788
3.772
3.757
3.003
2.978
2.801
2.784
2.730
2.712
2.692
2.679
2.637
2.624
2.605
2.592
1.439
1.418
10.80
12.75
7.94
1.41
1.55
1.59
5.50
3.56
5.37
4.00
24.00
9.5
9.0
8.5
8.0
7.5
7.0
6.5
6.0
5.5
5.0
4.5
4.0
3.5
3.0
2.5
2.0
1.5
1.0
ppm

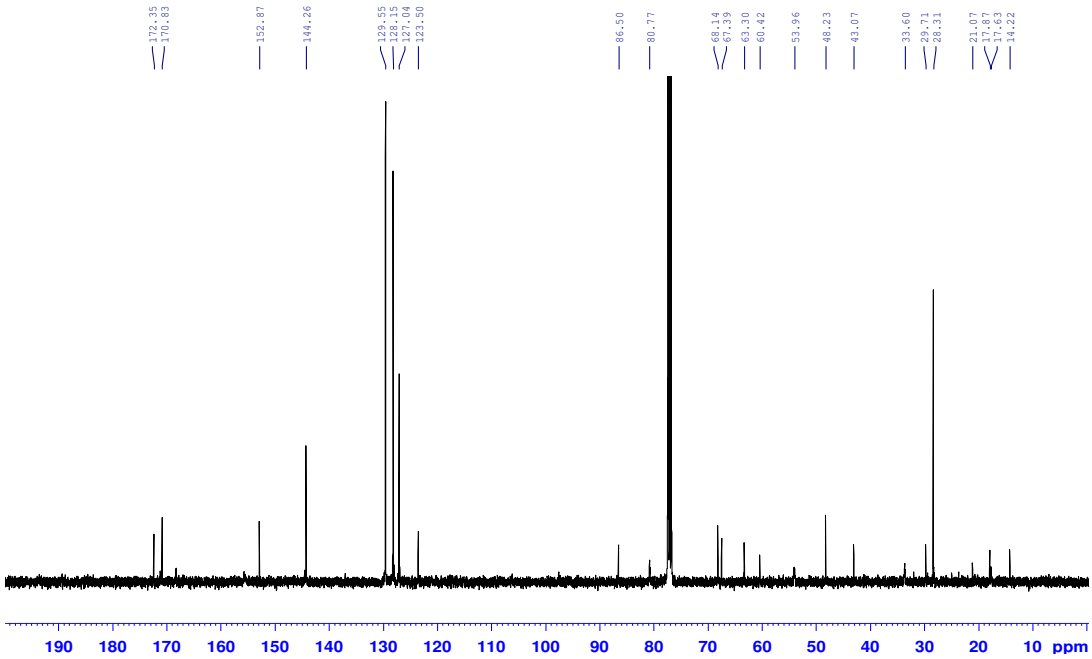
172.35
170.83
152.87
144.26
129.55
128.15
127.04
123.50
86.50
80.77
68.14
67.39
63.30
60.42
53.96
48.23
43.07
33.60
29.71
28.31
21.07
17.87
17.63
14.22
190
180
170
160
150
140
130
120
110
100
90
80
70
60
50
40
30
20
10
ppm

**3.23**

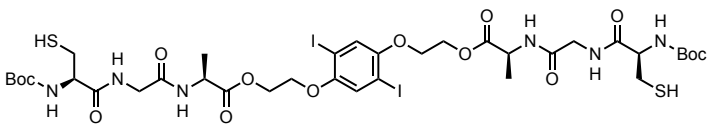

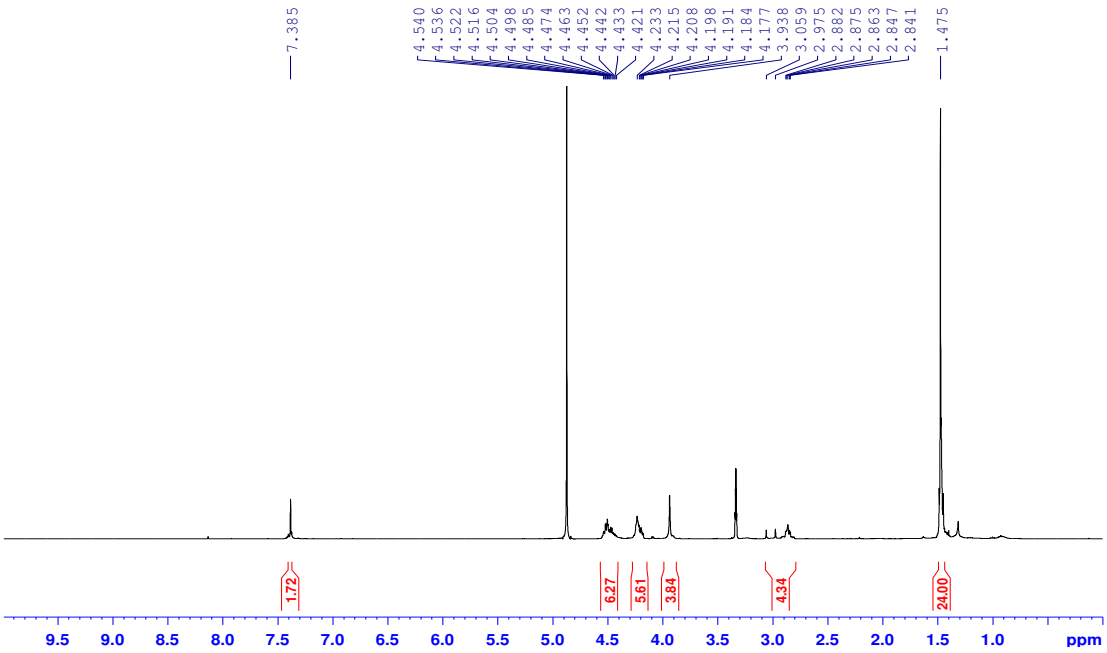
7.385
4.540
4.536
4.522
4.516
4.504
4.498
4.485
4.474
4.463
4.452
4.442
4.433
4.421
4.233
4.215
4.208
4.198
4.191
4.184
4.177
3.938
3.059
2.975
2.882
2.875
2.863
2.847
2.841
1.475
1.72
6.27
5.61
3.84
4.34
24.00
9.5 9.0 8.5 8.0 7.5 7.0 6.5 6.0 5.5 5.0 4.5 4.0 3.5 3.0 2.5 2.0 1.5 1.0
ppm

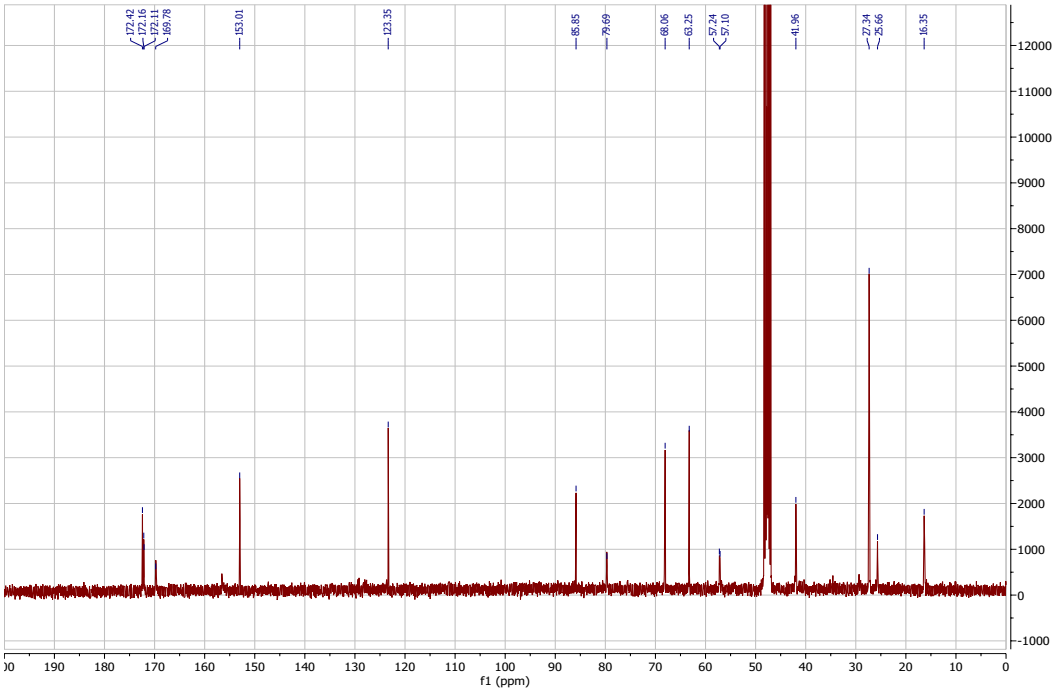
172.42
172.16
172.11
169.78
153.01
123.35
85.85
79.69
68.06
63.25
57.24
57.10
41.96
27.34
25.66
16.35
12000
11000
10000
9000
8000
7000
6000
5000
4000
3000
2000
1000
0
-1000
190 180 170 160 150 140 130 120 110 100 90 80 70 60 50 40 30 20 10 0
f1 (ppm)

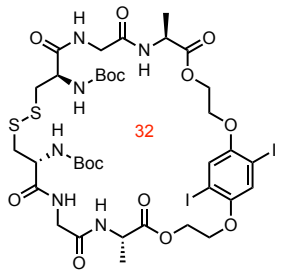
32
Boc
Boc
I
I

**3.24**

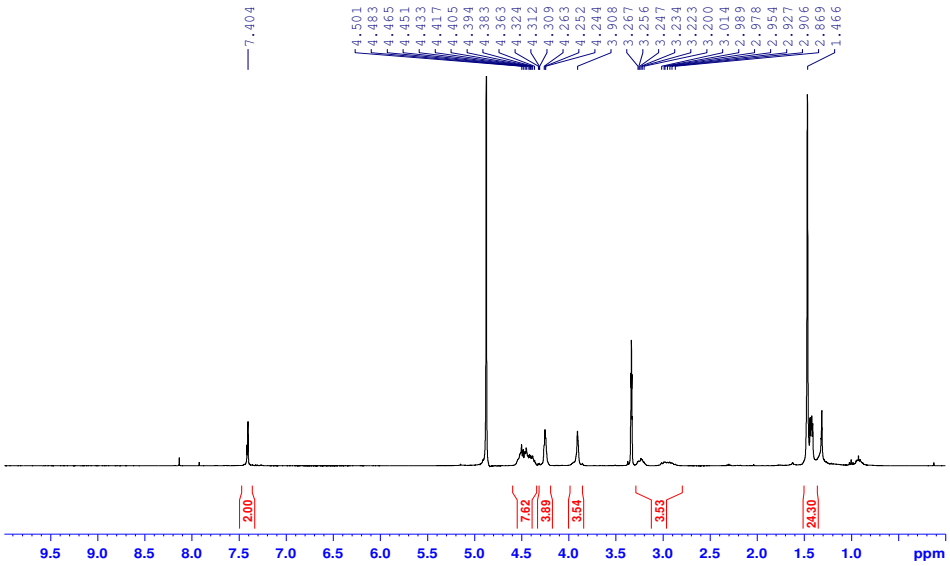
7.404
4.501
4.483
4.465
4.451
4.433
4.417
4.405
4.394
4.383
4.363
4.324
4.312
4.309
4.263
4.252
4.244
3.908
3.267
3.256
3.247
3.234
3.223
3.200
3.014
2.989
2.978
2.954
2.927
2.906
2.869
1.466
2.00
7.62
3.89
3.54
3.53
24.30
9.5 9.0 8.5 8.0 7.5 7.0 6.5 6.0 5.5 5.0 4.5 4.0 3.5 3.0 2.5 2.0 1.5 1.0
ppm

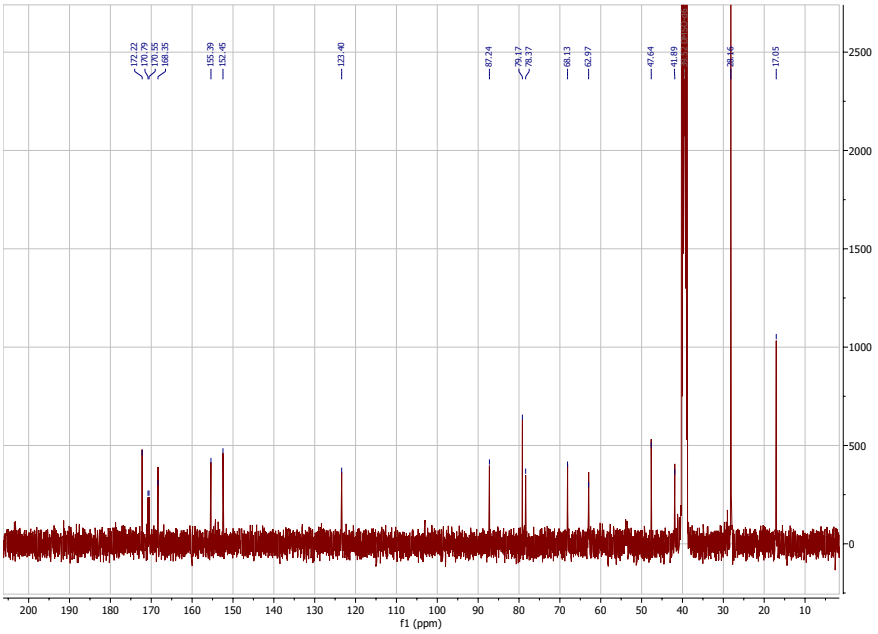
172.22
170.79
170.55
168.35
155.39
152.45
123.40
87.24
79.17
78.37
68.13
62.97
47.64
41.89
28.46
17.05
2500
2000
1500
1000
500
0
200 190 180 170 160 150 140 130 120 110 100 90 80 70 60 50 40 30 20 10
f1 (ppm)

# Appendix 2: Experimental Procedures and Spectral Data for Chapter 5

## Supplemental Information

### EXPERIMENTAL PROCEDURES AND CHARACTERIZATION DATA

### SYNTHESIS OF NEW ALKYNES AND ALKYNYL SULFIDES

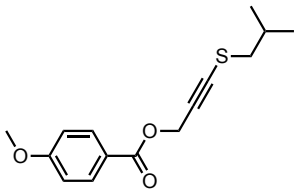

**3-(Isobutylthio)prop-2-yn-1-yl 4-methoxybenzoate (S1)**: A 118.5 mM solution of $Cu(MeCN)_4PF_6$ (0.088 g, 0.237 mmol) in acetonitrile (2 mL) was prepared under nitrogen. The solution was then sonicated under nitrogen until complete homogeneity was obtained. The bromoalkyne (0.250 g, 0.929 mmol, 1.0 equiv.), the thiol (0.111 mL, 1.02 mmol, 1.1 equiv.), dtbbpy (0.051 g, 0.186 mmol, 20 mol%) and 2,6-lutidine (0.216 mL, 1.86 mmol, 2.0 equiv.) were added to a 25 mL round bottom flask equipped with a stir bar. A septum was used to seal the vial and it was secured with parafilm. The vial was then purged with nitrogen for 2 minutes under vacuum. Afterwards, degassed acetonitrile (15 mL) was added to the flask under nitrogen. The $Cu(MeCN)_4PF_6$ solution (0.787 mL, 0.093 mmol, 10 mol%) was added to the flask in one portion. The reaction mixture was stirred for 90 minutes. Upon completion of the reaction (TLC), it was concentrated under vacuum to provide a crude reaction mixture which was purified by column chromatography on silica-gel. Following purification by column chromatography (0-4% EtOAc in Hexanes), the desired product was obtained as a colorless oil (259 mg, 85%). $^1$H NMR (400 MHz, Chloroform-*d*) δ 8.05 (d, *J* = 9.0 Hz, 2H), 6.95 (d, *J* = 8.9 Hz, 2H), 5.01 (s, 2H), 3.88 (s, 3H), 2.66 (d, *J* = 6.9 Hz, 2H), 2.06-1.96 (m, 1H), 1.05 (d, *J* = 6.7 Hz, 6H); $^{13}$C NMR (101 MHz, $CDCl_3$) δ 165.7, 163.6, 131.9, 122.1, 113.7, 87.7, 78.8, 55.5, 53.4, 44.4, 28.5, 21.5; HRMS (ESI) m/z calculated for $C_{15}H_{18}O_3S$ $[M+Na]^+$ 301.0869; found 301.0872.

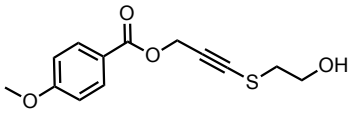

**3-((2-Hydroxyethyl)thio)prop-2-yn-1-yl 4-methoxybenzoate (5.1)**: A 118.5 mM solution of $Cu(MeCN)_4PF_6$ (0.088 g, 0.237 mmol) in acetonitrile (2 mL) was prepared under nitrogen. The solution was then sonicated under nitrogen until complete homogeneity was obtained. The bromoalkyne (0.750 g, 2.79 mmol, 1.0 equiv.), the thiol (0.215 mL, 3.07 mmol, 1.1 equiv.), dtbbpy (0.153 g, 0.557 mmol, 20 mol%) and 2,6-lutidine (0.649 mL, 5.57 mmol, 2.0 equiv.) were added to a 100 mL round bottom flask equipped with a stir bar. A septum was used to seal the vial and it was secured with parafilm. The vial was then purged with nitrogen for 2 minutes under vacuum. Afterwards, degassed acetonitrile (45 mL) was added to the flask under nitrogen. The $Cu(MeCN)_4PF_6$ solution (2.35 mL, 0.279 mmol, 10 mol %) was added to the flask in one portion. The reaction mixture was stirred for 90 minutes. Upon completion of the reaction (TLC), it was concentrated under vacuum to provide a crude reaction mixture which was purified by column chromatography on silica-gel. Following purification by column chromatography (20-33% EtOAc in Hexanes), the desired product was obtained as a colorless oil (528 mg, 71%). Characterization data was identical to that in the literature.[1]

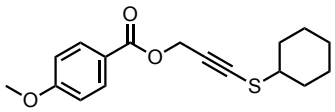

**3-(Cyclohexylthio)prop-2-yn-1-yl 4-methoxybenzoate (S2)**: A 118.5 mM solution of $Cu(MeCN)_4PF_6$ (0.088 g, 0.237 mmol) in acetonitrile (2 mL) was prepared under nitrogen. The solution was then sonicated under nitrogen until complete homogeneity was obtained. The bromoalkyne (0.205 g, 0.762 mmol, 1.0 equiv.), the thiol (0.087 mL, 0.838 mmol, 1.1 equiv.), dtbbpy (0.042 g, 0.152 mmol, 20 mol %) and 2,6-lutidine (0.177 mL, 1.52 mmol, 2.0 equiv.) were added to a 25 mL round bottom flask equipped with a stir bar. A septum was used to seal the vial and it was secured with parafilm. The vial was then purged with nitrogen for 2 minutes under vacuum. Afterwards, degassed acetonitrile (15 mL) was added to the flask under nitrogen. The $Cu(MeCN)_4PF_6$ solution (0.642 mL, 0.076 mmol, 10 mol %) was added to the flask in one portion. The reaction mixture was stirred for 90 minutes. Upon completion of the reaction (TLC), it was concentrated under vacuum to provide a crude reaction mixture which was purified by column chromatography on silica-gel. Following purification by column chromatography (2% EtOAc in Hexanes), the desired product was obtained as a colorless oil (169 mg, 73%). Characterization data was identical to that in the literature.[1]

[1] Godin, É.; Santandrea, J.; Caron, A.; Collins, S. K. General Cu-Catalyzed Csp-S Coupling. *Org. Lett.* **2020**, *22*, 5905–5909.

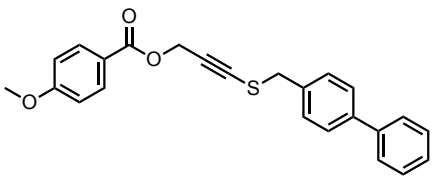

**3-(([1,1'-Biphenyl]-4-ylmethyl)thio)prop-2-yn-1-yl 4-methoxybenzoate (S3)**: A 118.5 mM solution of $Cu(MeCN)_4PF_6$ (0.088 g, 0.237 mmol) in acetonitrile (2 mL) was prepared under nitrogen. The solution was then sonicated under nitrogen until complete homogeneity was obtained. The bromoalkyne (0.100 g, 0.372 mmol, 1.0 equiv.), the thiol (0.082 mL, 0.409 mmol, 1.1 equiv.), dtbbpy (0.020 g, 0.074 mmol, 20 mol %) and 2,6-lutidine (0.087 mL, 0.743 mmol, 2.0 equiv.) were added to a 100 mL round bottom flask equipped with a stir bar. A septum was used to seal the vial and it was secured with parafilm. The vial was then purged with nitrogen for 2 minutes under vacuum. Afterwards, degassed acetonitrile (5.6 mL) was added to the flask under nitrogen. The $Cu(MeCN)_4PF_6$ solution (0.327 mL, 0.037 mmol, 10 mol %) was added to the flask in one portion. The reaction mixture was stirred for 90 minutes. Upon completion of the reaction (TLC), it was concentrated under vacuum to provide a crude reaction mixture which was purified by column chromatography on silica-gel. Following purification by column chromatography (0-5% EtOAc in Hexanes), the desired product was obtained as a white solid (528 mg, 71%). Characterization data was identical to that in the literature.[1]

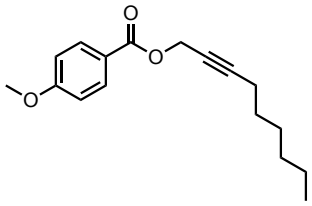

**Non-2-yn-1-yl 4-methoxybenzoate (5.4)**: To a solution of 4-methoxybenzoic acid (0.130 g, 0.856 mmol) in $CH_2Cl_2$ (2 mL) was added 2-nonyn-1-ol (0.103 mL, 0.713 mmol), DMAP (0.009 g, 0.071 mmol) and DCC (0.221 g, 1.07 mmol). The mixture was stirred for 18 hours at room temperature. Upon completion of the reaction (TLC), it was filtered and concentrated under vacuum to provide a crude reaction mixture which was purified by column chromatography on silica-gel. Following purification by column chromatography (0-2% ethyl acetate in hexanes), the desired product was obtained as a colorless oil (110 mg, 51%). $^1$H NMR (400 MHz, Chloroform-*d*) δ 8.06 (d, *J* = 9.2 Hz, 2H), 6.95 (d, *J* = 9.2 Hz, 2H), 4.91 (s, 2H), 3.88 (s, 3H), 2.27-2.23 (m, 2H), 1.58-1.51 (m, 2H), 1.44-1.26 (m, 6H), 0.90 (t, *J* = 6.7 Hz, 3H); $^{13}$C NMR (101 MHz, $CDCl_3$) δ 165.8, 163.5, 131.9, 122.2, 113.6, 87.7, 74.2, 55.4, 53.1, 31.3, 28.5, 28.4, 22.5, 18.8, 14.1; HRMS (ESI) m/z calculated for $C_{17}H_{22}O_3$ $[M+H]^+$ 275.1642; found 275.1653.

**REACTION SET-UP**

**General considerations for the photochemical reactions:**

All photocatalysis reactions for reaction optimization were performed in 15 mL screw cap vials equipped with a stir bar that were placed in a homemade photoreactor consisting of metal cylinder lined with a light-emitting diode (LED) strip connected to a power source on top of a stir plate. LED strips were purchased from Creative Lightings (https://www.creativelightings.com/ ). An external fan was used to maintain an average temperature below 30 °C.

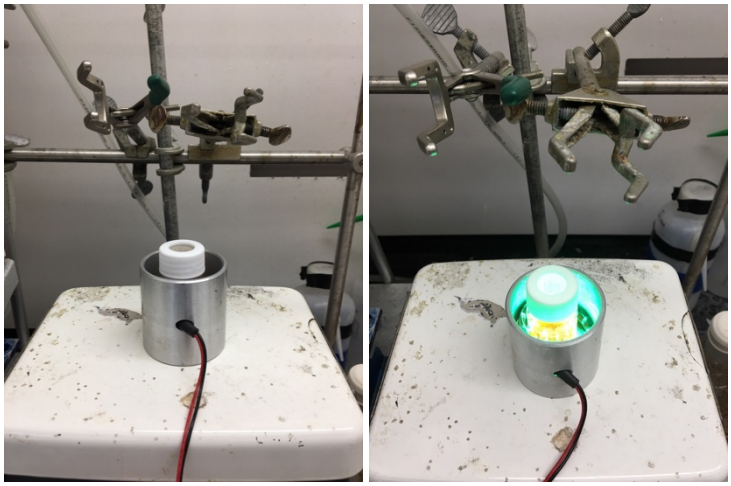

Figure **S1** – Homemade photoreactor used for the photochemical thiol-yne reaction.

**EXPERIMENTAL PROCEDURES AND CHARACTERIZATION DATA:**

**THIOL YNE REACTION ON INTERNAL ALKYNE**

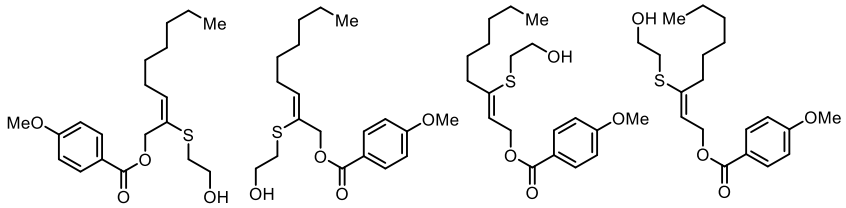


**Thiol-yne reaction on an internal alkyne**: To a 15 mL screw cap vial equipped with a stir bar was added the internal alkyne (0.110 g, 0.401 mmol, 1 equiv.), the thiol (0.031 mL, 0.441 mmol, 1.1 equiv.), TMEDA (0.066 mL, 0.441 mmol, 1.1 equiv.), and Eosin Y (0.005 g, 0.008 mmol, 2 mol %). Acetonitrile (8 mL) was added to the vial. The vial was placed in the middle of a metal cylinder containing green LEDs. The cylinder with the vial was positioned on a stir plate cooled by a fan. The LEDs were turned on and the reaction mixture was stirred for 24h at room temperature. Upon completion of the reaction (TLC), it was concentrated under vacuum to provide a crude reaction mixture which was purified by column chromatography on silica-gel. Following purification by column chromatography (10-20% EtOAc in Hexanes), a mix of the different isomers of the desired product was obtained as an oil (15 mg, 13%). HRMS (ESI) m/z calculated for $C_{19}H_{28}O_4S$ $[M+Na]^+$ 375.1601; found 375.1601.

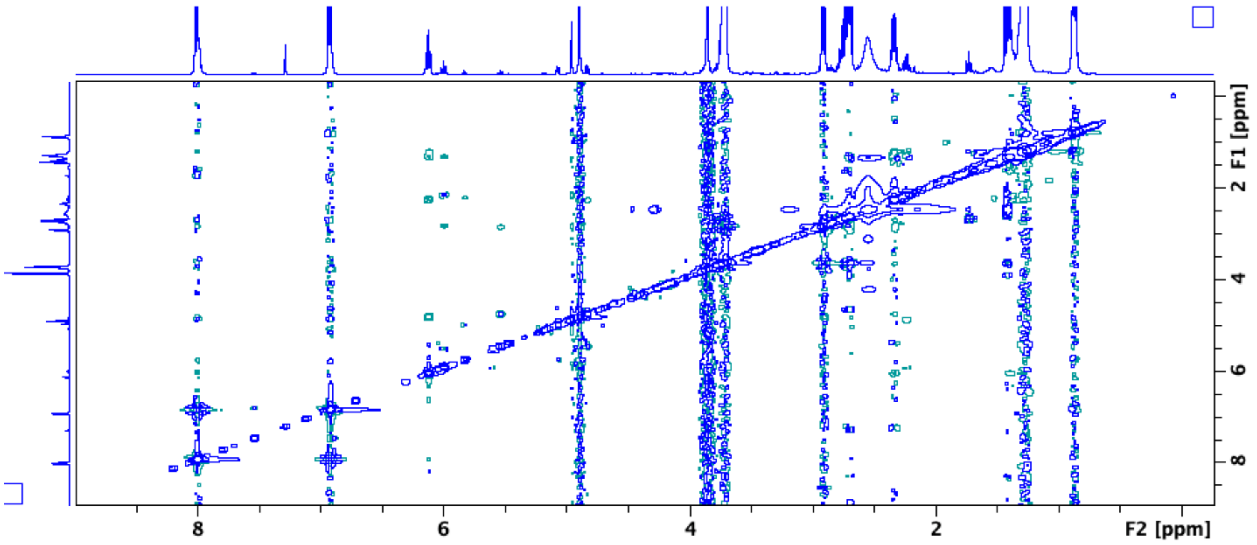

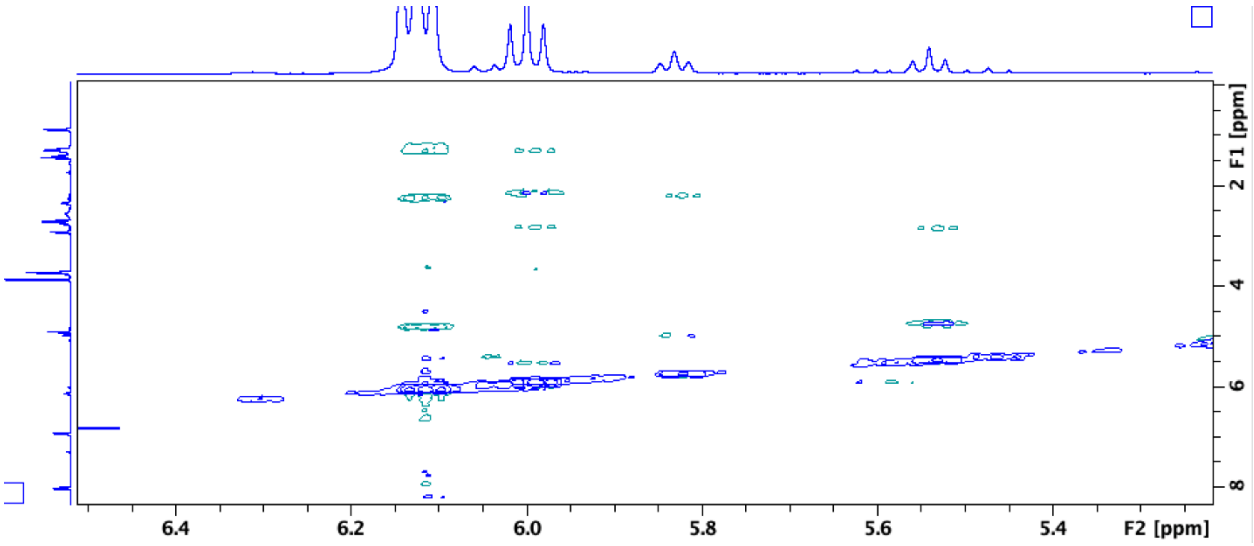
F1 [ppm]
2
4
6
8
6.4
6.2
6.0
5.8
5.6
5.4
F2 [ppm]

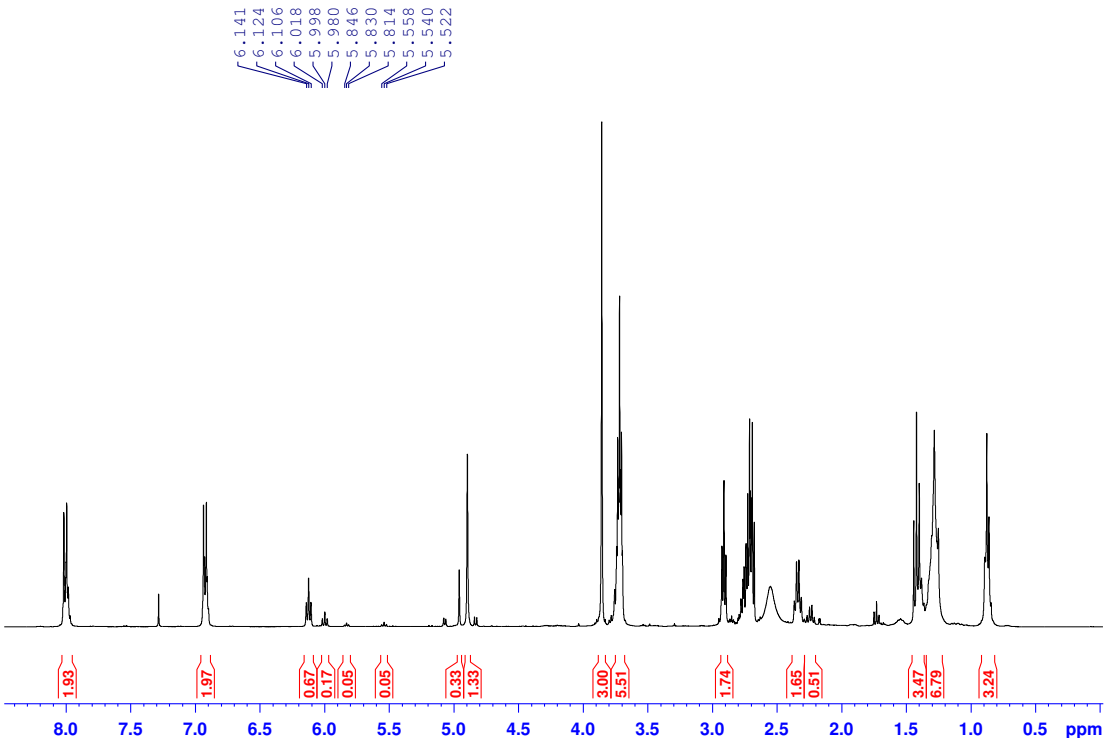
6.141
6.124
6.106
6.018
5.998
5.980
5.846
5.830
5.814
5.558
5.540
5.522
1.93
1.97
0.67
0.17
0.05
0.05
0.33
1.33
3.00
5.51
1.74
1.65
0.51
3.47
6.79
3.24
8.0
7.5
7.0
6.5
6.0
5.5
5.0
4.5
4.0
3.5
3.0
2.5
2.0
1.5
1.0
0.5
ppm

**EXPERIMENTAL PROCEDURES AND CHARACTERIZATION DATA:**

**PRODUCTS FROM THIOL YNE REACTION ON ALKYNYL SULFIDES**

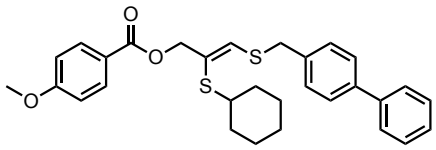

**(*Z*)-3-(([1,1'-Biphenyl]-4-ylmethyl)thio)-2-(cyclohexylthio)allyl 4-methoxybenzoate (5.5):** To a 15 mL screw cap vial equipped with a stir bar was added the alkynyl sulfide (0.050 g, 0.129 mmol, 1 equiv.), the thiol (0.015 mL, 0.142 mmol, 1.1 equiv.), TMEDA (0.021 mL, 0.142 mmol, 1.1 equiv.), and Eosin Y (0.0017 g, 0.0026 mmol, 2 mol%). Acetonitrile (2.6 mL) was added to the vial. The vial was placed in the middle of a metal cylinder containing green LEDs. The cylinder with the vial was positioned on a stir plate cooled by a fan. The LEDs were turned on and the reaction mixture was stirred for 24h at room temperature. Upon completion of the reaction (TLC), it was concentrated under vacuum to provide a crude reaction mixture which was purified by column chromatography on silica-gel. Following purification by column chromatography (2-10% EtOAc in Hexanes), the desired product was obtained as an oil (31 mg, 48%). $^{1}$H NMR (400 MHz, Chloroform-*d*) δ 7.99 (d, *J* = 9.0 Hz, 2H), 7.59-7.37 (m, 9H), 6.91 (d, *J* = 8.9 Hz, 2H), 6.77 (s, 1H), 4.86 (s, 2H), 4.00 (s, 2H), 3.84 (s, 3H), 3.21-3.14 (m, 1H), 1.97-1.25 (m, 10H); $^{13}$C NMR (101 MHz, $CDCl_3$) δ 165.8, 163.5, 140.7, 140.2, 136.7, 136.2, 131.7, 129.4, 128.8, 127.4, 127.1, 124.5, 122.4, 113.6, 67.9, 55.4, 45.0, 37.6, 33.7, 26.0, 25.7; HRMS (ESI) m/z calculated for $C_{30}H_{32}O_3S_2$ $[M+Na]^+$ 527.1685; found 527.1667.

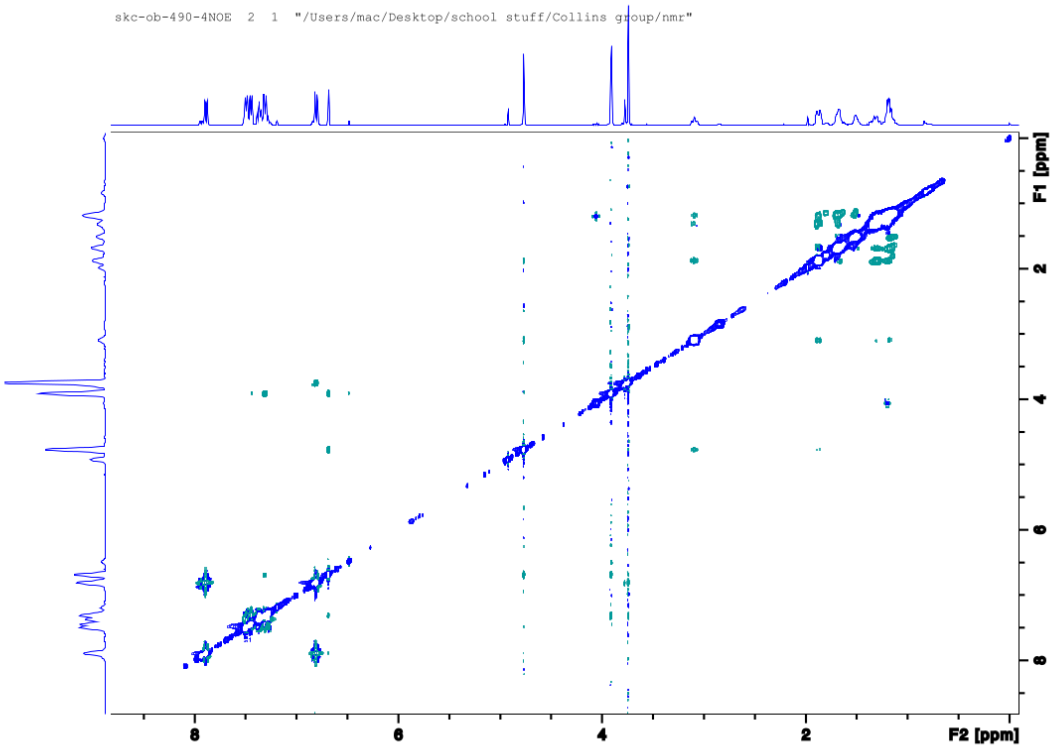

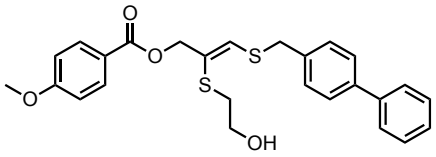

**(*Z*)-3-(([1,1'-Biphenyl]-4-ylmethyl)thio)-2-((2-hydroxyethyl)thio)allyl 4-methoxybenzoate (5.6):** To a 15 mL screw cap vial equipped with a stir bar was added the alkynyl sulfide (0.052 g, 0.134 mmol, 1 equiv.), the thiol (0.010 mL, 0.147 mmol, 1.1 equiv.), TMEDA (0.022 mL, 0.147 mmol, 1.1 equiv.), and Eosin Y (0.002 g, 0.0027 mmol, 2 mol%). Acetonitrile (1.4 mL) was added to the vial. The vial was placed in the middle of a metal cylinder containing green LEDs. The cylinder with the vial was positioned on a stir plate cooled by a fan. The LEDs were turned on and the reaction mixture was stirred for 24h at room temperature. Upon completion of the reaction (TLC), it was concentrated under vacuum to provide a crude reaction mixture which was purified by column chromatography on silica-gel. Following purification by column chromatography (2-10% EtOAc in Hexanes), the desired product was obtained as a white solid (25 mg, 40%). $^{1}$H NMR (400 MHz, Chloroform-*d*) δ 7.98 (d, *J* = 9.0 Hz, 2H), 7.60-54 (m, 4H), 7.49-7.38 (m, 5H), 6.92 (d, *J* = 8.9 Hz, 2H), 6.83 (s, 1H), 4.87 (s, 2H), 4.03 (s, 2H), 3.85 (s, 3H), 3.67 (t, *J* = 5.5 Hz, 2H), 2.97 (t, *J* = 5.6 Hz, 2H); $^{13}$C NMR (101 MHz, $CDCl_3$) δ 165.8, 163.6, 140.6, 140.4, 137.7, 136.2, 131.7, 129.3, 128.8, 127.5, 127.1, 123.7, 122.1, 113.7, 66.9, 60.3, 55.4, 37.5, 36.0; HRMS (ESI) m/z calculated for $C_{26}H_{26}O_4S_2$ $[M+Na]^+$ 489.1165; found 489.1151.

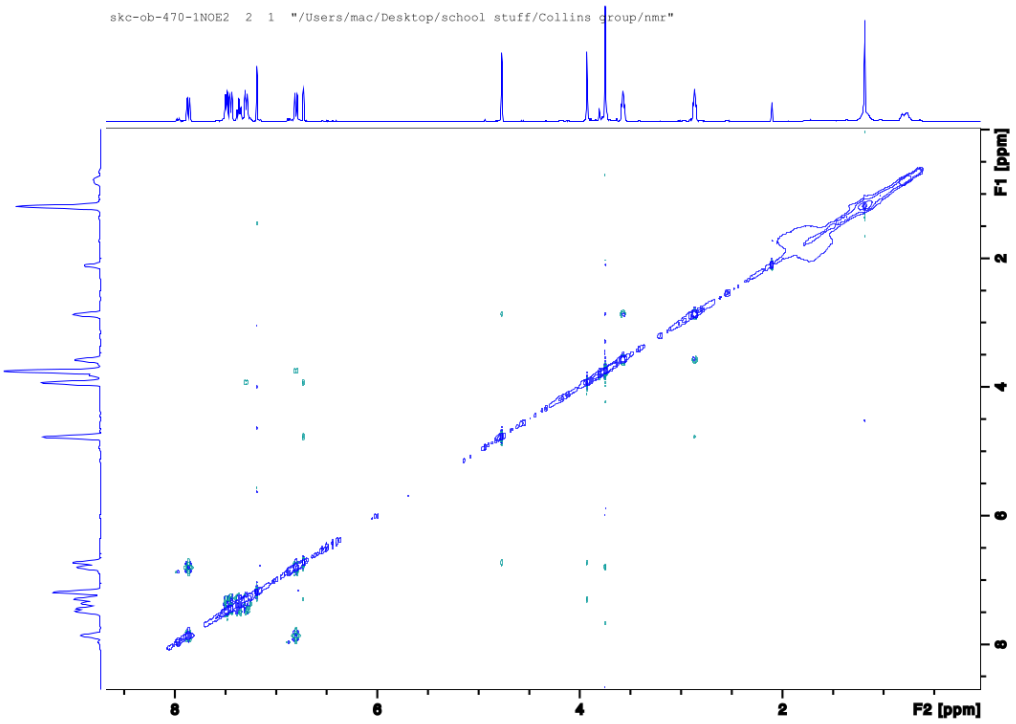

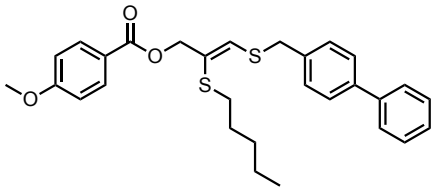

**(*Z*)-3-(([1,1'-Biphenyl]-4-ylmethyl)thio)-2-(pentylthio)allyl 4-methoxybenzoate (5.7):** To a 15 mL screw cap vial equipped with a stir bar was added the alkynyl sulfide (0.063 g, 0.162 mmol, 1 equiv.), the thiol (0.019 g, 0.178 mmol, 1.1 equiv.), TMEDA (0.027 mL, 0.178 mmol, 1.1 equiv.), and Eosin Y (0.002 g, 0.0032 mmol, 2 mol%). Acetonitrile (3.2 mL) was added to the vial. The vial was placed in the middle of a metal cylinder containing green LEDs. The cylinder with the vial was positioned on a stir plate cooled by a fan. The LEDs were turned on and the reaction mixture was stirred for 24h at room temperature. Upon completion of the reaction (TLC), it was concentrated under vacuum to provide a crude reaction mixture which was purified by column chromatography on silica-gel. Following purification by column chromatography (2-10% EtOAc in Hexanes), the desired product was obtained as a white solid (39 mg, 49%). $^{1}$H NMR (400 MHz, Chloroform-*d*) δ 7.97 (d, *J* = 9.0 Hz, 2H), 7.60 (dd, *J* = 8.2 Hz, 4H), 7.48-7.35 (m, 5H), 6.91 (d, *J* = 9.0 Hz, 2H), 6.67 (s, 1H), 4.87 (s, 2H), 4.01 (s, 2H), 3.84 (s, 3H), 2.80 (t, *J* = 7.4 Hz, 2H), 1.64-1.57 (m, 2H), 1.41-1.31 (m, 4H), 0.90-0.87 (t, *J* = 7.2 Hz, 3H); $^{13}$C NMR (101 MHz, $CDCl_3$) δ 165.8, 163.5, 140.7, 140.3, 136.6, 133.8, 131.7, 129.4, 128.8, 127.4, 127.1, 125.5, 122.4, 113.7, 67.0, 55.4, 37.6, 32.3, 30.9, 29.7, 22.3, 14.0; HRMS (ESI) m/z calculated for $C_{29}H_{32}O_3S_2$ $[M+Na]^+$ 515.1685; found 515.1692.

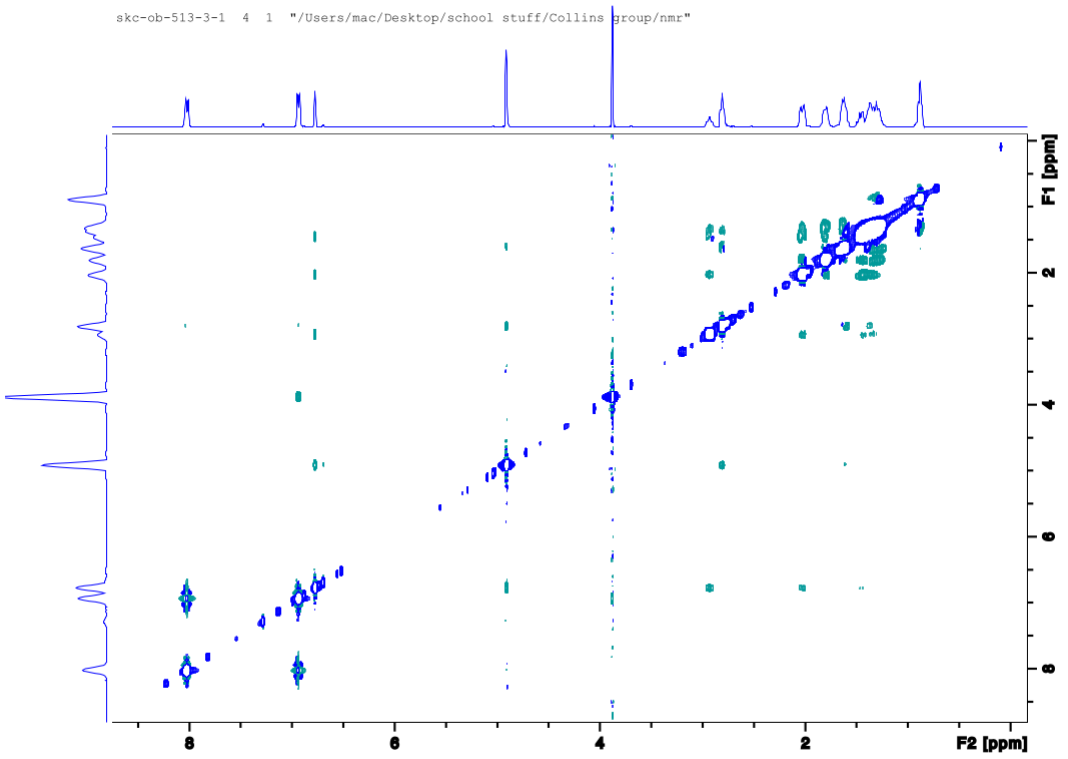

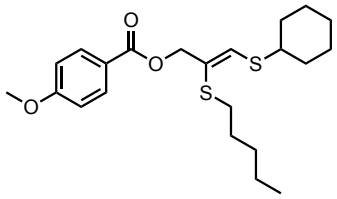

**(*Z*)-3-(Cyclohexylthio)-2-(pentylthio)allyl 4-methoxybenzoate (5.8):** To a 15 mL screw cap vial equipped with a stir bar was added the alkynyl sulfide (0.045 g, 0.148 mmol, 1 equiv.), the thiol (0.017 mL, 0.163 mmol, 1.1 equiv.), TMEDA (0.025 mL, 0.163 mmol, 1.1 equiv.), and Eosin Y (0.0021 g, 0.002 mmol, 2 mol%). Acetonitrile (3 mL) was added to the vial. The vial was placed in the middle of a metal cylinder containing green LEDs. The cylinder with the vial was positioned on a stir plate cooled by a fan. The LEDs were turned on and the reaction mixture was stirred for 24h at room temperature. Upon completion of the reaction (TLC), it was concentrated under vacuum to provide a crude reaction mixture which was purified by column chromatography on silica-gel. Following purification by column chromatography (2-6% Diethyl ether in Hexanes), the desired product was obtained as a colorless oil (34 mg, 56%). $^{1}$H NMR (400 MHz, Chloroform-*d*) δ 8.04 (d, *J* = 9.0 Hz, 2H), 6.95 (d, *J* = 9.0 Hz, 2H), 6.78 (s, 1H), 4.91 (s, 2H), 2.97-2.90 (m, 1H), 2.81 (t, *J* = 7.4 Hz, 3H), 2.04-2.01 (m, 2H), 1.81-1.79 (m, 2H), 1.65-1.58 (m, 3H), 1.50-1.25 (m, 9H), 0.88 (t, *J* = 7.2 Hz, 3H); $^{13}$C NMR (101 MHz, $CDCl_3$) δ 166.0, 163.5, 135.0, 131.7, 124.2, 122.5, 113.6, 67.7, 55.5, 46.1, 33.9, 32.1, 31.0, 29.7, 25.5, 22.3, 14.0; HRMS (ESI) m/z calculated for $C_{22}H_{32}O_3S_2$ $[M+K]^+$ 447.1424; found 447.1412.

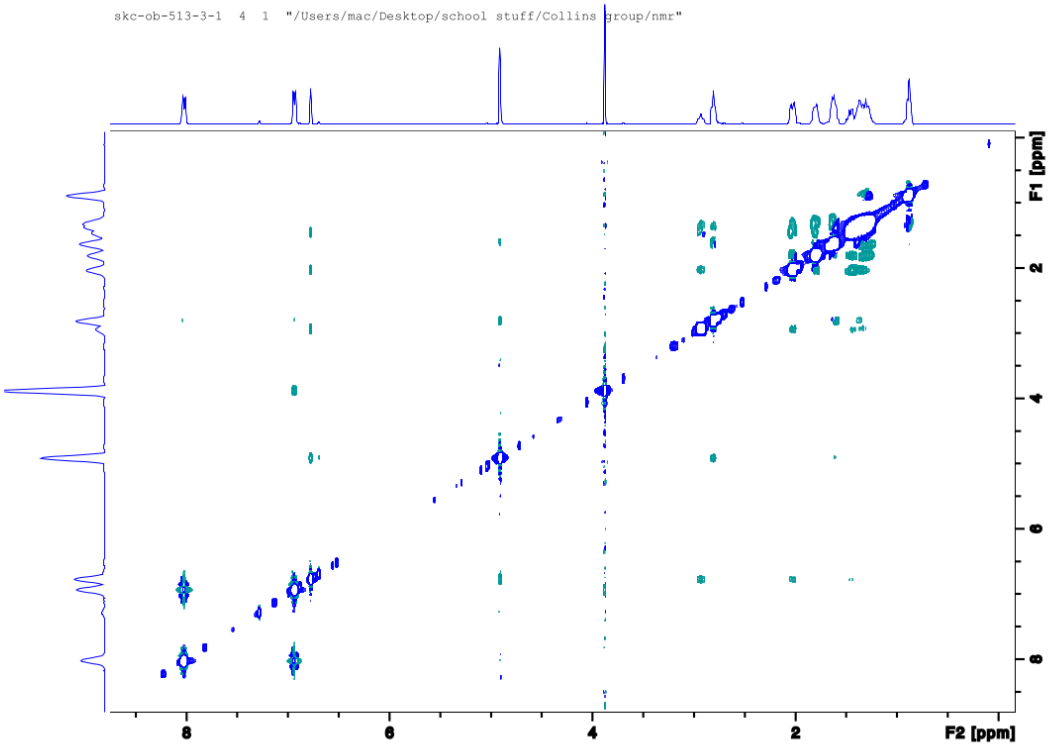

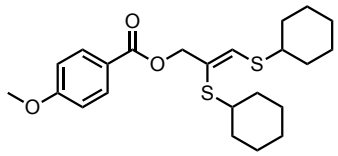

**(*Z*)-2,3-Bis(cyclohexylthio)allyl 4-methoxybenzoate (5.9)**: To a 15 mL screw cap vial equipped with a stir bar was added the alkynyl sulfide (0.050 g, 0.164 mmol, 1 equiv.), the thiol (0.022 mL, 0.181 mmol, 1.1 equiv.), TMEDA (0.027 mL, 0.181 mmol, 1.1 equiv.), and Eosin Y (0.0021 g, 0.0033 mmol, 2 mol%). Acetonitrile (3.3 mL) was added to the vial. The vial was placed in the middle of a metal cylinder containing green LEDs. The cylinder with the vial was positioned on a stir plate cooled by a fan. The LEDs were turned on and the reaction mixture was stirred for 24h at room temperature. Upon completion of the reaction (TLC), it was concentrated under vacuum to provide a crude reaction mixture which was purified by column chromatography on silica-gel. Following purification by column chromatography (2-5% Diethyl ether in Hexanes), the desired product was obtained as a colorless oil (43 mg, 63%). $^{1}$H NMR (400 MHz, Chloroform-*d*) δ 8.04 (d, *J* = 8.9 Hz, 2H), 6.95 (d, *J* = 8.9 Hz, 2H), 6.88 (s, 1H), 4.90 (s, 2H), 3.89 (s, 3H), 3.23-3.16 (m, 1H), 2.95-2.90 (m, 1H), 2.04-1.27 (m, 20H); $^{13}$C NMR (101 MHz, $CDCl_3$) δ 166.0, 163.5, 137.6, 131.7, 123.2, 122.6, 113.6, 68.6, 55.5, 46.0, 44.8, 33.9, 33.7, 26.0, 25.7, 25.5; HRMS (ESI) m/z calculated for $C_{23}H_{32}O_3S_2$ $[M+K]^+$ 459.1424; found 459.1427.

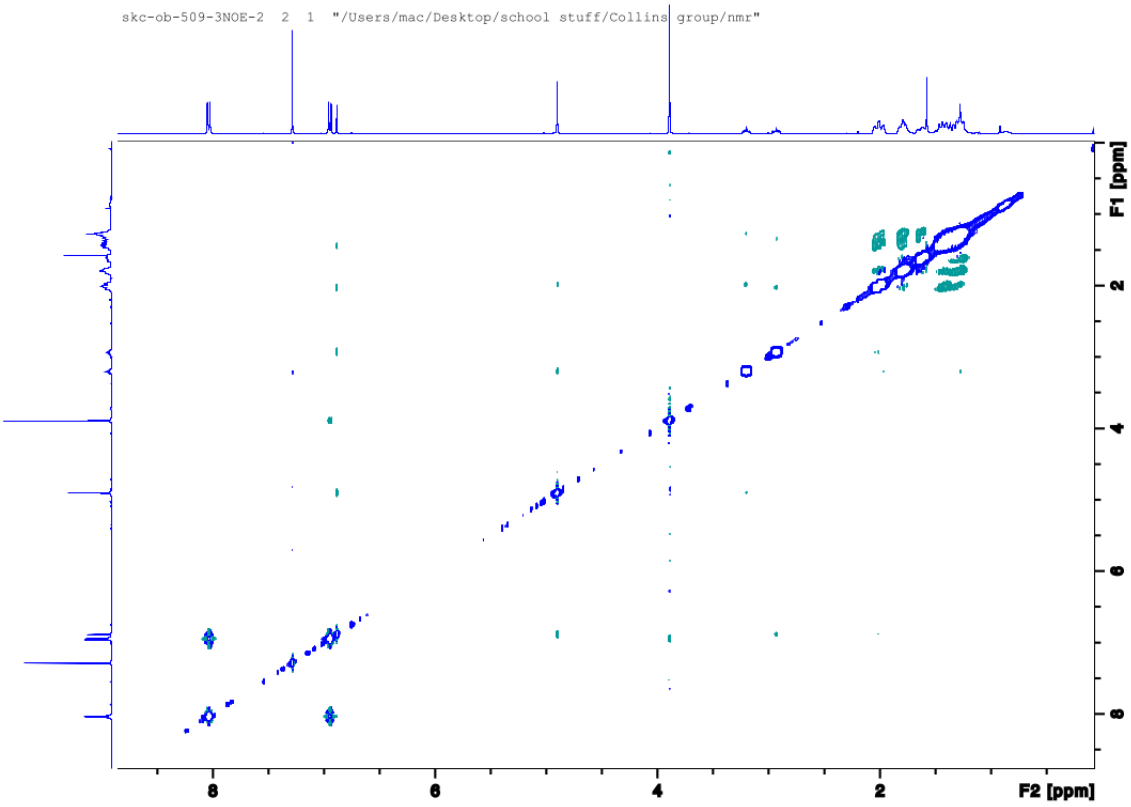

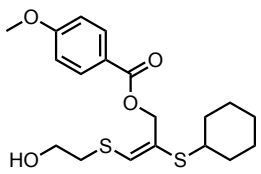

**(*E*)-2-(Cyclohexylthio)-3-((2-hydroxyethyl)thio)allyl 4-methoxybenzoate (5.10):** To a 15 mL screw cap vial equipped with a stir bar was added the alkynyl sulfide (0.052 g, 0.194 mmol, 1 equiv.), the thiol (0.025 g, 0.214 mmol, 1.1 equiv.), TMEDA (0.032 mL, 0.214 mmol, 1.1 equiv.), and Eosin Y (0.0025 g, 0.0039 mmol, 2 mol%). Acetonitrile (3.9 mL) was added to the vial. The vial was placed in the middle of a metal cylinder containing green LEDs. The cylinder with the vial was positioned on a stir plate cooled by a fan. The LEDs were turned on and the reaction mixture was stirred for 24h at room temperature. Upon completion of the reaction (TLC), it was concentrated under vacuum to provide a crude reaction mixture which was purified by column chromatography on silica-gel. Following purification by column chromatography (20-40% EtOAc in Hexanes), the desired product was obtained as an oil (12 mg, 16%). $^{1}$H NMR (400 MHz, Chloroform-*d*) δ 8.06 (d, *J* = 9.0 Hz, 2H), 6.95 (d, *J* = 8.8 Hz, 2H), 6.56 (s, 1H), 5.06 (s, 2H), 3.89 (s, 3H), 3.82 (t, *J* = 5.7 Hz, 2H), 3.07-2.98 (m, 1H), 2.94 (t, *J* = 5.8 Hz, 2H), 1.96 (d, *J* = 10.3 Hz, 2H), 1.77-1.75 (m, 2H), 1.61-1.59 (m, 1H), 1.33-1.23 (m, 5H); $^{13}$C NMR (101 MHz, $CDCl_3$) δ 166.1, 163.5, 133.4, 131.9, 128.0, 122.3, 113.7, 64.3, 61.4, 55.5, 45.1, 38.0, 33.3, 29.7, 25.9, 25.7; HRMS (ESI) m/z calculated for $C_{19}H_{26}O_4S_2$ $[M+Na]^+$ 405.1165; found 405.1165.

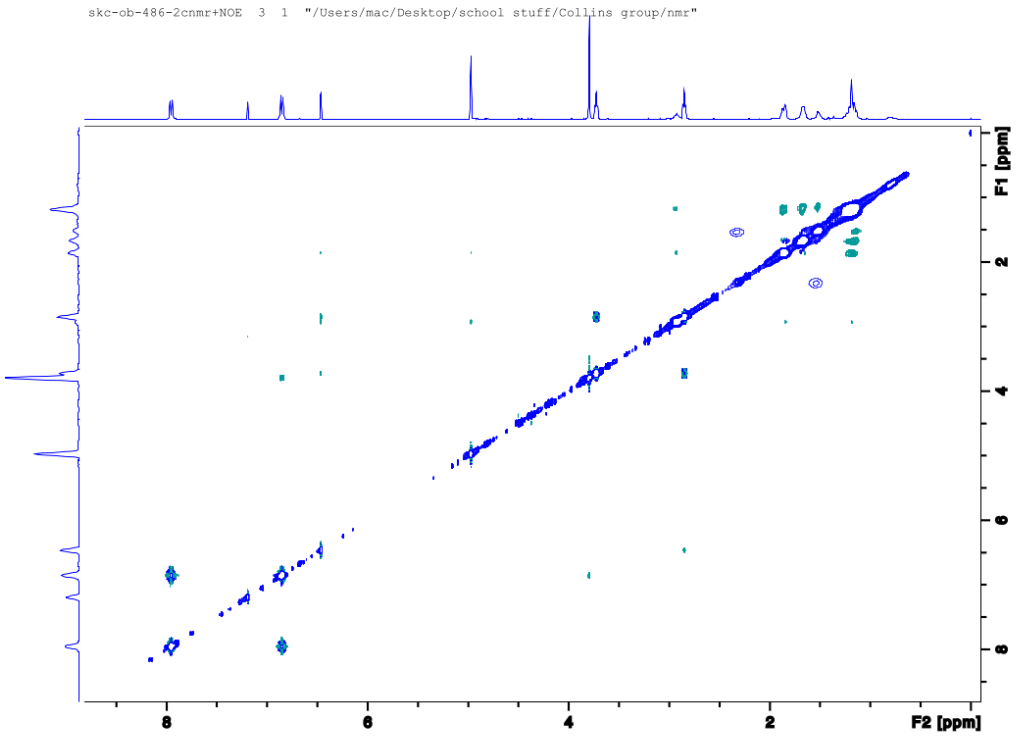

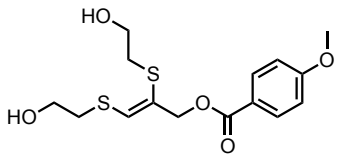


**(*Z*)-2,3-Bis((2-hydroxyethyl)thio)allyl 4-methoxybenzoate (5.11)**: To a 15 mL screw cap vial equipped with a stir bar was added the alkynyl sulfide (0.051 g, 0.192 mmol, 1 equiv.), the thiol (0.017 g, 0.211 mmol, 1.1 equiv.), TMEDA (0.032 mL, 0.211 mmol, 1.1 equiv.), and Eosin Y (0.003 g, 0.0038 mmol, 2 mol%)Acetonitrile (3.8 mL) was added to the vial. The vial was placed in the middle of a metal cylinder containing green LEDs. The cylinder with the vial was positioned on a stir plate cooled by a fan. The LEDs were turned on and the reaction mixture was stirred for 24h at room temperature. Upon completion of the reaction (TLC), it was concentrated under vacuum to provide a crude reaction mixture which was purified by column chromatography on silica-gel. Following purification by column chromatography (60% EtOAc in Hexanes), the desired product was obtained as an oil (38 mg, 58%). $^{1}$H NMR (400 MHz, Acetone-*d6*) δ 8.02 (d, *J* = 8.8 Hz, 2H), 7.06 (d, *J* = 8.8 Hz, 2H), 7.02 (s, 1H), 4.94 (s, 2H), 3.90 (s, 3H), 3.76 (t, *J* = 6.4 Hz, 2H), 3.70 (t, *J* = 6.8 Hz, 2H), 2.98-2.93 (m, 4H); $^{13}$C NMR (101 MHz, $CDCl_3$) δ 165.9, 163.7, 139.1, 131.8, 124.5, 122.1, 113.8, 67.0, 61.8, 60.3, 55.5, 37.1, 35.9; HRMS (ESI) m/z calculated for $C_{15}H_{20}O_5S_2$ $[M+Na]^+$ 367.0644; found 367.0645.

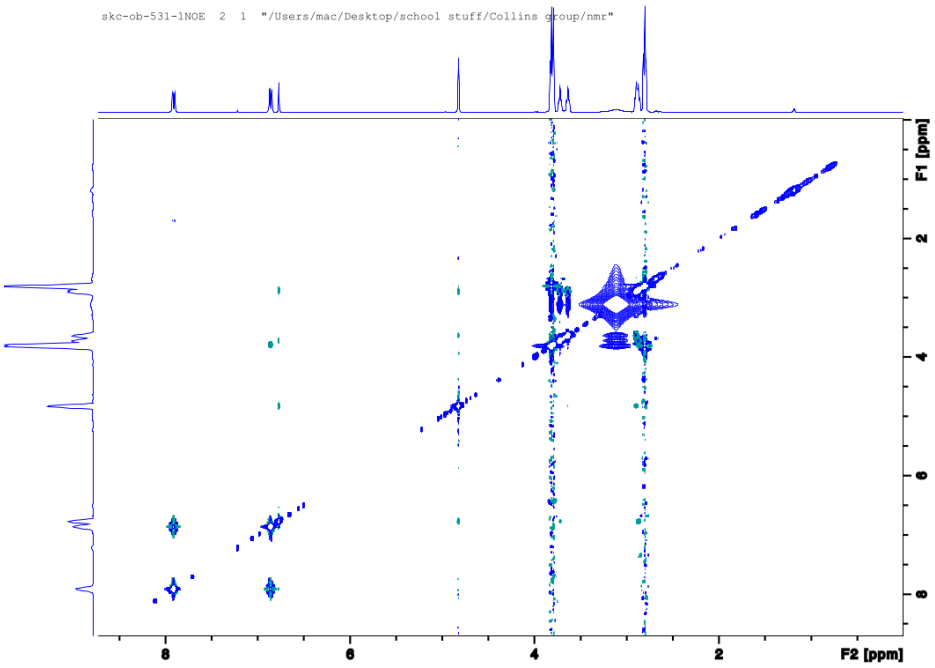

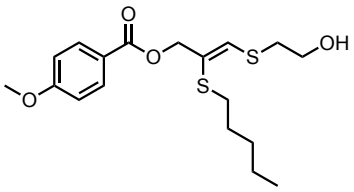

**(*Z*)-3-((2-Hydroxyethyl)thio)-2-(pentylthio)allyl 4-methoxybenzoate (5.12):** To a 15 mL screw cap vial equipped with a stir bar was added the alkynyl sulfide (0.085 g, 0.319 mmol, 1 equiv.), the thiol (0.037 g, 0.351 mmol, 1.1 equiv.), TMEDA (0.053 mL, 0.351 mmol, 1.1 equiv.), and Eosin Y (0.004 g, 0.0064 mmol, 2 mol%). Acetonitrile (6.4 mL) was added to the vial. The vial was placed in the middle of a metal cylinder containing green LEDs. The cylinder with the vial was positioned on a stir plate cooled by a fan. The LEDs were turned on and the reaction mixture was stirred for 24h at room temperature. Upon completion of the reaction (TLC), it was concentrated under vacuum to provide a crude reaction mixture which was purified by column chromatography on silica-gel. Following purification by column chromatography (10-15% Acetone in Hexanes), the desired product was obtained as an oil (62 mg, 45%). $^{1}$H NMR (400 MHz, Chloroform-*d*) δ 8.03 (d, *J* = 8.8 Hz, 2H), 6.94 (d, *J* = 8.8 Hz, 2H), 6.67 (s, 1H), 4.91 (s, 2H), 3.88 (s, 3H), 3.83 (t, *J* = 8 Hz, 2H), 2.96 (t, *J* = 5.9 Hz, 2H), 2.82 (t, *J* = 7.4 Hz, 2H), 1.98 (s, 1H), 1.66-1.59 (m, 2H), 1.66-1.59 (m, 2H), 1.41-1.28 (m, 4H), 0.89 (t, *J* = 7.2 Hz, 3H); $^{13}$C NMR (101 MHz, $CDCl_3$) δ 165.9, 163.6, 134.3, 131.8, 126.6, 122.3, 113.7, 67.0, 61.7, 55.5, 37.0, 32.2, 30.9, 29.7, 22.3, 14.0; HRMS (ESI) m/z calculated for $C_{18}H_{26}O_4S_2$ $[M+NH_4]^+$ 388.1611; found 388.1616.

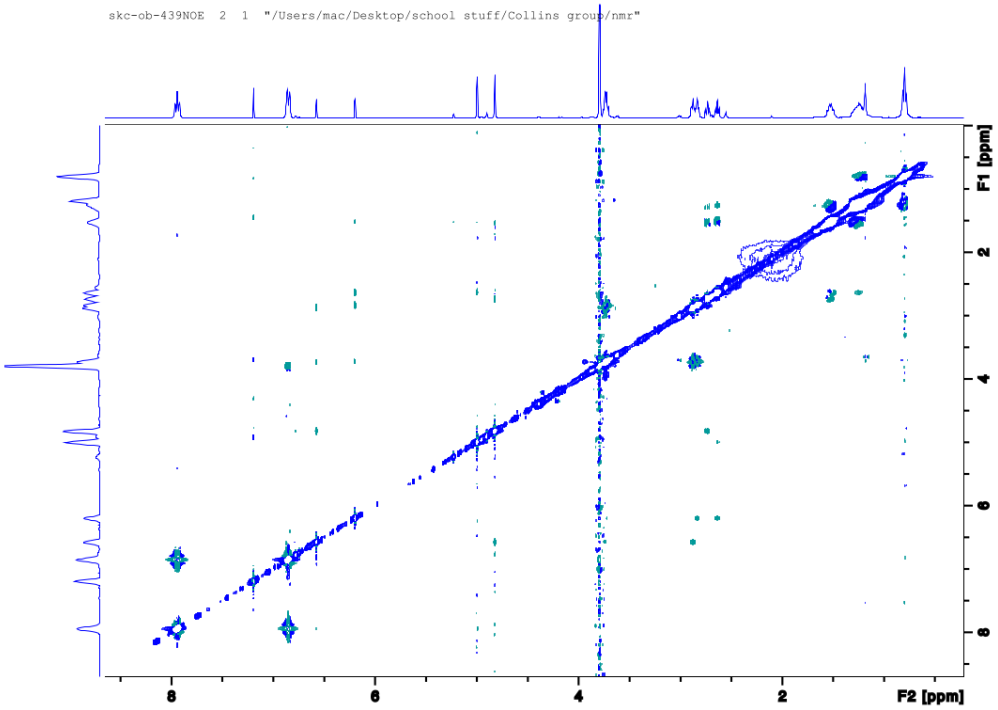

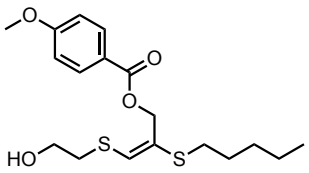

**(*E*)-3-((2-Hydroxyethyl)thio)-2-(pentylthio)allyl 4-methoxybenzoate (5.12a):** To a 15 mL screw cap vial equipped with a stir bar was added the alkynyl sulfide (0.085 g, 0.319 mmol, 1 equiv.), the thiol (0.037 g, 0.351 mmol, 1.1 equiv.), TMEDA (0.053 mL, 0.351 mmol, 1.1 equiv.), and Eosin Y (0.004 g, 0.0064 mmol, 2 mol%). Acetonitrile (6.4 mL) was added to the vial. The vial was placed in the middle of a metal cylinder containing green LEDs. The cylinder with the vial was positioned on a stir plate cooled by a fan. The LEDs were turned on and the reaction mixture was stirred for 24h at room temperature. Upon completion of the reaction (TLC), it was concentrated under vacuum to provide a crude reaction mixture which was purified by column chromatography on silica-gel. Following purification by column chromatography (10-15% Acetone in Hexanes), the desired product was obtained as an oil (15 mg, 20%). $^{1}$H NMR (400 MHz, Chloroform-*d*) δ 8.05 (d, *J* = 8.8 Hz, 2H), 6.95 (d, *J* = 8.8 Hz, 2H), 6.29 (s, 1H), 5.09 (s, 2H), 3.88 (s, 3H), 3.81 (t, *J* = 5.6 Hz, 2H), 2.93 (t, *J* = 5.7 Hz, 2H), 2.73 (t, *J* = 7.4 Hz, 2H), 1.64-1.57 (m, 2H), 1.38-1.28 (m, 4H), 0.89 (t, *J* = 7 Hz, 3H); $^{13}$C NMR (101 MHz, $CDCl_3$) δ 166.1, 163.6, 131.9, 130.7, 127.1, 122.2, 113.7, 63.5, 61.3, 55.5, 38.1, 32.7, 30.9, 29.7, 28.7, 22.3, 14.0; HRMS (ESI) m/z calculated for $C_{18}H_{26}O_4S_2$ $[M+Na]^+$ 393.1165; found 393.1179.

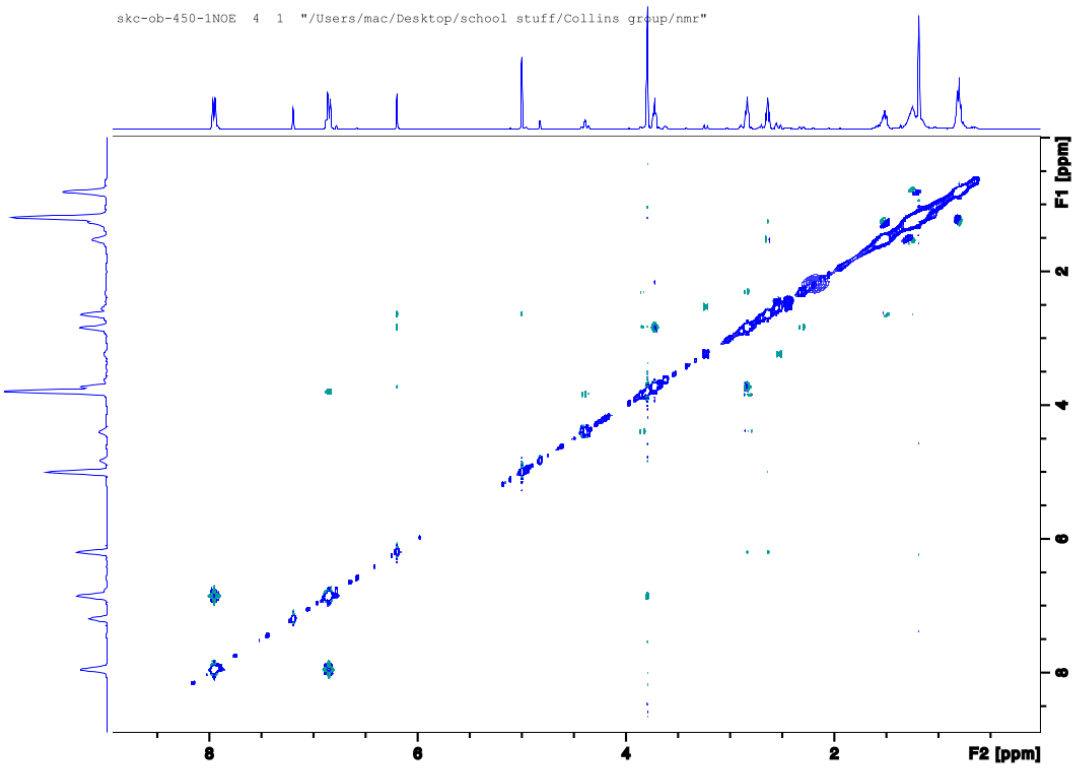

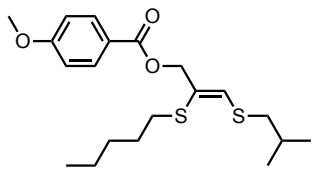

**(*Z*)-3-(Isobutylthio)-2-(pentylthio)allyl 4-methoxybenzoate (5.13)**: To a 15 mL screw cap vial equipped with a stir bar was added the alkynyl sulfide (0.045 g, 0.162 mmol, 1 equiv.), the thiol (0.022 mL, 0.178 mmol, 1.1 equiv.), TMEDA (0.027 mL, 0.178 mmol, 1.1 equiv.), and Eosin Y (0.0021 g, 0.003 mmol, 2 mol %). Acetonitrile (3.2 mL) was added to the vial. The vial was placed in the middle of a metal cylinder containing green LEDs. The cylinder with the vial was positioned on a stir plate cooled by a fan. The LEDs were turned on and the reaction mixture was stirred for 24h at room temperature. Upon completion of the reaction (TLC), it was concentrated under vacuum to provide a crude reaction mixture which was purified by column chromatography on silica-gel. Following purification by column chromatography (4% Diethyl ether in Hexanes), the desired product was obtained as a colorless oil (42 mg, 68%). $^{1}$H NMR (400 MHz, Chloroform-*d*) δ 8.04 (d, *J* = 9.0 Hz, 2H), 6.96 (d, *J* = 9.0 Hz, 2H), 6.68 (s, 1H), 4.90 (s, 2H), 3.89 (s, 3H), 2.82 (t, *J* = 7.4 Hz, 2H), 2.68 (d, *J* = 6.8 Hz, 2H), 1.93-1.83 (m, 1H), 1.68-1.59 (m, 2H), 1.45-1.27 (m, 4H), 1.03 (d, *J* = 6.7 Hz, 6H), 0.88 (t, *J* = 7.2 Hz, 3H); $^{13}$C NMR (101 MHz, $CDCl_3$) δ 166.0, 163.5, 1, 137.5, 131.7, 123.9, 122.5, 113.7, 67.5, 55.5, 43.2, 32.2, 31.0, 29.7, 29.4, 22.3, 21.7, 14.0; HRMS (ESI) m/z calculated for $C_{20}H_{30}O_3S_2$ $[M+Na]^+$ 405.1529; found 405.1530.

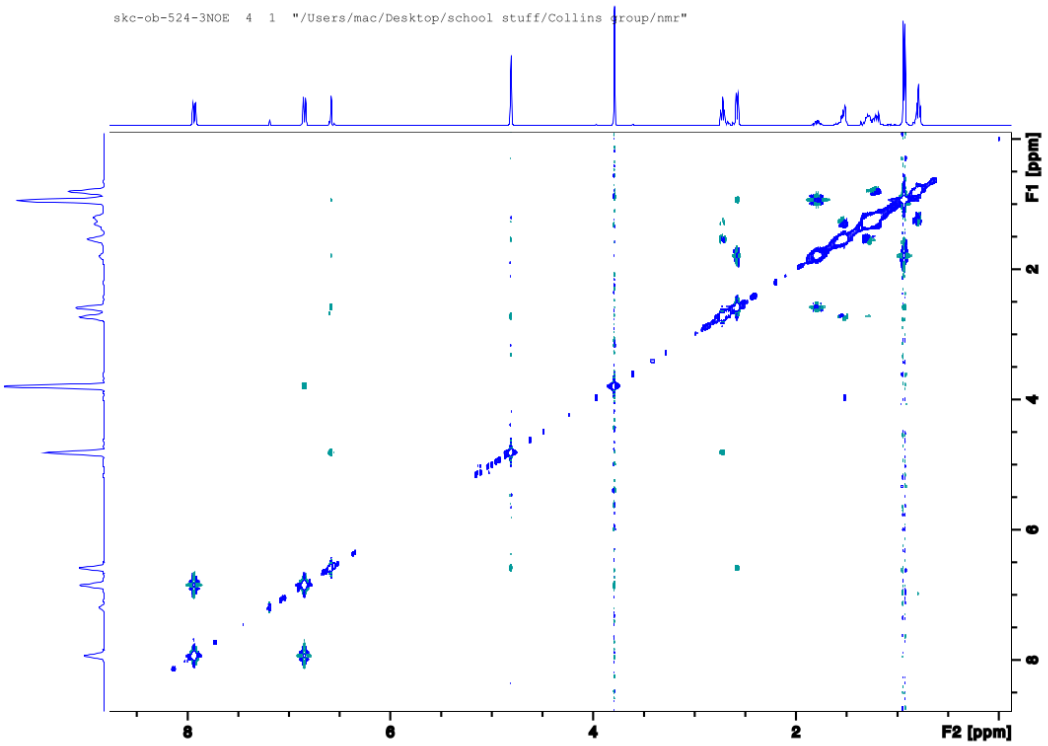

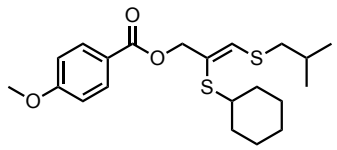

**(*Z*)-2-(Cyclohexylthio)-3-(isobutylthio)allyl 4-methoxybenzoate (5.14)**: To a 15 mL screw cap vial equipped with a stir bar was added the alkynyl sulfide (0.054 g, 0.194 mmol, 1 equiv.), the thiol (0.025 mL, 0.213 mmol, 1.1 equiv.), TMEDA (0.032 mL, 0.213 mmol, 1.1 equiv.), and Eosin Y (0.0025 g, 0.004 mmol, 2 mol %). Acetonitrile (3.9 mL) was added to the vial. The vial was placed in the middle of a metal cylinder containing green LEDs. The cylinder with the vial was positioned on a stir plate cooled by a fan. The LEDs were turned on and the reaction mixture was stirred for 24h at room temperature. Upon completion of the reaction (TLC), it was concentrated under vacuum to provide a crude reaction mixture which was purified by column chromatography on silica-gel. Following purification by column chromatography (2-4% Diethyl ether in Hexanes), the desired product was obtained as a colorless oil (46 mg, 60%). $^{1}$H NMR (400 MHz, Chloroform-*d*) δ 8.04 (d, *J* = 8.9 Hz, 2H), 6.96 (d, *J* = 8.9 Hz, 2H), 6.77 (s, 1H), 4.89 (s, 2H), 3.89 (s, 3H), 3.25-3.18 (m, 1H), 2.67 (d, *J* = 6.8 Hz, 2H), 2.00-1.25 (m, 14H), 1.03 (t, *J* = 6.6 Hz, 6H); $^{13}$C NMR (101 MHz, $CDCl_3$) δ 166.0, 163.5, 140.0, 131.7, 122.9, 122.5, 113.7, 68.5, 55.5, 44.8, 43.1, 33.7, 29.5, 26.0, 25.7, 21.7; HRMS (ESI) m/z calculated for $C_{21}H_{30}O_3S_2$ $[M+Na]^+$ 417.1529; found 417.1527.

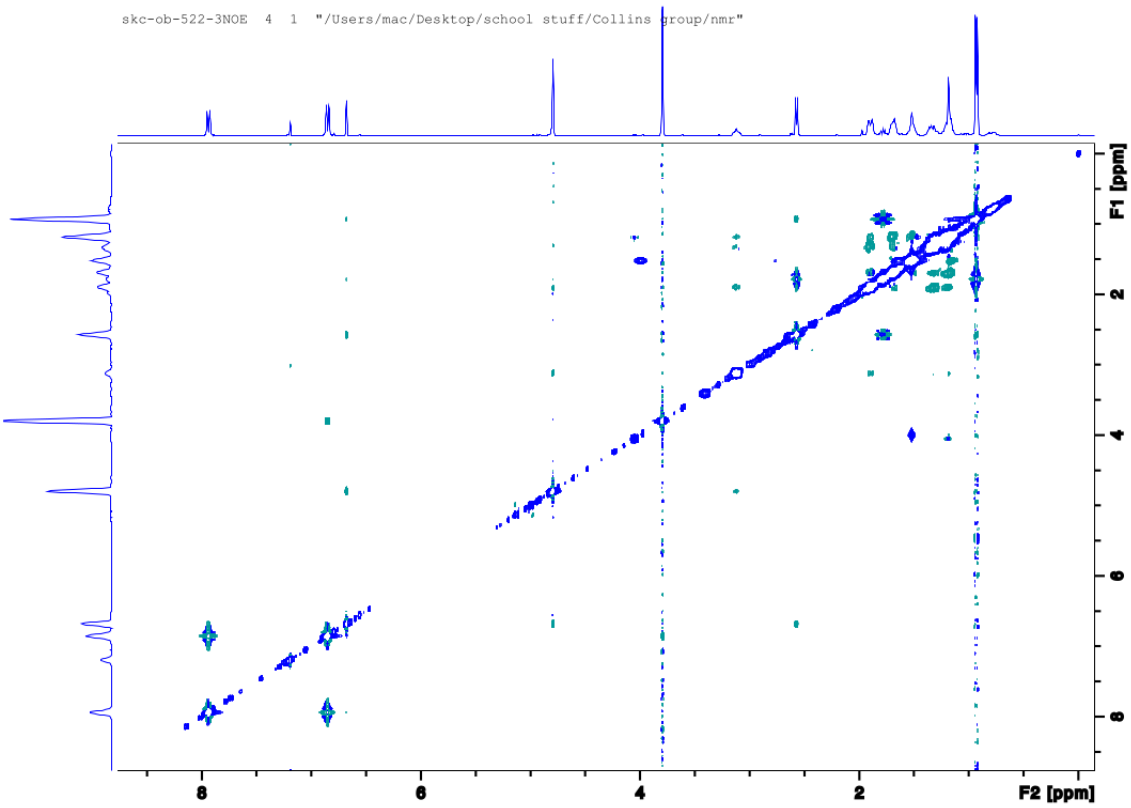

## NMR DATA FOR NEW COMPOUNDS

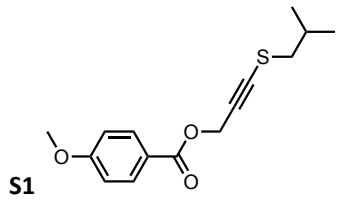

**S1**

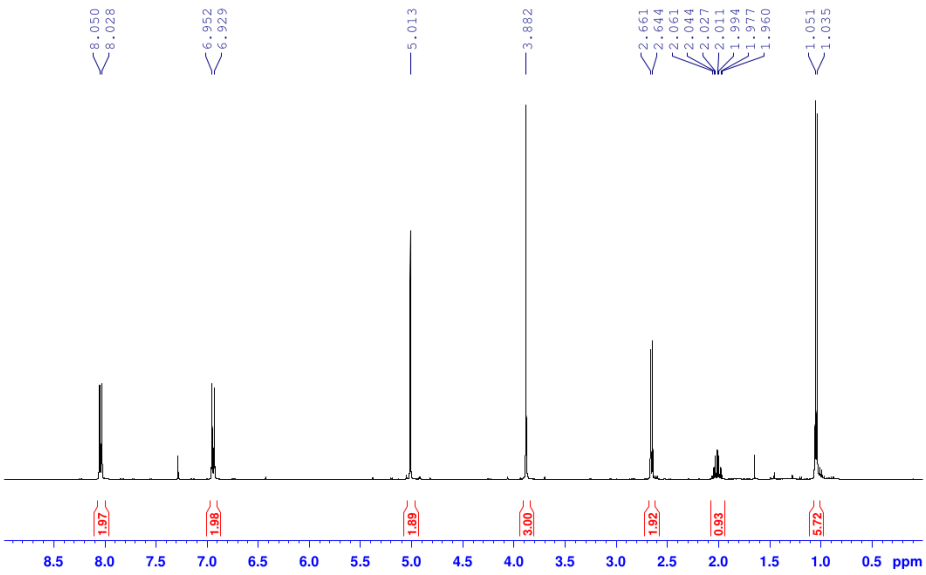


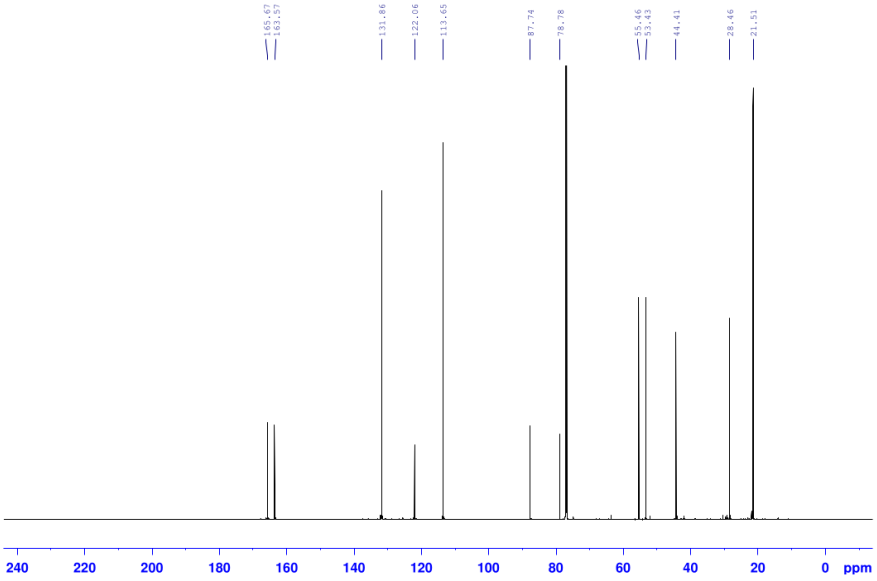

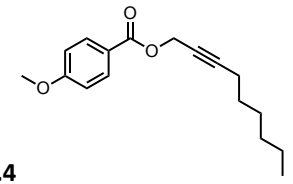

**5.4**

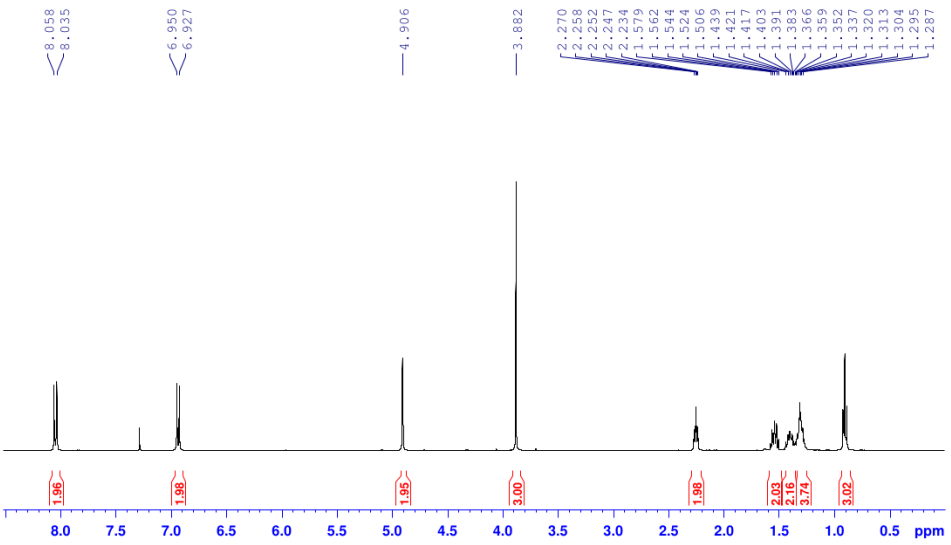
8.058
8.035
6.950
6.927
4.906
3.882
2.270
2.258
2.252
2.247
2.234
1.579
1.562
1.544
1.524
1.506
1.439
1.421
1.417
1.403
1.391
1.383
1.366
1.359
1.352
1.337
1.320
1.313
1.304
1.295
1.287
1.96
1.98
1.95
3.00
1.98
2.03
2.16
3.74
3.02
8.0 7.5 7.0 6.5 6.0 5.5 5.0 4.5 4.0 3.5 3.0 2.5 2.0 1.5 1.0 0.5 ppm

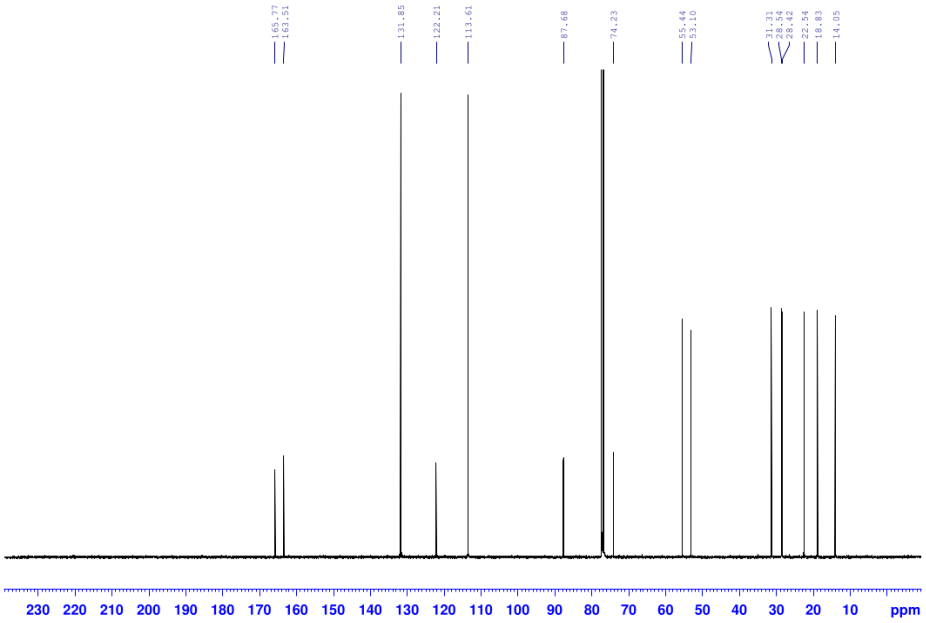
165.77
163.51
131.85
122.21
113.61
87.68
74.23
55.44
55.10
31.31
28.54
28.42
22.54
18.83
14.05
230 220 210 200 190 180 170 160 150 140 130 120 110 100 90 80 70 60 50 40 30 20 10 ppm

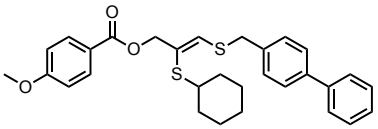

**5.5**

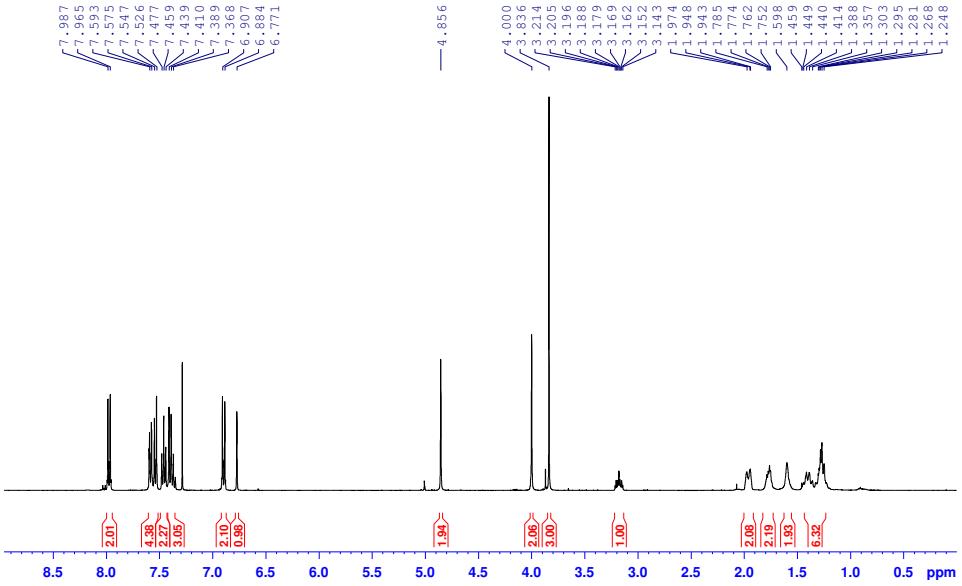
7.987
7.965
7.593
7.575
7.547
7.526
7.477
7.459
7.439
7.410
7.389
7.368
6.907
6.884
6.771
4.856
4.000
3.836
3.214
3.205
3.196
3.188
3.179
3.169
3.162
3.152
3.143
1.974
1.948
1.943
1.785
1.774
1.762
1.752
1.598
1.459
1.449
1.440
1.414
1.388
1.357
1.303
1.295
1.281
1.268
1.248
2.01
4.38
2.27
3.05
2.10
0.98
1.94
2.06
3.00
1.00
2.08
2.19
1.93
6.32
8.5 8.0 7.5 7.0 6.5 6.0 5.5 5.0 4.5 4.0 3.5 3.0 2.5 2.0 1.5 1.0 0.5 ppm

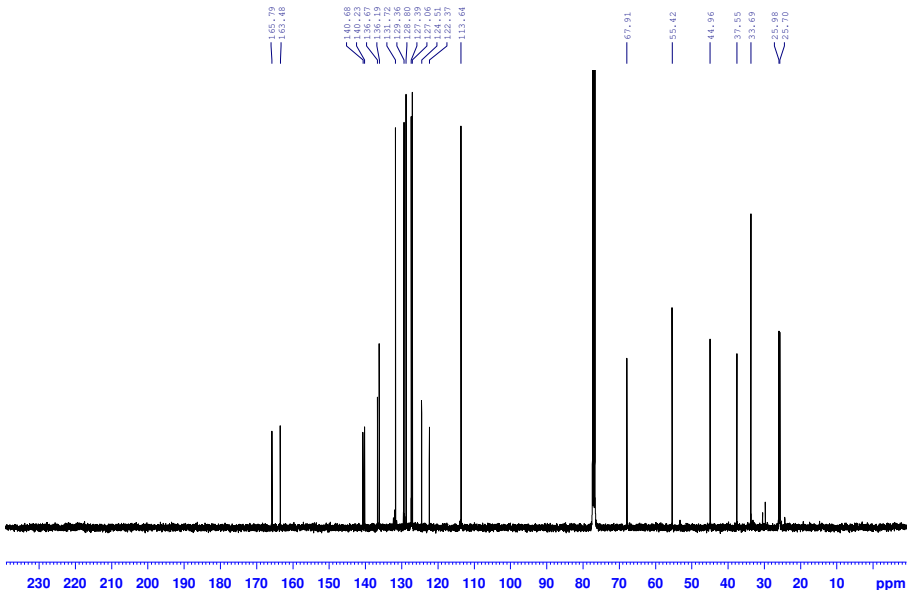
165.79
163.48
140.68
140.23
136.67
136.19
131.72
129.36
128.80
127.39
127.06
124.51
124.37
113.64
67.91
55.42
44.96
37.55
33.69
25.98
25.70
230 220 210 200 190 180 170 160 150 140 130 120 110 100 90 80 70 60 50 40 30 20 10 ppm

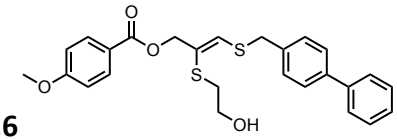

**5.6**

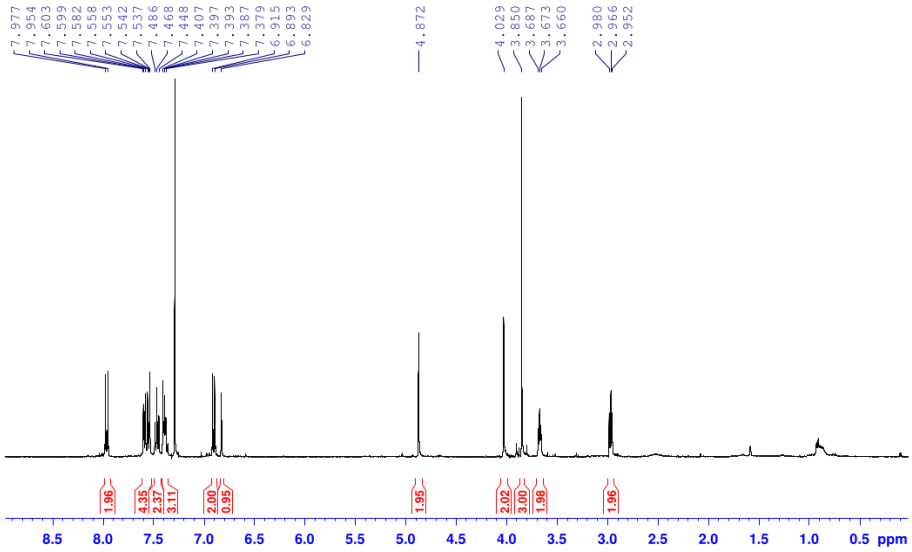
7.977
7.954
7.603
7.599
7.582
7.558
7.553
7.542
7.537
7.486
7.468
7.448
7.407
7.397
7.393
7.387
7.379
6.915
6.893
6.829
4.872
4.029
3.850
3.687
3.673
3.660
2.980
2.966
2.952
1.96
4.35
2.37
3.11
2.00
0.95
1.95
2.02
3.00
1.98
1.96
8.5 8.0 7.5 7.0 6.5 6.0 5.5 5.0 4.5 4.0 3.5 3.0 2.5 2.0 1.5 1.0 0.5 ppm

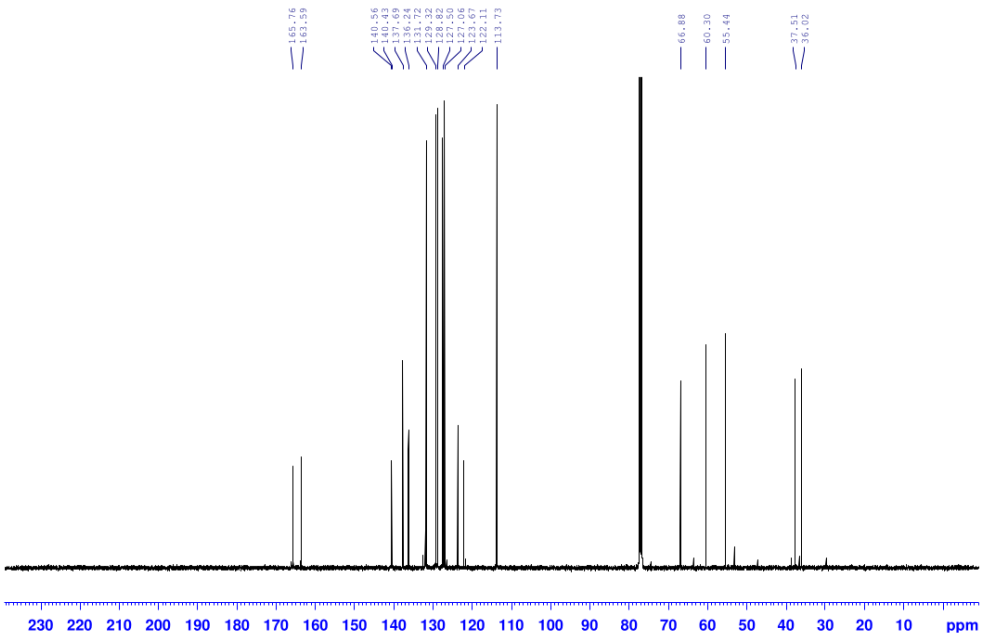
165.76
165.59
140.56
140.43
137.69
136.24
135.72
133.32
128.82
127.50
127.06
125.67
123.11
113.73
66.88
60.30
55.44
37.51
36.02
230 220 210 200 190 180 170 160 150 140 130 120 110 100 90 80 70 60 50 40 30 20 10 ppm

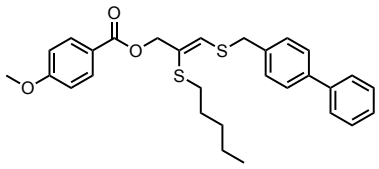

**5.7**

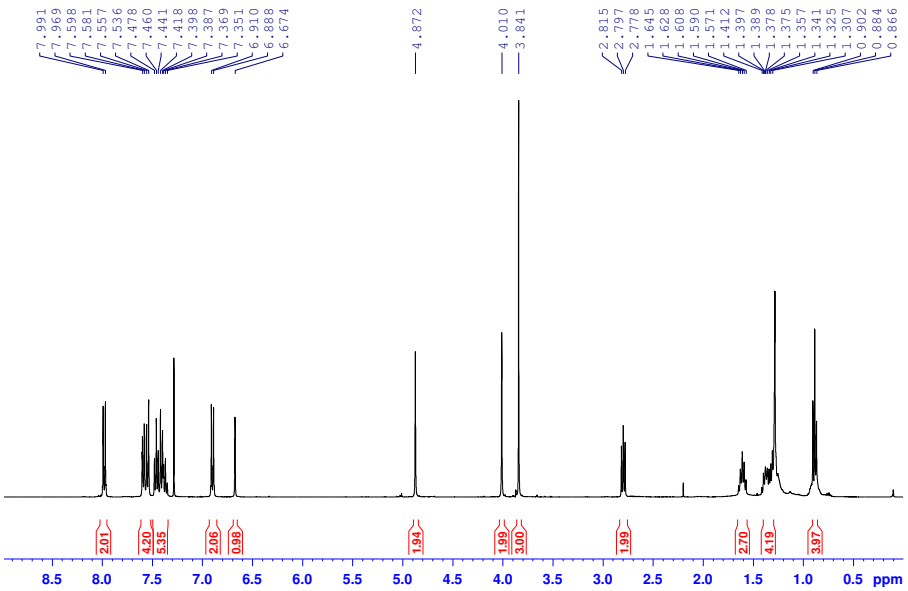
7.991
7.969
7.598
7.581
7.557
7.536
7.478
7.460
7.441
7.418
7.398
7.387
7.369
7.351
6.910
6.888
6.674
4.872
4.010
3.841
2.815
2.797
2.778
1.645
1.628
1.608
1.590
1.571
1.412
1.397
1.389
1.378
1.375
1.357
1.341
1.325
1.307
0.902
0.884
0.866
2.01
4.20
5.35
2.06
0.98
1.94
1.99
3.00
1.99
2.70
4.19
3.97
8.5 8.0 7.5 7.0 6.5 6.0 5.5 5.0 4.5 4.0 3.5 3.0 2.5 2.0 1.5 1.0 0.5 ppm

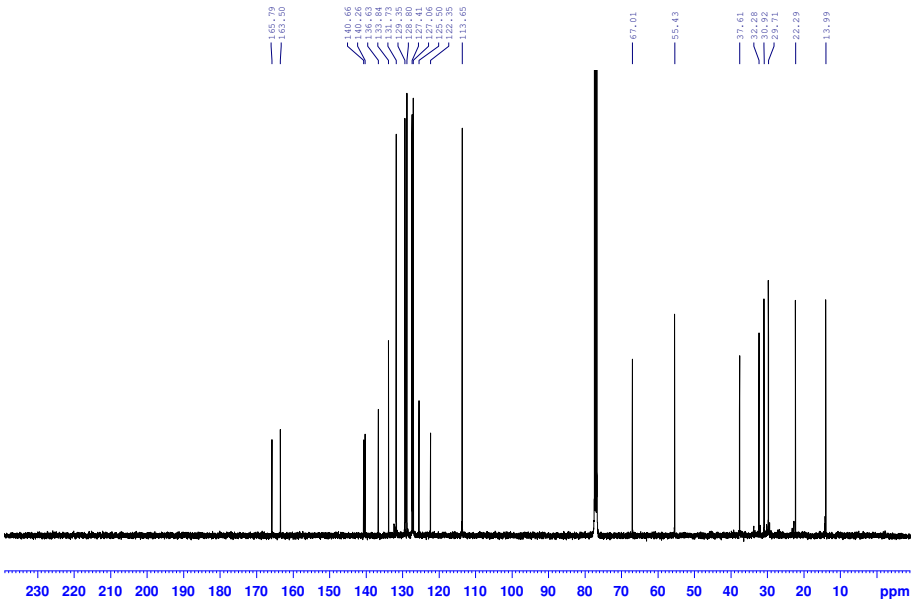
165.79
163.50
140.66
140.26
136.63
133.84
131.73
129.35
128.80
127.41
127.06
125.50
124.35
113.65
67.01
55.43
37.61
32.28
30.92
29.71
22.29
13.99
230 220 210 200 190 180 170 160 150 140 130 120 110 100 90 80 70 60 50 40 30 20 10 ppm

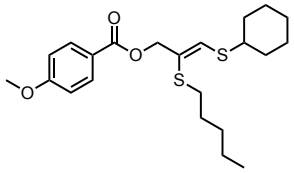

**5.8**

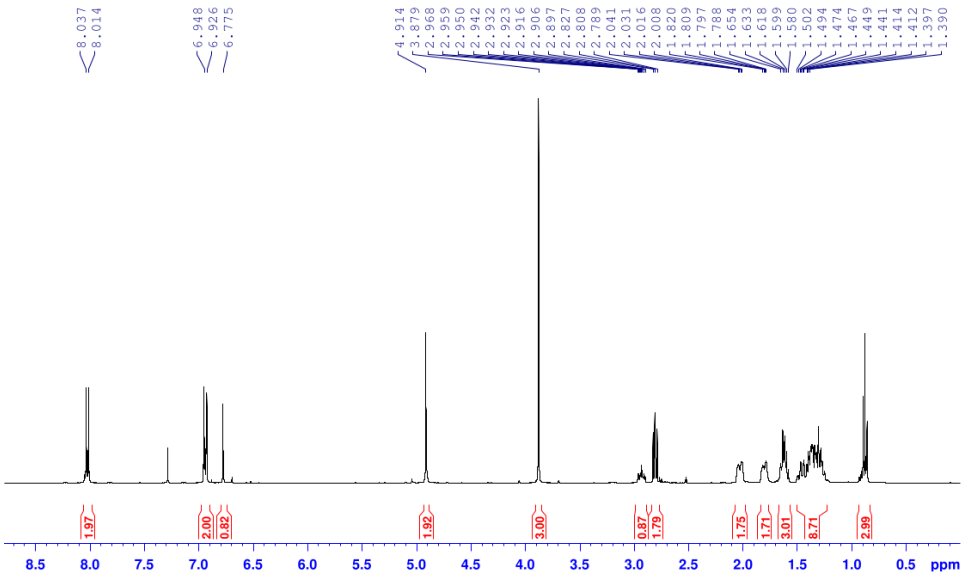
8.037
8.014
6.948
6.926
6.775
4.914
3.879
2.968
2.959
2.950
2.942
2.932
2.923
2.916
2.906
2.897
2.827
2.808
2.789
2.041
2.031
2.016
2.008
1.820
1.809
1.797
1.788
1.654
1.633
1.618
1.599
1.580
1.502
1.494
1.474
1.467
1.449
1.441
1.414
1.412
1.397
1.390
1.97
2.00
0.82
1.92
3.00
0.87
1.79
1.75
1.71
3.01
8.71
2.99
8.5 8.0 7.5 7.0 6.5 6.0 5.5 5.0 4.5 4.0 3.5 3.0 2.5 2.0 1.5 1.0 0.5 ppm

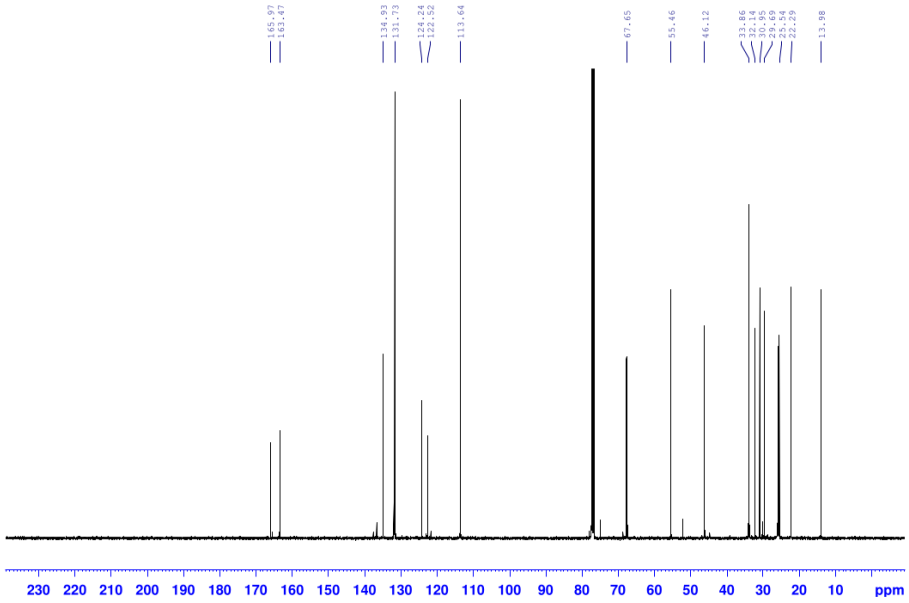
165.97
163.47
134.93
131.73
124.24
122.52
113.64
67.65
55.46
46.12
33.86
32.14
30.95
30.60
25.54
22.29
13.98
230 220 210 200 190 180 170 160 150 140 130 120 110 100 90 80 70 60 50 40 30 20 10 ppm

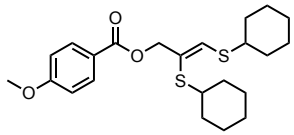

**5.9**

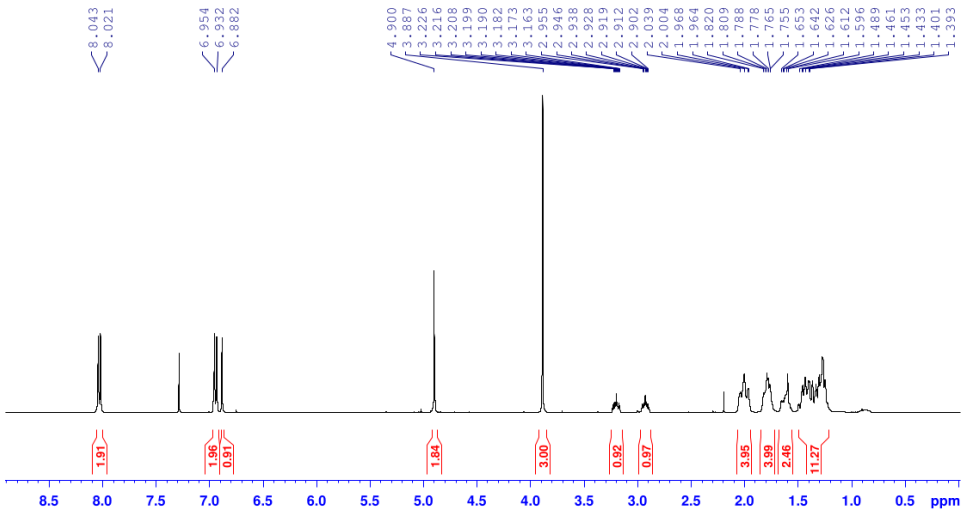
8.043
8.021
6.954
6.932
6.882
4.900
3.887
3.226
3.216
3.208
3.199
3.190
3.182
3.173
3.163
2.955
2.946
2.938
2.928
2.919
2.912
2.902
2.039
2.004
1.968
1.964
1.820
1.809
1.788
1.778
1.765
1.755
1.653
1.642
1.626
1.612
1.596
1.489
1.461
1.453
1.433
1.401
1.393
1.91
1.96
0.91
1.84
3.00
0.92
0.97
3.95
3.99
2.46
11.27
8.5 8.0 7.5 7.0 6.5 6.0 5.5 5.0 4.5 4.0 3.5 3.0 2.5 2.0 1.5 1.0 0.5 ppm

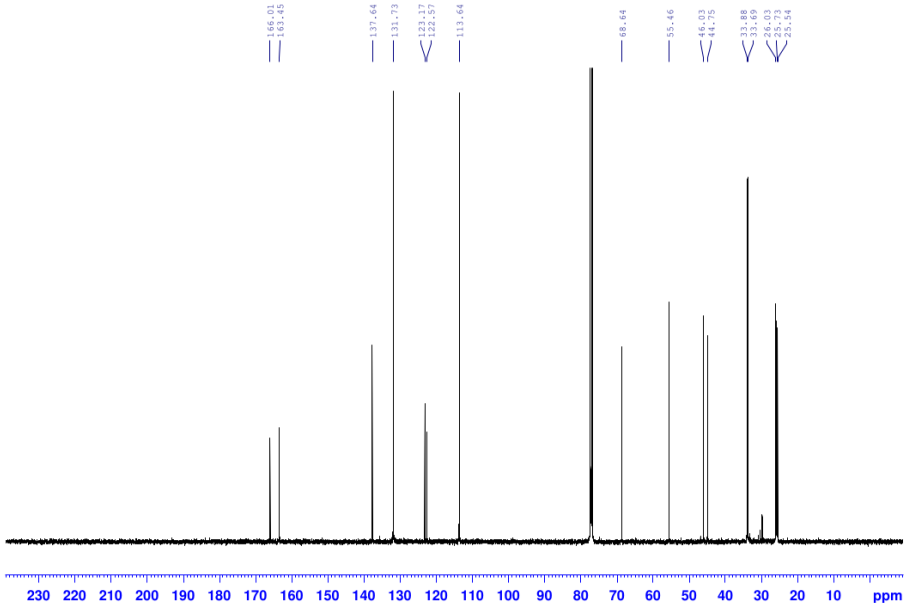
168.01
163.45
137.64
131.73
123.17
122.97
113.64
68.64
55.46
46.03
44.76
33.88
33.60
26.03
25.73
25.54
230 220 210 200 190 180 170 160 150 140 130 120 110 100 90 80 70 60 50 40 30 20 10 ppm

**5.10**

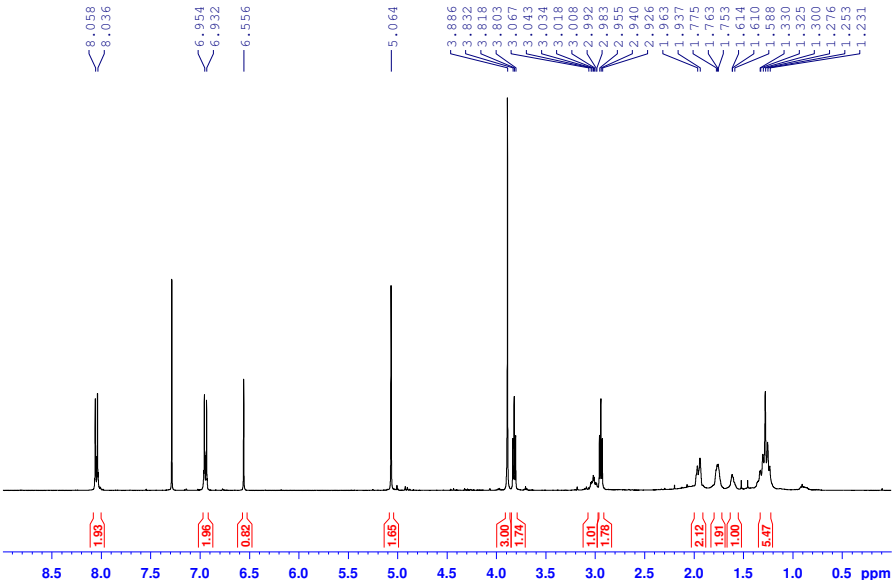
8.058
8.036
6.954
6.932
6.556
5.064
3.886
3.832
3.818
3.803
3.067
3.043
3.034
3.018
3.008
2.992
2.983
2.955
2.940
2.926
1.963
1.937
1.775
1.763
1.753
1.614
1.610
1.588
1.330
1.325
1.300
1.276
1.253
1.231
1.93
1.96
0.82
1.65
3.00
1.74
1.01
1.78
2.12
1.91
1.00
5.47
8.5 8.0 7.5 7.0 6.5 6.0 5.5 5.0 4.5 4.0 3.5 3.0 2.5 2.0 1.5 1.0 0.5 ppm

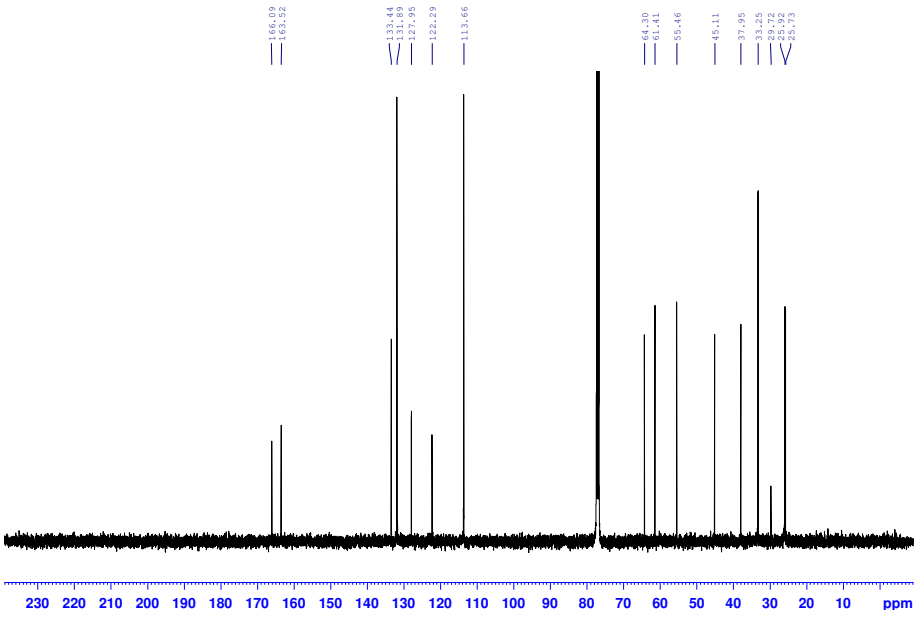
166.09
160.52
133.44
131.89
127.95
122.29
113.66
64.30
61.41
55.46
45.11
37.95
33.25
29.72
25.92
25.73
230 220 210 200 190 180 170 160 150 140 130 120 110 100 90 80 70 60 50 40 30 20 10 ppm

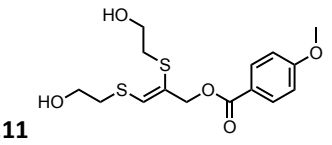
HO
S
HO
S
O
O
O

**5.11**

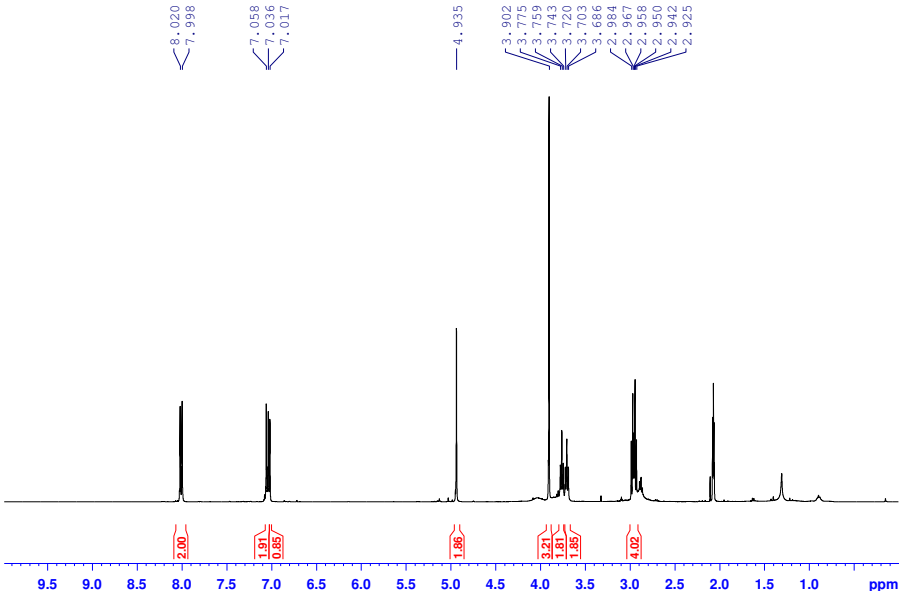
8.020
7.998
7.058
7.036
7.017
4.935
3.902
3.775
3.759
3.743
3.720
3.703
3.686
2.984
2.967
2.958
2.950
2.942
2.925
2.00
1.91
0.85
1.86
3.21
1.81
1.85
4.02
9.5 9.0 8.5 8.0 7.5 7.0 6.5 6.0 5.5 5.0 4.5 4.0 3.5 3.0 2.5 2.0 1.5 1.0 ppm

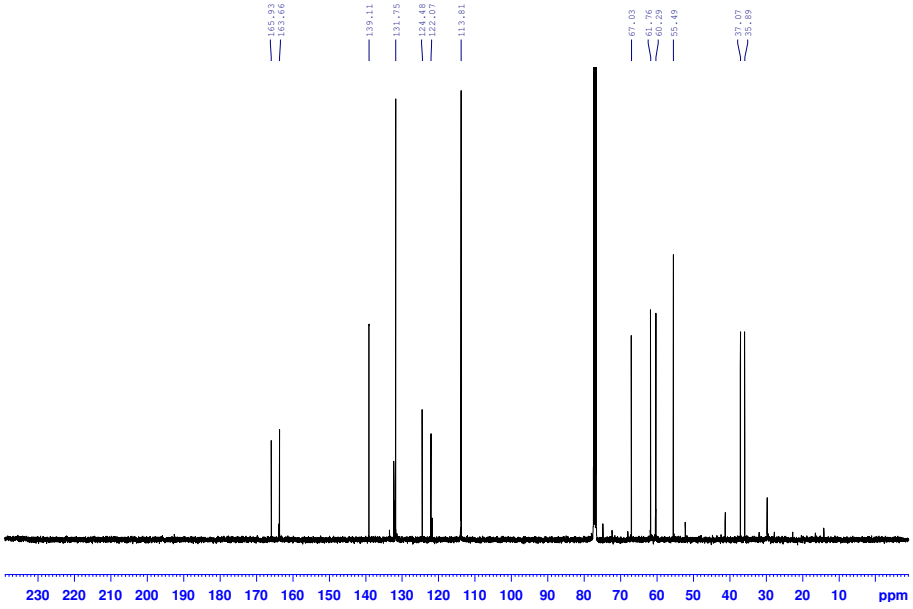
165.93
163.66
139.11
131.75
124.48
122.07
113.81
67.03
61.76
60.29
55.49
37.07
35.89
230 220 210 200 190 180 170 160 150 140 130 120 110 100 90 80 70 60 50 40 30 20 10 ppm

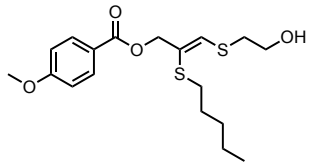
O
O
O
S
OH
S

**5.12**

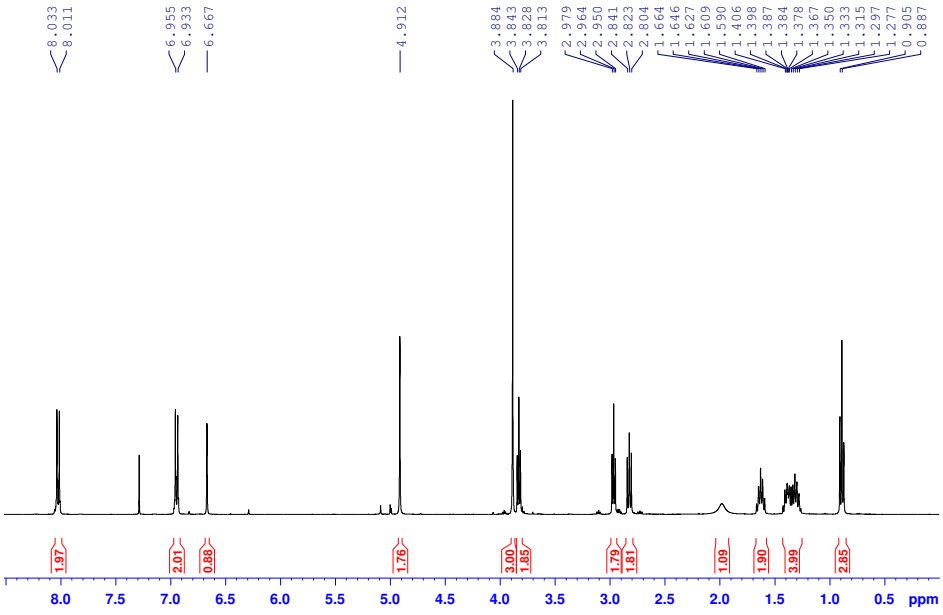
8.033
8.011
6.955
6.933
6.667
4.912
3.884
3.843
3.828
3.813
2.979
2.964
2.950
2.841
2.823
2.804
1.664
1.646
1.627
1.609
1.590
1.406
1.398
1.387
1.384
1.378
1.367
1.350
1.333
1.315
1.297
1.277
0.905
0.887
1.97
2.01
0.88
1.76
3.00
1.85
1.79
1.81
1.09
1.90
3.99
2.85
8.0 7.5 7.0 6.5 6.0 5.5 5.0 4.5 4.0 3.5 3.0 2.5 2.0 1.5 1.0 0.5 ppm

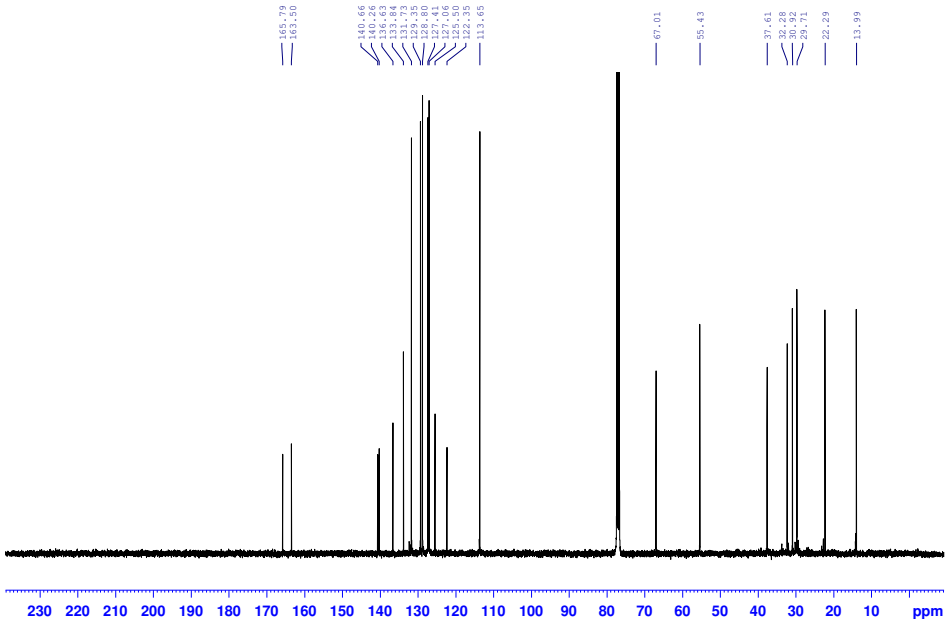
165.79
163.50
140.66
140.26
136.63
133.84
131.73
130.35
128.80
127.41
127.06
125.50
122.36
113.65
67.01
55.43
37.61
32.28
30.92
29.71
22.29
13.99
230 220 210 200 190 180 170 160 150 140 130 120 110 100 90 80 70 60 50 40 30 20 10 ppm

**5.12a**

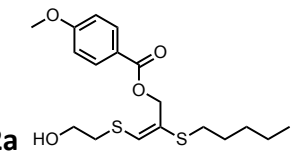
O
O
O
HO
S
S

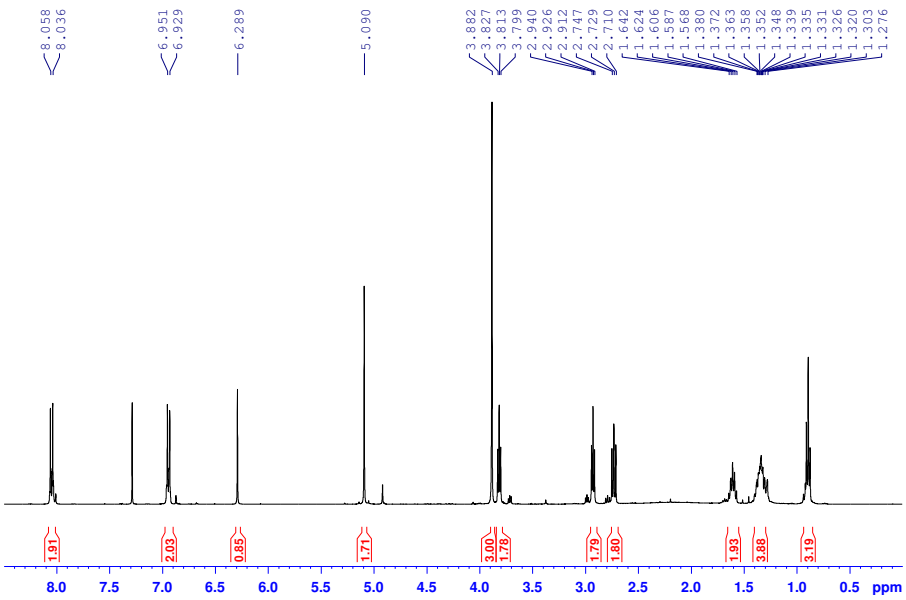
8.058
8.036
6.951
6.929
6.289
5.090
3.882
3.827
3.813
3.799
2.940
2.926
2.912
2.747
2.729
2.710
1.642
1.624
1.606
1.587
1.568
1.380
1.372
1.363
1.358
1.352
1.348
1.339
1.335
1.331
1.326
1.320
1.303
1.276
1.91
2.03
0.85
1.71
3.00
1.78
1.79
1.80
1.93
3.88
3.19
8.0
7.5
7.0
6.5
6.0
5.5
5.0
4.5
4.0
3.5
3.0
2.5
2.0
1.5
1.0
0.5
ppm

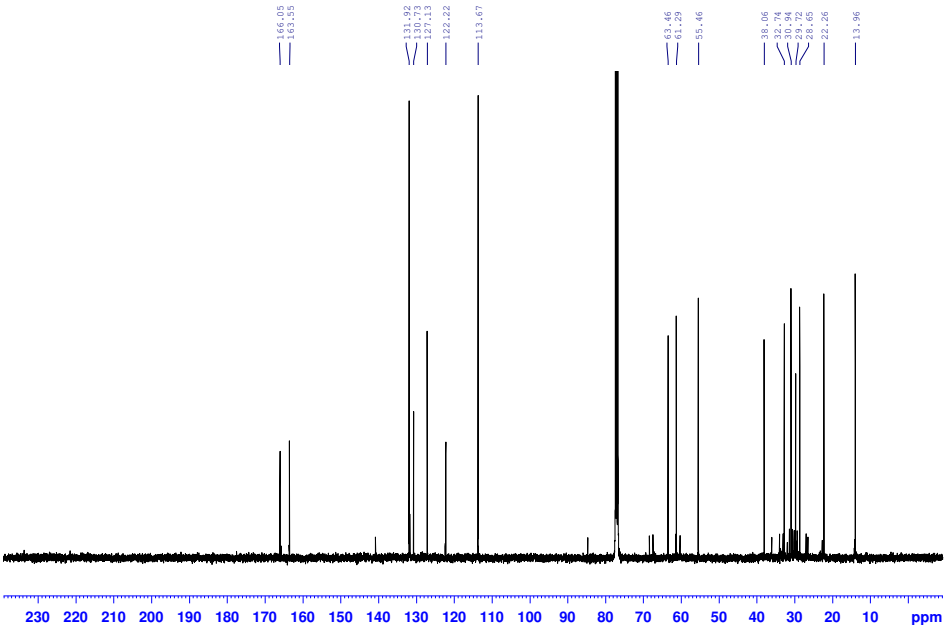
166.05
163.55
131.92
130.73
127.13
122.22
113.67
63.46
61.29
55.46
38.06
32.74
30.94
29.72
28.65
22.26
13.96
230
220
210
200
190
180
170
160
150
140
130
120
110
100
90
80
70
60
50
40
30
20
10
ppm

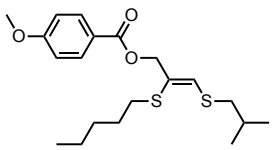

**5.13**

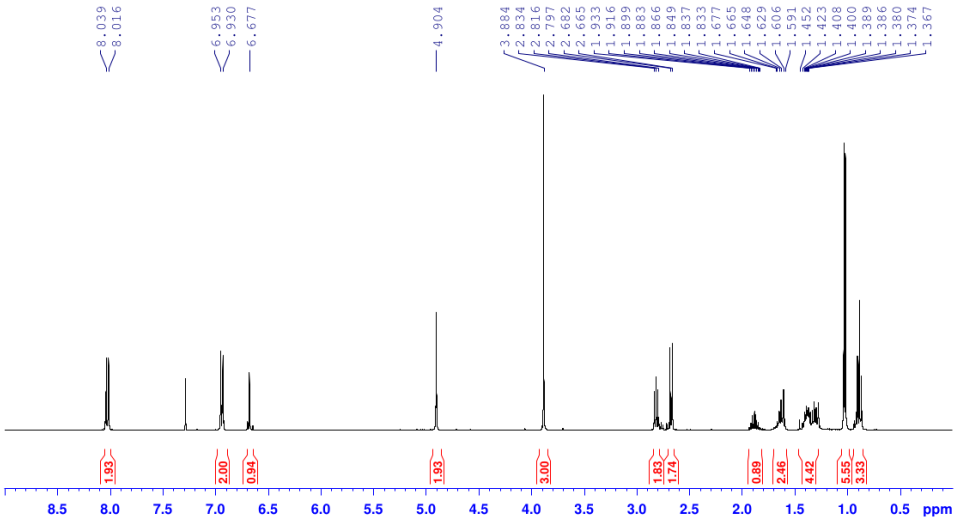
8.039
8.016
6.953
6.930
6.677
4.904
3.884
2.834
2.816
2.797
2.682
2.665
1.933
1.916
1.899
1.883
1.866
1.849
1.837
1.833
1.677
1.665
1.648
1.629
1.606
1.591
1.452
1.423
1.408
1.400
1.389
1.386
1.380
1.374
1.367
1.93
2.00
0.84
1.93
3.00
1.83
1.74
0.89
2.46
4.42
5.55
3.33
8.5 8.0 7.5 7.0 6.5 6.0 5.5 5.0 4.5 4.0 3.5 3.0 2.5 2.0 1.5 1.0 0.5 ppm

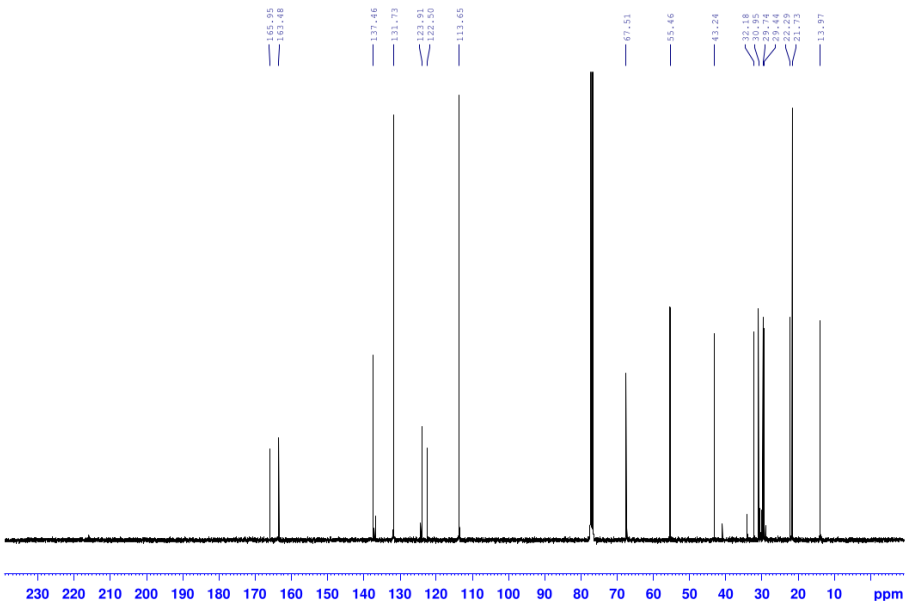
165.95
163.48
137.46
131.73
123.91
122.50
113.65
67.51
55.46
43.24
32.18
30.55
29.74
29.44
22.29
21.73
13.97
230 220 210 200 190 180 170 160 150 140 130 120 110 100 90 80 70 60 50 40 30 20 10 ppm

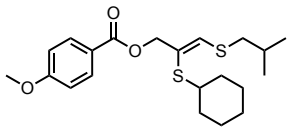

**5.14**

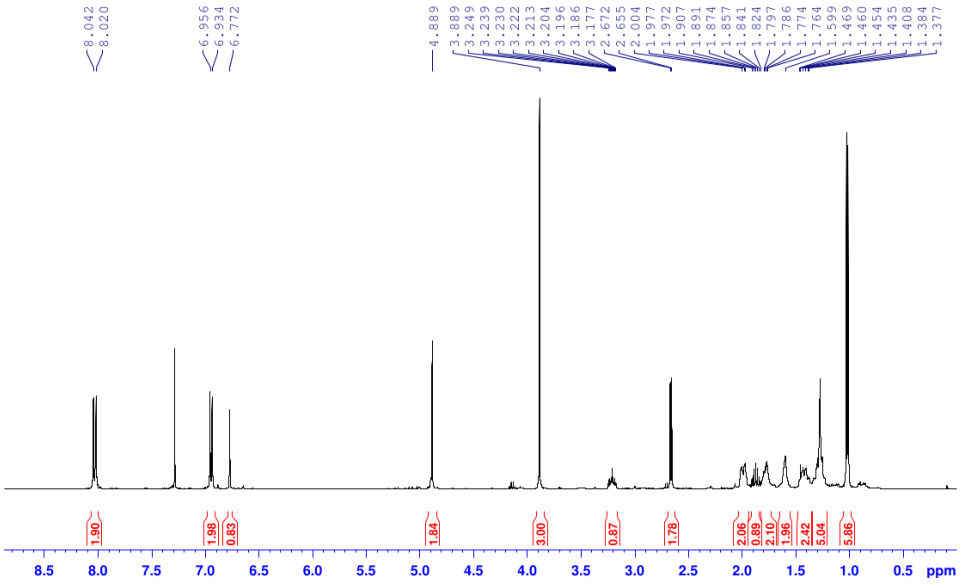
8.042
8.020
6.956
6.934
6.772
4.889
3.889
3.249
3.239
3.230
3.222
3.213
3.204
3.196
3.186
3.177
2.672
2.655
2.004
1.977
1.972
1.907
1.891
1.874
1.857
1.841
1.824
1.797
1.786
1.774
1.764
1.599
1.469
1.460
1.454
1.435
1.408
1.384
1.377
1.90
1.98
0.83
1.84
3.00
0.87
1.78
2.06
0.89
2.10
1.96
2.42
5.04
5.86
8.5 8.0 7.5 7.0 6.5 6.0 5.5 5.0 4.5 4.0 3.5 3.0 2.5 2.0 1.5 1.0 0.5 ppm

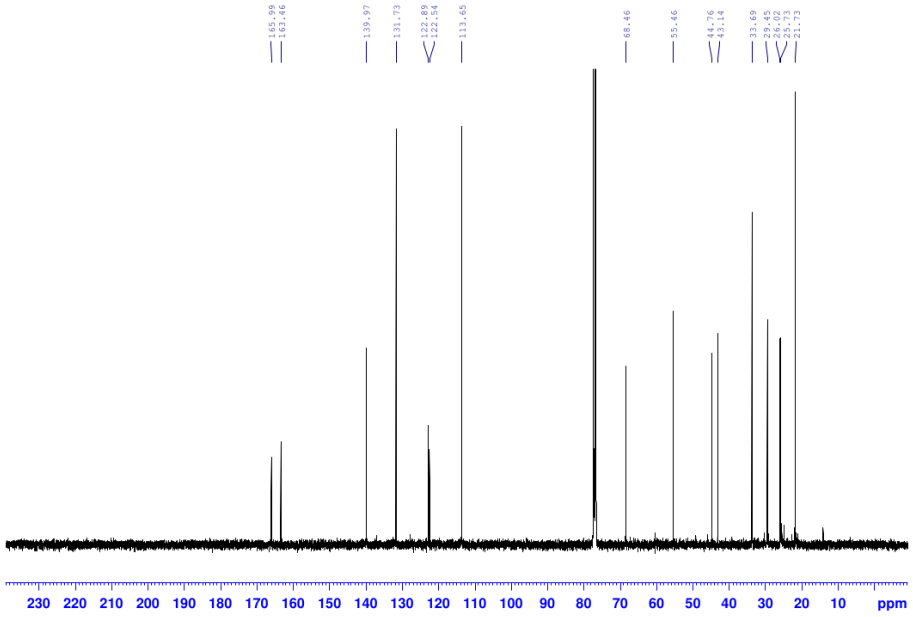
165.99
163.46
139.97
131.73
122.89
122.54
113.65
68.46
55.46
44.76
43.14
33.69
29.45
26.02
25.73
21.73
230 220 210 200 190 180 170 160 150 140 130 120 110 100 90 80 70 60 50 40 30 20 10 ppm

**NOESY spectral data for uncharacterized *cis* and *trans*-isomers of products**

Uncharacterized *cis*- or *trans*-isomers of products co-eluted with either unreacted starting material, or as a mixture of isomers. NOESYs of mixtures of *cis*- and *trans*-isomers will be indicated as mixtures and NOESYs of *cis*- or *trans*-isomers with unreacted starting material will be indicated as such.

**S4**

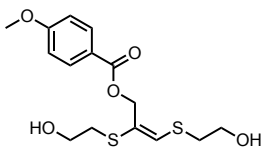


Mixture

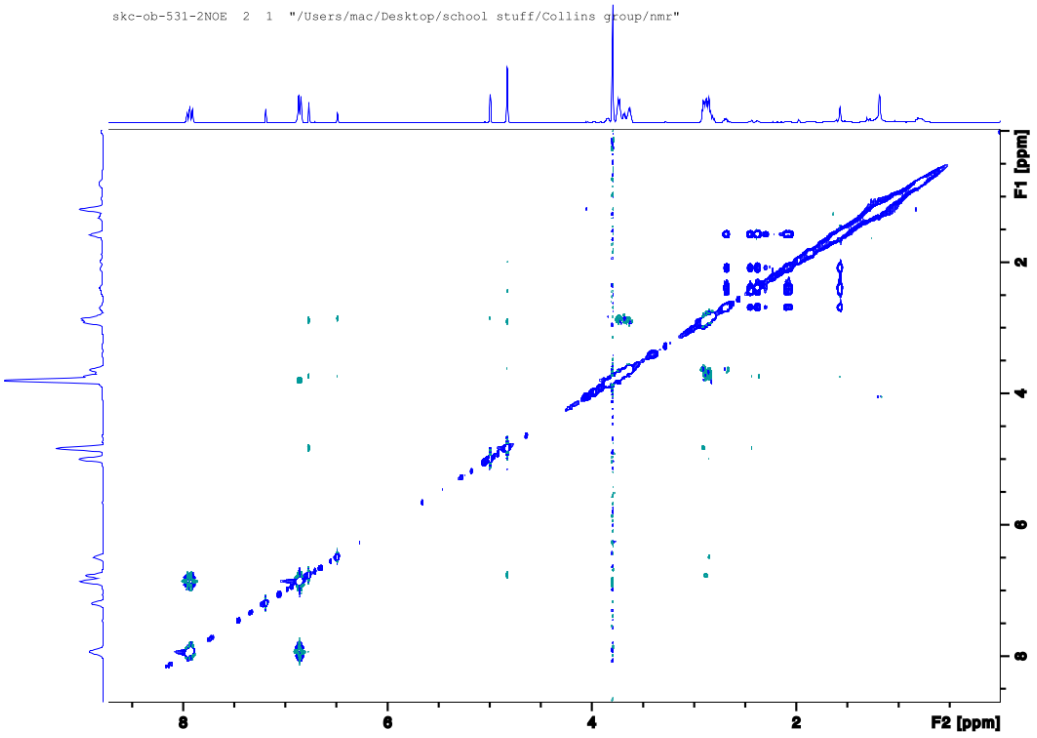

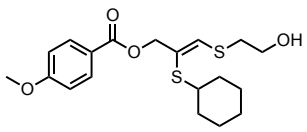


**S5**

(*cis* + unreacted starting material)

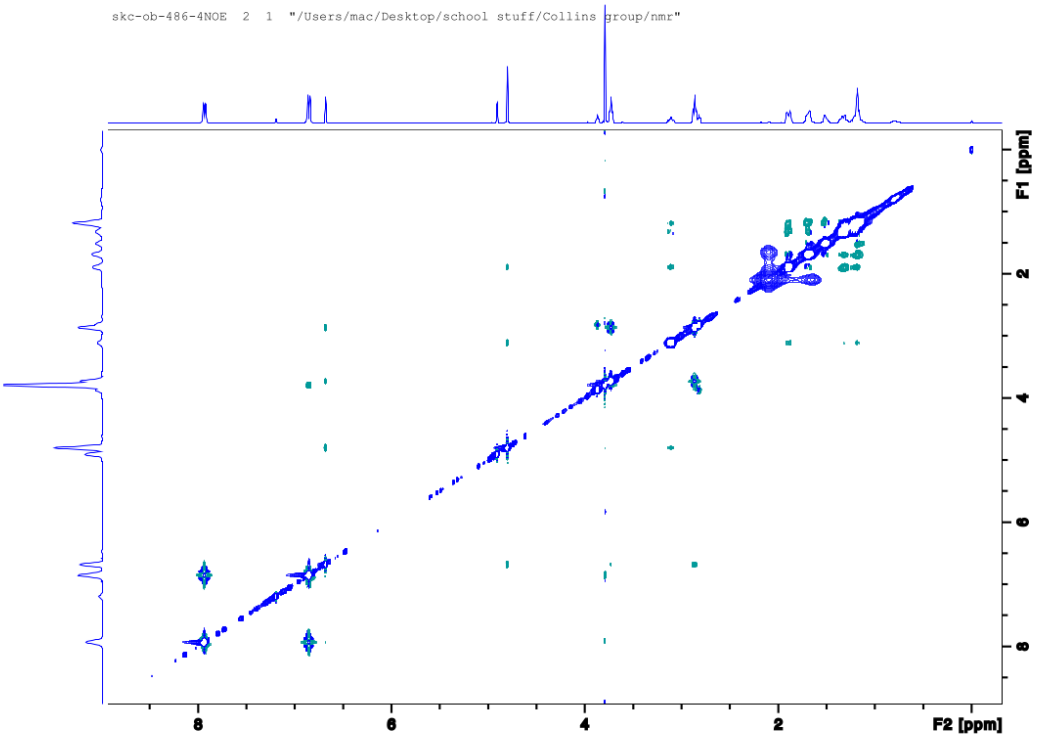

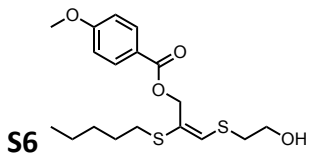
O
O
O
S
S
OH

**S6**

Mixture

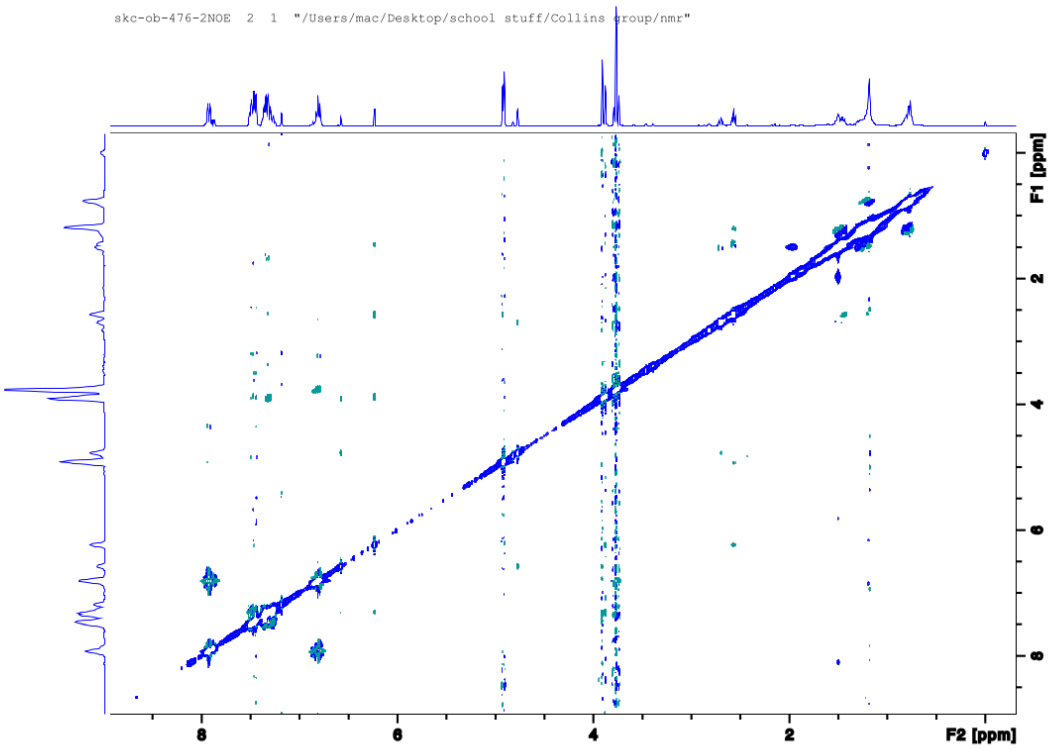
skc-ob-476-2NOE 2 1 "/Users/mac/Desktop/school stuff/Collins group/nmr"
F1 [ppm]
F2 [ppm]
8
6
4
2

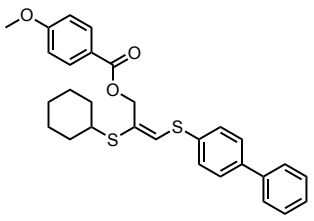

**S7**

(*trans* + unreacted starting material)

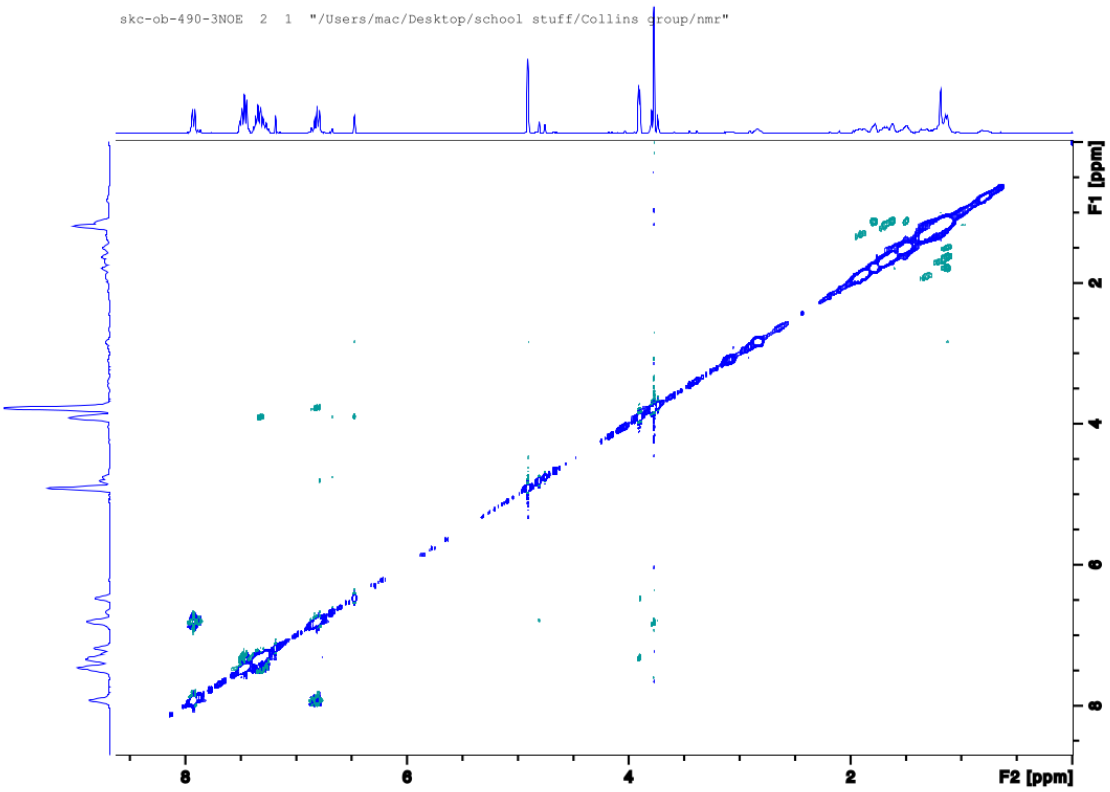

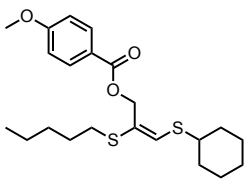

**S8**

Mixture

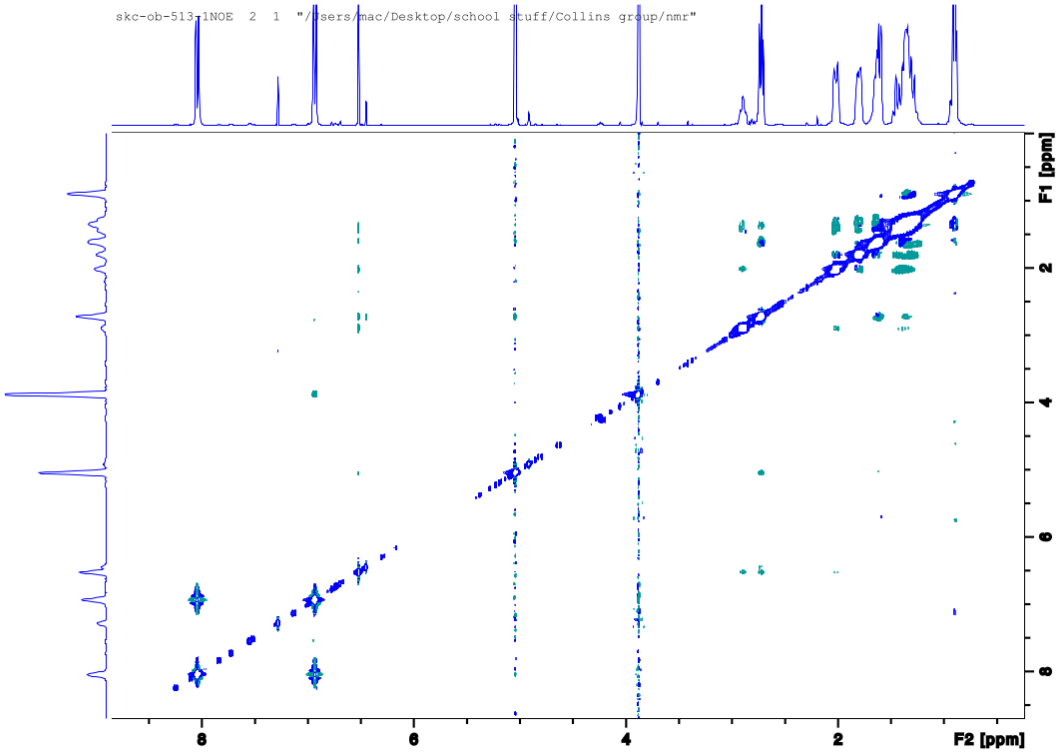
skc-ob-513-1NOE 2 1 "/Users/mac/Desktop/school stuff/Collins group/nmr"
F1 [ppm]
F2 [ppm]
8
6
4
2

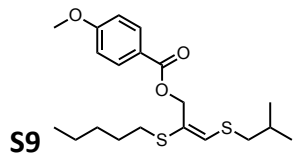

**S9**

(*trans* + unreacted starting material)

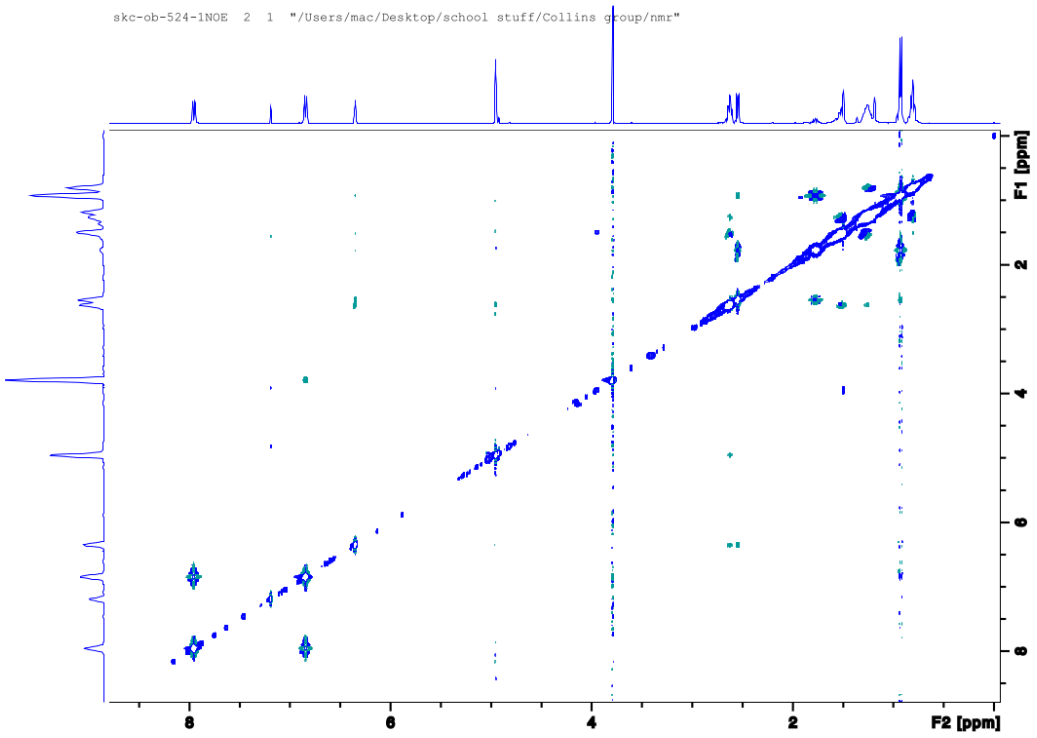

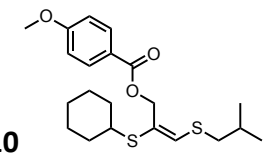

**S10**

(*trans* + unreacted starting material)